THÈSE en cotutelle

Présentée à

L'Université de Lille - Sciences et Technologies
Avec **l'Université de Mons**

Pour obtenir le titre de
DOCTEUR EN CHIMIE
Spécialité: Sciences de la matière du rayonnement et de l'environnement (ED SMRE)
par
Kifah NASR

Enzyme-catalyzed synthesis of polyesters by step-growth polycondensation: a promising approach towards a greener synthetic pathway.

Catalyse enzymatique de polycondensation pour les polyesters biosourcés : une approche prometteuse vers une voie de synthèse plus verte.

Soutenance le 20 septembre 2021 devant la commission d'examen

Rapporteurs:
M. Florent ALLAIS, Professeur, AgroParisTech (France)
M. Frédéric PERUCH, Professeur, Université de Bordeaux (France)

Examinateurs:
Mme. Katrien BERNAERTS, Maître de conférences, Maastricht University (Pays-Bas)
Mme. Veronique BOUNOR-LEGAR, Directeur de recherche, Université de Lyon 1 (France)
M. Pascal GERBAUX, Professeur, Université de Mons (Belgique)-**Président du jury**

Directeurs:
M. Jean-Marie RAQUEZ, Professeur, Université de Mons (Belgique)
M. Philippe ZINCK, Professeur, Université de Lille (France)

Co-encadrant:

Mme. Audrey FAVRELLE-HURET, Maître de conférences, Université de Lille (France)

Acknowledgement

I would like to express my deepest appreciation to my supervisors from the University of Lille, Prof. Philippe ZINCK and Dr. Audrey FAVRELLE-HURET, and from the University of Mons, Prof. Jean-Marie RAQUEZ for their continuous support, advice, and guidance. I consider research under their supervision a privilege. Their supportive attitudes are a model of what a successful researcher should acquire.

Thanks to Prof. Florent ALLAIS and Prof. Frédéric PERUCH for accepting the role as referees to my thesis, and to Dr. Katrien BERNAERTS, Dr. Veronique BOUNOR-LEGAR, Prof. Pascal GERBAUX for their roles as examiners.

I would like to extend my appreciation to all members of *Unité de Catalyse et Chimie du Solide* (UCCS, UMR 8181) and the Laboratory of Polymeric and Composite Materials (LPCM) for maintaining a good scientific environment and a high team spirit. I would also like to thank the organizers and members of the Interreg-ALPO project for their extensive effort invested in improving every aspect of this research, and the funders of this project that made this research possible.

I would like to thank all my colleagues and friends for the professional atmosphere they reflected, the good memories and encouragement: Franck, Andy, Julie, Michael, Robert, Catarina, Olda, Adrian, Lucas, Jean-Emile, Chiara, Meriam, Robert. W, Mirella, Ivaldo.Jr., Grace, Mira, Ali, Diaa, Chadi, Juliana, Josette, Imen, Karim and Sawssan.

Finally, a big thanks to my family for their never-ending support and love. Khalida, Ghassan, Ziad and Yara. Without you, none of this would have been possible.

Content

Abstract

Enzyme-catalyzed polymerization have been witnessing a growing attention in recent years as an eco-friendly substitute to metal-based catalysis. The objective of our work is to synthesize a series of polyesters *via* enzymatic catalysis based on different aliphatic and aromatic diols and diesters, where we focused on the influence of reaction parameters, monomer structures, and depicted the advantages and limitation of enzymatic catalysis in polymer synthesis. The enzyme used throughout our work was Novozym 435, a lipase from *Candida antarctica*, immobilized on an acrylic resin. In **Chapter 1,** we reviewed the different methods and approaches used in the literature to synthesize polymers *via* enzymatic catalysis. In **Chapter 2**, we performed the reaction between hexane-1,6-diol and diethyl adipate *via* a two-step polycondensation approach where we monitored the effect of certain parameters on the number average molecular weight (M_n). The influence of temperature, vacuum, and the amount of enzyme loading were determined using a central composite design. Other factors such as the reaction media, oligomerization time, and catalyst recyclability were also assessed. In **Chapter 3** furan-based copolyesters were synthesized, where we showed that we can incorporate higher amounts of furan when using aliphatic diols with longer chains such as dodecane-1,12-diol. In **Chapter 4**, levoglucosan, an anhydrous 6-carbon ring structure and a pyrolysis product of carbohydrates such as starch and cellulose, was reacted against different chain length diesters in the presence of aliphatic diols and Novozym 435 as a catalyst. The polyesters produced were limited in their number average molecular weight (M_n) and the amount of levoglucosan that was successfully incorporated into the polymeric structure. Nevertheless, by increasing the chain length of the diester, we were able to produce a copolymer containing higher amounts of levoglucosan and a higher molecular weight.

Résumé

La polymérisation catalysée par des enzymes a fait l'objet d'une attention croissante ces dernières années en tant qu'alternative écologique à la catalyse à base de métal. L'objectif de notre travail est de synthétiser une série de polyesters par catalyse enzymatique basée sur différents diols et diesters aliphatiques et aromatiques, où nous nous sommes concentrés sur l'influence des paramètres de réaction, des structures de monomères et avons décrit les avantages et les limites de la catalyse enzymatique dans la synthèse de polymères. L'enzyme utilisée tout au long de nos travaux était la Novozym 435, une lipase de *Candida antarctica*, immobilisée sur une résine macroporeuse acrylique. Dans le **Chapitre 1**, nous avons passé en revue les différentes méthodes et approches utilisées dans la littérature pour synthétiser des polymères par catalyse enzymatique. Dans le **Chapitre 2**, nous avons effectué la réaction entre l'hexane-1,6-diol et l'adipate de diéthyle *via* une approche de polycondensation en deux étapes où nous avons évalué l'effet de certains paramètres sur la masse molaire moyennee en nombre (M_n). L'effet de la température, du vide et de la charge enzymatique a été déterminé à l'aide d'un plan d'expérience de type plan composite centré. D'autres facteurs tels que le milieu réactionnel, le temps d'oligomérisation et la recyclabilité de l'enzyme ont également été évalués. Dans le **Chapitre 3**, des copolyesters à base de furane ont été synthétisés, où nous avons montré que nous pouvons incorporer des quantités plus élevées de dérivés furaniques lors de l'utilisation de diols aliphatiques avec des chaînes plus longues tels que le dodécane-1,12-diol. Dans le **Chapitre 4**, le lévoglucosan, un dérivé anhydre du glucose issu de la pyrolyse de polysaccharides tels que l'amidon et la cellulose, a réagi avec des diesters de différentes longueurs de chaîne en présence de diols aliphatiques et de Novozym 435 comme catalyseur. Les polyesters produits étaient limités en termes de masse molaire moyenne en nombre (M_n) et de quantité de lévoglucosan incorporée. En augmentant la longueur du diester, nous avons augmenté la quantité de lévoglucosan incorporée ainsi que la masse molaire moyenne en nombre.

List of abbreviations

[MOEMIm][dca]: 1-(2-hydroxyethyl)-3-methylimidazolium dicyanamide

[BMIM][Tf2N]: 1-butyl-3-methylimidazolium bis(trifluoromethane)sulfonimide

[BMIM][Cl]:1-butyl-3-methylimidazolium chloride

[BMIM][PF6]:1-Butyl-3-methylimidazolium hexafluorophosphate

BHMF: 2,5-bis-(hydroxymethyl)furan

HMFA: 5-hydroxymethylfuran-2-carboxylic acid

BDO: butane-1,4-diol

CALA: *Candida antarctica* lipase A /EC number: 3.1.1.3

CALB: *Candida antarctica* lipase B / EC number: 3.1.1.3

CR: *Candida rugosa* lipase / EC number: 3.1.1.3

CCD: central composite design

$CDCl_3$: Chloroform D

ΔH_c: crystallization enthalpy

CLEA cutinase: cutinases from *Fusarium solani pisi* cross-linkeded to form enzyme aggregates / EC number: 3.1.1.74

iCutinase: cutinases from *Fusarium solani pisi* immobilized on Lewatit beads / EC number: 3.1.1.74

D.P.: degree of polymerization

DMSO-d6: deuterated dimethyl sulfoxide

DBA: dibutyl adipate

DBSe: dibutyl sebacate

DBS: dibutyl succinate

DEA: diethyl adipate

DESe: diethyl sebacate

DES: diethyl succinate

DSC: Differential Scanning Calorimetry

DMA: dimethyl adipate

DMFDC: dimethyl furan-2,5-dicarboxylate

DMSe: dimethyl sebacate

DMS: dimethyl succinate

DMF: dimethylformamide

FDCA: furan-2,5-dicarboxylic acid

T_g: glass transition temperature

HDO: hexane-1,6-diol

HRP: horseradish peroxidase / EC number: 1.11.1.7

log P: logarithmic value of the partition coefficient

T_m: melting endotherm

ĐM: molar mass dispersity

X-furan: molar percent of alkylene furan-2,5-dicarboxylate unit in the copolymer

MM: *Mucor miehei* lipase / EC number: 3.1.1.3

N435: Novozym 435

M_n: number average molecular weight

ODO: octane-1,8-diol

OFAT: one-factor-at-a-time approach

X-levo: percentage of levoglucosan incorporated into the polymeric structure

P3HB: poly(3-hydroxybutyrate)

nylon-4,10: poly(butamethylene sebacamide)

PBS: poly(butylene succinate)

PEF: poly(ethylene furanoate)

PET: poly(ethylene terephthalate)

nylon-6,10: poly(hexamethylene sebacamide)

PHA: poly(hydroxyalkalkanoates)

PLA: poly(lactic acid)

nylon-8,10: poly(octamethylene sebacamide)

PTT: poly(trimethylene terephthalate)

PA: polyadipates

PBAF: polybutylene adipate furanoate

PBAT: polybutylene adipate terephthalate

PBF: polybutylene furanoate

PBT: polybutylene terephthalate

PE: polyethylene

PP: polypropylene

PPF: polypropylene furanoate

PPL: porcine pancreatic lipase

MALDI-MS: Positive-ion Matrix assisted LASER Desorption/Ionization-Mass Spectrometry

PC: *Pseudomonas cepacia* lipase / EC number: 3.1.1.3

REx: reactive extrusion

RSM: response surface methodology

RNA: ribonucleic acid

ROP: ring-opening polymerization

TPA: terephthalic acid

M_w: weight average molecular weight

WAXS: Wide-angle X-ray scattering

ε-CL: ε-caprolactone

PDL: ω-pentadecalactone

General introduction

The increasing environmental concerns of fossil fuel-based materials and their pronounced negative impact on our environment has been shifting the research focus towards a more sustainable synthetic pathway to develop polymers with adequate properties and a low carbon footprint. Such an approach is strongly supported with the increasing research works on the valorization of biomass to produce biobased polymeric materials.[1–5]

Although shifting to biobased polymers is a very important step to ensure environmental sustainability, it is however, insufficient. In fact, when discussing biobased polymers, it is crucial to investigate their manufacturing process and assess the environmental concerns accordingly. In other words, the overall production process of such biobased polyesters should be optimized to insure minimal environmental damage. For example, such assessment should take into consideration the extraction process of the biobased building blocks, the energy consumption during extraction and synthesis, and the impact of other factors such as the solvents and catalysts used, etc.

Focusing on optimizing the production of biobased polymers, enzymatic catalysis has been introduced as a greener synthetic approach towards the production of polyesters, owing to its non-toxic nature, high selectivity, and the possibility of processing under mild conditions.[6–8] When compared to current metal catalysts used for polyester synthesis, they are advantageous by avoiding any residual traces of harmful metals after synthesis and by preventing any discoloration and side reactions that can occur with metallic catalysis due to the elevated temperatures required.[9] In addition, the high selectivity of some enzymes can allow performing some reactions in minimal steps by avoiding additional steps like protection/deprotection chemistries that would otherwise require *via* these conventional catalyses.[10,11]

Aims of the study

The aims of the research conducted throughout this thesis is to develop efficient and green synthetic pathways for the manufacturing of biobased polymers via enzymatic catalysis. This work aims to highlight and define the impact of key-parameters that affect polymer growth *via*

enzymatic polycondensation. In addition, it sheds light over the limitations of using Novozym 435 for the synthesis of polyesters containing cyclic compounds and aims at developing appropriate approaches and strategies to overcome them.

Outline of the thesis

Novozym 435 (N435), a *Candida antarctica* lipase B (CALB) immobilized on a macroporous hydrophobic resin was used throughout this study to catalyze the polycondensation reactions of different monomeric units.

Chapter 1 starts with a general literature overview of the growing field of biobased polymers, their sources and challenges faced in production and competition. This chapter extends to focus on the use of enzymes as alternative catalysts for polymer synthesis, discussing the different types of enzymes, and polymers produced *via* enzymatic catalysis, and factors affecting it. In **Chapter 2**, we present a statistical approach to predict key-parameters affecting enzymatic catalysis, focusing on the impact of temperature, enzyme loading, reaction medium and vacuum variation. **Chapter 3** concerns the enzyme-catalyzed synthesis of furan-based copolyesters, where the effect of aromatic content, diol and diester length is assessed and studied. In **Chapter 4**, Novozym 435 was used to synthesize polyesters containing levoglucosan, an anhydrous derivative of glucose where different approached were assessed to incorporate it into a polymeric structure.

References:

(1) Babu, R. P.; O'Connor, K.; Seeram, R. Current Progress on Bio-Based Polymers and Their Future Trends. *Prog. Biomater.* **2013**, *2* (1), 8. https://doi.org/10.1186/2194-0517-2-8.

(2) Aeschelmann, F.; Carus, M. Biobased Building Blocks and Polymers in the World: Capacities, Production, and Applications–Status Quo and Trends Towards 2020. *Ind. Biotechnol.* **2015**, *11* (3), 154–159. https://doi.org/10.1089/ind.2015.28999.fae.

(3) Hamaide, T.; Deterre, R.; Feller, J.-F. *Environmental Impact of Polymers*; ISTE Ltd; John Wiley & Sons: London, UK; Hoboken, NJ, USA, 2014.

(4) Hottle, T. A.; Bilec, M. M.; Landis, A. E. Sustainability Assessments of Bio-Based Polymers. *Polym. Degrad. Stab.* **2013**, *98* (9), 1898–1907. https://doi.org/10.1016/j.polymdegradstab.2013.06.016.

(5) Vilela, C.; Sousa, A. F.; Fonseca, A. C.; Serra, A. C.; Coelho, J. F. J.; Freire, C. S. R.; Silvestre, A. J. D. The Quest for Sustainable Polyesters – Insights into the Future. *Polym. Chem.* **2014**, *5* (9), 3119–3141. https://doi.org/10.1039/C3PY01213A.

(6) Jiang, Y.; Woortman, A. J. J.; Ekenstein, G. O. R. A. van; Loos, K. A Biocatalytic Approach towards Sustainable Furanic–Aliphatic Polyesters. *Polym. Chem.* **2015**, *6* (29), 5198–5211. https://doi.org/10.1039/C5PY00629E.

(7) Gross, R. A.; Ganesh, M.; Lu, W. Enzyme-Catalysis Breathes New Life into Polyester Condensation Polymerizations. *Trends Biotechnol.* **2010**, *28* (8), 435–443. https://doi.org/10.1016/j.tibtech.2010.05.004.

(8) Chaudhary, A. K.; Lopez, J.; Beckman, E. J.; Russell, A. J. Biocatalytic Solvent-Free Polymerization To Produce High Molecular Weight Polyesters. *Biotechnol. Prog.* **1997**, *13* (3), 318–325. https://doi.org/10.1021/bp970024i.

(9) Jacquel, N.; Freyermouth, F.; Fenouillot, F.; Rousseau, A.; Pascault, J. P.; Fuertes, P.; Saint-Loup, R. Synthesis and Properties of Poly(Butylene Succinate): Efficiency of Different

Transesterification Catalysts. *J. Polym. Sci. Part Polym. Chem.* **2011**, *49* (24), 5301–5312. https://doi.org/10.1002/pola.25009.

(10) Adrio, J. L.; Demain, A. L. Microbial Enzymes: Tools for Biotechnological Processes. *Biomolecules* **2014**, *4* (1), 117–139. https://doi.org/10.3390/biom4010117.

(11) Jiang, Y.; Loos, K. Enzymatic Synthesis of Biobased Polyesters and Polyamides. *Polymers* **2016**, *8* (7), 243. https://doi.org/10.3390/polym8070243.

1. Bibliography

With the growing environmental concerns regarding the production of fossil fuel-based polymers and their significant polluting effect, research had been shifting attention towards finding alternative renewable resources to produce polymers with adequate properties, smaller carbon footprint, and an efficient economical synthetic pathway. Amongst the various approaches employed to reach such a goal, enzyme-based polymerization came to light as one of the green alternatives to conventional polymerization techniques, owing to their various advantageous properties such as their green renewable nature, selectivity, and the milder energy input they require in polymer production. In the following chapter we briefly report the different sources and challenges to produce biobased polymers. In addition, a thorough description of the use of enzymes as biocatalysts in the production of polymers have been reported. This chapter shows the advantages, capabilities, as well as limitations of enzyme-catalyzed polymerization focusing on the production of polyesters, polyamides and poly(ester-*co*-amide)s. The effect of monomer type, reaction parameters, and media, are detailed.

Keywords: biopolymers; enzymatic polymerization; polyesters; polyamides; poly(ester-*co*-amide)s; lipase.

1.1 An introduction to biobased polymers

Biobased polymers can be defined as polymers that are sustainable in nature, produced from renewable resources such as biomass and characterized by possessing neutral CO_2 emission. Such definition encompasses polymers produced totally or partially from renewable resources. Although different criteria can be used to distinguish between the different types of biobased polymers and their production route, it can mainly be divided into 3 main pathways: (1) natural polymers extracted and/or modified such as starch and cellulose; (2) macrostructures produced and extracted from microorganisms such as the use of bacteria to ferment sugars and oils to produce poly(hydroxyalkanoates); (3) polymerization of biomonomers to form e.g polyesters, polyamides, and polyurethanes. Although the first two approaches are known for a long time, they however

suffer from a low structural flexibility, and require intensive extraction methods to purify them.[1–3]

Before deepening into the current advances in biobased polymers, it is important to clarify the concept of biobased polymers against that of biodegradable polymers, as both groups are often misconceived as one. In brief, a biobased polymer only reflects the fact that a polymer is produced from renewable resources, but in terms of end-life it can be biodegradable or non-biodegradable. On the other hand, biodegradable polymers are polymers that can break down within an acceptable period of time due to the actions imposed by microorganisms: such polymers can be either bio-based or fossil-fuel based.[4] Figure 1 shows a classification of different polymers based on their biodegradability and the source of their raw materials.

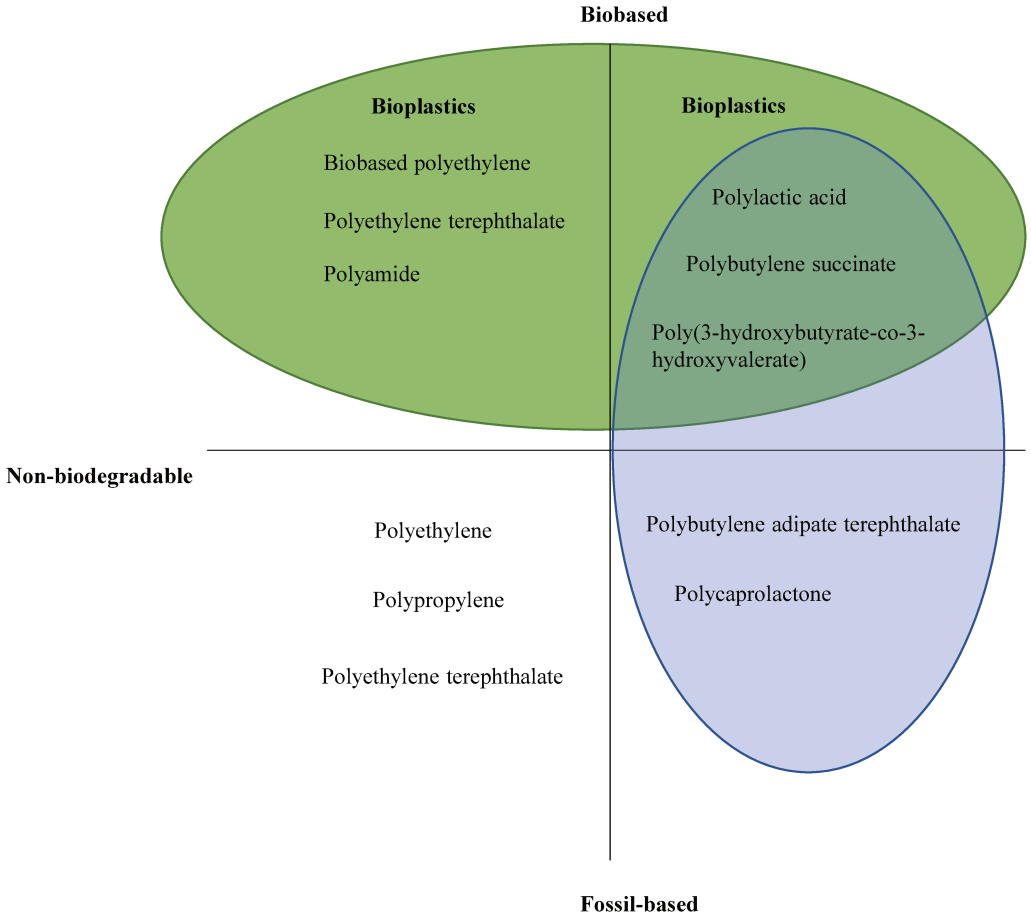

Figure 1. Different polymers as a function of their origin and biodegradability.[5]

As attractive as it might seem, biobased polymers are still facing with lots of limitations, especially in regard to their price, as their production is not capable of competing due to the high cost of raw materials, and low volume production in comparison to the fossil-fuel based polymers. Therefore, it is becoming essential to develop a green, fast, continuous, and reliable manufacturing pathway that could promote biobased polymers to a more competing status. In fact, the current market of biobased polymers does not exceed 1% of the total amount of polymers produced. Expectations for 2024, show a possible increase by 282 thousand tons (Figure 2), a 13% increase from 2018. However, this increase is still considered very modest in comparison to fossil-fuel based plastic market.[6,7]

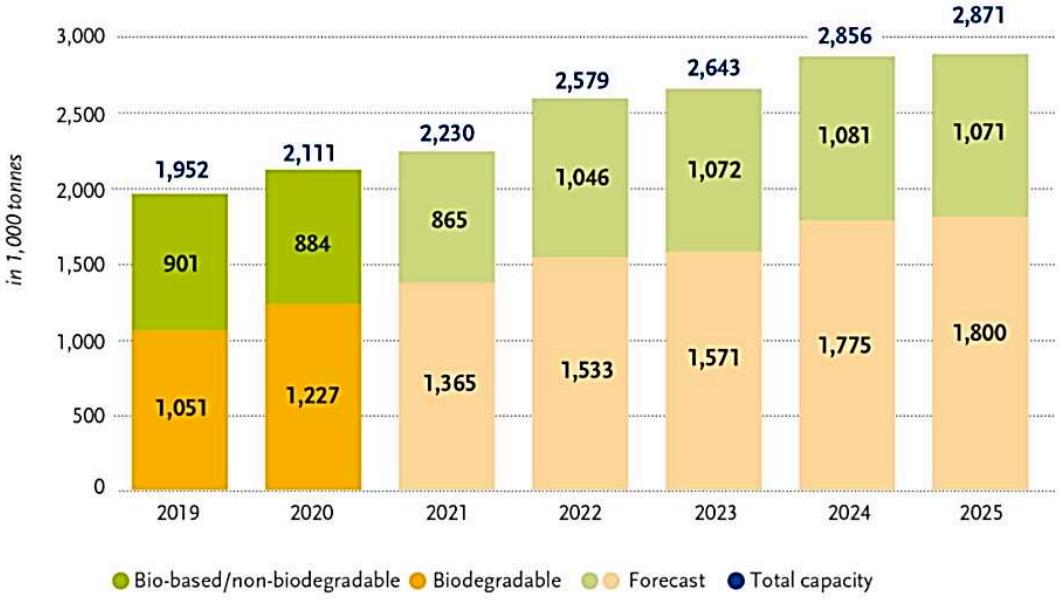

Figure 2. The expectation of biobased polymer production growth till 2024.[6,7]

The current applications of biobased polymers are limited and sparsely diversified, where up to 53% is solely used in packaging. Other applications include textiles, agriculture, coatings, and adhesives, etc. Several biobased polymers have been developed in the past years and are showing a promising growth in production rate, due to their wide range of applications, the most common among them are biobased polypropylene (PP) and poly(hydroxyalkalkanoates) (PHA) with expectations to increase by 3 and 6 times in 2024, respectively. The current biobased plastic market

is dominated by starch blends that account for 21.3% of the total biobased plastics market, followed by polylactic acid at 13.9% and polybutylene adipate terephthalate (PBAT) at 13.4%. Other biobased polymers produced at a significant level include polyethylene (PE), poly(ethylene terephthalate) (PET), poly(trimethylene terephthalate) (PTT), polyadipates (PA), and to a lesser extent, poly(butylene succinate) (PBS) at 4.3%. Additionally, a promising biobased polymer poly(ethylene furanoate) (PEF) is expected to become industrially produced in the few years to come, PEF possess similar properties and characteristics to PET, but has superior barrier properties, and can be totally produced from bioresources.[6,7]

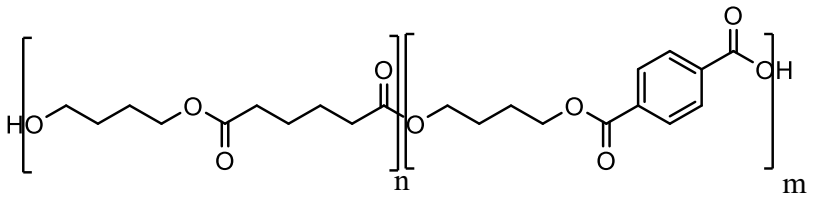

PBAT

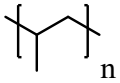

Bio-based PP

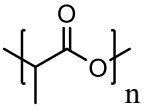

PLA

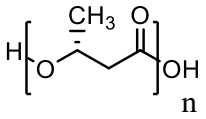

PHA

Scheme 1. Structures of common biobased polymers.

1.2 Biobased polymers sources and challenges

One of the major arguments against biobased polymers is the growing risk of the competition with food resources, especially when edible biomass is used in their production. Such a problem could only be exacerbated by competition on land and water resources, in addition to the deforestation

of huge areas and replacing a wide variety of plant species with only one (such as the case of palm trees for palm oil production). Such approaches would result in severe damage to our ecosystem, and cause problems that can be as significant as the damage done by fossil-fuel based polymers. Therefore, it is important to search for resources that do not inflict such damage and it is also important to tread carefully before branding a product as green or environment friendly. To address this problem, different strategies have been used to avoid the use of food related biomass and find alternative bioresources. For example, food waste is being a main contributor to all biowastes, can serve as a possible source for biogas production. Studies in this field have shown the possibility of producing biogas, biomethane, and other chemicals *via* different strategies and chemical procedures, such as anaerobic digestion of food waste to produce biomethane and biohydrogen that could serve as an energy source for electricity production.[8] In addition, food wastes due to its richness in sugars, proteins, and oils, can serve as an important source of chemicals that are essential in producing biobased polymers.[4] For example, monomers such as succinic acid, lactic acid, itaconic acid, including polymers such as PHA can be derived from fatty acids and sugars present in food waste through fermentation. Another important monomer (propane-1,3-diol) which is mainly used in the production of PTT, can be derived from glycerol, which is by turn a byproduct of biodiesel production.[9]

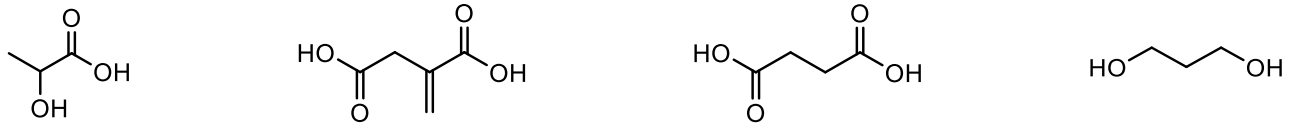

Lactic acid Itaconic acid Succinic acid Propane-1,3-diol

Scheme 2. Structures of some monomers that can be synthesized *via* fermentation of biomass.

Lignocellulosic biomass is another non-food competitive source for the production of biobased polymers, as such feedstock is considered to be the most abundant biomass in the world and encompasses a variety of green products such as trees, grass, and agricultural residues, etc. The main constituents of lignocellulosic biomass are mainly lignin and structural polysaccharides

(mainly pectin, cellulose, and hemicellulose). Although lignin remains difficult to get processed into small usable molecules, polysaccharides have shown to be efficiently used as building blocks. Indeed, microbial enzymes or chemicals can be used to decompose these polysaccharides into simple sugars that by turn can be used in biopolymer production.[9–11]

The use of microalgae has been recently attracting much more attention as a relatively new chemical and energy source due to the many advantages such as superior production rate related with high efficiency in photosynthesis (compared to lignocellulosic biomass) and high tolerance to extreme environmental conditions related with their ability to grow in non-arable lands using wastewater and in some cases sea water depending on the species. Therefore, microalgae can be considered to be non-competitive with food resources. The main products of microalgae vary and differ in amount from species to another. Generally, microalgae can produce polysaccharides, lipids, and proteins. Depending on the targeted class or molecule intended to be produced, certain microalgae species can be favored over others. For example, *Porphyridium cruentum* is a microalgae species with a high carbohydrate composition constituting between 40 to 57% w/w. On the other hand, *Chlorella pyrenoidosa* and *Chlorella vulgaris* are mainly dominated by their protein content which exceeds 50% w/w. Similarly, lipids constitute a major part of other species such as *Schizochytrium* species with lipid content ranging between 50 and 77% w/w. Currently, microalgae are mainly used in dietary supplements and their advertisement takes advantage of many studies that show their high health benefits (anti-inflammatory, anti-viral, anti-cancer properties, etc.) due to the variety of nutrients in them. Microalgae is also a source of high value bioproducts such as β-carotene, Astaxanthin, and Omega-3 fatty acids.[12–16]

The production of biobased monomers using microalgae as a source is not widely studied. However, as such species are rich in carbohydrates, lipids, and proteins, it is practically feasible to use them for that purpose. In fact, Hirayama and Ueda previously reported the direct production of PLA *via* dark anaerobic fermentation of starch produced by *Nannochlorum* sp. 26A4.[17] Similarly, bacterial fermentation of *Hydrodictyon reticulum* micro algae yielded L-lactic acid.[18] Other examples include the extraction of cellulose from certain species of microalgae, and their use as reinforcing material for biobased polymers, or in the production of nanocellulose fibers as presented by Kim *et al*.[19] by using electrospinning of polycaprolactone and *Spirulina* sp. mixture. In this study, the polycaprolactone-*Spirulina* nanofiber mat was used in cell culture and was found

to enhance the growth and metabolic activity of primary astrocytes (glial cells in the central nervous system) in comparison to polycaprolactone alone. In another study, PHA was successfully extracted from four different species of microalgae giving variable yields and some variations in the PHA's physical properties. Although microalgae show superiority over other feedstocks resources in different aspects, it is however more expensive and is still non-competitive, especially as a source of biobased molecules.[20] However, certain approaches can be and are being taken to enhance the production: cost ratio and improve efficiency, such as the optimization of the cultivation, processing, and extraction methods, in addition to genetic improvements and modifications. This can increase the desired aspects in microalgae such as increasing the light to biomass conversion, pathogen resistance, temperature, and light adaptability.[12,21,22] In fact, our current work falls within the framework of the ALPO-INTERREG project that aims at extracting and separating building blocks from micro-algal biomass that can be suitable for bioplastic material synthesis.

1.3 Enzymes in polymer synthesis

Enzymes are life essential substances that act as catalysts for thousands of biochemical reactions. Although some enzymes exist as ribonucleic acid (RNA) molecules, the majority however, are protein structures consisting of repeating units in amino acids and are considered essential in catalyzing most of the biological reactions that otherwise would take a very long time to occur. In fact, enzymes can accelerate reaction rates by million times. Like other catalysts, enzymes are not consumed in the reaction, but they simply increase the rate of reaction. Regarding their mechanism, as observed in Figure 3, the substrates bind to specific regions within the enzyme to form a complex. Afterwards, the substrate is converted into a product and detached from the enzyme.[23,24]

1.3.1 General mechanism of enzymatic catalysis

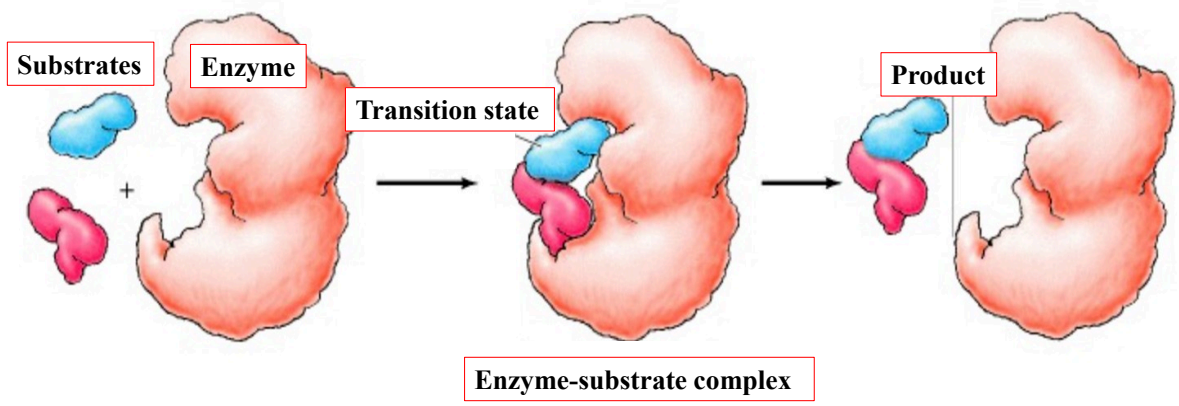

Figure 3. Mechanism of enzymatic catalysis of a reaction between two substrates.[24]

To further elaborate on enzymatic catalysis, it is important to acquire adequate understanding about the three-dimensional structure of enzymes and how such structure facilitates the catalytic pathway. In fact, although the sequence of amino acids within enzymatic structures plays an important role to determine the function, the intermolecular interactions between amino acids affecting the peptide folding into a three-dimensional structure is the key that determines their overall functionality. Within their three-dimensional structures, enzymes possess pockets or active sites that allows for specific substrate interaction. A simple model that describes their catalytic mechanism is the lock and key model introduced by Emil Fisher in the 19th century.[25] In this model, it is suggested that the selectivity of enzymes allows substrates to fit accurately to the active site. However, in many cases, substrates alter the shape of the substrate-enzyme complex, allowing the substrates to achieve a specific transition state, which by turn increase the reaction rate. The role of enzymes is not limited to achieve the transitional state of substrates, but they can react with reaction intermediates *via* amino acids within the active sites that by turn accelerates the reaction.[26]

1.3.2 Enzymatic categories, advantages, and their role in polymerization

Enzymes are mainly categorized into six groups encompassing oxidoreductases, transferases, hydrolases, lyases, isomerases, and ligases. Although enzymes have found applications in different fields, the focus herein is on their application as catalysts in polymerization reactions, where three out of the six enzyme categories have found applications in *in-vitro* polymerization, particularly oxidoreductases, transferases, and hydrolases. Further information regarding these classes and their applications are detailed in Table 1. Although natural polymers are produced *in-vivo via* enzymatic catalysis, the use of enzymes for *in-vitro* polymer synthesis is considered relatively new. In fact, the first example of enzyme mediated polymerization was reported in 1951 by Parravano who reported oxidase mediated polymerization of methyl methacrylate[27]. However, it was not until the 1990s that the concept of enzymatic polymerization started growing rapidly, and the use of enzymes for synthesis and transformation of small molecules shifted towards polymerization. This interest arose from observations and experiments that shed light on the advantages of enzymes in polymerization, such as being highly selective, possess high catalytic power under mild condition as well as being regarded as non-toxic green catalyst. For example, enzymes selectivity was observed when enzymes had been successfully used to catalyze polymer synthesis. This yielded well-defined structures that would otherwise require extra protection and deprotection steps using conventional catalysts. Similarly, their non-toxic nature provided an alternative synthetic pathway for polymers, especially biodegradable polymers used in biomedical application. Such polymers are conventionally synthesized using metal-based catalysts, which can be harmful and require their complex removal in biomedical applications. Unlike conventional catalysts that require high temperatures in step growth polycondensation, another advantage is that enzymes can catalyze the reaction under mild conditions, thus avoiding side reactions and unwanted discoloration that might occur at elevated temperatures. Last but not least, the development of immobilized enzymes has been paving the way towards the use of enzymes on an industrial level owing to the increased stability of immobilized enzymes, as well as their recyclable and reusable nature.[24,28–32] The following part includes a brief description of the different

enzymatic classes used in polymerization, with a focus on hydrolases which are the core of this chapter.

Table 1. Enzyme classification, mechanism of action, and typical enzymatically synthesized polymers

Enzymatic group	**Mechanism of action**	**Typical examples**
oxidoreductases	oxidation/reduction	polyphenols, polyanilines, vinyl polymers
transferases	chemical group transfer	polysaccharides, polyesters
hydrolases	hydrolysis esterification	polysaccharides, polyesters, polycarbonates
lyases	cleavage	
isomerases	isomerization	
ligases	joining of molecules by bond formation	

1.3.3 Oxidoreductases: examples in polymerization

Tyrosinases and laccases are both subclasses of oxidoreductases that can facilitate polymerization due to the presence of copper in their structures. In a study made by Desentis-Mendoza *et al*,[33] both enzymes were successfully used to catalyze the transformation of quercitin (a flavonol) into low molecular weight aggregates that possessed higher antioxidant activity than the original monomer. Oxidoreductases have also found application in catalyzing oligomerization and polymerization reaction of different types of arylamines through oxidative coupling. Perhaps the most studied oxidoreductase for arylamine oxidative coupling is horseradish peroxidase (HRP) extracted from horseradish roots, HRP is a heme peroxidase that contains iron (III) protoporphyrin IX prosthetic group that catalyzes the oxidative coupling reactions of arylamines in the presence of hydrogen peroxide as the oxidizing agent. In many cases templates were added (such as polymers or micelles that can have a positive impact on polymerization). The oxidoreductase synthesized polyanilines were proposed to have several applications such as in immunoassays, water treatment, and sensors.[34,35]

1.3.4 Transferases: examples in polymerization

Transferases catalyze reactions of transferring groups from one molecule to another. Such transferred groups could contain aldehydes, ketones, sulfur, etc. Within this category, different subcategories are present with enzymes responsible for different reactions. For example, the *in-vitro* synthesis of poly(hydroxyalkanoate) (PHA) was demonstrated with the synthesis of poly(3-hydroxybutyrate) (P3HB) using polyester synthases as catalysts.[36,37] Another subcategory (transglutaminases), found applications in food, textiles and biomedical applications. In fact, this enzyme can catalyze the crosslinking of different protein types such as whey and soy proteins, etc. which results in better quality products.[38,39] In addition, the use of transglutaminases has been found to enhance properties of protein-based fabrics by increasing the resistance against proteolysis (breaking down of proteins). This resistance was assumed to be resulting from changes in protein structures imposed by transglutaminases that would render protease access sites harder to access.[40] In addition to food and fabrics, transglutaminases were used to cross-link collagen for applications in wound dressings that showed improved wound healing properties.[41] Other transferases such as glycosyltransferase that can be further subcategorized into (phosphorylases, glucansucrases, etc), have been exploited in the production of oligosaccharides and polysaccharides, such as amylose.[42,43]

1.3.5 Hydrolases: examples in polymerization and a focus on lipases

Perhaps the most used and promising enzymes in the field of polymer chemistry are hydrolases. Although their name implies about their ability to catalyze hydrolysis reactions, they can however function in a reversed manner by catalyzing polymerization through ester and amide bond formation. The application of hydrolases in polymerization reactions ranges from ring-opening polymerization (ROP) to polycondensation reactions leading to polyesters and polyamides among others. Proteases which is a subclass of hydrolases have been mainly used in catalyzing the

formation of peptide bonds in the synthesis of polypeptides. Although different techniques are available for the synthesis of polypeptides, proteases offer the advantages of providing high yields, in addition to being stereo and regioselective.[44,45] Moreover, proteases were used for incorporating other unnatural moieties into polypeptides such as nylon and unnatural amino acids.[46–48]

Cutinases which fall within another subclass of hydrolases are naturally occurring fungal enzymes. As their name suggests, they hydrolyze ester bonds in cutin which is a waxy natural polyester found in plants. The research on cutinases in the past years have been focusing on their hydrolytic ability on polyesters rather than polymerization.[26] However, an increasing amount of research on the polymerization capacity of cutinases have been on the rise. For example, in an article by Stavila *et al.*[49] the author shed light on the effect of modifying cutinases by immobilization or formation of aggregates on its catalytic activity. As of such, cutinases from *Fusarium solani pisi* were first modified to form cross-linked enzyme aggregates (CLEA cutinase) or were immobilized on Lewatit beads (iCutinase immobilized on Lewatit) and were used to catalyze several polycondensation reactions between several diamines (butane-1,4-diamine, hexane-1,6-diamine, and octane-1,8-diamine) and diethyl sebacate. As observed in Table 2, following a two-step polycondensation reaction by applying vacuum through the second step, led to higher degree of polymerization (D.P.) regardless of the enzyme used. Moreover, results showed that when in the form of aggregates, cutinase possessed superior catalytic activity to immobilized cutinases. Additionally, the selectivity of cutinase was found to be better oriented towards longer diols (see Table 2). Other examples on cutinases include polycondensation of dicarboxylic acids and their esters,[50,51] and ring-opening polymerization of lactones.[52,53]

Table 2. Effect of different catalysts on the degree of polymeriation (D.P.) of poly(butamethylene sebacamide) (nylon-4,10), poly(hexamethylene sebacamide) (nylon-6,10), and poly(octamethylene sebacamide) (nylon-8,10).[49]

Nylons	Catalysts	One-step reaction	Two-step reaction
		D.P. (MALDI)	D.P. (MALDI)
Nylon-4,10	iCutinase immobilized on Lewatit	–	4
	CLEA cutinase	4	8
	Novozym 435	5	8
Nylon-6,10	iCutinase immobilized on Lewatit	–	5
	CLEA cutinase	8	11
	Novozym 435	7	10
Nylon-8,10	iCutinase immobilized on Lewatit	5	5
	CLEA cutinase	13	16
	Novozym 435	12	12

Within the class of hydrolases, lipases belonging to the subclass of serine hydrolases are one of the most studied and applied enzymes in polymerization. Although the focus here is on the role of lipases in catalyzing polymerization reactions, it is important to mention other applications of this enzymatic category, including the treatment of lipid-rich waste water, detergents to aid in fat hydrolysis, as well as in food processing.[54] Lipases possess certain advantages over other enzymes in being stable in non-conventional media e.g organic media, ionic liquids, supercritical fluids as well as their adequate functionality towards a broad range of substrates. In nature, lipases are enzymes responsible for hydrolysis of fatty acids. Although hydrolysis usually occurs in aqueous media, when put in low water content media, some lipases act as catalysts in the synthesis of polyesters, polyamides, polycarbonates, as well as polythioesters. Lipases used in polymerization reactions are diverse, including *Candida rugosa* lipase (CR) also known as *Candida cylindracea*, *Aspergillus niger* lipase (AN), *Candida antarctica* lipase A (CALA), *Mucor miehei* lipase (MM), porcine pancreatic lipase (PPL), *Pseudomonas cepacia* lipase (PC), *Candida antarctica* lipase B (CALB), etc. Lipases are known as interfacial enzymes mainly due to their mechanism of action that is called interfacial activation. Lipases contain large pocket like structures that are hydrophobic in nature, usually protected by a polypeptide chain known as a lid which by turn have

an inner hydrophobic surface and an outer hydrophilic surface. When in contact with other hydrophobic substrates such as glyceride drops (see Figure 4), the lid opens and adsorbs on them, allowing for an accessible path between glycerides and the active site of the enzyme. Thus, this mechanism allows lipases to adsorb on hydrophobic surfaces of substrates.[55–58]

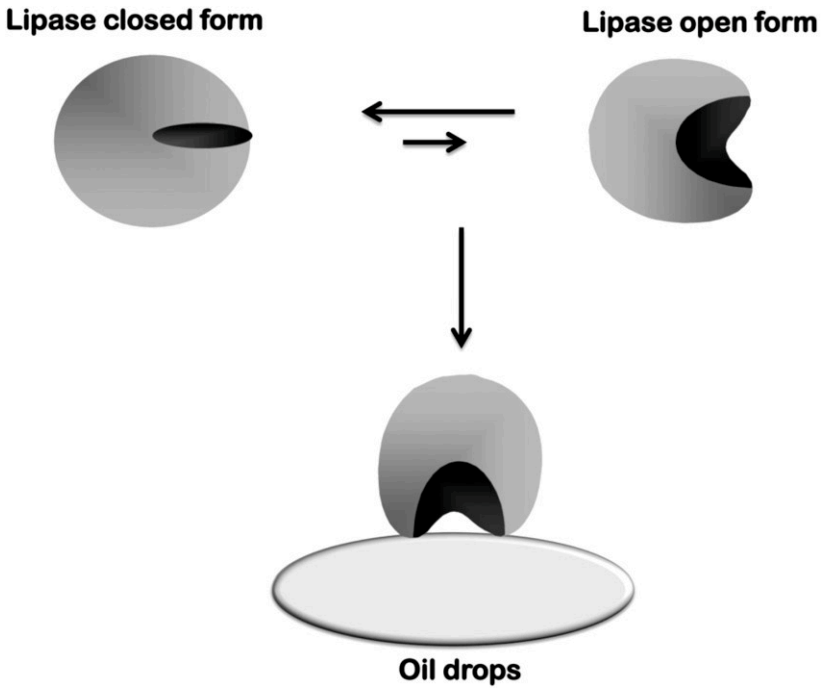

Figure 4. Conformational equilibrium and interfacial activation of lipases.[58]

The focus in the following part is on *Candida antarctica* lipase B (CALB), which is the most widely used lipase in the field of polymer chemistry, due to its high stability in organic solvents, its resistance to relatively high temperatures, as well as its enantioselectivity.[58] Starting with its structure, CALB consists of 317 amino acids, with a molecular weight of 33 kDa.[59] Like other lipases, CALB possess α/β hydrolase fold, where an α-helix is connected to the middle of a β-sheet array (only seven β-strands in case of CALB), i.e., their catalytic triad; which is the active site, consists of serine, histidine and aspartate.[60] Regarding its mechanism of action, first; as observed in Scheme 3, the substrate forms a complex with the enzyme known as Michaelis–Menten complex, this activates the hydroxyl group of the serine, allowing it to attack carbonyl groups of substrates such as carboxylic acids or their esters. This attack allows the formation of an

intermediate with a negatively charged oxygen within the carbonyl group known as a tetrahedral intermediate. This negative charge is then stabilized *via* hydrogen bonds occurring between the oxygen of the carbonyl group and the amide groups on the backbone of the enzyme also known as oxyanion hole. Similarly, the positively charged histidine is stabilized by interacting with aspartate. Following, proton is transferred to the alkyl oxygen on the substrate, allowing the release of alcohol of the substrate. This will result in the formation of the acyl-enzyme intermediate, which is then deacylated by a nucleophile attack such as alcohol, forming in place a second tetrahedral intermediate. After which, an enzyme-product complex forms and released, while the free enzyme is regenerated.[31,61–64]

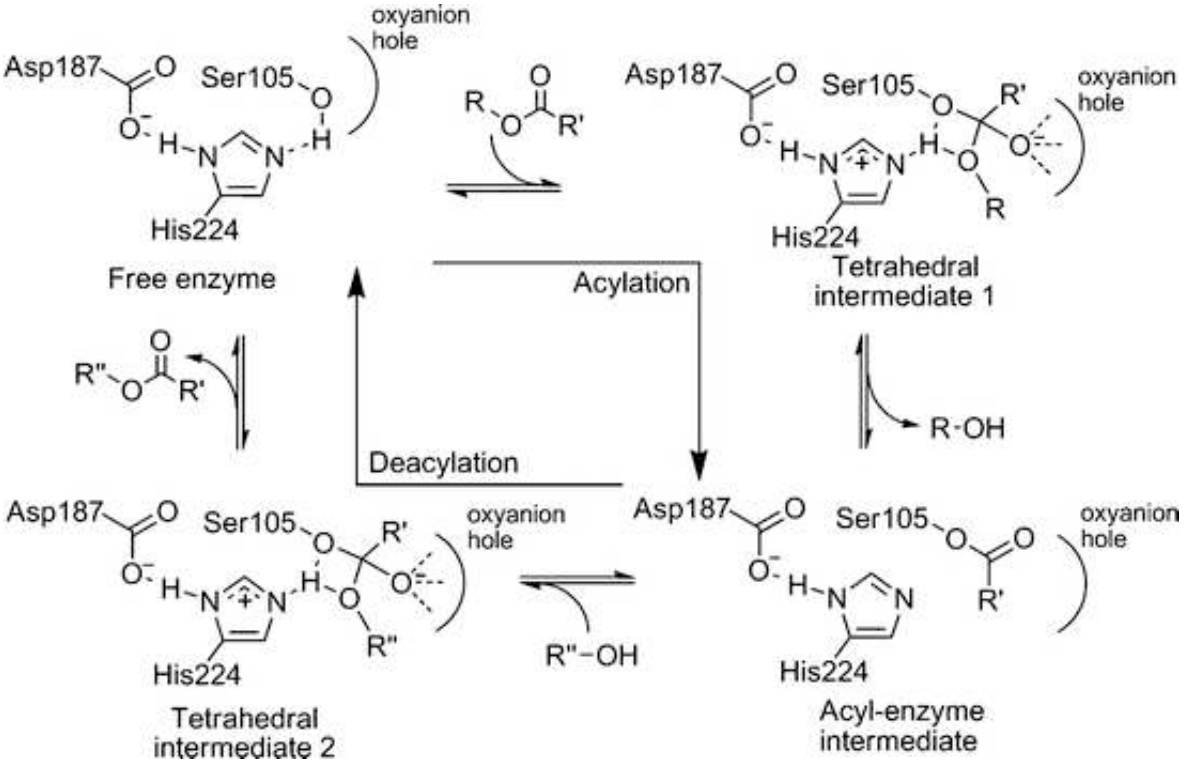

Scheme 3. Steps of the catalytic mechanism of CALB.[61]

1.3.6 Immobilization techniques: a focus on CALB immobilization

Although CALB showed better stability in solvents and better thermal resistance when compared to other lipases and other enzymes in general, it is still considered as a low stability catalyst. Accordingly, in the past years, increasing research started arising by focusing on methods that could further enhance the stability of enzymes, mainly protein engineering and enzymatic immobilization. The focus in the following part is on immobilization techniques, especially the immobilization of CALB. However, it is important to establish an understanding about protein engineering, and how this method improves the properties of enzymes. Simply put, protein engineering is the process of modifying the amino acid sequence within the enzyme in a certain way which will subsequently result in structural changes leading to improved properties such as stability, selectivity, etc.[65] There are many examples and techniques used in the literature regarding protein engineering, with applications in various fields such as the bread, beer, and detergent industries among many others. However, this will not be further reviewed here.

Enzyme immobilization can be defined as the process of binding an enzyme to a solid insoluble material which first arose as a technique aiming to facilitate the removal of enzyme from solvents and products. However, the advantages of immobilization were not limited to facilitating separation, but also extended towards other properties, such as modifying its selectivity and stability, enhancing dispersion of enzyme molecules as well as its ability to recycle and reuse. Such improvements have made enzymatic catalysis more attractive to both the research and industrial sectors. Different protocols and approaches towards enzymatic immobilization have immerged in the past years, but principally, they can be separated into three categories, being entrapment, cross-linking, and binding to support. The support to which the enzyme is immobilized is usually a synthetic resin or a polymer, but other biomaterials such as alginates and chitosan can be used. *Via* entrapment techniques, a polymeric network is synthesized while enzymes are present, leading to entrapment of enzymes within the network. Cross-linking on the other hand, proceeds by cross-linking enzymatic aggregates to form macroparticles. Immobilization *via* binding to support can be subcategorized into physical bonding, covalent bonding, and ionic bonding. Physical bonding, also known as adsorption, occurs when the enzyme forms weak interactions (*i.e.*, hydrophobic group interactions, Van der Waals interactions) with

the supporting material that had been surface modified. On the other hand, the bonds formed *via* covalent or ionic bonding methods are usually stronger and, in these methods, the support material is functionalized, allowing it to form covalent or ionic attachments with the enzyme. Further information on the advantages and disadvantages of different immobilization techniques is presented in Table 3.[65–70]

Table 3. General advantages and disadvantages of different enzyme immobilization techniques.

Method of immobilization	Advantages	Disadvantages
Physical binding	Relatively easy to prepare. Economical. High activity.	Enzyme leaching. Low stability.
Covalent binding	Strong enzyme-support bonds. Lower extent of enzyme leaching. High thermal stability.	Low activity due to lack of enzymatic free movement. Unrenewable support materials.
Entrapment	Allows easier movement for low molecular weight molecules.	Weak physical restraints. Low enzymatic loading.
Cross-linking	Insoluble enzymes allow recyclability.	Low activity. Low stability. Difficulties accessing active enzyme sites.

The mechanism of lipases based on hydrophobic interactions can cause problems such as enzyme aggregation that would limit the enzymatic activity. However, this mechanism can be used advantageously to immobilize the enzyme on hydrophobic surfaces, rendering the enzyme more stable and active. The most studied immobilized enzyme in the literature is Novozym 435 (N435), which is a *Candida antarctica* lipase B (CALB) immobilized on a macroporous hydrophobic resin of poly(methylmethacrylate) *via* interfacial activation.[58] The following part will focus on the use of Novozym 435 as a catalyst in different polymerization reactions, especially in the productions of polyesters and polyamides.

1.4 Enzymatic synthesis of aliphatic poly(alkylene dicarboxylate)s

Aliphatic poly(alkylene dicarboxylate)s are considered as a subgroup of the polyester family synthesized from aliphatic monomers such as aliphatic diols and dicarboxylic acids. The fact that most of poly(alkylene dicarboxylate)s can be synthesized from biobased monomers have attracted increasing attention from research with the aim to find an alternative to fossil-fuel based polymers.

1.4.1 Biobased poly(butylene succinate)

Perhaps one of the most studied aliphatic poly(alkylene dicarboxylate) which is obtained exclusively *via* polycondensation is poly(butylene succinate) (PBS) as synthesized in the presence of a catalyst *via* the polycondensation reaction of butane-1,4-diol and succinic acid or its anhydride. It is a biodegradable polymer that possess good mechanical and thermal properties that are comparable to those of polyethylene and polypropylene. In fact, PBS possess a T_g = -32 °C, which makes it easier for melt processing in comparison to PLA with a T_g = 60 °C.[71] Such properties have allowed PBS to find applications in packaging materials, textiles, etc. In addition to its good properties, the fact that succinic acid and later butane-1,4-diol, became available and commercialized from renewable resources, have made PBS more attractive as a biobased polymer, offering a possible alternative for some fossil fuel-based polymers.[72] Although the production of biobased succinic acid derived from sugar fermentation (see Figure 5), it is still at its infancy with respect to the production of fossil-based analogues, many research and emerging technologies are reducing the competition gap between both pathways. Such research includes genetic engineering of bacterial strains to give higher yields and less byproducts. Additionally, research has been focusing on enhancing the efficiency in extracting succinic acid from the fermentation broth through different technologies such as precipitation, sorption, reactive extraction, electrodialysis, and ion-exchange.[73,74]

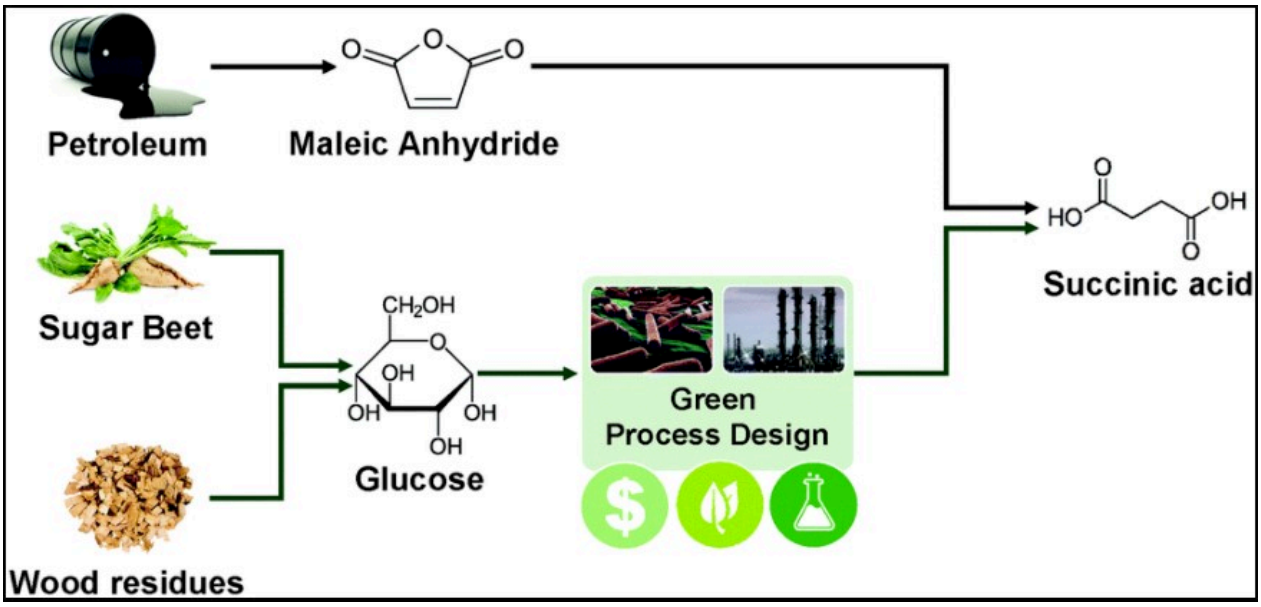

Figure 5. Succinic acid production pathways (fossil-fuel *vs*. biomass).[74]

Richard A. Gross and his team have studied the enzymatic synthesis of PBS using a two-step polycondensation method.[75] In this study, diethyl succinate was used as the acyl donor instead of succinic acid to avoid some problems related with phase separation in the reaction media caused by the poor solubility of succinic acid in butane-1,4-diol. As such, the reactions were carried out for 2 h under atmospheric pressure followed by a 72 h under vacuum (53 mbar), the temperature was constant in both stages (80 °C), and N435 was present in 10% w/w relative to total monomers. The molecular weight determined *via* polystyrene calibrated gel permeation chromatography (GPC) reached a maximum of 10,000 $g.mol^{-1}$ in diphenyl ether. In the same study, a significant increase in molecular weight from 10,000 to > 35,000 $g.mol^{-1}$ was achieved in diphenyl ether by simply increasing the reaction temperature from 80 to 95 °C after 21 h. This temperature increase allowed the formation of a monophasic mixture, prevented PBS precipitation, and thus gave a way to a further increase in molecular weight.

Similarly, Sugihara *et al.*[76] attempted a different strategy for the synthesis of high molecular weight PBS using N435 as a catalyst. In their work, they compared between two strategies to synthesize PBS, the first is the direct polycondensation of butane-1,4-diol and dimethyl succinate, while the second is the ring-opening polymerization (ROP) of cyclic oligoesters synthesized by the

condensation of the monomers in dilute toluene solution (see Scheme 4. Cyclization and direct polycondensation as methods in the synthesis of PBS.[76].The results showed that the last method resulted in a PBS having a number average molecular weight (M_n) ~ 81,000 g.mol^{-1} and a dispersity ~ 1.6, in comparison to an inferior M_n ~ 12,000 g.mol^{-1} and a dispersity of 3.7 obtained *via* the direct polycondensation method.

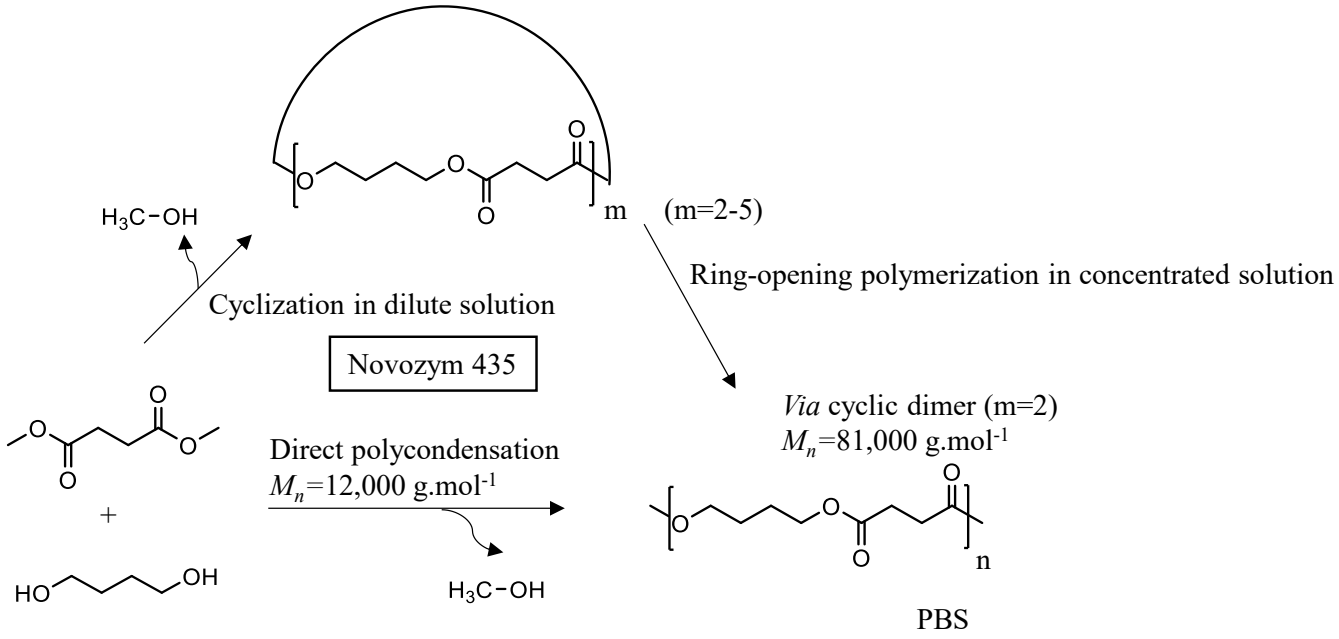

Scheme 4. Cyclization and direct polycondensation as methods in the synthesis of PBS.[76]

1.4.2 Biobased poly(lactic acid) (PLA)

Poly(lactic acid) (PLA) is a biodegradable and biobased thermoplastic polyester, currently used in medical implants such as bone fixation, drug delivery systems, as well as decomposable packaging material.77 PLA is considered as one of the most industrially produced biobased polymers, its global production capacity in 2019 exceeded that of PBS by more than 3-folds.6 The usual synthetic method of PLA is through the ring-opening polymerization of lactide, but, it can also be synthesized via the polycondensation reaction of lactic acid. However, this method is not preferred due to the low molecular weight it yields due to water formation as a byproduct (see Scheme 5).[78]

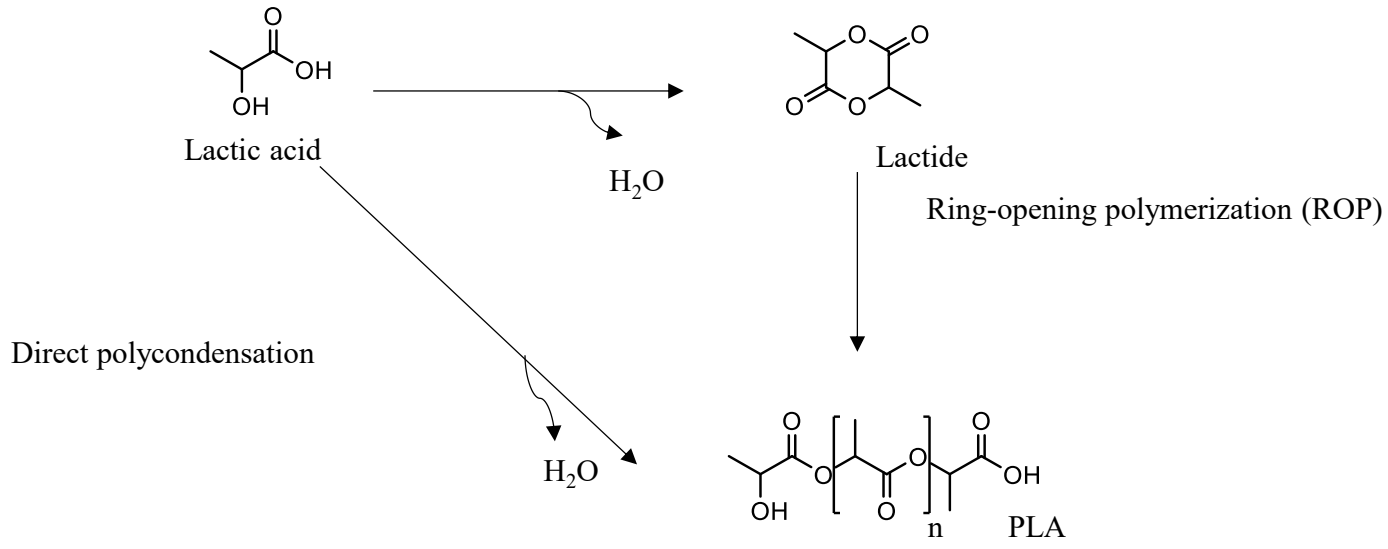

Scheme 5. Reaction pathways towards the synthesis of PLA.

Lactic acid, the starting monomer of PLA, can be obtained from corn and other sugars *via* fermentation,[79] which makes it very attractive as a replacement for polymers produced from fossil fuels. Lactic acid exists in the D- or L-form, and the ratio of these forms can influence the properties of the PLA produced.[72,80] The lipase catalyzed synthesis of PLA has been reported in the literature and has been proposed as an adequate alternative for harmful metal catalysts, especially when PLA is exploited in biomedical applications. However, the specificity of lipases towards L- and D-lactide is ambiguous.[78] In fact, the enzyme catalyzed ring-opening polymerization of D, L-lactide was previously reported by Mutsumara *et al.* yielding a PLA with a weight-average molecular weights (M_w) of 126,000 g.mol^{-1} in bulk after 7 days of incubation at 130 °C. However, the successful conversion was achieved with *Pseudomonas cepacia* lipase (PS) rather than Novozyme 435 (N435) that showed no conversion in this case.[81] On the other hand, Omay *et al*. obtained PLA having a M_n of 21,000 and 26,000 g.mol^{-1} *via* ROP of D,L-lactide in toluene at 80 °C using free CALB and N435, respectively.[82] In another study, the use of CALB did not produce any polymers when starting with L,L-lactide, but the use of D,D-lactide led to 80% conversion after a 2-days reaction at 50 °C in toluene with 15% w/w N435.[83] Similarly, Duchiron *et al.* showed N435 is selective towards D-lactide polymerization, while lipase from *Burkholderia cepacia* is selective towards L-lactide.[84] However, other research showed that N435

is not stereospecific to the ROP of lactides, and both D,D- and L,L-lactides can be produced with good yields.[85] These inconsistencies between results obtained from the enzymatic ROP of lactides have been proposed to originate from different factors such as water content, medium nature, lipase type, lipase form (immobilized or free form) and initiator used.[78,86] Another study showed that using O-carboxylic anhydride derivative of lactic acid rather than lactide resulted in an improved reaction efficiency in terms of molecular weight, and reaction yields of PLA when using both N435 and *Pseudomonas cepacia* lipase (PS) as catalyst for the ROP reaction (see Scheme 6).[87]

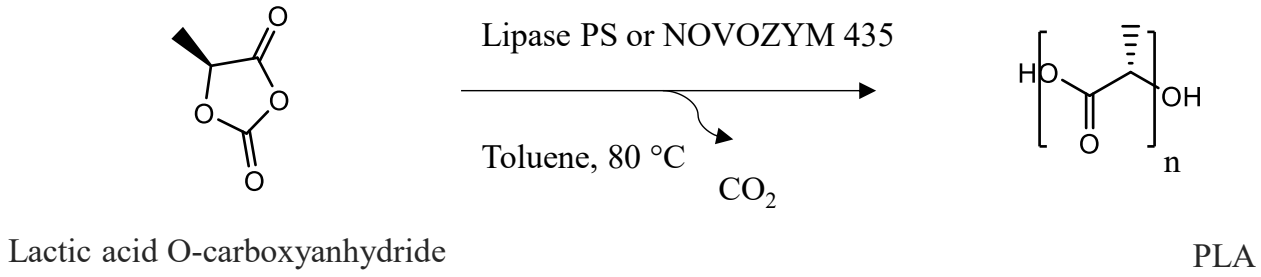

Scheme 6. Ring-opening polymerization of lactic acid O-carboxyanhydride towards the synthesis of PLA.

As mentioned before, the production of high molecular weight PLA *via* polycondensation of lactic acid is more challenging due to the small value of its equilibrium constant. A direct polycondensation method to produce high molecular weight PLA from lactic acid has been previously reported in a study by Chen *et al.* [88] where PLLA was synthesized using titanium (IV) butoxide as a catalyst. This was achieved within a period of 7 h, reaching a molecular weight of 130,000 g.mol^{-1}. However, the use of lipases in catalyzing the polycondensation reaction of lactic acid did not prove efficient in achieving high molecular weights and gave low molecular weight PLA (< 2,000 g.mol^{-1}) with various lipases (Porcine Pancreas Lipase, Lipozyme IM20, and Chirazyme), and at different conditions.[89]

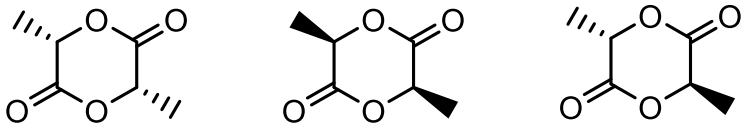

Scheme 7. Stereoisomers of lactide.[86]

1.4.3 Other aliphatic polyesters based on different diacids and diols

Aside from the well-known polyesters such as PBS and PLA, many biobased or potentially biobased diols and diacids were successfully used to synthesize different biobased poly(alkylene dicarboxylate)s *via* lipase catalyzed polycondensation.

In one study, aliphatic diacids and diols with varying chain lengths were reacted together in bulk and catalyzed by immobilized CALB yielding aliphatic polyesters with different molecular weights and yields. Although the difference in chain length of the diols and the diacids influenced the polymers' molecular weight and yield, no definitive relation was obtained between them. In fact, when sebacic acid was reacted with different diols, the M_n (determined *via* gel permeation chromatography -GPC) of the polymer produced increased from 1,700 g.mol^{-1} with ethane-1,2-diol up to 4,100 with octane-1,8-diol, suggesting a positive relation between chain length and M_n, however, this direct relation between chain length and D.P. was not always the case, where the use of decane-1,10-diol led to a decrease in M_n, while dodecane-1,12-diol did not yield any polymers.[90] Similarly in a study by Linko *et al.*[91] varying the aliphatic diol or diacid length in an enzyme-catalyzed polycondensation reaction showed a rather random relation between D.P. and the monomer length. In a much recent study by Pellis *et al.*[92] CALB was used to catalyze a solvent-free polycondensation reaction between different aliphatic diols varying in chain length between C4 and C8 and aliphatic diesters varying in chain length between C4 and C10. The maximum M_n was recorder for the reaction between octane-1,8-diol and dimethyl adipate reaching ~7,100 g.mol^{-1}. What was additionally observed in this study was that starting with methyl and ethyl diesters gave rise to polymers with higher molecular weights when compared to molecular weights achieved with butyl diesters, which according to the authors resulted from the differences in

boiling points of their respective byproducts, where butanol, the byproduct of butyl diester had the highest boiling point and was thus harder to evacuate from the system leading to lower conversion and polymer growth (see Figure 6).

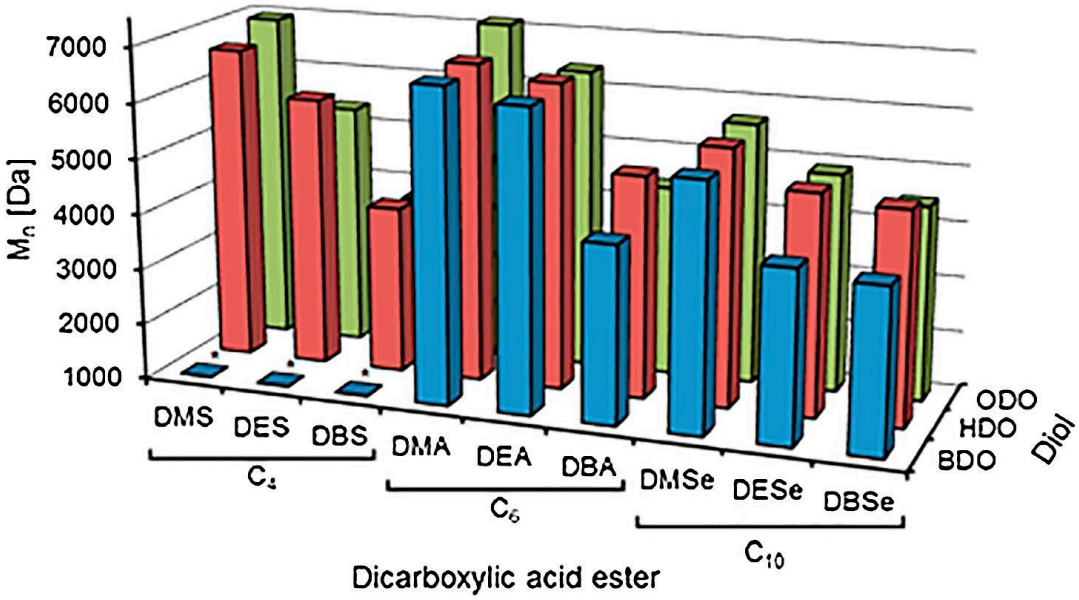

Figure 6. Number average molecular weights (M_n) calculated via GPC analysis of the crude polycondensation products using a polystyrene calibration curve (1 Da equivalent to 1 g.mol^{-1}). DMS=dimethyl succinate; DES=diethyl succinate; DBS=dibutyl succinate; DMA=dimethyl adipate; DEA=diethyl adipate; DBA=dibutyl adipate; DMSe=dimethyl sebacate; DESe=diethyl sebacate; DBSe=dibutyl sebacate; BDO=butane-1,4-diol; HDO=hexane-1,6-diol; ODO=octane-1,8-diol.[92]

In another study, bis(2,2,2-trifluoroethyl) sebacate was reacted with different aliphatic diols varying in their chain length between (C2-C6) catalyzed by *Mucor miehei* lipase in diphenyl ether.[93] The degree of polymerization (D.P.) increased as a function of increasing the diol length from 30 with ethane-1,2-diol up to 155 with pentane-1,5-diol, to slightly decrease thereafter with hexane-1,6-diol to reach a D.P. of ~135. This relation between polymer growth and diol length in enzymatic polymerization was previously reported by Morrow,[94] who showed similar increasing

trends in molecular weight as a function of increasing the diol length up to C6 as in the case of hexane-1,6-diol.

1.5 Enzymatic synthesis of semi-aromatic poly(alkylene dicarboxylate)s

Semi-aromatic poly(alkylene dicarboxylate)s are a subgroup of the polyester family usually synthesized by incorporating an aromatic monomer into the polyesterification reaction, such as the case of the reaction between terephthalic acid and ethylene glycol yielding poly(ethylene terephthalate) (PET). The use of aromatic structures in polymer synthesis have a positive effect on polymers' properties, as they increase the strength, thermal stability, and general performance of the produced polymer.[95] The following part will be mainly focused on two semi-aromatic poly(alkylene dicarboxylate)s subclasses being, polyesters based on terephthalic acid such as PET, and polyesters based on furan such as poly(ethylene furanoate) (PEF).

1.5.1 Polyesters based on 6-membered aromatic rings such as PET

PET is a the most commonly produced thermoplastic polyesters present in the market today, and is expected to reach a global market value of 68 billion U.S. dollars in 2023.[96,97] It is mainly produced in two grades as fiber-grade used in the production of cloth fibers with molecular weights ranging between 15,000 and 20,000 $g.mol^{-1}$ and bottle-grade PET, used in food and drink containers with molecular weights ranging between 24,000 and 36,000 $g.mol^{-1}$.[98,99] PET is the product of the polycondensation reaction between ethylene glycol and terephthalic acid or its diester. The attractiveness of PET does not only originate from its good properties and applications, but also from the fact that ethylene glycol can be sourced from biomass rather than fossil fuels. This attractiveness however is limited due to difficulties in producing terephthalic acid from biomass, rendering PET a partially biobased polymer that have been produced under different trademarks, such as PlantBottle™ with up to 30% biosourcing .[100–104]

The enzymatic catalysis for PET synthesis or PET-like polyesters has been challenging and scarcely reported in the literature.[97] Uyama *et al.*[105] showed that a reaction between terephthalic acid divinyl ester and ethylene glycol did not achieve a yield higher than 5%, with no detectable M_n. On the other hand, using longer chained diols such as butane-1,4-diol, hexane-1,6-diol, and decane-1,10-diol achieved moderate yields of 34, 72, and 58% and low M_n of 1,100, 2,300, and 2,000 g.mol^{-1} respectively. In another study, Linko *et al.*[91] showed that using N435 to catalyze the polycondensation reaction between terephthalic acid and different diols being butane-1,4-diol or hexane-1,6-diol did not yield any product with detectable molecular weight. However, when replacing terephthalic acid by isophthalic acid, the polycondensation reaction between the later and butane-1,4-diol yielded a M_w of 2,300 g.mol^{-1} at 60 °C, and 38,000 g.mol^{-1} with hexane-1,6-diol. This finding suggests that the type of diol as well as the relative position of the carboxylic functional groups on the benzene ring play a critical role and have a significant influence on polymer growth.

1.5.2 Polyesters based on furan-2,5-dicarboxylic acid (FDCA): a focus on poly(ethylene furanoate) (PEF)

The synthesis of polyesters based on FDCA is not so new. In fact, the synthesis of poly(ethylene furanoate) (PEF) was reported in a patent dating back to 1946.[106] Later on, in 1977, Moore and Kelly also derived polyesters based on FDCA.[107] However, it was not until recent years that research on FDCA based polymers started getting thrived.[108] As a matter of fact, polyesters based on FDCA are becoming more frequently regarded as biobased substitutions to polyesters based on terephthalic acid. This increased attention towards FDCA stems from two main reasons, first, the rigid structure of FDCA possess similar physical and chemical properties when compared to terephthalic acid (TPA). Secondly, and more importantly, FDCA can be produced from 5-(hydroxymethyl)furfural which is by turn derived from carbohydrates, rendering FDCA a biobased monomer. This is an attractive property when comparing it to TPA that is still facing limitations to be produced from biomass.[79,109–112]The general reaction of FDCA and ethane-1,2-diol is given in Scheme 8.

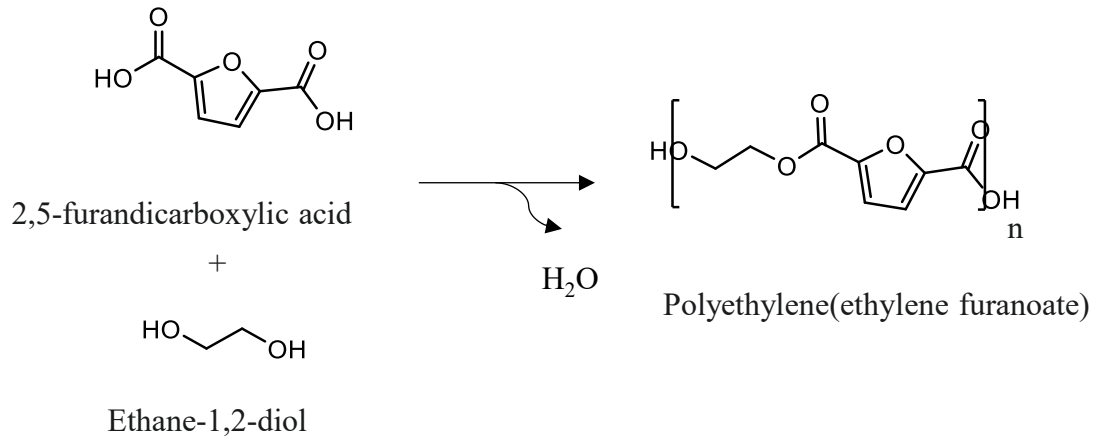

Scheme 8. General reaction pathway towards the synthesis of poly(ethylene furanoate).

In recent years, many works focusing on the synthesis and properties of FDCA based polyesters have been immerging.[113–115] Gandini *et al*.[116] described the synthesis and properties of PEF and other furan based polyesters synthesized with different diols *via* metallic catalysis.[117] Other research found that FDCA based polyesters have shown properties that are in many cases superior to those of TPA based, especially in terms of their gas barrier properties, where PEF had shown superior gas barrier properties when compared to PET: it decreased O_2 permeability 11 times more efficiently than PET, CO_2 permeability was decreased by nineteen times, and H_2O permeability by 2.1 times.[118–120]

The synthetic method used to produce furan-based polyesters usually takes place at temperatures around 200 °C and uses metal catalysts. These conditions result in undesired problems such as side reactions and coloration.[108,114,121] Enzymatic catalysis was proposed as a method to avoid the aforementioned issues in the production of furan-based polyesters. The enzymatic oligomerization reactions of FDCA, 5-hydroxymethylfuran-2-carboxylic acid (HMFA), and 2,5-bis-(hydroxymethyl)furan (BHMF), along with other aliphatic dicarboxylic acids and diols such as succinic acid, adipic acid, and butane-1,4-diol were previously reported using N435 as a catalyst at a temperature of 65 °C in toluene and *tert*-butanol solution. However, oligomers rather than polymers were produced, where the reaction between FDCA and butane-1,4-diol for 24 h led to products that did not exceed 2,100 $g.mol^{-1}$ in terms of weight average molecular weight (M_w).[122] Later on, N435 catalyzed transesterification reactions between dimethyl furan-2,5-dicarboxylate

(DMFDC) and different aliphatic diols with varied chain lengths was carried on in toluene and *tert*-butanol solution at 75 °C, yielding only linear oligomers with shorter diols (C2, C3), but also cyclic esters with longer diols (C4 to C12). Such findings show that the length and flexibility of diols play a major role in the formation of cyclic esters.[123] Jiang *et al.*[124] reported the enzymatic oligomerization between BHMF and different diacid ethyl esters with varying chain lengths (C2 to C10) at 80 °C in diphenyl ether using N435 (Scheme 9). However, unlike previous research, that found an increase in the molecular weight of polyesters as a function of increasing the chain length of the diacid esters;[125,126] this research found no significant change in molecular weight arising from variations in the chain length of the produced oligoesters. This was proposed to result from the formation of ethers resulting from the dehydration of BHMF molecules together.

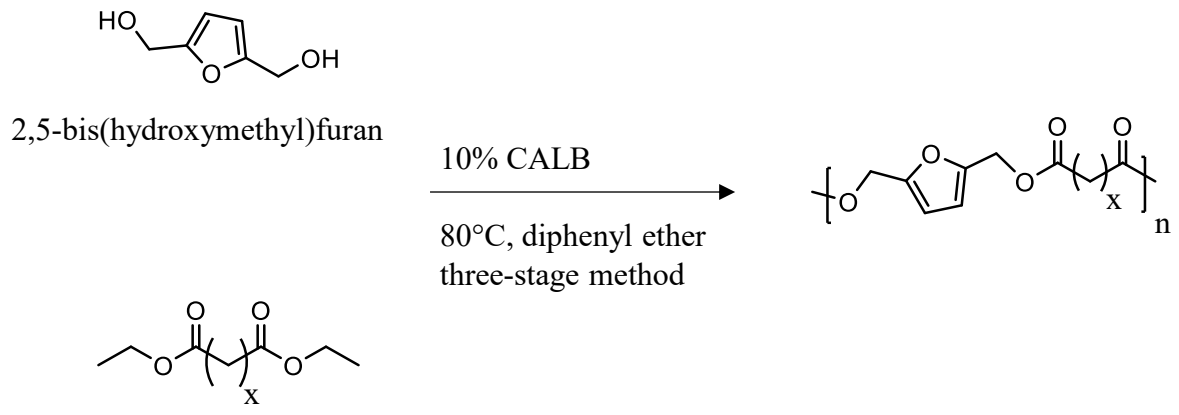

Scheme 9. CALB-catalyzed synthesis of 2,5-bis(hydroxymethyl)furan-based polyesters.[124]

1.6 Enzymatic synthesis of polyamides

Polyamides are considered as an important class of polymers possessing adequate properties such as high thermal resistance and improved mechanical properties that make them suitable for different applications ranging from textiles to electronics.[127] Although they could occur naturally

like in the case of proteins, there exists multiple synthetic pathways that can be utilized to yield polyamides, mainly through the polycondensation of diamines along with diacids or their esters, or aminoacids, or through the ROP of lactams. Polyamides can be classified based on their composition into aliphatic, semi-aromatic, and aromatic polymers.

Aliphatic polyamides such as Nylon 6 and Nylon 66 currently dominate the global market as the most produced polyamides. Nylon 6 also called polycaprolactam is usually synthesized *via* the ROP of caprolactam and used in electronics, automobiles, and textiles. Nylon 66 on the other hand or poly(hexamethylene adipamide) is synthesized through the polycondensation reaction of hexamethylenediamine and adipic acid, and is mainly used in applications demanding high mechanical properties and chemical resistance such as in pipes, airbags, etc..

Various enzymes such as proteases and lipases are capable of catalyzing the synthesis of polyamides. However, there are not many studies on the subject, mainly due to several limitations imposed by the nature of the monomers or the enzyme itself.[128] In fact, amines are not as nucleophilic as alcohols in lipase-catalyzed reactions, which imposes a negative effect on the reaction rate. Secondly, amines possess high melting points that can make them inadequate for enzymatic catalysis that require modest temperatures, and thirdly, amines are not very soluble in common organic solvents. All these reasons among others, have limited the success in synthesizing polyamides via enzymatic catalysis, especially when aiming at high molecular weights. For example, Ragupathy *et al.*[129] synthesized low M_n polyamides by reacting diethyl sebacate and 1,8-diaminooctane for 48 h in toluene at 60 °C, catalyzed by N435 (Scheme 10).

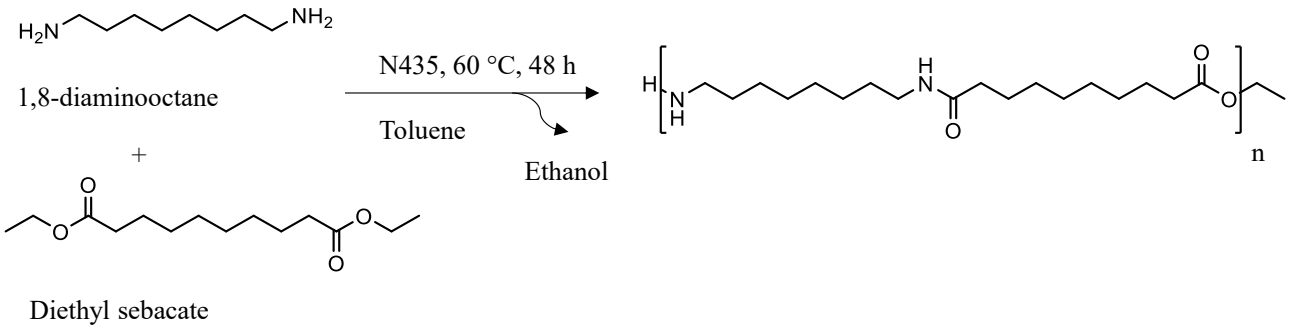

Scheme 10. Polycondensation reaction between 1,8-diaminooctane and diethyl sebacate.[129]

The resulting oligomer did not exceed an M_n of 2,000 g.mol^{-1} determine *via* calibrated GPC. In the same work, Ragupathy *et al.* performed a three-step polycondensation reaction in diphenyl ether between diethyl sebacate and 1,8-diaminooctane catalyzed by N435, starting at 60 °C and 667 mbar for 20 h, in the second step, the temperature was raised to 100 °C while the pressure was decreased to 133 mbar for 24 h, and finally a third step for 12 h with a gradual increase in temperature up to 150 °C. However, the polyamide synthesized from this method did not exceed an M_n of 4,650 g.mol^{-1}. In another example, Cheng *et al.*[130] performed a series of enzyme-catalyzed polycondensation reactions of diamines and diesters in bulk condition, the resulting polymers did not exceed a M_n of 8,600 g.mol^{-1}.

Another attempt on the synthesis of polyamides was performed by Fan *et al.*[131] First, amino acid-containing diesters were prepared by reacting different amino acid methyl ester hydrochlorides with sebacoyl chloride catalyzed by triethylamine. In the second step, the prepared amino acid-containing diesters were reacted with hexamethylene-1,6-diamine in the presence of different proteases. Results showed that α-Chymotrypsin gave the highest yield and intrinsic viscosity with the monomer prepared from L-phenylalanine. As for the solvents used, it was found that reactions in toluene gave the highest yields, and slightly lower yields were found with chloroform and dimethylformamide (DMF). Poulhès *et al*[132]. performed a 240-h enzyme-catalyzed polymerization reaction to produce polyamides. In a comparison between different starting monomers (see Scheme 11), it was found that ω-amino-α-alkoxy acetate (structure 1) showed 93% conversion within only 30 min in comparison to only 36 and 31% with structures 2 and 3. The superiority of structure 1 was attributed to the presence of an oxygen atom in the beta position, and achieved a M_n value of 3,880 g.mol^{-1} in bulk under 10 mbar of vacuum.

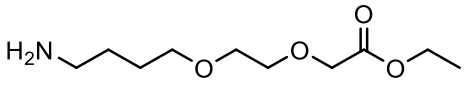

1

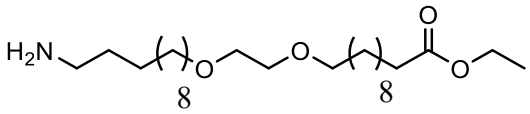

2

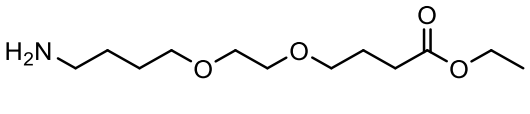

3

Scheme 11. Different amino-ester monomers.[132]

1.7 Enzymatic synthesis of poly(ester-*co*-amide)

Biobased poly(ester-*co*-amide)s have shown promising properties as biodegradable polymers for applications in the medical field. The presence of ester moieties enhance the biodegradable properties of such polymers, while the amide moieties contribute to their thermo-mechanical properties, which make it feasible to use poly(ester-*co*-amide)s in drug delivery, tissue engineering, among other applications.[133–135] However, the enzymatic catalysis towards the production of poly(ester-*co*-amide)s was not frequently pursued in the literature. In a research work by Raguphathy *et al.*[129], a combination of ROP and polycondensation was employed in an attempt to enhance polymer growth (see Scheme 12). The highest molecular weight achieved *via* this method was M_n = 17,550 g.mol^{-1} when pentadecanolide was reacted with equimolar ratios of 1,8-diaminooctane and 1,12-diaminododecane in toluene, followed by the addition of diethyl sebacate in the second step. However, reacting pentadecanolide with only one diamine led to a drop in M_n to 12,930 g.mol^{-1} when the diamine was 1,12-diaminododecane and to M_n = 2050 g.mol^{-1} with 1,8-diaminooctane.

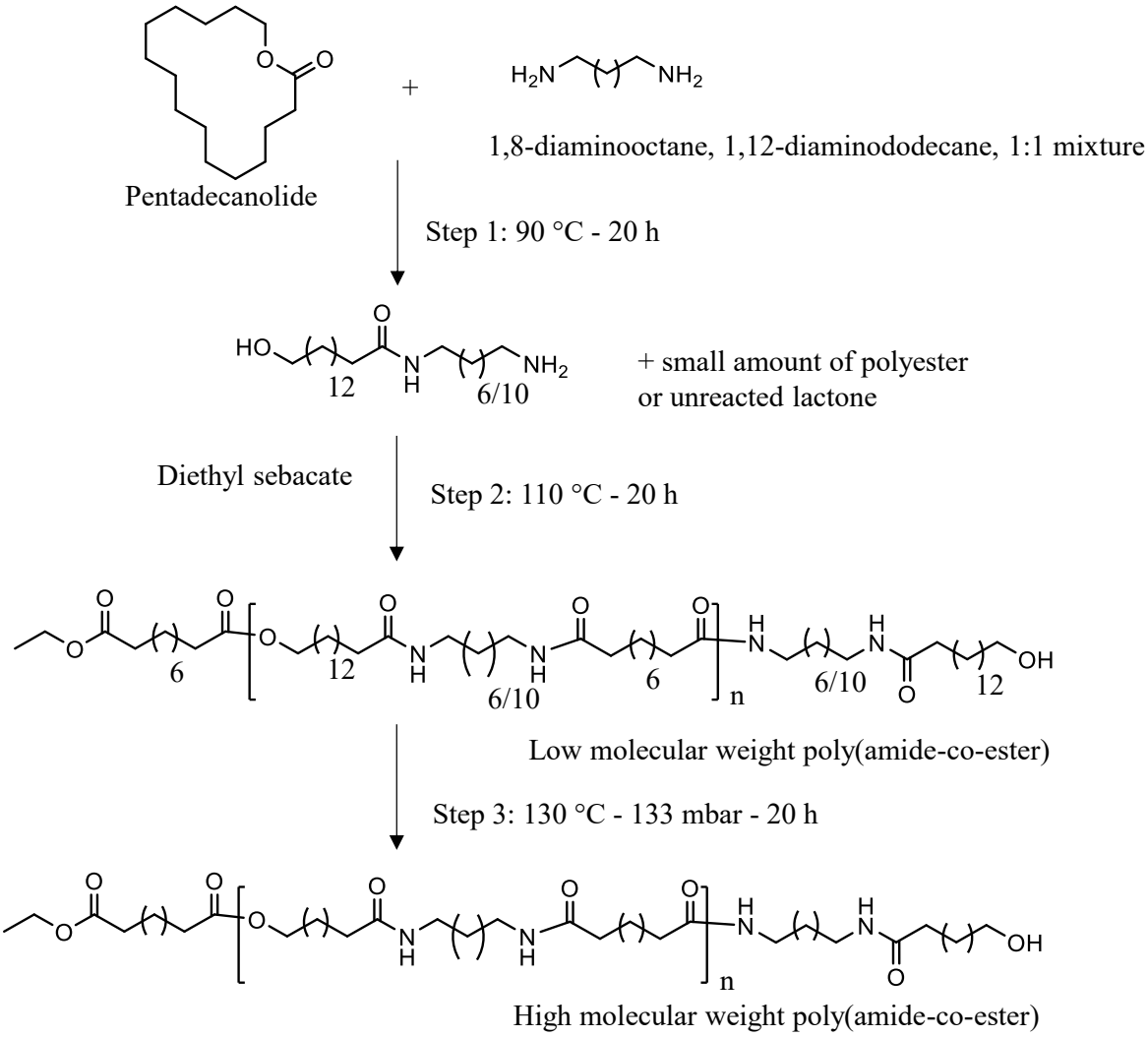

Scheme 12. Synthesis of poly(amide-*co*-ester)s by three step N-435- catalyzed polymerization.[129]

In another example, Sharma et al.[136] conducted a two-step polycondensation reaction in bulk, reacting different feed mole ratios of octane-1,8-diol, diethyl adipate, and α,ω-(diaminopropyl)polydimethylsiloxane using N435 as a catalyst at 10% w/w relative to the total monomers. The 70-h reaction conducted at 70 °C produced copolymers with M_n values ranging between 6,000 to 11,000 g.mol^{-1}. In this study, amide linkages were formed at a faster rate than ester links leading to a more block-oriented repeating sequence rather than a random copolymer. At high molar content of α,ω-(diaminopropyl)polydimethylsiloxane, the copolymer became more

glue-like with low melting points that apparently decreased as a function of increasing the siliconamide units in the polymer.

Furan-based poly(ester-*co*-amide)s were synthesized by reacting different chain-length diols, diamines and dimethyl-2,5-furandicarboxylate in toluene or in an ionic liquid. These lipase-catalyzed reactions led to polymers with higher molecular weights when longer diols and diamines were used, resulting in a polymer with an M_n of 13,000 g.mol^{-1} using dodecane-1,12-diol, 1,12-dodecanediamine, and dimethyl-2,5-furandicarboxylate as starting monomers as observed in Scheme 13.[137]

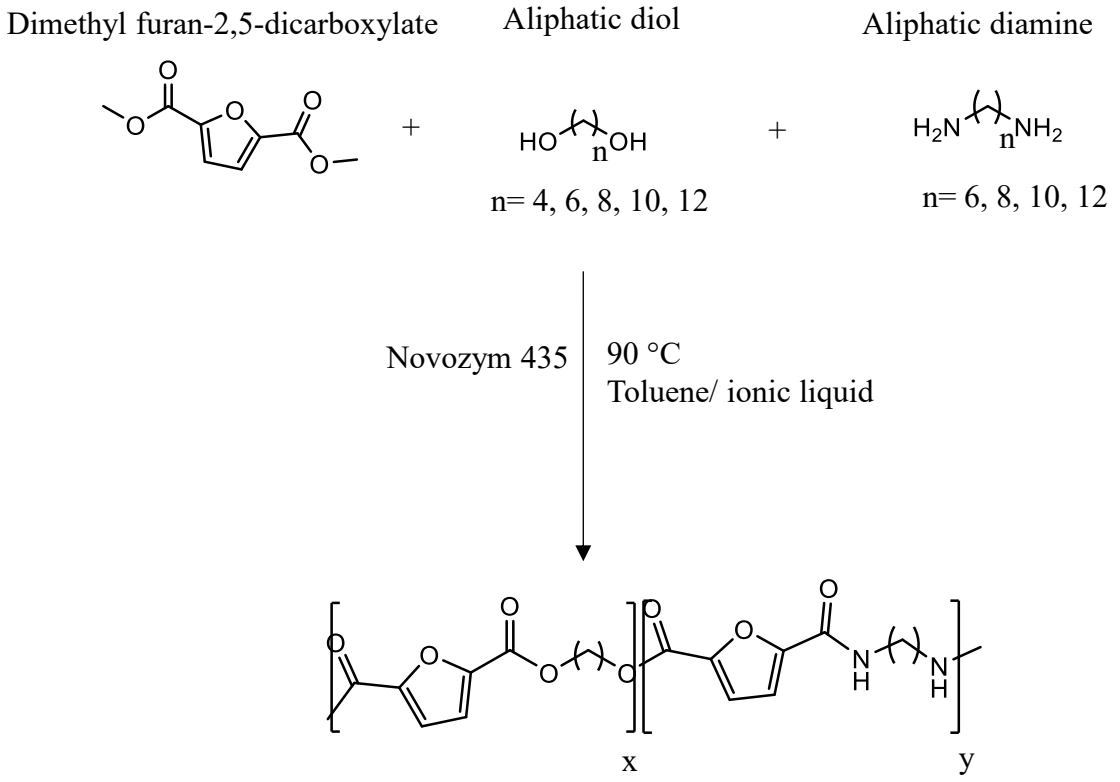

Scheme 13. Enzymatic synthesis of furan-based poly(ester amide)s

Stavila et al.[138] compared the catalytic efficiency of three enzymes being N435, icutinase, and CLEA cutinase, in three different polycondensation reactions in an attempt to produce polyamides. All reactions were performed in either toluene or diphenyl ether (see Scheme 14). The first reaction

was the reaction between p-xylylenediamine and diethyl sebacate, the second reaction was between dimethyl terephthalate and 1,8-diaminooctane, and the third reaction was between p-xylylenediamine and dimethyl terephthalate. For the first and second reactions, N435 was found to achieve higher conversion than the other enzymes, but both N435 and CLEA cutinase achieved polymers with similar degree of polymerization (D.P.). However, only short-chained amide products were produced in the third reaction between aromatic moieties, which was attributed to the bulkiness of aromatic groups and the formation of a conjugated system between the benzene ring and the ester which hindered the enzymatic catalysis.

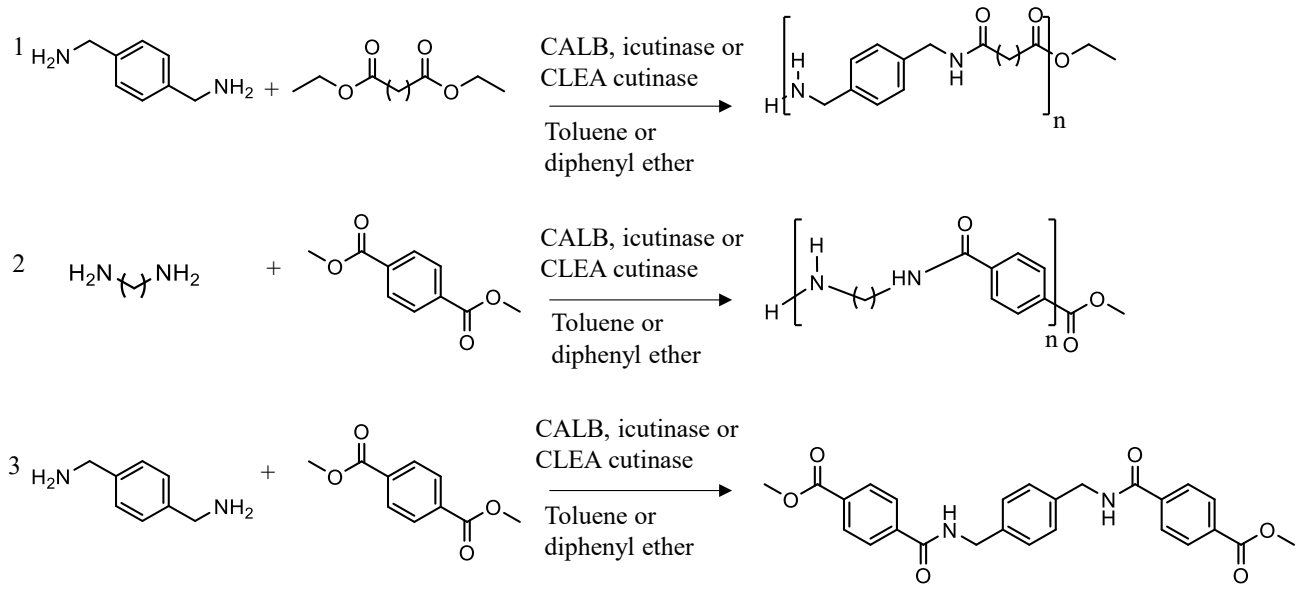

Scheme 14. Enzymatic polycondensation for the production of aromatic and semi-aromatic polyamides in toluene and diphenyl ether.[138]

In another recent work by Meimoun et al.[139] poly(ester-*co*-amide)s based on secondary diols were prepared for the first time *via* enzymatic catalysis. The secondary diols were first synthesized by diacylation of diamines followed by the reduction of ketones to alcohols. The produced diols were then reacted against different diesters and diacids. The polymers produced had a M_n ranging from 1,300 to 7,200 g.mol^{-1} and a dispersity <1.8. (Scheme 15).

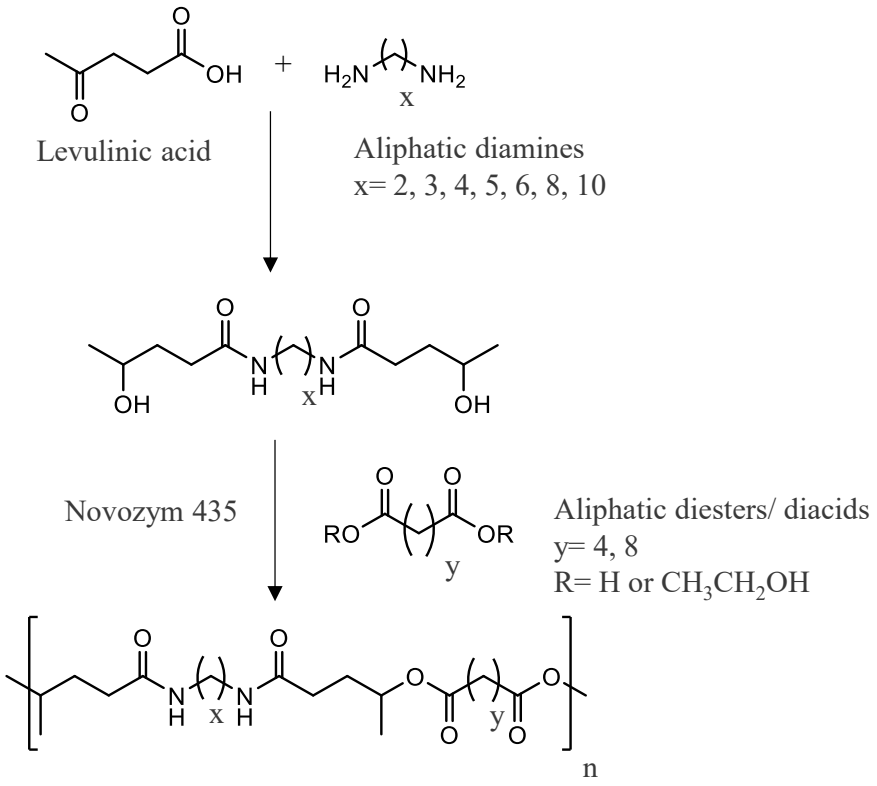

Scheme 15. Synthesis of poly(ester-*co*-amide)s by enzymatic polycondensation.[139]

1.8 Influence of reaction parameters and reaction media

Reaction parameters such as time and temperature are key factors that influence enzymatic polymerization. Choosing optimal values for these conditions is therefore critical to avoid the denaturation of enzymes and insure adequate polymerization. In a study by Azim *et al.*[75] the M_n of PBS was increased from 2,000 to 8,000 g.mol^{-1} by increasing the reaction temperature from 60 °C to 80 °C. Increasing the reaction time from 24 to 72 h did not impose any significant changes on M_n but was reported to decrease dispersity due to the diffusion of low molecular weight oligomers towards the catalyst, allowing for further transesterification reactions. Contrary to these findings, Mahapatro *et al.*[140] performed an enzyme-catalyzed reaction between octane-1,8-diol and adipic acid in bulk conditions. Varying the reaction temperature between 65 and 90 °C did not show any major influence on the M_n. Using the same monomers in the presence of N435, Yao *et al.*[140]

increased the M_n of the polymers from 4,300 to 7,600 g.mol^{-1} with increasing the temperature from 50 to 80 °C followed by a drop to 6,400 g.mol^{-1} after a further temperature increase up to a 90 °C. in terms of reaction time, the M_n increased significantly between 6 and 48 h at 70 °C, and continued without significant change upon extending the reaction for 72 h.

Besides reaction temperature and time, water content plays a very important role in enzymatic polymerization. Water molecules can combine to the surface of the enzyme (also known as essential water) and can also be incorporated within its structure and is known then as "structural water".[84,141,142] In a study by Engel *et al.*[143] the influence of water content was examined for its effect on the ROP of ε-caprolactone (ε-CL) in toluene. Results showed that increasing water content from 12 to 359 ppm led to an increase in M_n (determined *via* GPC) from 6,400 to 7,700 g.mol^{-1} followed by a decrease to 7,200 g.mol^{-1} after increasing the water content to 442 ppm. Though this change is not considered significant, the change in dispersity was more pronounced, decreasing from 4.1 to 2.3, to increase again to 2.5 when the water content increase from 12 to 359 and 442 ppm, respectively. In a similar reaction, the increase in water content in 1-Butyl-3-methylimidazolium hexafluorophosphate [BMIM][PF_6] from 0.02 to 0.09 w/w %, led to a drop in the M_n from 9,900 to 6,600 g.mol^{-1}.[78] In another study, freeze drying was used as a method to decrease essential water from N435 while preserving the content of structural water. The ROP of lactide showed an increment of up to 40% in M_n of polylactide.[84]

It is obvious from the literature that there are many factors influencing enzymatic polymerization. Evidently, throughout this chapter, factors such as reaction time, temperature, enzyme nature, monomer structure and different reaction pathways were mentioned. The following part focuses on the effect of the reaction media on enzyme-catalyzed polymerization reactions. In fact, enzymatic polymerization reactions were performed in either bulk or solution media, and special emphasis was put on determining an optimal media suitable for achieving high conversions and molecular weights.

Although the type of the solvent is considered to be a major factor in enzyme-catalyzed reactions, the relation between the properties of such solvents and the efficiency of the enzyme is not yet fully understood. In fact, different properties of such solvents such as their water solubility, polarity, dielectric constant and log *P* values (the logarithmic value of the partition coefficient) can play different roles with different degree of influence on the enzymatic activity.[144,145] In a study

by Azim *et al.*[75] the polycondensation reaction between diethyl succinate and butane-1,4-diol was performed in bulk and different solvents, being dodecane, diglyme, and diphenyl ether. A M_n of 10,000 g.mol^{-1} was achieved in diphenyl ether compared to only 2,500, 4,400 and 3,300 g.mol^{-1} in dodecane, diglyme, and bulk respectively (see Figure 7)

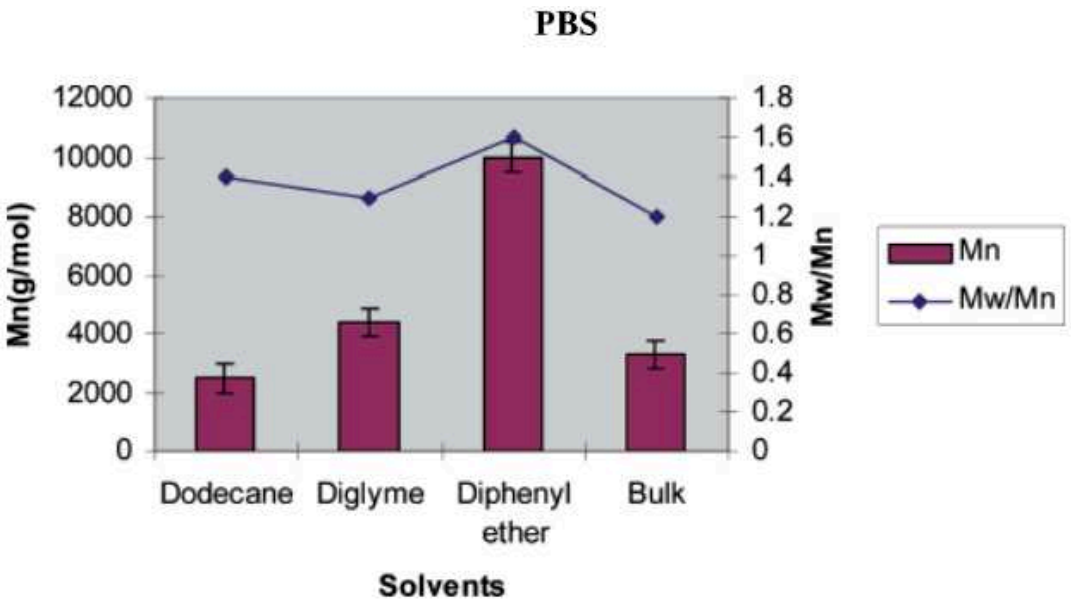

Figure 7. Effects of solvent on PBS molecular weight and dispersity.[75]

The superiority of diphenyl ether as a solvent suitable for enzymatic polymerization continued to reoccur in the literature for different polycondensation reactions, where it was found to yield the highest M_n in the synthesis of poly(butylene succinate-*co*-itaconate) catalyzed by N435.[146] In the same research, the effect of the concentration in diphenyl ether was also assessed, where M_n was found to increase as a function of increasing the amount of diphenyl ether up to 150 w/w % relative to the total of monomers, to decrease significantly thereafter upon further increase in the amount of diphenyl ether. In fact, the enhancement in M_n up to a certain point was assumed to result from the dilution effect that allowed for better heat and mass transfer within the system, however, dilution can also impact the reaction rate negatively, and make it harder to evacuate byproducts by vacuum application.[146]

In a study by Linko *et al.*[93] the polycondensation reaction between butane-1,4-diol and bis(2,2,2-trifluoroethyl) sebacate was found to yield the highest molecular weight when conducted in diphenyl ether with *Mucor miehei* lipase as a catalyst, reaching a M_w value of 27,700 g.mol^{-1}, in comparison to 17,400 g.mol^{-1} in veratrole, and not exceeding 9,000 g.mol^{-1} in hexyl ether, isoamyl ether, triethylene glycol dimethyl ether, and dodecane. These results came in agreement with previous documented results showing the superiority of diphenyl ether in the polycondensation reaction between butane-1,4-diol and sebacic acid.[147] Contrary to these results, in a study by Morrow.[94] veratrole was found to be superior to diphenyl ether in the polymerization reaction between butane-1,4-diol and bis(2,2,2-trifluoroethyl) glutarate catalyzed by porcine pancreatic lipase. This differences in results between the last-mentioned studies was attributed to the different enzymes used, which could further complicate the approach towards determining the key parameters affecting enzyme catalysis in different solvents.

The catalytic activity of N435 was assessed in several ROP reactions of ε-caprolactone (ε-CL) conducted in different organic solvents having different log *P* values ranging from -1.1 to 4.5.[148] Results showed that solvents with log *P* values ranging from −1.1 to 0.49 such as dioxane, acetonitrile and tetrahydrofuran showed low conversion not exceeding 30% in 4 h time, and low M_n values limited to a maximum of 5,200 g.mol^{-1}. On the other hand, solvents with log *P* values ranging from 1.9 to 4.5 such as isopropyl ether, toluene, butyl ether and isooctane showed higher conversions exceeding 60% and M_n values superior to 11,500 g.mol^{-1}. However, the increase in conversion and M_n was not in a direct relation with log *P*, as the maximum conversion and M_n of ~80% and 15,000 g.mol^{-1} respectively, were achieved in toluene with a log *P* value of 2.5, while reactions conducted in butyl ether that has a higher log *P* value of 2.9 showed lower percent conversion and M_n of ~60% and 12,900 g.mol^{-1}, respectively (see Figure 8). Such observation signifies that the catalytic activity of N435 is not solely governed by the partition coefficient value of its solvent. Other factors such as the polarity[149], water solubility[123], dielectric constant[145] and Hildebrand solubility parameter (δ)[144] can influence also influence the polymerization reaction.[26]

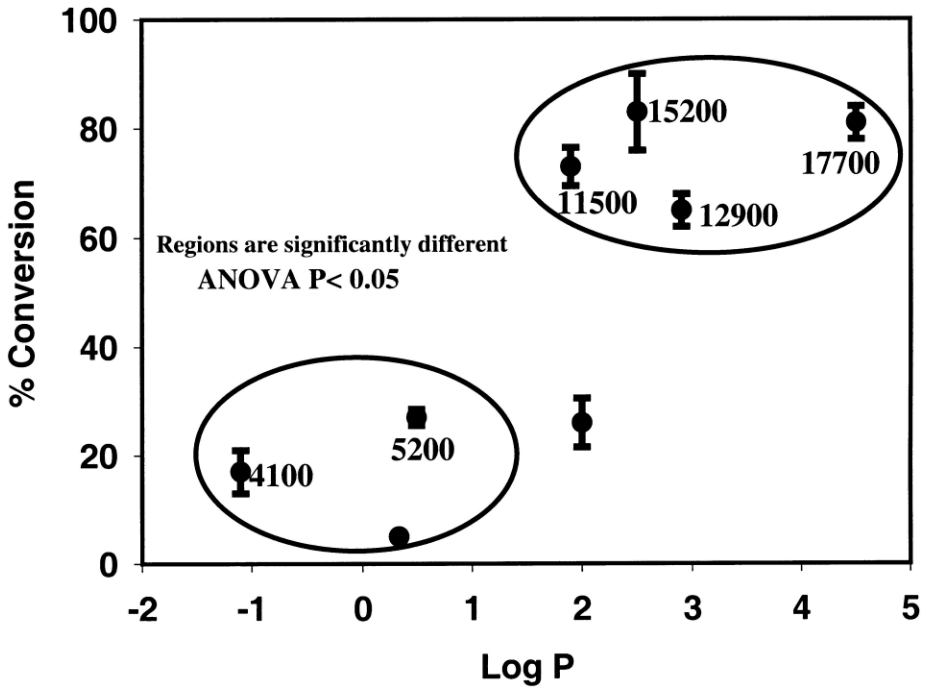

Figure 8. Relationship between the dielectric constant of the solvent and the conversion for N435 catalyzed polymerization of ε-CL at a monomer/solvent ratio 1:3 for 4 h at 70 °C.[148]

The effect of solvent type on the ROP of ε-caprolactone in the presence of N435 as a catalyst was also assessed by Yang *et al.*[150] where it was found that higher percent conversion and M_n were achieved with hydrophobic hydrocarbon solvents such as toluene, cyclohexane and n-hexane.

In addition to organic solvents, CALB was successfully used for the ROP of five different lactones in ionic liquids. Even at low enzyme loading equivalent to 1% w/w relative to the weight of lactone, a high degree of polymerization of 170 was obtained in the ROP of β-propiolactone conducted in 1-butyl-3-methylimidazolium bis(trifluoromethane)sulfonimide ([BMIM][Tf2N]). It was also observed that water immiscible ionic liquids were a better choice than water miscible ionic liquids leading to higher conversion.[151] The use of ionic liquids as solvents is due to the many advantages they possess that make them good candidates for enzymatic polymerization, such as their high vapor pressure, low viscosity, and thermal stability.[152]

Yoshizawa-Fujita *et* al. performed the ROP of L-lactide in bulk, toluene, and different ionic liquids. A maximum M_n of 54,600 g.mol^{-1} was achieved in 1-butyl-3-methylimidazolium chloride

(ionic liquid) ([BMIM][Cl]) at 110 °C after a 24-h reaction, but a superior yield was achieved in bulk (54.1%). However, not all tested ionic liquids gave high molecular weight PLA. In fact, the maximum M_n reached in 1-butyl-3-methylimidazolium hexafluorophosphate ([BMIM][PF6]) was limited to 3,900 g.mol^{-1} due to the low solubility of PLLA in it, leading to early precipitation.[153]

Besides ionic liquids, other medias such as supercritical CO_2 were tested for enzymatic polymerization.[154] In a study by García-Arrazola *et al.*[155] N435 was successfully used to catalyze the ring-opening polymerization of L-lactide using supercritical CO_2 at 65 °C yielding a weight average molecular weight (M_w) of 12,900 g.mol^{-1}, the activity of N435 was linked to their initial water content, where the molecular weight decreased with the increase in water content. In another study, enzyme was used in the ROP of poly(ε-caprolactone) in supercritical CO_2, reaching a M_n of 13,700 g.mol^{-1} and up to 90% w/w yield.[156]

1.9 Enzymatic polymerization in unconventional systems

Besides the nature of the reaction media, the use of unconventional systems such as microwave assisted polymerization and reactive extrusion were also reported for enzyme-catalyzed polymerization reactions. In a study by Pellis *et al.*[157] the authors compared between microwave and heat assisted polymerization of dimethyl succinate and butane-1,4-diol catalyzed by N435. It was observed that both conditions yielded polymers with similar conversion with no notable positive or negative effect imposed by microwave energy in comparison to a traditional oil bath. The only detected difference was detected in bulk condition as a decrease in conversion only when using high power microwave energy.

The use of enzymes in reactive extrusion (REx) have been mainly limited to depolymerization reactions in the literature.[158,159] However, the first enzyme-catalyzed polymerization reaction was reported by Spinella *et al.*[160] in the ROP of ω-pentadecalactone catalyzed by N435. In comparison to bulk and solution polymerization, the M_n achieved with REx reached 90,000 g.mol^{-1} in only 15 min, in comparison to 22,100 and 80,000 in bulk and in solution, respectively after a 72-h reaction. The superiority of reactive extrusion was attributed to its efficient mixing that allows for a much faster polymer growth. Later, using N435, Li *et al.*[161] performed a lipase-catalyzed ring-opening

copolymerization of ω-pentadecalactone and δ-valerolactone by reactive extrusion reaching within a 6-h time a M_n of 71,300 g.mol^{-1} at 90 °C. It was also observed that the degree of randomness of the copolymer is related to the time of the reaction, where the polymeric structure changed from a blocky arrangement after a 1-h reaction, to a random arrangement after 6 h. This change was due to the decrease in monomer concentration which results in increasing the prevalence of transesterification reactions.

In a similar study, Li *et al.*[162] performed a lipase-catalyzed copolymerization of ε-caprolactone and ω-pentadecalactone *via* REx. In this work, REx was found to lead to high monomer conversion and molecular weight, where after a 3 h reaction at 90 °C the conversion exceeded 98% and the M_n reached 51,300 g.mol^{-1} (see Figure 9) in comparison to only 25,600 g.mol^{-1} in bulk under similar conditions. In addition, increasing the time of the reaction was also found to increase the degree of randomness of the copolymer structure, which came in agreement to what was previously reported.[161]

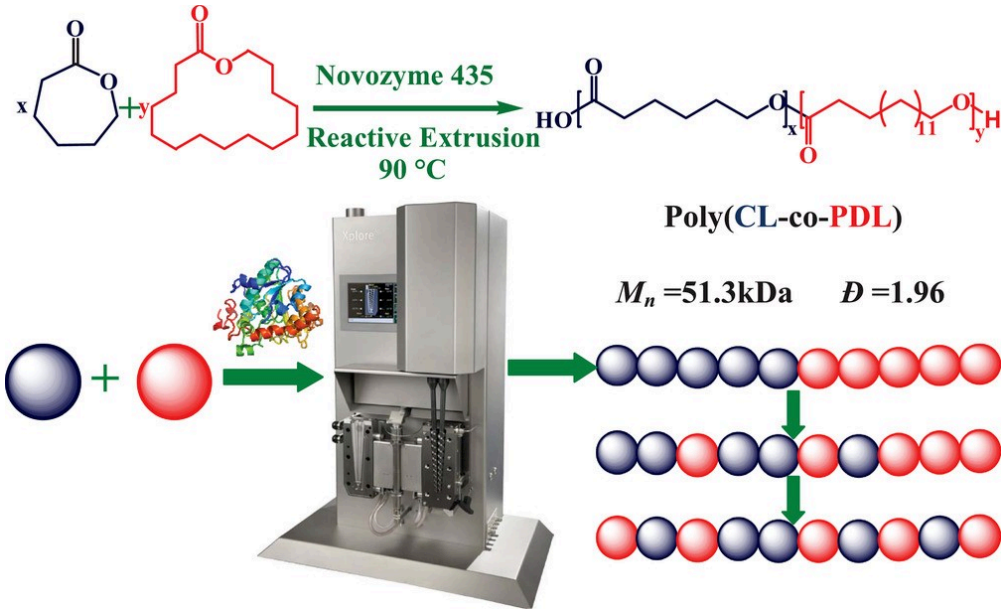

Figure 9. N435-catalyzed REX ring-opening copolymerization of ε-caprolactone (ε-CL) and ω-pentadecalactone (PDL) (51.3 kDa = 51,300 g.mol^{-1}).[162]

1.10 Conclusion

In this chapter, the various sources of biobased polymers were introduced, with a focus on their production methods and the challenges encountered. The use of biomass to produce biobased polymers can serve as an adequate approach to decrease the carbon footprint in polymer production and pave the way towards a greener chemistry. This chapter then focuses on the use of different classes of enzymes in polymerization reactions and focuses on the use of lipases such as Novozym 435 as appropriate catalysts for the synthesis of polyesters, polyamides, and poly(ester-co-amide). This chapter is then directed to establish proper relations between the efficiency of enzymatic catalysis and certain parameters such as temperature, solvent, and nature of the reactants. Although the literature provided important information regarding conditions and settings that enhance enzymatic catalysis and vice versa, it remained ambiguous to establish optimal conditions or a confident degree of control regarding the expected outcome of enzymatic catalysis. As such, in the next chapter, the influence of certain parameters and the extent of such influence will be assessed *via* a statistical approach that compares between in-solution and in-bulk enzyme-catalyzed polycondensation and test the effect of certain factors on the molecular weight. Such approach would provide us with a handy tool that offers higher degree of control in polymer synthesis.

1.11 References

(1) Gandini, A.; Lacerda, T. M. From Monomers to Polymers from Renewable Resources: Recent Advances. *Prog. Polym. Sci.* **2015**, *48*, 1–39. https://doi.org/10.1016/j.progpolymsci.2014.11.002.

(2) Jiang, Y.; Loos, K. Enzymatic Synthesis of Biobased Polyesters and Polyamides. *Polymers* **2016**, *8* (7), 243. https://doi.org/10.3390/polym8070243.

(3) Nakajima, H.; Dijkstra, P.; Loos, K. The Recent Developments in Biobased Polymers toward General and Engineering Applications: Polymers That Are Upgraded from Biodegradable Polymers, Analogous to Petroleum-Derived Polymers, and Newly Developed. *Polymers* **2017**, *9* (10), 523. https://doi.org/10.3390/polym9100523.

(4) Ramesh Kumar, S.; Shaiju, P.; O'Connor, K. E.; P, R. B. Bio-Based and Biodegradable Polymers - State-of-the-Art, Challenges and Emerging Trends. *Curr. Opin. Green Sustain. Chem.* **2020**, *21*, 75–81. https://doi.org/10.1016/j.cogsc.2019.12.005.

(5) Shen, L.; Haufe, J.; Patel, M. K. *Group Science, Technology and Society (STS) Copernicus Institute for Sustainable Development and Innovation Utrecht University*; p 243.

(6) Bioplastics market data https://www.european-bioplastics.org/market/ (accessed 2020 -04 -03).

(7) Bio-based economy - Services of the nova-Institut GmbH http://bio-based.eu/ (accessed 2020 -04 -03).

(8) Ren, Y.; Yu, M.; Wu, C.; Wang, Q.; Gao, M.; Huang, Q.; Liu, Y. A Comprehensive Review on Food Waste Anaerobic Digestion: Research Updates and Tendencies. *Bioresour. Technol.* **2018**, *247*, 1069–1076. https://doi.org/10.1016/j.biortech.2017.09.109.

(9) Attard, T. M.; Clark, J. H.; McElroy, C. R. Recent Developments in Key Biorefinery Areas. *Curr. Opin. Green Sustain. Chem.* **2020**, *21*, 64–74. https://doi.org/10.1016/j.cogsc.2019.12.002.

(10) Paul, S.; Dutta, A. Challenges and Opportunities of Lignocellulosic Biomass for Anaerobic Digestion. *Resour. Conserv. Recycl.* **2018**, *130*, 164–174. https://doi.org/10.1016/j.resconrec.2017.12.005.

(11) Kohli, K.; Prajapati, R.; Sharma, B. K. Bio-Based Chemicals from Renewable Biomass for Integrated Biorefineries. *Energies* **2019**, *12* (2), 233. https://doi.org/10.3390/en12020233.

(12) Barkia, I.; Saari, N.; Manning, S. R. Microalgae for High-Value Products Towards Human Health and Nutrition. *Mar. Drugs* **2019**, *17* (5). https://doi.org/10.3390/md17050304.

(13) Becker, E. W. Micro-Algae as a Source of Protein. *Biotechnol. Adv.* **2007**, *25* (2), 207–210. https://doi.org/10.1016/j.biotechadv.2006.11.002.

(14) Chisti, Y. Biodiesel from Microalgae. *Biotechnol. Adv.* **2007**, *25* (3), 294–306. https://doi.org/10.1016/j.biotechadv.2007.02.001.

(15) Lauritano, C.; Andersen, J. H.; Hansen, E.; Albrigtsen, M.; Escalera, L.; Esposito, F.; Helland, K.; Hanssen, K. Ø.; Romano, G.; Ianora, A. Bioactivity Screening of Microalgae for Antioxidant, Anti-Inflammatory, Anticancer, Anti-Diabetes, and Antibacterial Activities. *Front. Mar. Sci.* **2016**, *3*. https://doi.org/10.3389/fmars.2016.00068.

(16) Lee, J.-B.; Hayashi, K.; Hirata, M.; Kuroda, E.; Suzuki, E.; Kubo, Y.; Hayashi, T. Antiviral Sulfated Polysaccharide from Navicula Directa, a Diatom Collected from Deep-Sea Water in Toyama Bay. *Biol. Pharm. Bull.* **2006**, *29* (10), 2135–2139. https://doi.org/10.1248/bpb.29.2135.

(17) Hirayama, S.; Ueda, R. Production of Optically Pure D-Lactic Acid by Nannochlorum Sp. 26A4. *Appl. Biochem. Biotechnol.* **2004**, *119* (1), 71–78. https://doi.org/10.1385/abab:119:1:71.

(18) Nguyen, C. M.; Kim, J.-S.; Hwang, H. J.; Park, M. S.; Choi, G. J.; Choi, Y. H.; Jang, K. S.; Kim, J.-C. Production of L-Lactic Acid from a Green Microalga, Hydrodictyon Reticulum, by Lactobacillus Paracasei LA104 Isolated from the Traditional Korean Food, Makgeolli. *Bioresour. Technol.* **2012**, *110*, 552–559. https://doi.org/10.1016/j.biortech.2012.01.079.

(19) Kim, S. H.; Shin, C.; Min, S. K.; Jung, S.-M.; Shin, H. S. In Vitro Evaluation of the Effects of Electrospun PCL Nanofiber Mats Containing the Microalgae Spirulina (Arthrospira) Extract on Primary Astrocytes. *Colloids Surf. B Biointerfaces* **2012**, *90*, 113–118. https://doi.org/10.1016/j.colsurfb.2011.10.004.

(20) Roja, K.; Ruben Sudhakar, D.; Anto, S.; Mathimani, T. Extraction and Characterization of Polyhydroxyalkanoates from Marine Green Alga and Cyanobacteria. *Biocatal. Agric. Biotechnol.* **2019**, *22*, 101358. https://doi.org/10.1016/j.bcab.2019.101358.

(21) Zhang, C.; Show, P.-L.; Ho, S.-H. Progress and Perspective on Algal Plastics – A Critical Review. *Bioresour. Technol.* **2019**, *289*, 121700. https://doi.org/10.1016/j.biortech.2019.121700.

(22) Benedetti, M.; Vecchi, V.; Barera, S.; Dall'Osto, L. Biomass from Microalgae: The Potential of Domestication towards Sustainable Biofactories. *Microb. Cell Factories* **2018**, *17* (1), 173. https://doi.org/10.1186/s12934-018-1019-3.

(23) Blanco, A.; Blanco, G. Chapter 8 - Enzymes. In *Medical Biochemistry*; Blanco, A., Blanco, G., Eds.; Academic Press, 2017; pp 153–175. https://doi.org/10.1016/B978-0-12-803550-4.00008-2.

(24) Cooper, G. M. The Central Role of Enzymes as Biological Catalysts. In *The Cell: A Molecular Approach. 2nd edition*; Sinauer Associates, 2000.

(25) Fischer, E. Einfluss Der Configuration Auf Die Wirkung Der Enzyme. *Berichte Dtsch. Chem. Ges.* **1894**, *27* (3), 2985–2993. https://doi.org/10.1002/cber.18940270364.

(26) Douka, A.; Vouyiouka, S.; Papaspyridi, L.-M.; Papaspyrides, C. D. A Review on Enzymatic Polymerization to Produce Polycondensation Polymers: The Case of Aliphatic Polyesters, Polyamides and Polyesteramides. *Prog. Polym. Sci.* **2018**, *79*, 1–25. https://doi.org/10.1016/j.progpolymsci.2017.10.001.

(27) Parravano, G. Chain Reactions Induced by Enzymic Systems. *J. Am. Chem. Soc.* **1951**, *73* (1), 183–184. https://doi.org/10.1021/ja01145a063.

(28) Kobayashi, S.; Uyama, H.; Kimura, S. Enzymatic Polymerization. *Chem. Rev.* **2001**, *101* (12), 3793–3818. https://doi.org/10.1021/cr9901211.

(29) Gross, R.; Kalra, B.; Kumar, A. Polyester and Polycarbonate Synthesis by in Vitro Enzyme Catalysis. *Appl. Microbiol. Biotechnol.* **2001**, *55* (6), 655–660. https://doi.org/10.1007/s002530100617.

(30) Gross, R. A.; Kumar, A.; Kalra, B. Polymer Synthesis by in Vitro Enzyme Catalysis. *Chem. Rev.* **2001**, *101* (7), 2097–2124. https://doi.org/10.1021/cr0002590.

(31) Varma, I. K.; Albertsson, A.-C.; Rajkhowa, R.; Srivastava, R. K. Enzyme Catalyzed Synthesis of Polyesters. *Prog. Polym. Sci.* **2005**, *30* (10), 949–981. https://doi.org/10.1016/j.progpolymsci.2005.06.010.

(32) Yang, Y.; Zhang, J.; Wu, D.; Xing, Z.; Zhou, Y.; Shi, W.; Li, Q. Chemoenzymatic Synthesis of Polymeric Materials Using Lipases as Catalysts: A Review. *Biotechnol. Adv.* **2014**, *32* (3), 642–651. https://doi.org/10.1016/j.biotechadv.2014.04.011.

(33) Desentis-Mendoza, R. M.; Hernández-Sánchez, H.; Moreno, A.; Rojas del C., E.; Chel-Guerrero, L.; Tamariz, J.; Jaramillo-Flores, M. E. Enzymatic Polymerization of Phenolic Compounds Using Laccase and Tyrosinase from Ustilago Maydis. *Biomacromolecules* **2006**, *7* (6), 1845–1854. https://doi.org/10.1021/bm060159p.

(34) Ćirić-Marjanović, G.; Milojević-Rakić, M.; Janošević-Ležaić, A.; Luginbühl, S.; Walde, P. Enzymatic Oligomerization and Polymerization of Arylamines: State of the Art and Perspectives. *Chem. Pap.* **2017**, *71* (2), 199–242. https://doi.org/10.1007/s11696-016-0094-3.

(35) Zdarta, J.; Meyer, A. S.; Jesionowski, T.; Pinelo, M. Developments in Support Materials for Immobilization of Oxidoreductases: A Comprehensive Review. *Adv. Colloid Interface Sci.* **2018**, *258*, 1–20. https://doi.org/10.1016/j.cis.2018.07.004.

(36) Stubbe, J.; Tian, J.; He, A.; Sinskey, A. J.; Lawrence, A. G.; Liu, P. NONTEMPLATE-DEPENDENT POLYMERIZATION PROCESSES: Polyhydroxyalkanoate Synthases as a Paradigm. *Annu. Rev. Biochem.* **2005**, *74* (1), 433–480. https://doi.org/10.1146/annurev.biochem.74.082803.133013.

(37) Gerngross, T. U.; Martin, D. P. Enzyme-Catalyzed Synthesis of Poly[(R)-(-)-3-Hydroxybutyrate]: Formation of Macroscopic Granules in Vitro. *Proc. Natl. Acad. Sci.* **1995**, *92* (14), 6279–6283. https://doi.org/10.1073/pnas.92.14.6279.

(38) DeJong, G. a. H.; Koppelman, S. J. Transglutaminase Catalyzed Reactions: Impact on Food Applications. *J. Food Sci.* **2002**, *67* (8), 2798–2806. https://doi.org/10.1111/j.1365-2621.2002.tb08819.x.

(39) Jaros, D.; Partschefeld, C.; Henle, T.; Rohm, H. Transglutaminase in Dairy Products: Chemistry, Physics, Applications. *J. Texture Stud.* **2006**, *37* (2), 113–155. https://doi.org/10.1111/j.1745-4603.2006.00042.x.

(40) Cortez, J.; Bonner, P. L. R.; Griffin, M. Transglutaminase Treatment of Wool Fabrics Leads to Resistance to Detergent Damage. *J. Biotechnol.* **2005**, *116* (4), 379–386. https://doi.org/10.1016/j.jbiotec.2004.12.007.

(41) Garcia, Y.; Wilkins, B.; Collighan, R. J.; Griffin, M.; Pandit, A. Towards Development of a Dermal Rudiment for Enhanced Wound Healing Response. *Biomaterials* **2008**, *29* (7), 857–868. https://doi.org/10.1016/j.biomaterials.2007.10.053.

(42) van der Vlist, J.; Loos, K. Transferases in Polymer Chemistry. In *Enzymatic Polymerisation*; Palmans, A. R. A., Heise, A., Eds.; Advances in Polymer Science; Springer: Berlin, Heidelberg, 2011; pp 21–54. https://doi.org/10.1007/12_2010_73.

(43) Homann, A.; Seibel, J. Towards Tailor-Made Oligosaccharides—Chemo-Enzymatic Approaches by Enzyme and Substrate Engineering. *Appl. Microbiol. Biotechnol.* **2009**, *83* (2), 209–216. https://doi.org/10.1007/s00253-009-1989-5.

(44) Gimenez-Dejoz, J.; Tsuchiya, K.; Numata, K. Insights into the Stereospecificity in Papain-Mediated Chemoenzymatic Polymerization from Quantum Mechanics/Molecular Mechanics Simulations. *ACS Chem. Biol.* **2019**, *14* (6), 1280–1292. https://doi.org/10.1021/acschembio.9b00259.

(45) Tsuchiya, K.; Numata, K. Chemoenzymatic Synthesis of Polypeptides for Use as Functional and Structural Materials. *Macromol. Biosci.* **2017**, *17* (11), 1700177. https://doi.org/10.1002/mabi.201700177.

(46) Yazawa, K.; Gimenez-Dejoz, J.; Masunaga, H.; Hikima, T.; Numata, K. Chemoenzymatic Synthesis of a Peptide Containing Nylon Monomer Units for Thermally Processable Peptide Material Application. *Polym. Chem.* **2017**, *8* (29), 4172–4176. https://doi.org/10.1039/C7PY00770A.

(47) Yazawa, K.; Numata, K. Papain-Catalyzed Synthesis of Polyglutamate Containing a Nylon Monomer Unit. *Polymers* **2016**, *8* (5), 194. https://doi.org/10.3390/polym8050194.

(48) Tsuchiya, K.; Numata, K. Chemoenzymatic Synthesis of Polypeptides Containing the Unnatural Amino Acid 2-Aminoisobutyric Acid. *Chem. Commun.* **2017**, *53* (53), 7318–7321. https://doi.org/10.1039/C7CC03095A.

(49) Stavila, E.; Arsyi, R. Z.; Petrovic, D. M.; Loos, K. Fusarium Solani Pisi Cutinase-Catalyzed Synthesis of Polyamides. *Eur. Polym. J.* **2013**, *49* (4), 834–842. https://doi.org/10.1016/j.eurpolymj.2012.12.010.

(50) Feder, D.; Gross, R. A. Exploring Chain Length Selectivity in HIC-Catalyzed Polycondensation Reactions. *Biomacromolecules* **2010**, *11* (3), 690–697. https://doi.org/10.1021/bm901272r.

(51) Pellis, A.; Ferrario, V.; Cespugli, M.; Corici, L.; Guarneri, A.; Zartl, B.; Acero, E. H.; Ebert, C.; Guebitz, G. M.; Gardossi, L. Fully Renewable Polyesters *via* Polycondensation Catalyzed by Thermobifida Cellulosilytica Cutinase 1: An Integrated Approach. *Green Chem.* **2017**, *19* (2), 490–502. https://doi.org/10.1039/C6GC02142E.

(52) Hunsen, M.; Azim, A.; Mang, H.; Wallner, S. R.; Ronkvist, A.; Xie, W.; Gross, R. A. A Cutinase with Polyester Synthesis Activity. *Macromolecules* **2007**, *40* (2), 148–150. https://doi.org/10.1021/ma062095g.

(53) Gross, R. A.; Ganesh, M.; Lu, W. Enzyme-Catalysis Breathes New Life into Polyester Condensation Polymerizations. *Trends Biotechnol.* **2010**, *28* (8), 435–443. https://doi.org/10.1016/j.tibtech.2010.05.004.

(54) Anobom, C. D.; Pinheiro, A. S.; De-Andrade, R. A.; Aguieiras, E. C. G.; Andrade, G. C.; Moura, M. V.; Almeida, R. V.; Freire, D. M. From Structure to Catalysis: Recent Developments in the Biotechnological Applications of Lipases. *BioMed Res. Int.* **2014**, *2014*, 684506. https://doi.org/10.1155/2014/684506.

(55) Schmid, R. D.; Verger, R. Lipases: Interfacial Enzymes with Attractive Applications. *Angew. Chem. Int. Ed.* **1998**, *37* (12), 1608–1633. https://doi.org/10.1002/(SICI)1521-3773(19980703)37:12<1608::AID-ANIE1608>3.0.CO;2-V.

(56) Brzozowski, A. M.; Derewenda, U.; Derewenda, Z. S.; Dodson, G. G.; Lawson, D. M.; Turkenburg, J. P.; Bjorkling, F.; Huge-Jensen, B.; Patkar, S. A.; Thim, L. A Model for Interfacial

Activation in Lipases from the Structure of a Fungal Lipase-Inhibitor Complex. *Nature* **1991**, *351* (6326), 491–494. https://doi.org/10.1038/351491a0.

(57) Grochulski, P.; Li, Y.; Schrag, J. D.; Bouthillier, F.; Smith, P.; Harrison, D.; Rubin, B.; Cygler, M. Insights into Interfacial Activation from an Open Structure of Candida Rugosa Lipase. *J. Biol. Chem.* **1993**, *268* (17), 12843–12847.

(58) Ortiz, C.; Ferreira, M. L.; Barbosa, O.; Santos, J. C. S. dos; Rodrigues, R. C.; Berenguer-Murcia, Á.; Briand, L. E.; Fernandez-Lafuente, R. Novozym 435: The "Perfect" Lipase Immobilized Biocatalyst? *Catal. Sci. Technol.* **2019**, *9* (10), 2380–2420. https://doi.org/10.1039/C9CY00415G.

(59) Strzelczyk, P.; Bujacz, G. D.; Kiełbasiński, P.; Błaszczyk, J. Crystal and Molecular Structure of Hexagonal Form of Lipase B from Candida Antarctica. *Acta Biochim. Pol.* **2016**, *63* (1), 103–109. https://doi.org/10.18388/abp.2015_1065.

(60) Li, C.; Tan, T.; Zhang, H.; Feng, W. Analysis of the Conformational Stability and Activity of Candida Antarctica Lipase B in Organic Solvents INSIGHT FROM MOLECULAR DYNAMICS AND QUANTUM MECHANICS/SIMULATIONS. *J. Biol. Chem.* **2010**, *285* (37), 28434–28441. https://doi.org/10.1074/jbc.M110.136200.

(61) Veld, M. A. J.; Palmans, A. R. A. Hydrolases Part I: Enzyme Mechanism, Selectivity and Control in the Synthesis of Well-Defined Polymers. In *Enzymatic Polymerisation*; Palmans, A. R. A., Heise, A., Eds.; Advances in Polymer Science; Springer: Berlin, Heidelberg, 2011; pp 55–78. https://doi.org/10.1007/12_2010_86.

(62) *Industrial Enzymes: Structure, Function and Applications*; Polaina, J., MacCabe, A. P., Eds.; Springer Netherlands, 2007. https://doi.org/10.1007/1-4020-5377-0.

(63) Kobayashi, S.; Makino, A. Enzymatic Polymer Synthesis: An Opportunity for Green Polymer Chemistry. *Chem. Rev.* **2009**, *109* (11), 5288–5353. https://doi.org/10.1021/cr900165z.

(64) Pellis, A.; Guarneri, A.; Brandauer, M.; Acero, E. H.; Peerlings, H.; Gardossi, L.; Guebitz, G. M. Exploring Mild Enzymatic Sustainable Routes for the Synthesis of Bio-Degradable Aromatic-Aliphatic Oligoesters. *Biotechnol. J.* **2016**, *11* (5), 642–647. https://doi.org/10.1002/biot.201500544.

(65) Singh, R. K.; Tiwari, M. K.; Singh, R.; Lee, J.-K. From Protein Engineering to Immobilization: Promising Strategies for the Upgrade of Industrial Enzymes. *Int. J. Mol. Sci.* **2013**, *14* (1), 1232–1277. https://doi.org/10.3390/ijms14011232.

(66) Bernal, C.; Rodríguez, K.; Martínez, R. Integrating Enzyme Immobilization and Protein Engineering: An Alternative Path for the Development of Novel and Improved Industrial Biocatalysts. *Biotechnol. Adv.* **2018**, *36* (5), 1470–1480. https://doi.org/10.1016/j.biotechadv.2018.06.002.

(67) Mateo, C.; Palomo, J. M.; Fernandez-Lorente, G.; Guisan, J. M.; Fernandez-Lafuente, R. Improvement of Enzyme Activity, Stability and Selectivity *via* Immobilization Techniques. *Enzyme Microb. Technol.* **2007**, *40* (6), 1451–1463. https://doi.org/10.1016/j.enzmictec.2007.01.018.

(68) Silva, C.; Martins, M.; Jing, S.; Fu, J.; Cavaco-Paulo, A. Practical Insights on Enzyme Stabilization. *Crit. Rev. Biotechnol.* **2018**, *38* (3), 335–350. https://doi.org/10.1080/07388551.2017.1355294.

(69) Sheldon, R. A.; Pelt, S. van. Enzyme Immobilisation in Biocatalysis: Why, What and How. *Chem. Soc. Rev.* **2013**, *42* (15), 6223–6235. https://doi.org/10.1039/C3CS60075K.

(70) Eş, I.; Vieira, J. D. G.; Amaral, A. C. Principles, Techniques, and Applications of Biocatalyst Immobilization for Industrial Application. *Appl. Microbiol. Biotechnol.* **2015**, *99* (5), 2065–2082. https://doi.org/10.1007/s00253-015-6390-y.

(71) Papaspyrides, C. D.; Vouyiouka, S.; Georgousopoulou, I.-N.; Marinkovic, S.; Estrine, B.; Joly, C.; Dole, P. Feasibility of Solid-State Postpolymerization on Fossil- and Bio-Based Poly(Butylene Succinate) Including Polymer Upcycling Routes. *Ind. Eng. Chem. Res.* **2016**, *55* (20), 5832–5842. https://doi.org/10.1021/acs.iecr.6b00588.

(72) Babu, R. P.; O'Connor, K.; Seeram, R. Current Progress on Bio-Based Polymers and Their Future Trends. *Prog. Biomater.* **2013**, *2* (1), 8. https://doi.org/10.1186/2194-0517-2-8.

(73) Bechthold, I.; Bretz, K.; Kabasci, S.; Kopitzky, R.; Springer, A. Succinic Acid: A New Platform Chemical for Biobased Polymers from Renewable Resources. *Chem. Eng. Technol.* **2008**, *31* (5), 647–654. https://doi.org/10.1002/ceat.200800063.

(74) Morales, M.; Ataman, M.; Badr, S.; Linster, S.; Kourlimpinis, I.; Papadokonstantakis, S.; Hatzimanikatis, V.; Hungerbühler, K. Sustainability Assessment of Succinic Acid Production Technologies from Biomass Using Metabolic Engineering. *Energy Environ. Sci.* **2016**, *9* (9), 2794–2805. https://doi.org/10.1039/C6EE00634E.

(75) Azim, H.; Dekhterman, A.; Jiang, Z.; Gross, R. A. Candida Antarctica Lipase B-Catalyzed Synthesis of Poly(Butylene Succinate): Shorter Chain Building Blocks Also Work. *Biomacromolecules* **2006**, *7* (11), 3093–3097. https://doi.org/10.1021/bm060574h.

(76) Sugihara, S.; Toshima, K.; Matsumura, S. New Strategy for Enzymatic Synthesis of High-Molecular-Weight Poly(Butylene Succinate) *via* Cyclic Oligomers. *Macromol. Rapid Commun.* **2006**, *27* (3), 203–207. https://doi.org/10.1002/marc.200500723.

(77) Jamshidian, M.; Tehrany, E. A.; Imran, M.; Jacquot, M.; Desobry, S. Poly-Lactic Acid: Production, Applications, Nanocomposites, and Release Studies. *Compr. Rev. Food Sci. Food Saf.* **2010**, *9* (5), 552–571. https://doi.org/10.1111/j.1541-4337.2010.00126.x.

(78) Zhao, H.; Nathaniel, G. A.; Merenini, P. C. Enzymatic Ring-Opening Polymerization (ROP) of Lactides and Lactone in Ionic Liquids and Organic Solvents: Digging the Controlling Factors. *RSC Adv.* **2017**, *7* (77), 48639–48648. https://doi.org/10.1039/C7RA09038B.

(79) Corma, A.; Iborra, S.; Velty, A. Chemical Routes for the Transformation of Biomass into Chemicals. *Chem. Rev.* **2007**, *107* (6), 2411–2502. https://doi.org/10.1021/cr050989d.

(80) Garlotta, D. A Literature Review of Poly(Lactic Acid). *J. Polym. Environ.* **2001**, *9* (2), 63–84. https://doi.org/10.1023/A:1020200822435.

(81) Matsumura, S.; Mabuchi, K.; Toshima, K. Lipase-Catalyzed Ring-Opening Polymerization of Lactide. *Macromol. Rapid Commun.* **1997**, *18* (6), 477–482. https://doi.org/10.1002/marc.1997.030180604.

(82) Omay, D.; Guvenilir, Y. Synthesis and Characterization of Poly(d,l-Lactic Acid) *via* Enzymatic Ring Opening Polymerization by Using Free and Immobilized Lipase. *Biocatal. Biotransformation* **2013**, *31* (3), 132–140. https://doi.org/10.3109/10242422.2013.795148.

(83) Hans, M.; Keul, H.; Moeller, M. Ring-Opening Polymerization of DD-Lactide Catalyzed by Novozyme 435. *Macromol. Biosci.* **2009**, *9* (3), 239–247. https://doi.org/10.1002/mabi.200800236.

(84) Duchiron, S. W.; Pollet, E.; Givry, S.; Avérous, L. Mixed Systems to Assist Enzymatic Ring Opening Polymerization of Lactide Stereoisomers. *RSC Adv.* **2015**, *5* (103), 84627–84635. https://doi.org/10.1039/C5RA18954C.

(85) Jeon, N. Y.; Ko, S.-J.; Won, K.; Kang, H.-Y.; Kim, B. T.; Lee, Y. S.; Lee, H. Synthesis of Alkyl (R)-Lactates and Alkyl (S,S)-O-Lactyllactates by Alcoholysis of Rac-Lactide Using Novozym 435. *Tetrahedron Lett.* **2006**, *47* (37), 6517–6520. https://doi.org/10.1016/j.tetlet.2006.07.034.

(86) Zhao, H. Enzymatic Ring-Opening Polymerization (ROP) of Polylactones: Roles of Non-Aqueous Solvents. *J. Chem. Technol. Biotechnol.* **2018**, *93* (1), 9–19. https://doi.org/10.1002/jctb.5444.

(87) Bonduelle, C.; Martin-Vaca, B.; Bourissou, D. Lipase-Catalyzed Ring-Opening Polymerization of the O-Carboxylic Anhydride Derived from Lactic Acid. *Biomacromolecules* **2009**, *10* (11), 3069–3073. https://doi.org/10.1021/bm9007343.

(88) Chen, G.-X.; Kim, H.-S.; Kim, E.-S.; Yoon, J.-S. Synthesis of High-Molecular-Weight Poly(l-Lactic Acid) through the Direct Condensation Polymerization of l-Lactic Acid in Bulk State. *Eur. Polym. J.* **2006**, *42* (2), 468–472. https://doi.org/10.1016/j.eurpolymj.2005.07.022.

(89) Kiran, K. R.; Divakar, S. Lipase-Catalysed Polymerization of Lactic Acid and Its Film Forming Properties. *World J. Microbiol. Biotechnol.* **2003**, *19* (8), 859–865. https://doi.org/10.1023/A:1026004229239.

(90) Uyama, H.; Inada, K.; Kobayashi, S. Lipase-Catalyzed Synthesis of Aliphatic Polyesters by Polycondensation of Dicarboxylic Acids and Glycols in Solvent-Free System. *Polym. J.* **2000**, *32* (5), 440–443. https://doi.org/10.1295/polymj.32.440.

(91) Linko, Y.-Y.; Lämsä, M.; Wu, X.; Uosukainen, E.; Seppälä, J.; Linko, P. Biodegradable Products by Lipase Biocatalysis. *J. Biotechnol.* **1998**, *66* (1), 41–50. https://doi.org/10.1016/S0168-1656(98)00155-2.

(92) Pellis, A.; Comerford, J. W.; Maneffa, A. J.; Sipponen, M. H.; Clark, J. H.; Farmer, T. J. Elucidating Enzymatic Polymerisations: Chain-Length Selectivity of Candida Antarctica Lipase B towards Various Aliphatic Diols and Dicarboxylic Acid Diesters. *Eur. Polym. J.* **2018**, *106*, 79–84. https://doi.org/10.1016/j.eurpolymj.2018.07.009.

(93) Linko, Y.-Y.; Wang, Z.-L.; Seppälä, J. Lipase-Catalyzed Linear Aliphatic Polyester Synthesis in Organic Solvent. *Enzyme Microb. Technol.* **1995**, *17* (6), 506–511. https://doi.org/10.1016/0141-0229(94)00095-9.

(94) Morrow, C. J. Biocatalytic Synthesis of Polyesters Using Enzymes. *MRS Bull.* **1992**, *17* (11), 43–47. https://doi.org/10.1557/S0883769400046650.

(95) Díaz, A.; Katsarava, R.; Puiggalí, J. Synthesis, Properties and Applications of Biodegradable Polymers Derived from Diols and Dicarboxylic Acids: From Polyesters to Poly(Ester Amide)s. *Int. J. Mol. Sci.* **2014**, *15* (5), 7064–7123. https://doi.org/10.3390/ijms15057064.

(96) PET market value worldwide 2023 https://www-statista-com.ressources-electroniques.univ-lille.fr/statistics/964331/market-value-polyethylene-terephthalate-worldwide/ (accessed 2020 -05 -29).

(97) Pellis, A.; Herrero Acero, E.; Ferrario, V.; Ribitsch, D.; Guebitz, G. M.; Gardossi, L. The Closure of the Cycle: Enzymatic Synthesis and Functionalization of Bio-Based Polyesters. *Trends Biotechnol.* **2016**, *34* (4), 316–328. https://doi.org/10.1016/j.tibtech.2015.12.009.

(98) Crawford, C. B.; Quinn, B. 4 - Physiochemical Properties and Degradation. In *Microplastic Pollutants*; Crawford, C. B., Quinn, B., Eds.; Elsevier, 2017; pp 57–100. https://doi.org/10.1016/B978-0-12-809406-8.00004-9.

(99) Al-Sabagh, A. M.; Yehia, F. Z.; Eshaq, Gh.; Rabie, A. M.; ElMetwally, A. E. Greener Routes for Recycling of Polyethylene Terephthalate. *Egypt. J. Pet.* **2016**, *25* (1), 53–64. https://doi.org/10.1016/j.ejpe.2015.03.001.

(100) Shen, L.; Worrell, E.; Patel, M. K. Comparing Life Cycle Energy and GHG Emissions of Bio-Based PET, Recycled PET, PLA, and Man-Made Cellulosics. *Biofuels Bioprod. Biorefining* **2012**, *6* (6), 625–639. https://doi.org/10.1002/bbb.1368.

(101) Tabone, M. D.; Cregg, J. J.; Beckman, E. J.; Landis, A. E. Sustainability Metrics: Life Cycle Assessment and Green Design in Polymers. *Environ. Sci. Technol.* **2010**, *44* (21), 8264–8269. https://doi.org/10.1021/es101640n.

(102) Chen, L.; Pelton, R. E. O.; Smith, T. M. Comparative Life Cycle Assessment of Fossil and Bio-Based Polyethylene Terephthalate (PET) Bottles. *J. Clean. Prod.* **2016**, *137*, 667–676. https://doi.org/10.1016/j.jclepro.2016.07.094.

(103) Neaţu, F.; Culică, G.; Florea, M.; Parvulescu, V. I.; Cavani, F. Synthesis of Terephthalic Acid by P-Cymene Oxidation Using Oxygen: Toward a More Sustainable Production of Bio-Polyethylene Terephthalate. *ChemSusChem* **2016**, *9* (21), 3102–3112. https://doi.org/10.1002/cssc.201600718.

(104) Ren, H.; Qiao, F.; Shi, Y.; Knutzen, M. W.; Wang, Z.; Du, H.; Zhang, H. PlantBottle™ Packaging Program Is Continuing Its Journey to Pursue Bio-Mono-Ethylene Glycol Using Agricultural Waste. *J. Renew. Sustain. Energy* **2015**, *7* (4), 041510. https://doi.org/10.1063/1.4929336.

(105) Uyama, H.; Yaguchi, S.; Kobayashi, S. Enzymatic Synthesis of Aromatic Polyesters by Lipase-Catalyzed Polymerization of Dicarboxylic Acid Divinyl Esters and Glycols. *Polym. J.* **1999**, *31* (4), 380–383. https://doi.org/10.1295/polymj.31.380.

(106) Drewitt, J. G. N.; Lincoln, J. Improvements in Polymers. GB621971A, April 25, 1949.

(107) Moore, J. A.; Kelly, J. E. Polyesters Derived from Furan and Tetrahydrofuran Nuclei. *Macromolecules* **1978**, *11* (3), 568–573. https://doi.org/10.1021/ma60063a028.

(108) Sousa, A. F.; Vilela, C.; Fonseca, A. C.; Matos, M.; Freire, C. S. R.; Gruter, G.-J. M.; Coelho, J. F. J.; Silvestre, A. J. D. Biobased Polyesters and Other Polymers from 2,5-Furandicarboxylic Acid: A Tribute to Furan Excellency. *Polym. Chem.* **2015**, *6* (33), 5961–5983. https://doi.org/10.1039/C5PY00686D.

(109) van Putten, R.-J.; van der Waal, J. C.; de Jong, E.; Rasrendra, C. B.; Heeres, H. J.; de Vries, J. G. Hydroxymethylfurfural, A Versatile Platform Chemical Made from Renewable Resources. *Chem. Rev.* **2013**, *113* (3), 1499–1597. https://doi.org/10.1021/cr300182k.

(110) Delidovich, I.; Hausoul, P. J. C.; Deng, L.; Pfützenreuter, R.; Rose, M.; Palkovits, R. Alternative Monomers Based on Lignocellulose and Their Use for Polymer Production. *Chem. Rev.* **2016**, *116* (3), 1540–1599. https://doi.org/10.1021/acs.chemrev.5b00354.

(111) Jiang, Y.; Maniar, D.; Woortman, A. J. J.; Loos, K. Enzymatic Synthesis of 2,5-Furandicarboxylic Acid-Based Semi-Aromatic Polyamides: Enzymatic Polymerization Kinetics, Effect of Diamine Chain Length and Thermal Properties. *RSC Adv.* **2016**, *6* (72), 67941–67953. https://doi.org/10.1039/C6RA14585J.

(112) Román-Leshkov, Y.; Chheda, J. N.; Dumesic, J. A. Phase Modifiers Promote Efficient Production of Hydroxymethylfurfural from Fructose. *Science* **2006**, *312* (5782), 1933–1937. https://doi.org/10.1126/science.1126337.

(113) Jiang, M.; Liu, Q.; Zhang, Q.; Ye, C.; Zhou, G. A Series of Furan-Aromatic Polyesters Synthesized *via* Direct Esterification Method Based on Renewable Resources. *J. Polym. Sci. Part Polym. Chem.* **2012**, *50* (5), 1026–1036. https://doi.org/10.1002/pola.25859.

(114) Knoop, R. J. I.; Vogelzang, W.; Haveren, J. van; Es, D. S. van. High Molecular Weight Poly(Ethylene-2,5-Furanoate); Critical Aspects in Synthesis and Mechanical Property Determination. *J. Polym. Sci. Part Polym. Chem.* **2013**, *51* (19), 4191–4199. https://doi.org/10.1002/pola.26833.

(115) Burgess, S. K.; Leisen, J. E.; Kraftschik, B. E.; Mubarak, C. R.; Kriegel, R. M.; Koros, W. J. Chain Mobility, Thermal, and Mechanical Properties of Poly(Ethylene Furanoate) Compared to Poly(Ethylene Terephthalate). *Macromolecules* **2014**, *47* (4), 1383–1391. https://doi.org/10.1021/ma5000199.

(116) Gandini, A.; Silvestre, A. J. D.; Neto, C. P.; Sousa, A. F.; Gomes, M. The Furan Counterpart of Poly(Ethylene Terephthalate): An Alternative Material Based on Renewable Resources. *J. Polym. Sci. Part Polym. Chem.* **2009**, *47* (1), 295–298. https://doi.org/10.1002/pola.23130.

(117) Gomes, M.; Gandini, A.; Silvestre, A. J. D.; Reis, B. Synthesis and Characterization of Poly(2,5-Furan Dicarboxylate)s Based on a Variety of Diols. *J. Polym. Sci. Part Polym. Chem.* **2011**, *49* (17), 3759–3768. https://doi.org/10.1002/pola.24812.

(118) Guidotti, G.; Genovese, L.; Soccio, M.; Gigli, M.; Munari, A.; Siracusa, V.; Lotti, N. Block Copolyesters Containing 2,5-Furan and Trans-1,4-Cyclohexane Subunits with Outstanding Gas Barrier Properties. *Int. J. Mol. Sci.* **2019**, *20* (9). https://doi.org/10.3390/ijms20092187.

(119) Burgess, S. K.; Karvan, O.; Johnson, J. R.; Kriegel, R. M.; Koros, W. J. Oxygen Sorption and Transport in Amorphous Poly(Ethylene Furanoate). *Polymer* **2014**, *55* (18), 4748–4756. https://doi.org/10.1016/j.polymer.2014.07.041.

(120) Burgess, S. K.; Kriegel, R. M.; Koros, W. J. Carbon Dioxide Sorption and Transport in Amorphous Poly(Ethylene Furanoate). *Macromolecules* **2015**, *48* (7), 2184–2193. https://doi.org/10.1021/acs.macromol.5b00333.

(121) de Jong, E.; Dam, M. A.; Sipos, L.; Gruter, G.-J. M. Furandicarboxylic Acid (FDCA), A Versatile Building Block for a Very Interesting Class of Polyesters. In *Biobased Monomers, Polymers, and Materials*; ACS Symposium Series; American Chemical Society, 2012; Vol. 1105, pp 1–13. https://doi.org/10.1021/bk-2012-1105.ch001.

(122) Narvaez, D. I. H. Biocatalytic Synthesis of Cyclic Ester Oligomers from Biobased Building Blocks. PhD, Wageningen University, The Netherlands, 2011.

(123) Cruz-Izquierdo, Á.; Broek, L. A. M. van den; Serra, J. L.; Llama, M. J.; Boeriu, C. G. Lipase-Catalyzed Synthesis of Oligoesters of 2,5-Furandicarboxylic Acid with Aliphatic Diols. *Pure Appl. Chem.* **2015**, *87* (1), 59–69. https://doi.org/10.1515/pac-2014-1003.

(124) Jiang, Y.; Woortman, A. J. J.; Alberda van Ekenstein, G. O. R.; Petrović, D. M.; Loos, K. Enzymatic Synthesis of Biobased Polyesters Using 2,5-Bis(Hydroxymethyl)Furan as the Building Block. *Biomacromolecules* **2014**, *15* (7), 2482–2493. https://doi.org/10.1021/bm500340w.

(125) Juais, D.; Naves, A. F.; Li, C.; Gross, R. A.; Catalani, L. H. Isosorbide Polyesters from Enzymatic Catalysis. *Macromolecules* **2010**, *43* (24), 10315–10319. https://doi.org/10.1021/ma1013176.

(126) Mahapatro, A.; Kalra, B.; Kumar, A.; Gross, R. A. Lipase-Catalyzed Polycondensations: Effect of Substrates and Solvent on Chain Formation, Dispersity, and End-Group Structure.

(127) McKeen, L. W. 6 - Polyamides (Nylons). In *The Effect of Temperature and other Factors on Plastics and Elastomers (Third Edition)*; McKeen, L. W., Ed.; Plastics Design Library; William

Andrew Publishing: Oxford, 2014; pp 233–340. https://doi.org/10.1016/B978-0-323-31016-1.00006-4.

(128) Finnveden, M.; Hendil-Forssell, P.; Claudino, M.; Johansson, M.; Martinelle, M. Lipase-Catalyzed Synthesis of Renewable Plant Oil-Based Polyamides. *Polymers* **2019**, *11* (11). https://doi.org/10.3390/polym11111730.

(129) Ragupathy, L.; Ziener, U.; Dyllick-Brenzinger, R.; von Vacano, B.; Landfester, K. Enzyme-Catalyzed Polymerizations at Higher Temperatures: Synthetic Methods to Produce Polyamides and New Poly(Amide-*Co*-Ester)s. *J. Mol. Catal. B Enzym.* **2012**, *76*, 94–105. https://doi.org/10.1016/j.molcatb.2011.11.019.

(130) Cheng, H. N.; Gu, Q.-M.; Maslanka, W. W. Enzyme-Catalyzed Polyamides and Compositions and Processes of Preparing and Using the Same. US6677427B1, January 13, 2004.

(131) Fan, Y.; Chen, G.; Tanaka, J.; Tateishi, T. Biosynthesis of Polyamides Containing Amino Acid Residues through the Specific Aminolysis of Amino Acid Ester Derivatives. *Mater. Sci. Eng. C* **2004**, *24* (6), 791–796. https://doi.org/10.1016/j.msec.2004.08.020.

(132) Poulhès, F.; Mouysset, D.; Gil, G.; Bertrand, M. P.; Gastaldi, S. Speeding-up Enzyme-Catalyzed Synthesis of Polyamides Using ω-Amino-α-Alkoxy-Acetate as Monomer. *Polymer* **2013**, *54* (14), 3467–3471. https://doi.org/10.1016/j.polymer.2013.05.011.

(133) Guo, K.; Chu, C. C. Controlled Release of Paclitaxel from Biodegradable Unsaturated Poly(Ester Amide)s/Poly(Ethylene Glycol) Diacrylate Hydrogels. *J. Biomater. Sci. Polym. Ed.* **2007**, *18* (5), 489–504. https://doi.org/10.1163/156856207780852569.

(134) Karimi, P.; Rizkalla, A. S.; Mequanint, K. Versatile Biodegradable Poly(Ester Amide)s Derived from α-Amino Acids for Vascular Tissue Engineering. *Materials* **2010**, *3* (4), 2346–2368. https://doi.org/10.3390/ma3042346.

(135) Guo, K.; Chu, C. C. Biodegradable and Injectable Paclitaxel-Loaded Poly(Ester Amide)s Microspheres: Fabrication and Characterization. *J. Biomed. Mater. Res. B Appl. Biomater.* **2009**, *89B* (2), 491–500. https://doi.org/10.1002/jbm.b.31239.

(136) Sharma, B.; Azim, A.; Azim, H.; Gross, R. A.; Zini, E.; Focarete, M. L.; Scandola, M. Enzymatic Synthesis and Solid-State Properties of Aliphatic Polyesteramides with

Polydimethylsiloxane Blocks. *Macromolecules* **2007**, *40* (22), 7919–7927. https://doi.org/10.1021/ma070671i.

(137) Maniar, D.; Silvianti, F.; Ospina, V. M.; Woortman, A. J. J.; van Dijken, J.; Loos, K. On the Way to Greener Furanic-Aliphatic Poly(Ester Amide)s: Enzymatic Polymerization in Ionic Liquid. *Polymer* **2020**, *205*, 122662. https://doi.org/10.1016/j.polymer.2020.122662.

(138) Stavila, E.; Alberda van Ekenstein, G. O. R.; Loos, K. Enzyme-Catalyzed Synthesis of Aliphatic–Aromatic Oligoamides. *Biomacromolecules* **2013**, *14* (5), 1600–1606. https://doi.org/10.1021/bm400243a.

(139) Meimoun, J.; Bernhard, Y.; Pelinski, L.; Bousquet, T.; Pellegrini, S.; Raquez, J.-M.; Winter, J. D.; Gerbaux, P.; Cazaux, F.; Tahon, J.-F.; Gaucher, V.; Chenal, T.; Favrelle-Huret, A.; Zinck, P. Lipase-Catalysed Polycondensation of Levulinic Acid Derived Diol-Diamide Monomers: Access to New Poly(Ester-*Co*-Amide)s. *Polym. Chem.* **2020**, *11* (47), 7506–7514. https://doi.org/10.1039/D0PY01301C.

(140) Mahapatro, A.; Kumar, A.; Kalra, B.; Gross, R. A. Solvent-Free Adipic Acid/1,8-Octanediol Condensation Polymerizations Catalyzed by Candida Antartica Lipase B. *Macromolecules* **2004**, *37* (1), 35–40. https://doi.org/10.1021/ma025796w.

(141) Mei, Y.; Kumar, A.; Gross, R. Kinetics and Mechanism of Candida Antarctica Lipase B Catalyzed Solution Polymerization of ε-Caprolactone. *Macromolecules* **2003**, *36* (15), 5530–5536. https://doi.org/10.1021/ma025741u.

(142) Lee, C. S.; Ru, M. T.; Haake, M.; Dordick, J. S.; Reimer, J. A.; Clark, D. S. Multinuclear NMR Study of Enzyme Hydration in an Organic Solvent. *Biotechnol. Bioeng.* **1998**, *57* (6), 686–693. https://doi.org/10.1002/(SICI)1097-0290(19980320)57:6<686::AID-BIT6>3.0.CO;2-H.

(143) Engel, S.; Höck, H.; Bocola, M.; Keul, H.; Schwaneberg, U.; Möller, M. CaLB Catalyzed Conversion of ε-Caprolactone in Aqueous Medium. Part 1: Immobilization of CaLB to Microgels. *Polymers* **2016**, *8* (10), 372. https://doi.org/10.3390/polym8100372.

(144) Brink, L. E.; Tramper, J. Optimization of Organic Solvent in Multiphase Biocatalysis. *Biotechnol. Bioeng.* **1985**, *27* (8), 1258–1269. https://doi.org/10.1002/bit.260270822.

(145) Laane, C.; Boeren, S.; Vos, K.; Veeger, C. Rules for Optimization of Biocatalysis in Organic Solvents. *Biotechnol. Bioeng.* **1987**, *30* (1), 81–87. https://doi.org/10.1002/bit.260300112.

(146) Jiang, Y.; Woortman, A. J. J.; Alberda van Ekenstein, G. O. R.; Loos, K. Enzyme-Catalyzed Synthesis of Unsaturated Aliphatic Polyesters Based on Green Monomers from Renewable Resources. *Biomolecules* **2013**, *3* (3), 461–480. https://doi.org/10.3390/biom3030461.

(147) Linko, Y.-Y.; Wang, Z.-L.; Seppälä, J. Lipase-Catalyzed Synthesis of Poly(1,4-Butyl Sebacate) from Sebacic Acid or Its Derivatives with 1,4-Butanediol. *J. Biotechnol.* **1995**, *40* (2), 133–138. https://doi.org/10.1016/0168-1656(95)00039-S.

(148) Kumar, A.; Gross, R. A. Candida Antartica Lipase B Catalyzed Polycaprolactone Synthesis: Effects of Organic Media and Temperature. *Biomacromolecules* **2000**, *1* (1), 133–138. https://doi.org/10.1021/bm990510p.

(149) Cremonesi, P.; Carrea, G.; Ferrara, L.; Antonini, E. Enzymatic Preparation of 20β-Hydroxysteroids in a Two-Phase System. *Biotechnol. Bioeng.* **1975**, *17* (8), 1101–1108. https://doi.org/10.1002/bit.260170802.

(150) Yang, Y.; Ge, Y.; Zhao, H.; Shi, W.; Li, Q. Lipase-Catalyzed Synthesis of Poly(εε-Caprolactone) and Characterization of Its Solid-State Properties. *Biocatal. Biotransformation* **2011**, *29* (6), 337–343. https://doi.org/10.3109/10242422.2011.638057.

(151) Gorke, J. T.; Okrasa, K.; Louwagie, A.; Kazlauskas, R. J.; Srienc, F. Enzymatic Synthesis of Poly(Hydroxyalkanoates) in Ionic Liquids. *J. Biotechnol.* **2007**, *132* (3), 306–313. https://doi.org/10.1016/j.jbiotec.2007.04.001.

(152) Sheldon, R. A.; Lau, R. M.; Sorgedrager, M. J.; Rantwijk, F. van; Seddon, K. R. Biocatalysis in Ionic Liquids. *Green Chem.* **2002**, *4* (2), 147–151. https://doi.org/10.1039/B110008B.

(153) Yoshizawa-Fujita, M.; Saito, C.; Takeoka, Y.; Rikukawa, M. Lipase-Catalyzed Polymerization of L-Lactide in Ionic Liquids. *Polym. Adv. Technol.* **2008**, *19* (10), 1396–1400. https://doi.org/10.1002/pat.1217.

(154) Tsai, W.-C.; Wang, Y. Progress of Supercritical Fluid Technology in Polymerization and Its Applications in Biomedical Engineering. *Prog. Polym. Sci.* **2019**, *98*, 101161. https://doi.org/10.1016/j.progpolymsci.2019.101161.

(155) García-Arrazola, R.; López-Guerrero, D. A.; Gimeno, M.; Bárzana, E. Lipase-Catalyzed Synthesis of Poly-l-Lactide Using Supercritical Carbon Dioxide. *J. Supercrit. Fluids* **2009**, *51* (2), 197–201. https://doi.org/10.1016/j.supflu.2009.08.014.

(156) Comim Rosso, S. R.; Bianchin, E.; de Oliveira, D.; Oliveira, J. V.; Ferreira, S. R. S. Enzymatic Synthesis of Poly(ε-Caprolactone) in Supercritical Carbon Dioxide Medium by Means of a Variable-Volume View Reactor. *J. Supercrit. Fluids* **2013**, *79*, 133–141. https://doi.org/10.1016/j.supflu.2013.02.009.

(157) Pellis, A.; Guebitz, G. M.; Farmer, T. J. On the Effect of Microwave Energy on Lipase-Catalyzed Polycondensation Reactions. *Molecules* **2016**, *21* (9), 1245. https://doi.org/10.3390/molecules21091245.

(158) Jbilou, F.; Dole, P.; Degraeve, P.; Ladavière, C.; Joly, C. A Green Method for Polybutylene Succinate Recycling: Depolymerization Catalyzed by Lipase B from Candida Antarctica during Reactive Extrusion. *Eur. Polym. J.* **2015**, *68*, 207–215. https://doi.org/10.1016/j.eurpolymj.2015.04.039.

(159) Gatt, E.; Rigal, L.; Vandenbossche Maréchal, V. Biomass Pretreatment with Reactive Extrusion Using Enzymes: A Review. *Ind. Crops Prod.* **2018**, *122*, 329–339. https://doi.org/10.1016/j.indcrop.2018.05.069.

(160) Spinella, S.; Ganesh, M.; Re, G. L.; Zhang, S.; Raquez, J.-M.; Dubois, P.; Gross, R. A. Enzymatic Reactive Extrusion: Moving towards Continuous Enzyme-Catalysed Polyester Polymerisation and Processing. *Green Chem.* **2015**, *17* (8), 4146–4150. https://doi.org/10.1039/C5GC00992H.

(161) Li, C.; Pan, S.; Xu, W.; Lu, Y.; Wang, P.; Zhang, F.; Gross, R. A. Lipase-Catalyzed Ring-Opening Copolymerization of ω-Pentadecalactone and δ-Valerolactone by Reactive Extrusion. *Green Chem.* **2020**, *22* (3), 662–668. https://doi.org/10.1039/C9GC04111G.

(162) Li, C.; Xu, W.; Lu, Y.; Gross, R. A. Lipase-Catalyzed Reactive Extrusion: Copolymerization of ε-Caprolactone and ω-Pentadecalactone. *Macromol. Rapid Commun.* **2020**, *41* (22), 2000417. https://doi.org/10.1002/marc.202000417.

2. Enzymatic polycondensation of hexane-1,6-diol and diethyl adipate: A statistical approach predicting the key-parameters in solution and in bulk

2.1 Introduction

These recent years have witnessed growing research on replacing metal-based catalysts with more eco-friendly organocatalysts and enzymes, both of which possessed certain advantages and limitations.[1] This work will focus on enzymatic catalysis as a replacement to conventional metal-based catalysts, due to their selectivity, eco-friendly, and recyclable nature [1–8]. The most popular biocatalyst used is Novozym 435 (N435 - lipase B from *Candida antarctica* immobilized on a porous acrylic resin), where it showed improved properties in terms of specificity, thermal stability, and selectivity, and was proposed in many research works as a versatile catalyst that can be beneficial in different synthetic routes, particularly in the case of aliphatic polyesters.[9,10]

Many of the research in the area of enzymatic polyesterification remains very empirical, *i.e.*, testing the viability and efficiency of different enzymes for the development of polyesters and optimizing the reaction conditions for achieving high molecular weights. However, the impact of certain parameters, or in a more accurate sense, the 'degree of impact' of these parameters can vary largely in different conditions and settings. Passing from solution to bulk remains very challenging and certain parameters, such as vacuum application can behave differently. Although the importance of vacuum in the two-step method is very well established,[2,11–13] most research included vacuum at a constant value, or otherwise compared it to reactions under atmospheric pressure. Poojari et al.[14] showed that an increase in vacuum gauge pressure from 66 to 400 mbar resulted in a significant increase in M_w and M_n in the polycondensation reactions between 1,3-bis(3-carboxypropyl)tetramethyldisiloxane and butane-1,4-diol or hexane-1,6-diol. In the presence of octane-1,8-diol, the vacuum effect was reversed. Jiang[15] showed the necessity of high vacuum

application to synthesize high molecular weight copolymers of ω-pentadecalactone, diethyl succinate, and butane-1,4-diol, by comparing the results achieved at high vacuum (<4 mbar) to very low levels of vacuum being ~ 800 and 1,013 mbar (atmospheric pressure) respectively, where the two latter conditions produced oligomers that did not exceed 1,000 g.mol^{-1} in M_n compared to values exceeding 10,000 g.mol^{-1} at high vacuum levels.

Traditional methods of optimization follow a one-factor-at-a-time approach (OFAT), which involves varying one factor while keeping other factors constant. The main drawback of this method is that it does not account for interactions between the tested variables, leading to inaccuracy in depicting the true effect of the factors tested. On the other hand, the use of response surface methodology (RSM) such as central composite design (CCD) allows for an accurate representation of the effect of the tested variables and their interaction.[16] RSM has been successfully employed in many research works as a tool of optimization.[17,18] For example, Itabaiana et al.[19] used a CCD to determine optimal conditions for lipase catalyzed esterification of waste fatty acids into useful esters. Similarly, Pellis et al.[20] used a fractional factorial design to evaluate the effect of temperature, pressure, and water content in the polycondensation reaction between butane-1,4-diol or octane-1,8-diol with dimethyl adipate catalyzed by either cutinase 1 from *Thermobifida cellulosilytica* or CALB, under solvent and thin film conditions.

In order to implement our response surface methodology, we select the step-growth synthesis of poly(hexylene adipate) conducted in solution and in bulk, following a two-step procedure, transesterification followed by polycondensation. After assessing the influence of oligomerization time and monomer concentration, the variable impact and interaction of different experimental parameters (temperature, % w/w enzyme loading, and vacuum) on the polycondensation reaction between hexane-1,6-diol and diethyl adipate in solvent (diphenyl ether) and bulk media, using N435 is reported. Two central composite designs were used to build second order quadratic models with equations that can predict the M_n based on the conditions used. As such, these models give users the exact parameters that can be considered to develop a polymer with a certain desired range of M_n, a method that can show to be very useful for providing an efficient tool in the enzymatic synthesis of polyesters using a step-growth method, where the control of M_n is of importance. Finally, the influence of the process, bulk *vs.* solution, on enzyme recycling was also studied.

2.2 Results and discussion

The solution polycondensation of equimolar amounts (4 mmol) of hexane-1,6-diol and diethyl adipate in the presence of N435 (see Scheme 16) was conducted in diphenyl ether, as it was reported to be the more suitable solvent to achieve higher molecular weights [21,22]. The effect of the monomer concentration on the yield and molecular weight was first assessed considering a 2 h oligomerization step followed by a 24 h polycondensation step under a vacuum of 10 mbar and a temperature of 100 °C. The overall concentrations were varied by changing the amount of diphenyl ether used. Typical ^{1}H NMR spectra of the monomers and synthesized polymer are presented in Figure 10, Figure 11 and Figure 12, whereas the results are given in

Table 4.

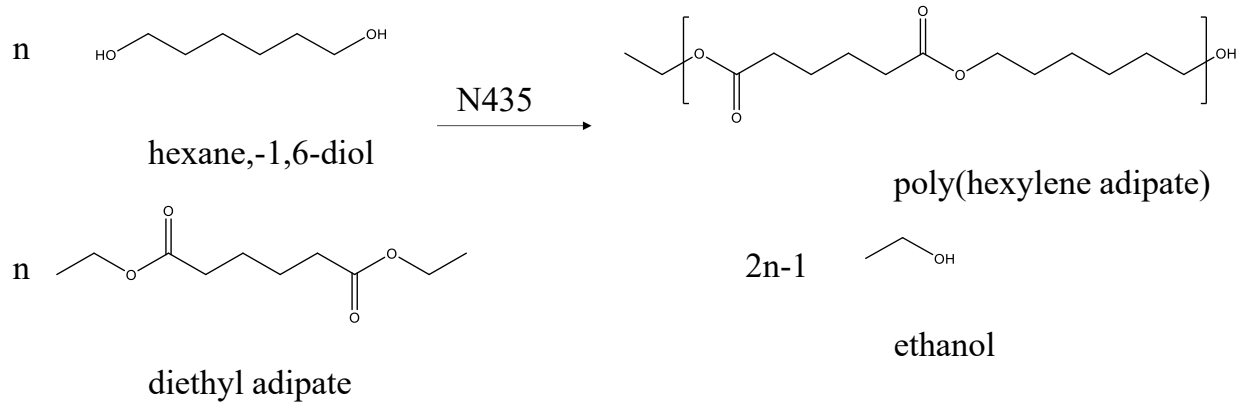

Scheme 16. Polycondensation of hexane-1,6-diol and diethyl adipate in the presence of N435 as catalyst.

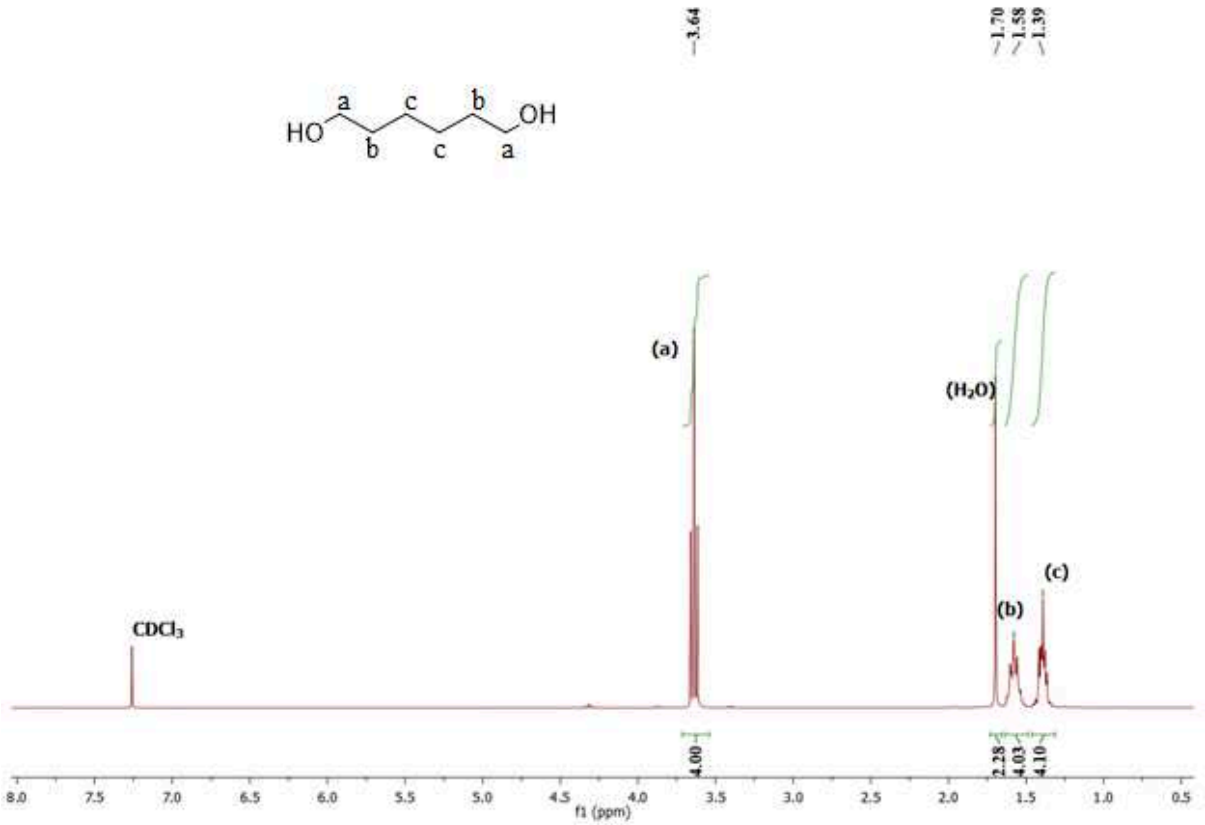

Figure 10. ^{1}H NMR spectrum ($CDCl_3$, 300 MHz) of hexane-1,6-diol ($C_6H_{14}O_2$): δ(ppm) 1.39 (m, 4H), 1.58 (m, 4H), 3.64 (t, J = 6.5 Hz, 4H).

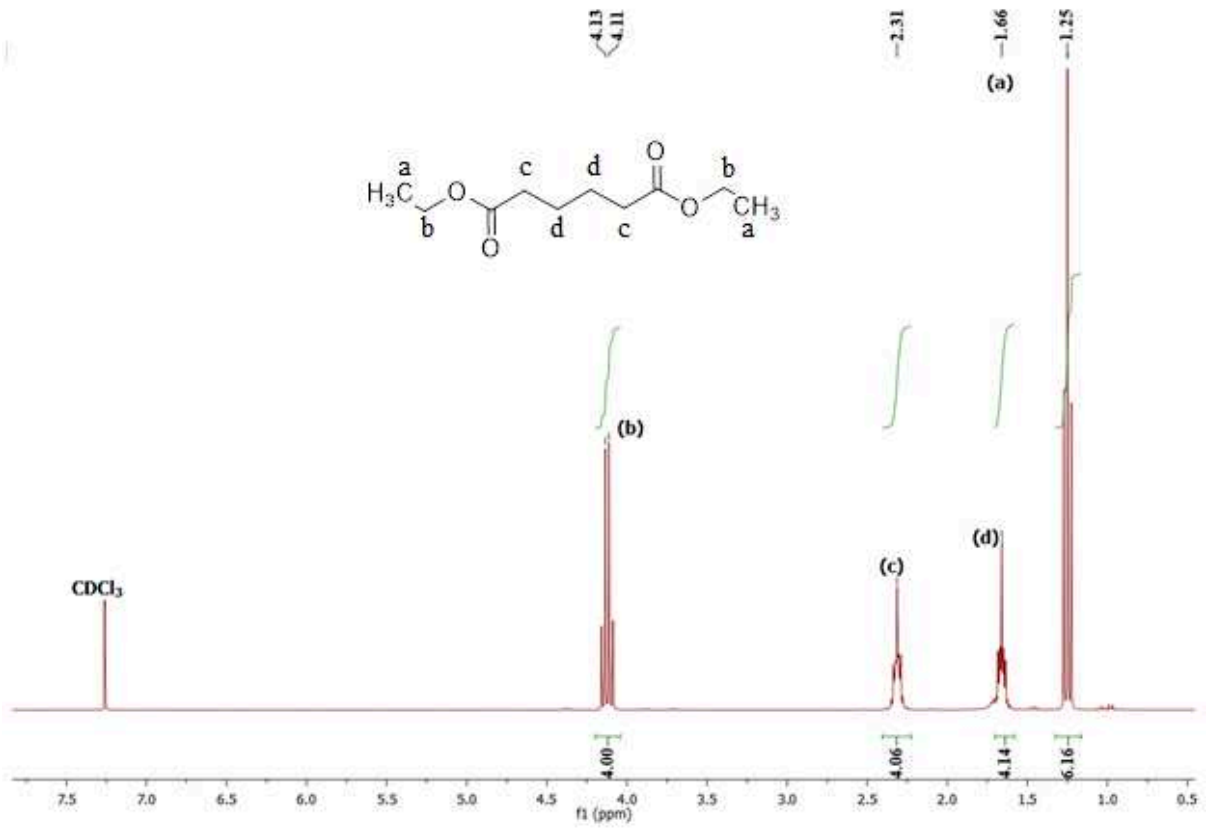

Figure 11. ^{1}H NMR spectrum ($CDCl_3$, 300 MHz) of diethyl adipate ($C_{10}H_{18}O_4$): δ(ppm) 1.25 (t, J = 7.1 Hz, 6H), 1.66 (m, 4H), 2.31 (t, J = 7.2 Hz, 4H), 4.11-4.13 (q, J = 7.1 Hz, 4H).

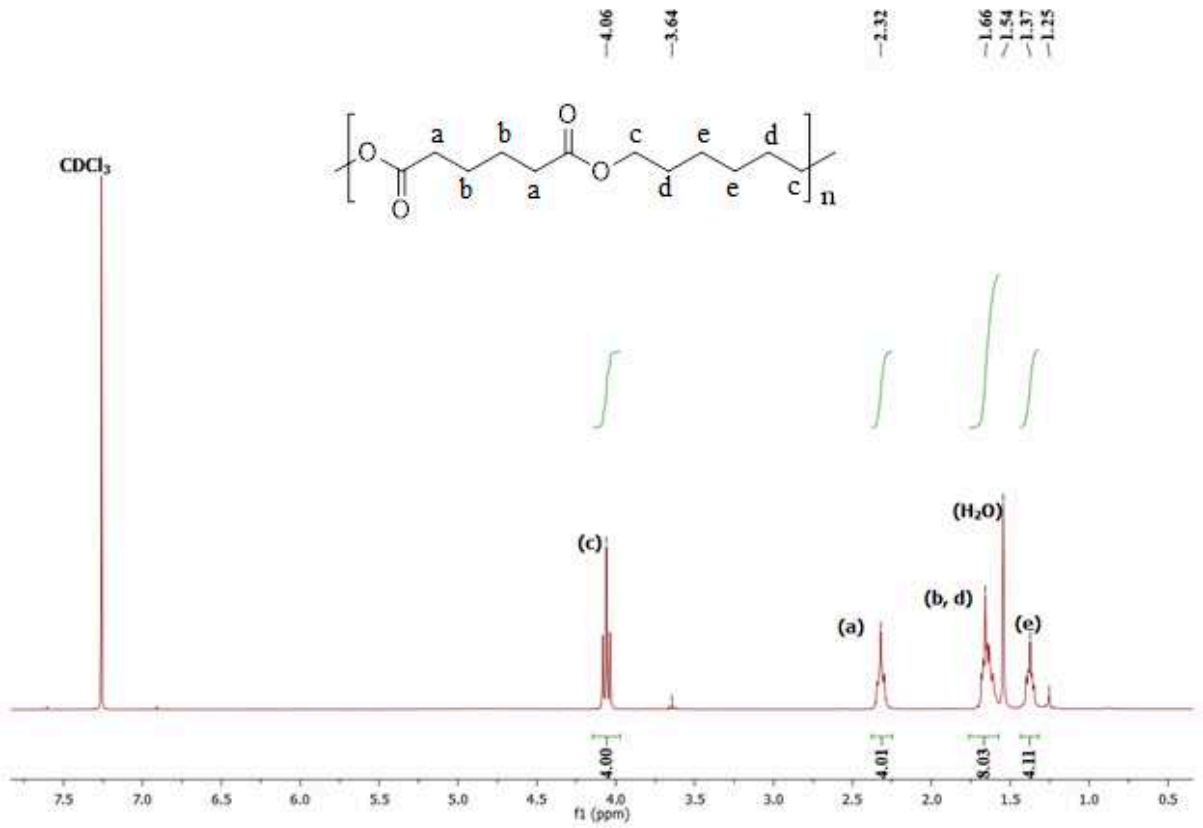

Figure 12. ^{1}H NMR spectrum ($CDCl_3$, 300 MHz) of poly(hexylene adipate) [-$O(CH_2)_6O_2C(CH_2)_4CO$-]n: δ(ppm) 1.37 (m, 4H), 1.66 (m, 8H), 2.32 (t, J = 7.1 Hz, 4H), 4.06 (t, J = 6.7 Hz, 4H).

Table 4. Effect of monomer concentration on yield, M_n and dispersity of poly(hexylene adipate).

Entry[1]	Concentration (mol.L^{-1})	Yield (%)	M_n (g.mol^{-1})[2]	$Đ_M$[3]
1	4	88	12,300	1.44
2	2	86	10,700	1.49
3	1	74	8,300	1.30
4	0.5	56	7,400	1.18

[1] All experiments were conducted following a two-step polycondensation reaction: 1st step reaction conducted under atmospheric pressure, followed by the 2nd step of 24 h under vacuum (10 mbar). Temperature and enzyme loading were kept constant in both steps at 100 °C and 10% w/w of N435. [2] The number average molecular weight (M_n) was obtained from GPC analyses ($CHCl_3$, 40 °C, polystyrene standards). [3] Molar mass dispersity $Đ_M = M_w/M_n$ was obtained from GPC analyses ($CHCl_3$, 40 °C, polystyrene standards).

An increase in M_n and yield with monomer concentration can be noticed, *i.e.*, where the M_n passed from 7,400 up to 12,300 g.mol^{-1} by increasing the monomer concentration from 0.5 to 4 mol.L^{-1}. Similarly, the yield increased from 56 to 88%. Therefore, for the next experiments carried out in solution, the volume of diphenyl ether was set constant at 1 mL to establish a monomer concentration of 4 mol.L^{-1}. This decrease in M_n as a function of decreasing monomer concentration can be attributed to the decrease in the polymerization rate in dilute solutions due to the decrease in molecular collision as proposed by the collision theory [15,23]. In fact, this drop in reactivity is reflected as a decrease in monomer conversion which would decrease the degree of polymerization (X_n) according to Carothers equation: $X_n = 1/(1-p)$ where p is defined as the conversion [24]. Another proposed cause can also be attributed to the decrease in the byproduct (ethanol) removal efficiency in lower concentration solutions [25]. As the vacuum application may result in the evaporation of small monomer fractions, the oligomerization step was varied between 1 and 6 h in both bulk and solution in order to determine a suitable time for oligomer growth before the vacuum application. hexane-1,6-diol and DEA were added in equimolar amounts (4 mmol) in both systems, while 1 mL of diphenyl ether was added for the solution polymerization method to obtain the previously optimized concentration (4 mol.L^{-1}) conditions. The monomer conversion in the first step was determined *via* ^{1}H NMR at different time intervals in order to assess the reaction kinetics

and the time needed to reach the equilibrium at different temperatures and % enzyme loading, as reported in Figure 15.

An example of the ^{1}H-NMR spectra is given in Figure 13 and Figure 14 representing the reaction of hexane-1,6-diol and diethyl adipate in diphenyl ether after 15 mins reaction at 80 °C and 1% w/w enzyme loading. Conversion was calculated *via* the ratio of the signal representing poly(hexylene adipate) at δ= 4.06 relative to the summation of signals representing DEA and poly(hexylene adipate) at δ= 4.11- 4.13 and at δ= 4.06, respectively. The totality of the unreacted monomer in addition to the produced polymer was presented as an integral of 1 that can be calculated *via* two ways, either by considering the integral for poly(hexylene adipate) and unreacted diethyl adipate (-OOC-CH_2-CH_2-CH_2-CH_2-COO-) represented at δ= 2.32 or by considering the combination of signals at δ= 4.11-4.14 of the methylene group (CH_3-CH_2-O-) of the unreacted diethyl adipate in addition to the signals at δ= 4.06 of the methylene (-O-CH_2-C_4H_8-CH_2-O-) of the produced poly(hexylene adipate). The conversion is considered as the ratio of the integral presenting the methylene (-O-CH_2-C_4H_8-CH_2-O-) of the produced poly(hexylene adipate) to the total mentioned above given in:

Equation 1. Conversion calculated *via* ^{1}H-NMR.

$$Conversion = 100 * \frac{Ib}{Ia + Ib}$$

where Ib is the integral of methylene (-O-CH_2-C_4H_8-CH_2-O-) of the produced poly(hexylene adipate), and Ia is the integral of the methylene group (CH_3-CH_2-O-) of the unreacted diethyl adipate. Due to partial peak overlapping between the triplets representing the methylene (-O-CH_2-C_4H_8-CH_2-O-) of poly(hexylene adipate) at δ= 4.06 and the right peak of the quartet representing the unreacted diethyl adipate (-OOC-CH_2-CH_2-CH_2-CH_2-COO-) at δ= 2.32, the conversion was calculated by including the mentioned peak as an integral of poly(hexylene adipate) and subtracting its value represented by the left peak of the quartet (0.38-0.08= 0.3= 30% conversion).

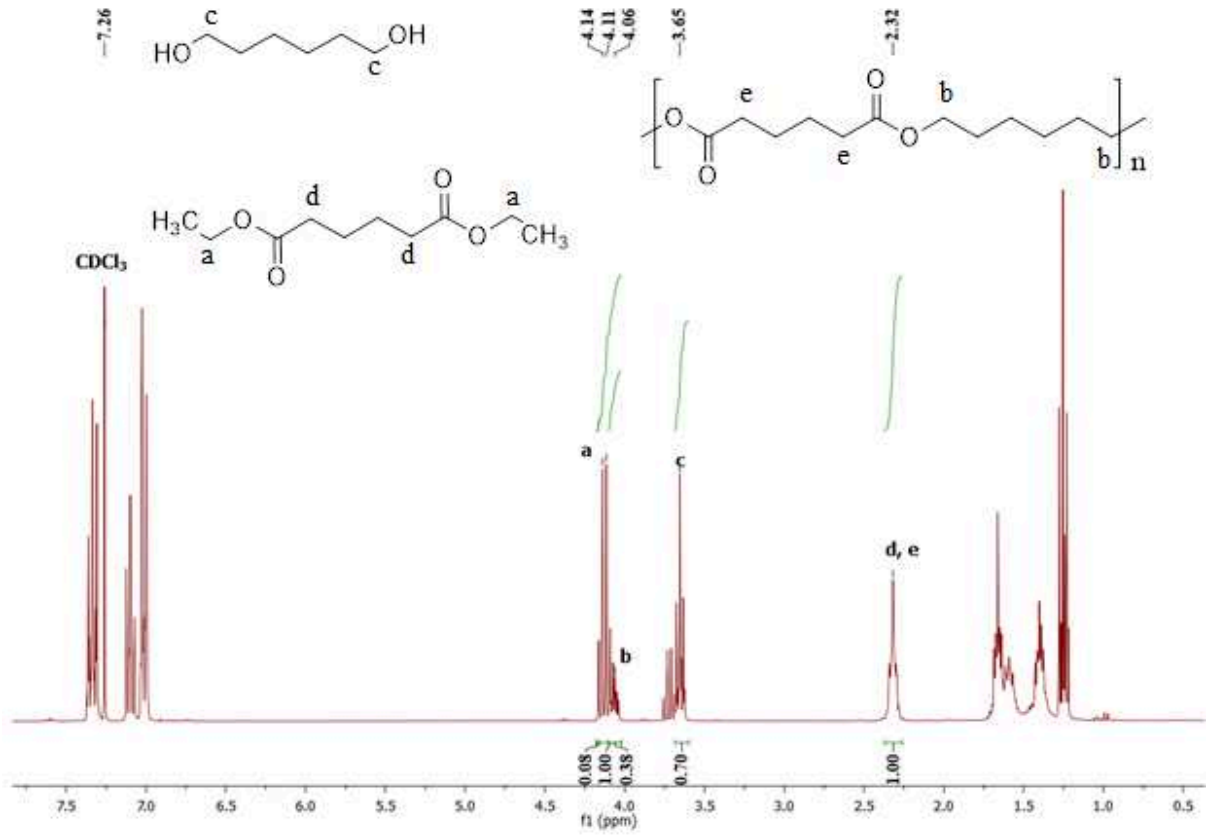

Figure 13. ^{1}H NMR spectrum ($CDCl_3$, 300 MHz) of the crude reaction of hexane-1,6-diol and diethyl adipate in diphenyl ether (1 mL), and the yielded poly(hexylene adipate) after 15 mins reaction at 80 °C and 1% w/w enzyme loading: δ(ppm) 1.25 (t, 6H), 1.37 (m, 8H), 1.66 (m, 12H), 2.32 (t, 8H), 3.65 (t, 4H), 4.06 (t, 4H), 4.11-4.13 (q, 4H). Note: δ ~7-7.5 represent diphenyl ether

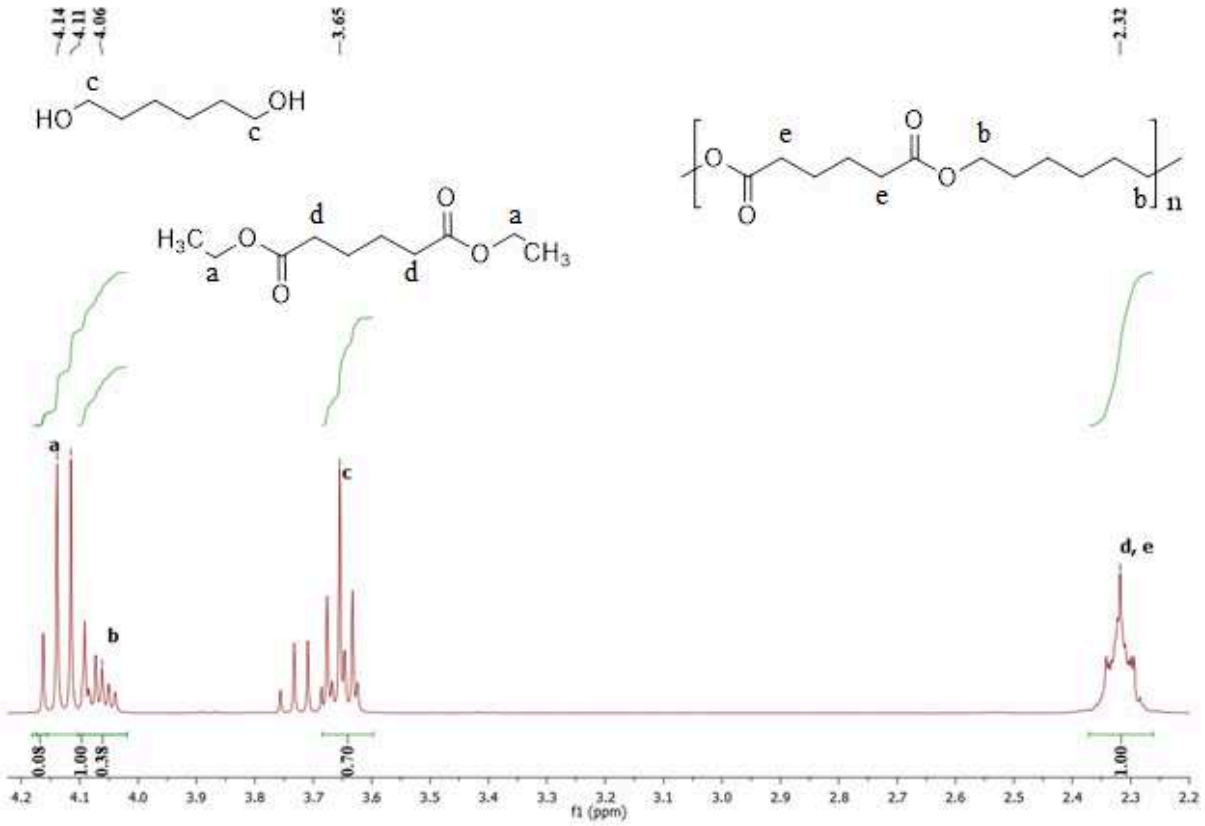

Figure 14. Enlarged view of figure 13 (between 2.2 and 4.2 ppm).

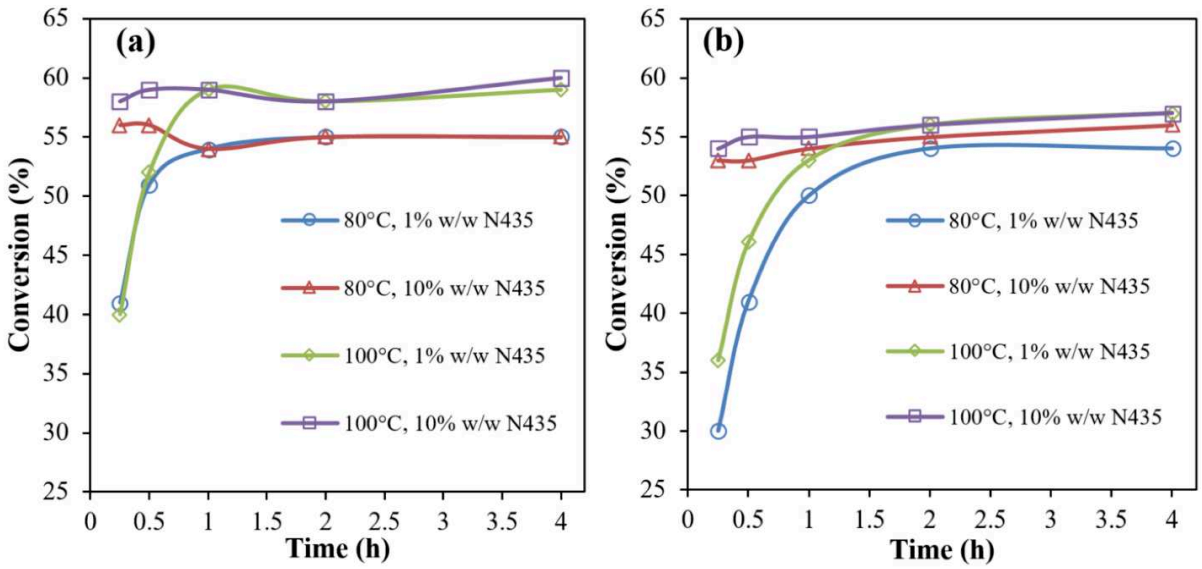

Figure 15. Conversion (expressed in %) after oligomerization step calculated *via* ^{1}H NMR as a function of temperature and enzyme loading in bulk (a) and diphenyl ether (b) conditions.

From Figure 15, it was noticed that the increase in % enzyme loading from 1 to 10% affected the rate of conversion, while at 10% enzyme, the maximum conversion reached a maximum within a time of 15 min in both solution and bulk, compared to 1 and 2 h with 1% N435 in both bulk and diphenyl ether conditions respectively. On the other hand, an increase in temperature by 20 °C did not influence the reaction rate, but rather increased the maximum monomer conversion by a modest value of ~4%.

To validate the 2 h oligomerization step, a two-step polycondensation reaction was set up to run at constant temperature, % enzyme loading, and vacuum. This test was set to determine if extending the oligomerization time would have any effect on the M_n of the final product after a 24 h vacuum application. The corresponding conditions are enclosed in

Table 5 where the only variable was the oligomerization time, followed by a 24 h of vacuum application. The results confirm that, for an average value of 5.5 w/w of enzyme, there is no influence between 2 or 6 h oligomerization time where, e.g., the M_n after 24 h were 6,700, 7,000, and 6,700 g.mol^{-1} for 2, 4, and 6 h oligomerization respectively. In other words, there is no need for prolongation, and an oligomerization step of 1 or 2 h is sufficient for further experiments.

Table 5. Effect of oligomerization time variation on yield, M_n, and dispersity of poly(hexylene adipate) after a 24 h (secondary step) under vacuum.

Entry	Reaction time (h)[1] 1st step/ 2nd step	Yield (%)	M_n (g.mol^{-1})[2]	$Đ_M$[3]
5	2/24	88	6,700	1.38
6	4/24	86	7,000	1.34
7	6/24	74	6,700	1.38

[1] 1st step reaction conducted under atmospheric pressure, followed by the 2nd step of 24 h under vacuum (30 mbar). Temperature and enzyme loading were kept constant in both steps at 90 °C and 5.5% w/w of N435. [2] The number average molecular weight (M_n) was obtained from GPC analyses ($CHCl_3$, 40 °C, polystyrene standards). [3] Molar mass dispersity $Đ_M = M_w/M_n$ was obtained from GPC analyses ($CHCl_3$, 40 °C, polystyrene standards).

Although the effect of temperature and catalyst loading were widely studied in the literature, the effect of vacuum variation was scarcely mentioned. The results obtained using the central composite design (CCD) of experiment did not only determine the effect of temperature, % enzyme loading, and vacuum, but also the interactions between these factors. The CCD design that is further explained in section 2.4.7.4 provided a series of reactions to perform at different conditions. For example, to determine the impact of vacuum at 10 mbar, a set of experiments was performed maintaining vacuum at 10 mbar while varying the values of enzyme loading and temperature between their minimal, middle, and maximal value. Experiments were conducted in a similar pattern at 30 and 50 mbar. The presence of midpoints ensures the proper definition of curvatures in the system that would allow for a high degree of confidence in modeling. Before stepping into the statistical analysis, ^{1}H NMR confirmed >90% conversion for all samples after a 24 h reaction under vacuum, calculated *via* Equation 1. Examples of the ^{1}H NMR spectra in both bulk and solution conditions are given in Figure 16 and Figure 17.

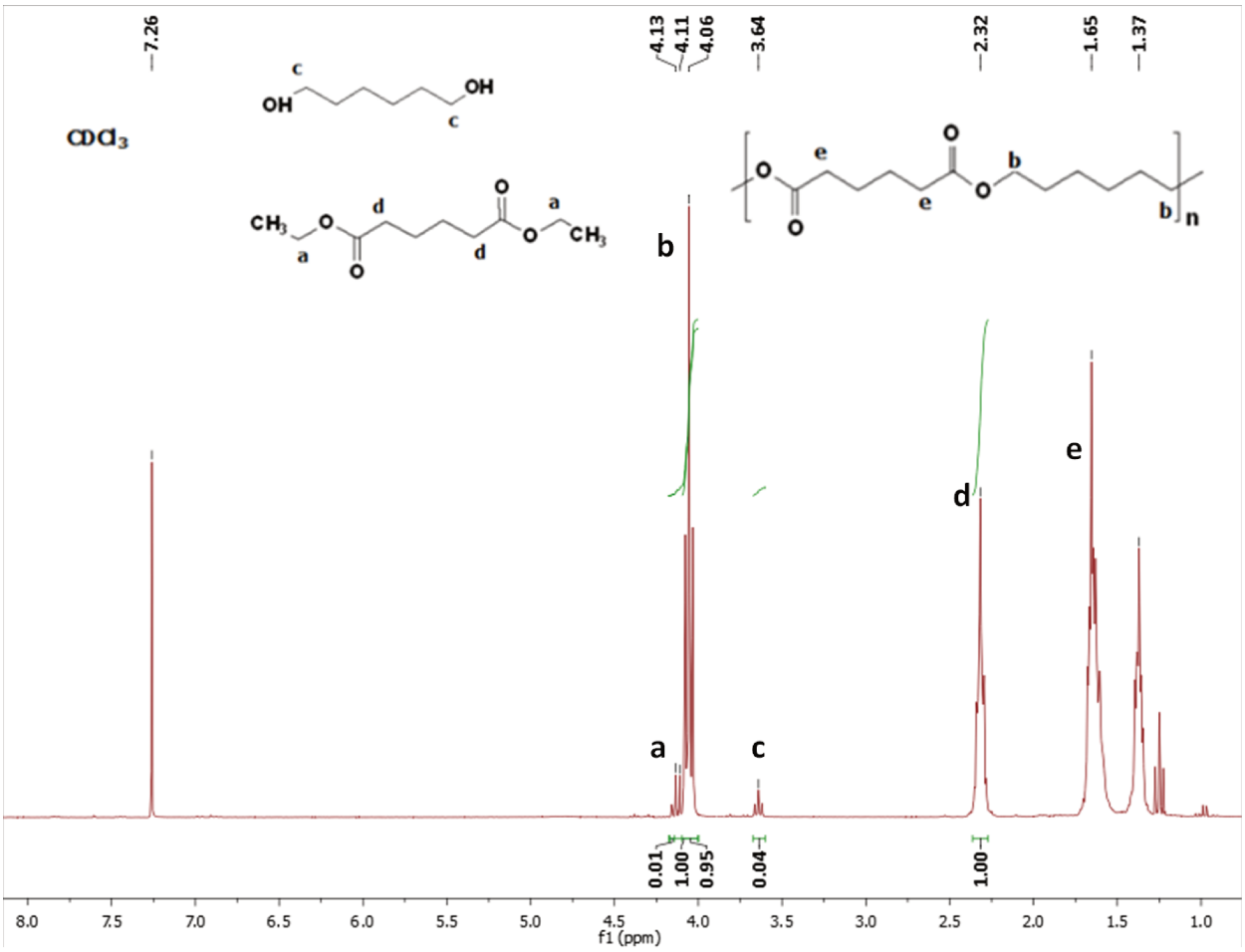

Figure 16. ^{1}H NMR spectrum ($CDCl_3$, 300 MHz) of the crude reaction of hexane-1,6-diol and diethyl adipate in bulk, and the yielded poly(hexylene adipate) after 24 h at 50 mbar vacuum application, at 90 °C and 5.5% w/w enzyme loading.

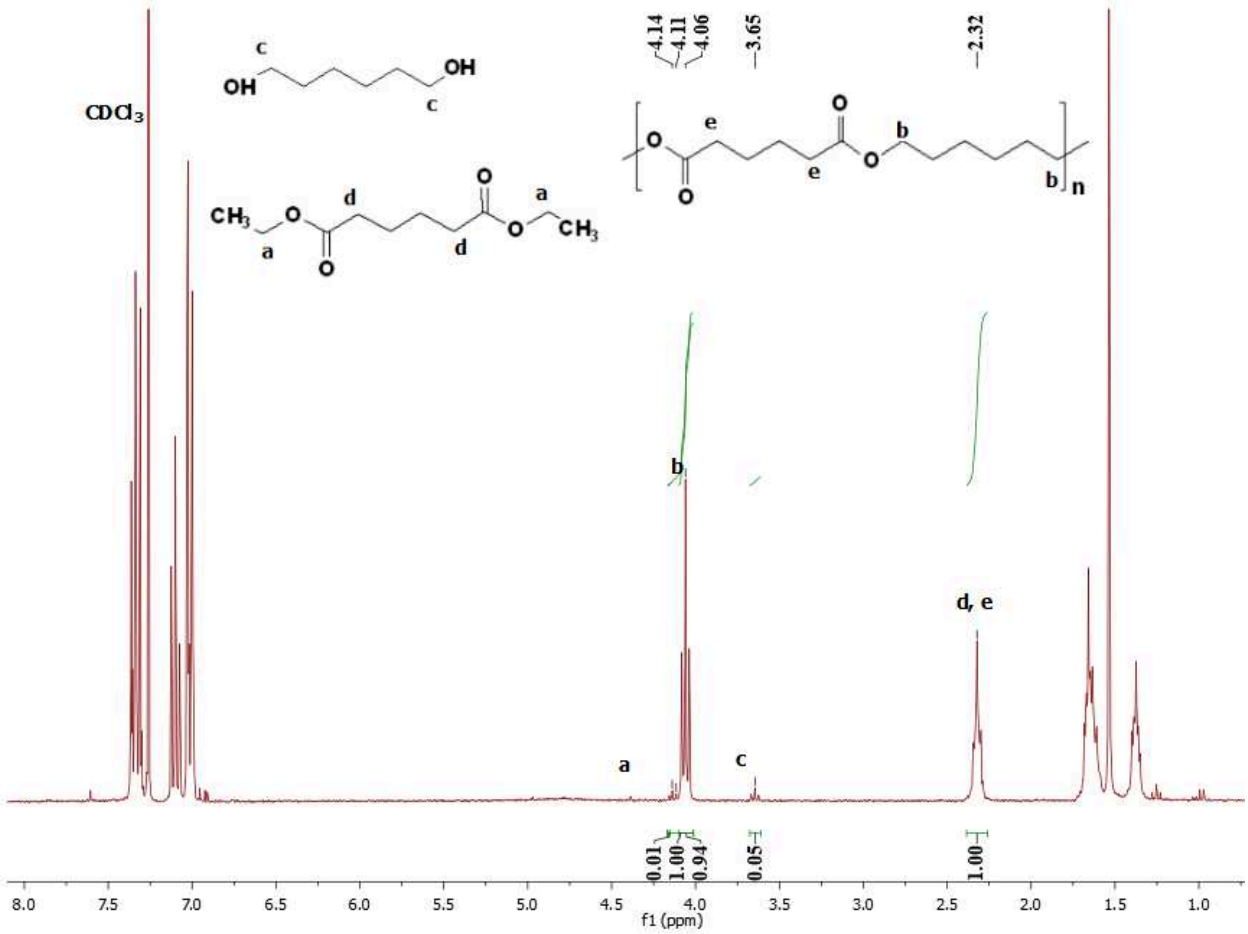

Figure 17. ^{1}H NMR spectrum ($CDCl_3$, 300 MHz) of the crude reaction of hexane-1,6-diol and diethyl adipate in 1 mL diphenyl ether, and the yielded poly(hexylene adipate) after 24 h at 10 mbar vacuum application, at 100 °C and 1% w/w enzyme loading. Note: δ ~7-7.5 represent diphenyl ether.

For solution polymerization, and following the method detailed under statistical analysis (Experimental section), a quadratic model was developed. Table 6 shows the build information of the design model employed herein whereas Table 7 shows the fit statistics information with a predicted R^2=0.92, which was in good agreement with the adjusted R^2 value of 0.96. The adequate Precision value of 25.5 representing the signal to noise ratio indicated an adequate signal, where according to the software's output, a ratio greater than 4 is desirable to permit the usage of the model to navigate the design space. Moreover, Figure 18 shows very good fit between the predicted and actual plots in solution polymerization. The model is presented as an equation in

terms of the actual factors given in Table 8. Finally, to confirm the model, additional runs were performed, the M_n of these additional experiments fell within 95% PI (prediction interval) range, which confirmed the suitability of the model (see Table 9).

Table 6. Build information of the design model for in solution polymerization.

Study Type	**Response Surface**		**Subtype**	**Randomized**
Design Type	I-optimal	Coordinate Exchange	**Runs**	18
Design Model	Quadratic		**Blocks**	No Blocks

Table 7. Fit statistics for in solution polymerization.

Std. Dev.	**415.60**	**R²**	**0.9851**
Mean	7288.56	**Adjusted R²**	0.9683
C.V. %	5.70	**Predicted R²**	0.9231
		Adeq Precision	25.5240

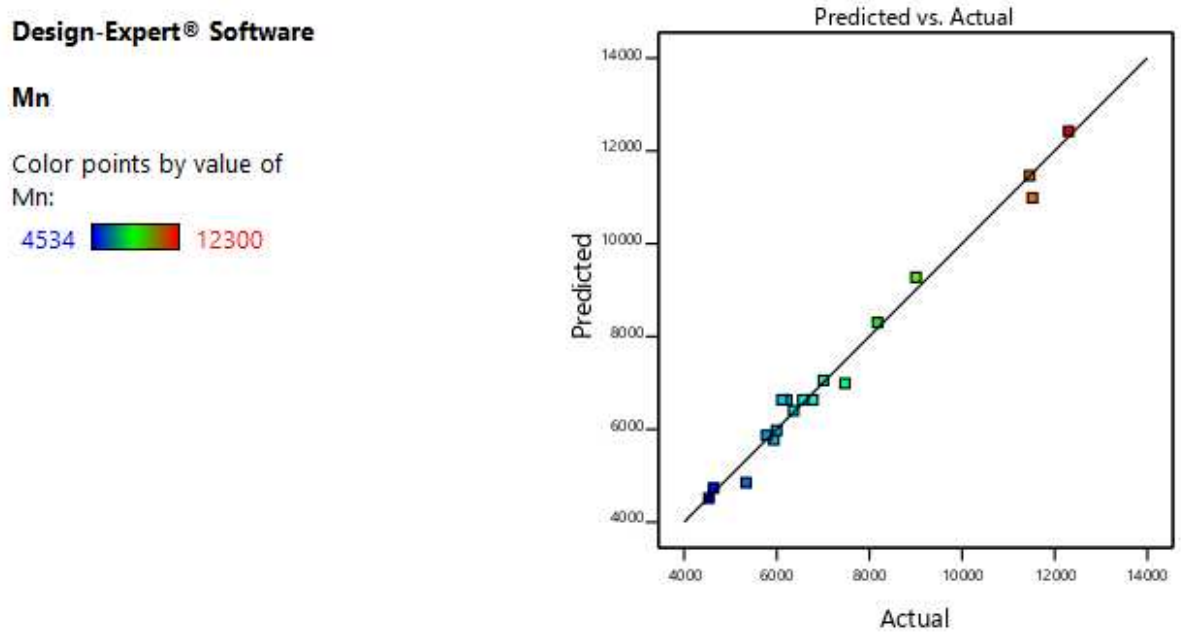

Figure 18. Graph of the predicted *vs*. actual plots in solution polymerization.

Table 8. Final equation in term of actual factors (in-solution polymerization).

M_n	=
-57746.63612	
+102.81721	% w/w enzyme loading
+1409.90006	Temperature
-170.83302	Vacuum
-0.091667	% enzyme * Temperature
-2.09306	% w/w enzyme loading * Vacuum
-2.38562	Temperature * Vacuum
+3.05879	% w/w enzyme loading²
-6.82060	Temperature²
+4.48610	Vacuum²

Table 9. Additional tested point for model confirmation for in solution polymerization.

Variables			***Mn* (g.mol^{-1})**							
Temperature (°C)	% w/w enzyme loading	Vacuum (mbar)	Predicted Mean	Predicted Median	Std Dev	n	SE Pred	95% PI low	Data Mean	95% PI high
90	10	50	6040.86	6040.86	415.602	1	544.717	4784.74	5955	7296.98
100	5.5	50	5814.91	5814.91	415.602	1	544.717	4558.79	6699	7071.03
90	10	10	11533	11533	415.602	1	544.717	10276.9	10340	12789.1
100	5.5	10	11884.6	11884.6	415.602	1	544.717	10628.4	11300	13140.7
100	1	10	11467.9	11467.9	415.602	2	472.773	10377.6	12250	12558.1

As for the effect of the tested variables, the results clearly show that vacuum was the most influential factor on the M_n achieved, where an increase from 50 to 10 mbar resulted in an increase of 4,400 g.mol^{-1} at 80 °C and up to 6,300 g.mol^{-1} at 100 °C showing that vacuum becomes more influential at elevated temperatures. Similarly, the temperature increase had a pronounced effect on the M_n, where an increase of 20 °C from 80 to 100 °C resulted in an increase in M_n by 3,300 g.mol^{-1} when the vacuum was 10 mbar. The effect of temperature did not have the same influence at the lower vacuum level of 50 mbar where the same temperature increase, resulted only in 1,400 g.mol^{-1} increase in M_n (see Figure 20 (a)) increased with the increase in M_n, with all values within a dispersity range of 1.2-1.7. These results arise from a significant interaction between variables, which in this case is an interaction between temperature and vacuum. In other words, the effect of vacuum on M_n is dependent on the level of temperature and vice versa. This vacuum-temperature interaction could be further justified by Clausius-Clapeyron equation where the vapor pressure of liquids increases with the increase in temperature in a non-linear manner [26,27], and thus, at higher temperatures, vacuum application becomes more efficient in the removal of ethanol due to a more pronounced increase in vapor pressure, thus pushing the reaction forward. Additionally, varying the % enzyme loading between 1 and 10% showed no significant effect on M_n (see Figure 20(b), Figure 20(c), suggesting that with 1% w/w N435, the catalyst exceeds the stoichiometric amount of reactive moieties present in the system and is therefore sufficient to catalyze the reaction.

Moving into bulk polymerization, a quadratic model was designed with an R^2=0.9 using the same variables and levels as in solution polycondensation conditions to facilitate comparison.

Table 10 shows the build information of the design model whereas the fit statistics information was introduced in Table 11 showing a predicted R^2=0.9, which was in good agreement with the adjusted R^2 value of 0.93. The adequate Precision value of 18.9 representing the signal to noise ratio indicated an adequate signal, that permits the usage of the model to navigate the design space. The actual *vs.* predicted plot in Figure 19 shows a very good fit between the predicted and actual plots in bulk polymerization. The equation representing the model is presented in terms of the actual factors given in Table 12. Finally, the model was confirmed by running additional experiments that fell within 95% PI (prediction interval) range (see Table 13).

Table 10. Build information of the design model for bulk polymerization.

Study Type	**Response Surface**	**Subtype**	**Randomized**
Design Type	Central Composite	**Runs**	18
Design Model	Quadratic	**Blocks**	No Blocks

Table 11. Fit statistics for bulk polymerization.

Std. Dev.	**292.34**	**R^2**	**0.9697**
Mean	7290.78	**Adjusted R^2**	0.9355
C.V. %	4.01	**Predicted R^2**	0.9000
		Adeq Precision	18.9389

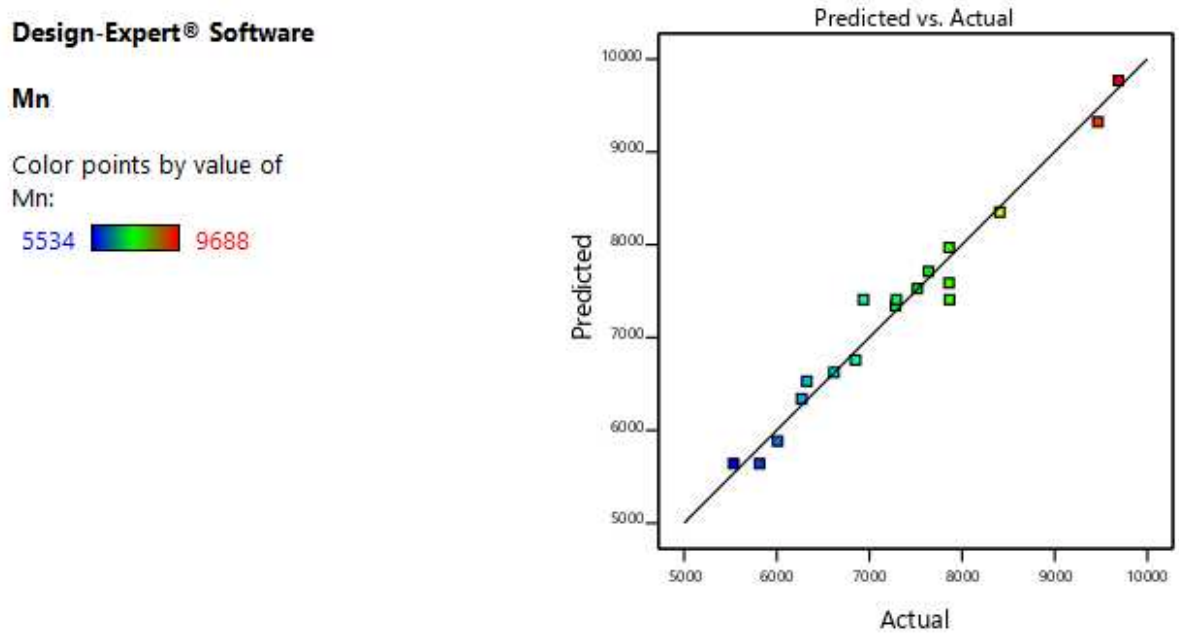

Figure 19. Graph of the predicted *vs.* actual plots in bulk polymerization.

Table 12. Final equation in term of actual factors (bulk polymerization).

M_n	=
-61780.81204	
+1489.13946	Temperature
-674.83906	% w/w enzyme loading
+43.99298	Vacuum
+3.38892	Temperature * % w/w enzyme loading
-0.090008	Temperature * Vacuum
-1.79724	% w/w enzyme loading * Vacuum
-7.95682	Temperature²
+54.80580	% w/w enzyme loading²
-0.874206	Vacuum²

Table 13 Additional tested point for model confirmation for in bulk polymerization.

Variables			**M_n (g.mol^{-1})**							
Temperature (°C)	% w/w enzyme loading	Vacuum (mbar)	Predicted Mean	Predicted Median	Std Dev	n	SE Pred	95% PI low	Data Mean	95% PI high
100	1	10	7528.28	7528.28	292.343	1	390.969	6626.7	7039	8429.85
90	1	10	7729.96	7729.96	292.343	1	383.149	6846.42	7065	8613.5
90	5.5	10	7587.89	7587.89	292.343	1	359.478	6758.93	8221	8416.85
80	10	50	6625.48	6625.48	292.343	1	391.098	5723.6	5832	7527.35
90	5.5	50	6530.09	6530.09	292.343	2	293.411	5853.49	6105.5	7206.7
80	10	10	7970.78	7970.78	292.343	1	390.969	7069.2	7678	8872.35
100	10	10	9768.78	9768.78	292.343	1	389.332	8870.98	9525	10666.6

However, in contrary to the results in solution, the factors tested here had different influence on the M_n of the synthesized polymer, where it was shown that enzyme loading had the most

pronounced effect (see Figure 20(d), Figure 20(e)), followed by temperature, and finally vacuum (see Figure 20(f)) giving a less pronounced effect. Additionally, the M_n achieved in bulk conditions was significantly lower than that achieved in solution following the same conditions. Dispersity (see Table 14) increased with M_n but did not vary beyond the range of 1.2-1.6. These variations are not surprising. In fact, it could be explained by the decrease in diffusion capabilities of growing chains in high viscous mediums. In contrast to solution polymerization, bulk polymerization shows fast and significant increase in viscosity within minutes of vacuum application, leading to complete stop of stirring applied *via* magnetic bars. Having the catalyst in its heterogeneous form, it becomes more and more crucial to maintain adequate mass transfer to allow the polymer growth. In fact, though 1% N435 proved to be as efficient as 10% in solution, the results in bulk conditions showed significant variation between both percentages. This variation should be mainly attributed to the limitations enforced by the decrease in mass transfer rather than the activity of the enzyme, where a higher loading of N435 would rationally occupy more space within the medium, resulting in more interaction between substrates and the enzyme active sites especially when chain movement in the medium is reduced.

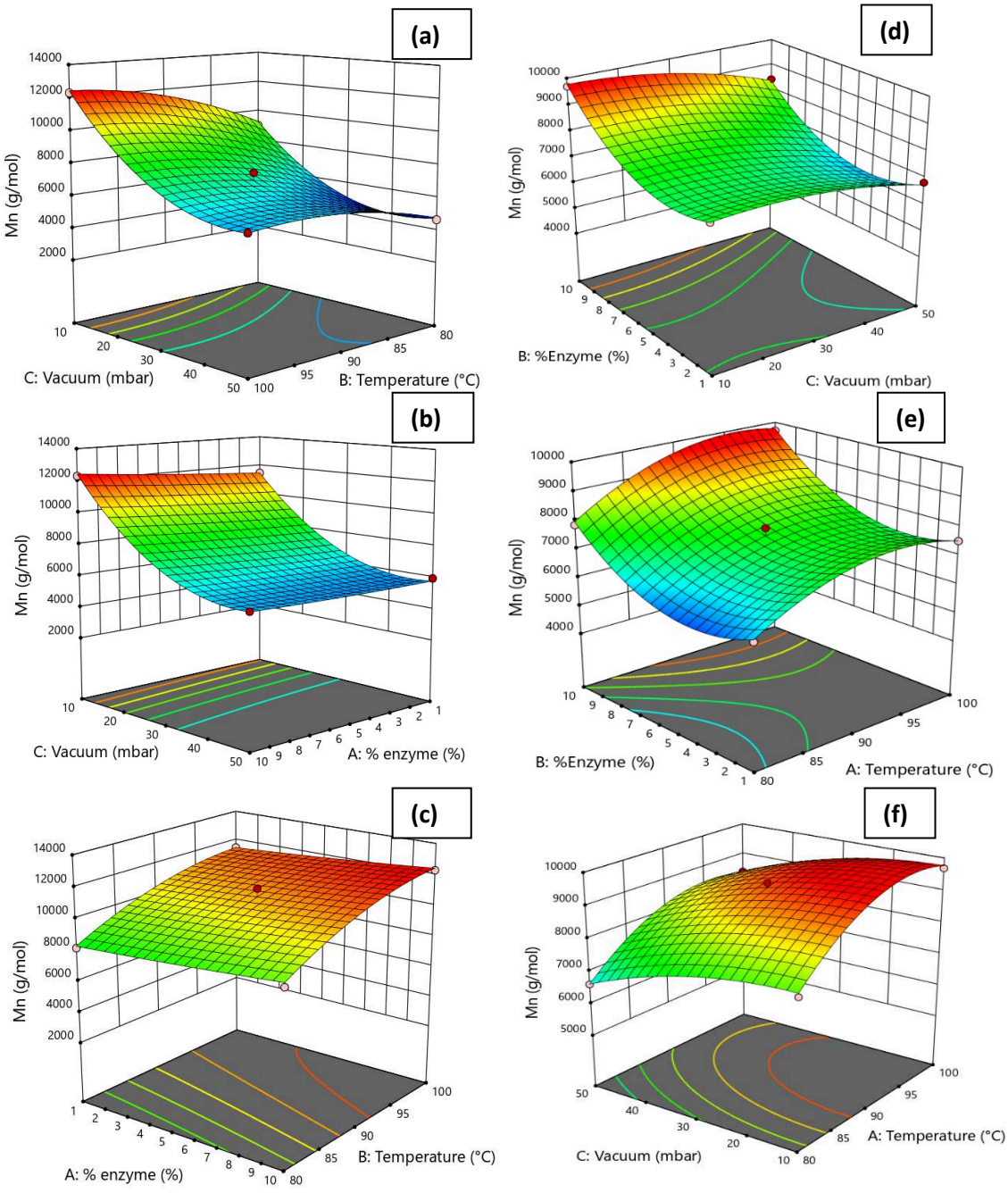

Figure 20. (a) Effect of vacuum and temperature on M_n (solution) at 10% enzyme loading. (b) Effect of vacuum and % enzyme loading on M_n (solution) at 100 °C. (c) Effect of % enzyme loading and temperature on M_n (solution) at 10 mbar of reduced pressure. (d) Effect of vacuum and % loading enzyme on M_n (bulk conditions) at 100 °C. (e) Effect of % enzyme loading and temperature on M_n (bulk conditions) at 10 mbar of vacuum. (f) Effect of vacuum and temperature on M_n (bulk conditions) at 10% enzyme loading. *(The red and pink points

MALDI-TOF MS was used to determine the nature of the end-groups present in the synthesized poly(hexylene adipate). However, due to the quite broad molar mass dispersity (*i.e.,* >1.2) of the polymer samples, mass spectrometry was not useful for determining the molar masses accurately [28]. As such, 16 polymer samples (8 solution and 8 bulk conditions) were analyzed to establish a comparison between both conditions as represented in Table 14. From the MS spectra in Figure 21 representing experiment 1S, three main polyester families were identified being end-functionalized as (1) ester-ester (2) alcohol-alcohol (3) ester-alcohol. Cyclic structure was also probable but only traces were detected. Based on the MALDI-TOF spectrum, ester-alcohol was found to possess the highest intensity, showing that these structures are the most abundant in the sample, as expected. Those results were consistent among all the tested samples in bulk and solution media with no apparent differences.

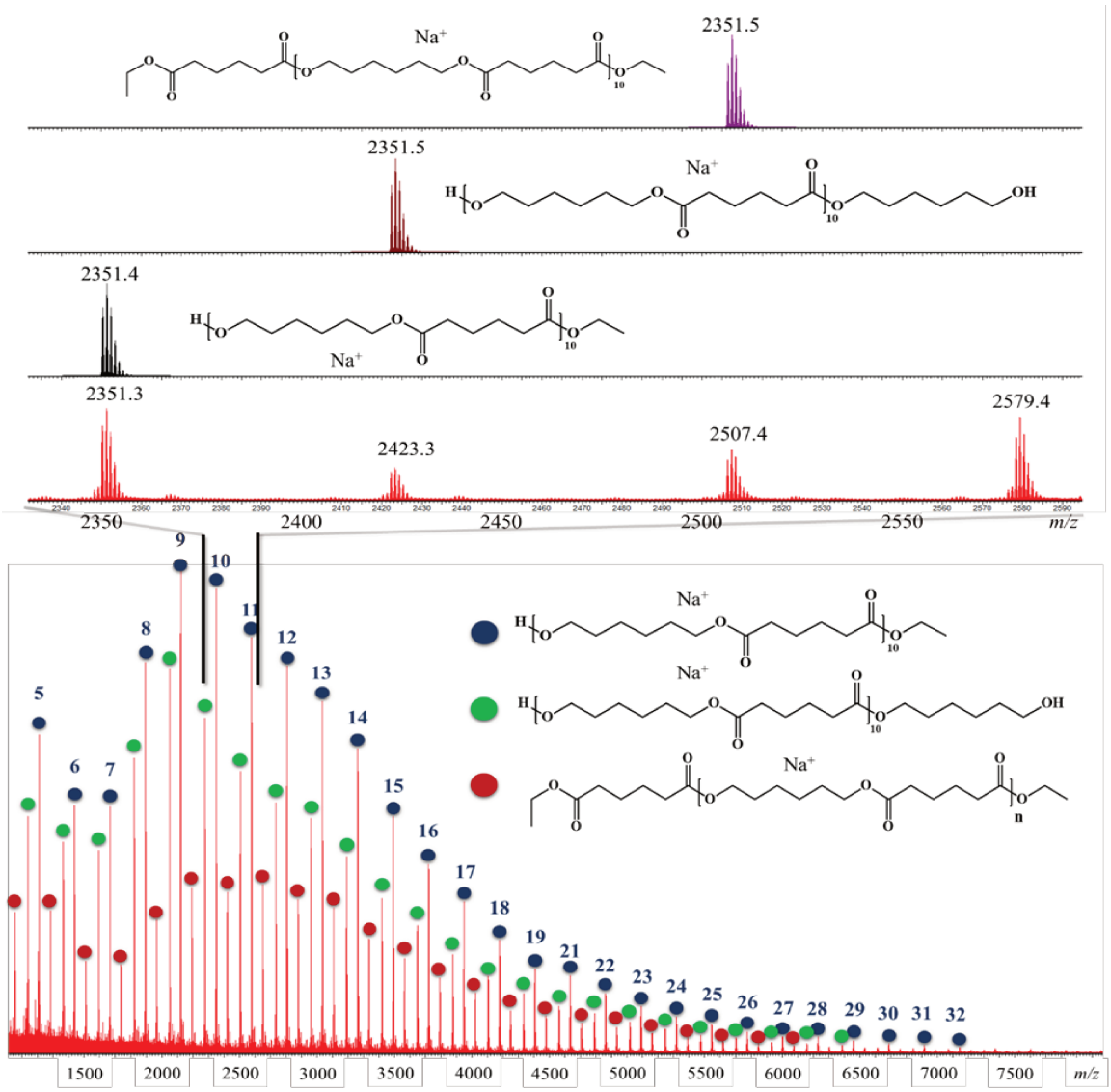

Figure 21. MALDI-TOF mass spectrum recorded for experiment 1S (see Table 14), lower part of the figure represents the global mass spectrum with the 3 main families present in the polymer sample, the number on each signal highlights the number of monomer units for the observed ions. The upper part of the spectrum corresponds to a magnification between m/z 2,300 and m/z 2,600 with a comparison between the theoretical isotopic models (for oligomers with 10 monomer units of diol and diester) and the experimental data confirming the presence of 3 end-groups moieties *i.e.*, ester-ester (red dots), alcohol-alcohol (green dots) and ester-alcohol (blue dots) respectively.

Table 14. Experiments analyzed *via* MALDI-TOF MS for end group determination.

Experimental conditions			**Bulk polycondensation**				**In-solution polycondensation**			
				Determined *via* GPC				Determined *via* GPC		
Enzyme	Temperature	Vacuum		M_n	M_w	dispersity		M_n	M_w	dispersity
% w/w	(°C)	(mbar)	Experiment	(g.mol^{-1})	(g.mol^{-1})		Experiment	(g.mol^{-1})	(g.mol^{-1})	
1	80	50	1B	5,500	6,800	1.2	1S	4,500	5,900	1.3
10	80	50	2B	6,600	8,200	1.2	2S	4,600	6,000	1.3
1	100	50	3B	6,900	9,100	1.3	3S	5,900	7,700	1.3
10	100	50	4B	8,400	10,700	1.3	4S	6,000	8,200	1.4
1	80	10	5B	6,300	8,400	1.3	5S	8,200	11,800	1.5
10	80	10	6B	7,900	11,200	1.4	6S	9,000	13,300	1.5
1	100	10	7B	7,500	10,100	1.3	7S	11,500	17,800	1.6
10	100	10	8B	9,700	15,700	1.6	8S	12,300	19,400	1.6

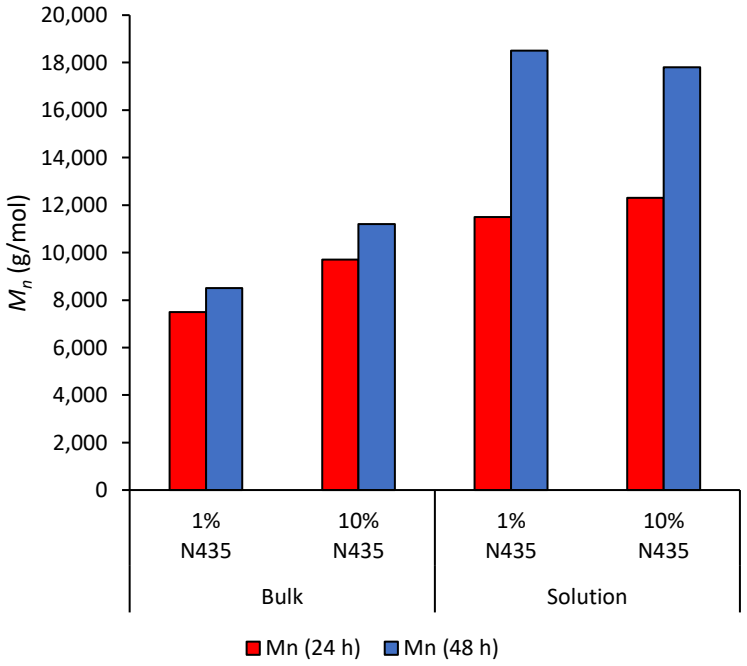

Figure 22 Effect of extending polymerization time on M_n in both solution and bulk conditions.

The limitation imposed by the decrease in mass transfer becomes more apparent when extending the reaction time (see Figure 22), where the M_n of polyesters synthesized in bulk increase only by

30% when extending the reaction time from 24 to 48 h. On the other hand, up to 70% increase in M_n was observed in solution, mainly due to both better mixing and mass transfer. The high positive influence of efficient mixing was previously highlighted using reactive extrusion for the ring-opening polymerization of ω-pentadecalactone, yielding an M_n of 90,000 g.mol^{-1} in only 15 min compared to 22,100 g.mol^{-1} after 72 h in bulk conditions.[29] In this work, the M_n of the first cycle in both mediums was considered as 100%, while the percentage yield was calculated by dividing the actual yield by the theoretical yield, taking into consideration the molar mass of the polyester achieved.

The recyclability of N435 was finally tested for three consecutive cycles in solution (1% w/w N435) (see Figure 23) and bulk conditions (0.5, 1, and 10% w/w N435) (see Figure 24). The results for solution polycondensation showed ~17% drop in M_n during the second cycle from 12,100 to 10,000 g.mol^{-1}, however, no significant changes were observed during the third cycle.

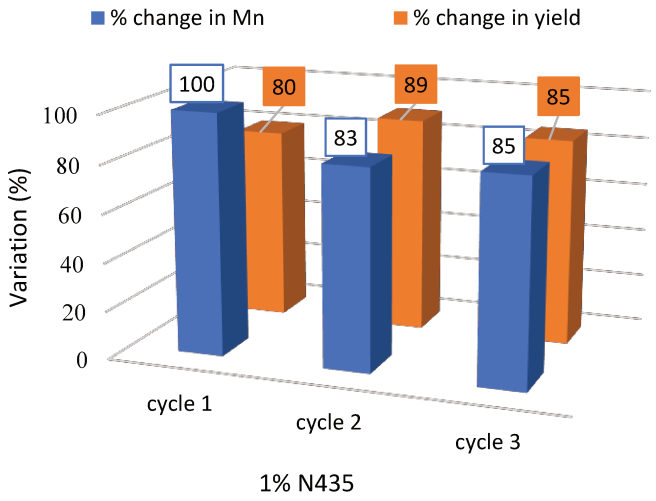

Figure 23. Effect of recycling 1% N435 on M_n and yield in solution.

On the other hand, the recyclability assays in bulk conditions showed better consistency during the three cycles where the M_n dropped by a maximum of 8% in the third cycle with 1% N435, and to a lower extent with 0.5 and 10% N435, knowing that it was considered insignificant as it falls

within the error range of the GPC analysis. As such, for bulk polymerization, even at relatively high temperature (100 °C), N435 can be effectively reused at least for three consecutive cycles giving similar results in terms of M_n and yield as observed in Figure 24. The more pronounced drop in N435 activity in diphenyl ether medium can be attributed to several reasons. First, the use of diphenyl ether as a solvent attributed to a better heat transfer in the system, and thus, the enzyme will be more prone to elevated temperatures in comparison to bulk, which would result in a more pronounced enzyme degradation or leaching. Additionally, due to the fact that N435 is prepared *via* interfacial activation of lipases *vs.* supports with hydrophobic surfaces, the enzyme becomes more susceptible to be released in the presence of organic solvents [9,30,31].

However, this remains a speculation within the current study and further studies are needed to determine the reason behind the drop in N435 activity in solution.

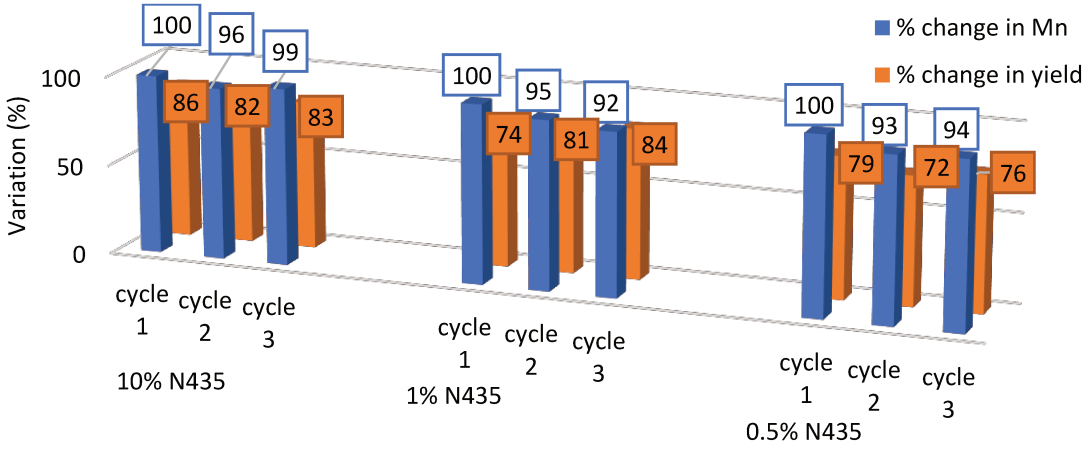

Figure 24. Effect of recycling 0.5, 1 and 10% N435 on M_n and yield in bulk conditions.

2.3 Conclusion

The polycondensation reaction of hexane-1,6-diol and diethyl adipate was studied in both diphenyl ether and bulk media using Novozym 435 as biocatalyst. The oligomerization time was optimized where the maximum monomer conversion was confirmed after a maximum of 2 h from the start of the reaction, thus preventing any unnecessary time extension for the oligomerization step. Following, a face centered central composite design was used to develop a quadratic model that showed how temperature, vacuum, and % enzyme loading can affect M_n. In diphenyl ether,

vacuum showed to be the most influential factor in relation to M_n, followed by temperature, and finally % enzyme loading that showed no significant effect. This relation between the independent variables and M_n showed an opposite relation in bulk where % enzyme loading had the most significant impact on M_n, followed by temperature and vacuum respectively. The models were confirmed by running additional experiments, where their results were within the acceptable prediction interval, confirming that the models can be adequately used to predict the M_n of the polymer at any level within the tested factor ranges. Recyclability assays showed a more efficient recycling for N435 in bulk conditions (consistent results up to 3 cycles) in comparison to diphenyl ether that showed a drop of activity by 17% for the second cycle. Finally, this work introduced a green method to produce poly(hexylene adipate) and control its M_n. After establishing a better understanding on the impact of key parameters, future research will enlarge on the findings of this work, to explore the feasibility of using Novozym 435 for the polymerization of different monomers. Mainly, next chapter will focus on the enzymatic catalysis of aromatic groups, where we will assess the efficiency of Novozym 435 in catalyzing the synthesis of semi-aromatic terpolymers, and how adjusting certain variables, such as the diol length, can lead to major differences in polymer growth.

2.4 Materials and Methods

2.4.1 Materials

hexane-1,6-diol (97%), diethyl adipate (99%) and diphenyl ether (99%) were purchased from Sigma-Aldrich (Lyon, France). Analytical grade methanol, tetrahydrofuran (THF), chloroform (99%) and toluene were purchased from VWR (Fontenay-sous-Bois, France). All the reagents and solvents were used as received. Novozym 435 (N435), a *Candida antarctica* Lipase B (CALB) immobilized on a porous acrylic resin was kindly provided by Novozymes (Bagsværd, Denmark) (activity = 10,000 propyl laurate units (PLU)/g). Chloroform D ($CDCl_3$) (99.8%) was purchased from Euriso-Top (Saint-Aubin, France).

2.4.2 General procedure of the enzymatic polycondensation of hexane-1,6-diol and diethyl adipate

Equimolar amounts (4 mmol) of hexane-1,6-diol and diethyl adipate were weighed and added into a schlenk tube. A predetermined amount varied between 1 and 10% w/w of N435 (relative to the total weight of the monomers) was weighed and added to the mixture. For solution polymerization, 1 mL of diphenyl ether was added as a solvent of choice, whereas for bulk polymerization, the reaction was commenced with no additional steps. The reaction proceeded under atmospheric pressure for 2 h at a preset temperature between 80 and 100 °C (using an oil bath with continuous stirring kept constant at 350 rpm). Afterwards, the schlenk tube was attached to a vacuum line, and the pressure was decreased gradually in 1 h to reach a predetermined value between 10 and 50 mbar to remove byproduct (ethanol). After applying the vacuum, the reaction was left to proceed for 24 h and got stopped by adding an excess amount of chloroform under atmospheric pressure after a cooling step, followed by direct filtration to remove the N435 beads. The filtrate was then partially evaporated using a rotavap, followed by the addition of excess amount of cold methanol to precipitate the obtained polymer. The mixture was then filtered, and the product obtained was left to dry at room temperature for 24 h before collecting and weighing.

2.4.3 Effect of solvent volume on the achieved number-average molecular weight (M_n)

For solution polymerization, diphenyl ether was chosen as a solvent. To determine the effect of volume variation, the polycondensation reaction was carried out with different volumes at 100 °C at 1% w/w N435 for 2 h oligomerization followed by an additional 24 h polymerization under 10 mbar of vacuum (see Table 4). The reaction was then confirmed *via* ^{1}H NMR analysis.

2.4.4 Effect of the oligomerization step time on conversion in solution and bulk

The conversion was monitored by exploiting the ^{1}H NMR signals at δ= 4.11- 4.14 of the methylene group (CH_3-CH_2-O-) of diethyl adipate (DEA) in addition to the signals at δ= 4.06 of the methylene (-O-CH_2-C_4H_8-CH_2-O-) of the poly(hexylene adipate).

2.4.5 Effect of the oligomerization step time on the achieved number-average molecular weight (M_n) after 24 h of post vacuum application in bulk

Two-step polycondensation reactions were set up to run with a tunable oligomerization time (2, 4, and 6 h) at constant temperature (90 °C), % w/w enzyme loading (5.5%), and followed by a secondary 24 h step under vacuum (10 mbar) application. M_n was determined by GPC analysis.

2.4.6 N435 recyclability

The polycondensation protocol of hexane-1,6-diol and diethyl adipate was followed as mentioned before, the temperature was kept constant at 100 °C and the oligomerization step at 2 h. At the end of each polymerization cycle, the separated N435 beads were washed 3 times with excess chloroform, then left to dry at room temperature for 24 h under atmospheric pressure and reused for three consecutive cycles.

2.4.7 Analytical methods

2.4.7.1 ^{1}H NMR analysis

Approximately 5 mg of hexane-1,6-diol, diethyl adipate, and the recovered poly(hexylene adipate) were directly dissolved in three NMR tubes containing 0.5 mL of $CDCl_3$. The ^{1}H NMR spectra of the monomers, and the recovered polymer were recorded at room temperature on a Bruker Avance 300 instrument (Bruker, Billerica, MA, USA), (delay time = 3 s, number of scans = 32) at 300.13 MHz. Chemical shifts (ppm) were calibrated using the residual signal of $CDCl_3$ at 7.26 ppm. Additionally, ^{1}H NMR was used to confirm conversion. Data acquisition and analysis were performed using the Bruker TopSpin 3.2.

2.4.7.2 GPC analysis

Gel permeation chromatography analysis was performed in THF as eluent (flow rate of 1 mL/min) at 40 °C using Alliance e2695 apparatus (Waters, Milford, MA, USA) with a sample concentration around 10-15 $mg.mL^{-1}$. A refractive index detector Optilab T-rEX (WYATT Optilab T-Rex, Santa Barbara, CA, USA) was used as a detector, and a set of columns: HR1, HR2 and HR4 (Water Styragel, (Water Styragel, Milford, MA, USA) were utilized. The molecular weight calibration curve was obtained using monodisperse polystyrene standards.

2.4.7.3 MALDI-TOF MS analysis

Positive-ion Matrix assisted LASER Desorption/Ionization-Mass Spectrometry (MALDI-MS) experiments were performed using a Waters QToF Premier mass spectrometer (Waters, Milford, MA, USA equipped with a Nd:YAG laser operating at 355 nm (third harmonic) with a maximum output of 65 μJ delivered to the sample in 2.2 ns pulses at 50Hz repeating rate. Time-of-flight mass

analysis was performed in the reflectron mode at a resolution of about 10 k (m/z 569). All samples were analyzed using trans-2-[3-(4-*tert*-butylphenyl)-2-methylprop-2-enylidene]malononitrile (DCTB) as a matrix. Polymer samples synthesized in bulk as well as in solution conditions were dissolved in THF to obtain 1 $mg.mL^{-1}$ solution. Additionally, 40 µL of 2 $mg.mL^{-1}$ NaI solution in acetonitrile was added to the polymer solution.

2.4.7.4 Statistical analysis

A face centered central composite design (CCD) was used to optimize the polycondensation reaction of poly(hexylene adipate) in terms of the established number-average molecular weight (M_n). A CCD is an experimental designed used to determine the effect and interaction of several factors and develop a response model. This design consists of 3 levels represented as (-1, 0, 1), where the center point (0) is replicated several times to determine variability and improve predictability. In the following work, 3 factors were tested at 3 levels being temperature (80, 90, 100 °C), % w/w enzyme loading (1, 5.5, 10%), vacuum (10, 30, 50 mbar). The models were developed and analyzed by Design-Expert 11®. The models were confirmed by running additional experiments that fell within 95% PI (prediction interval) range (see Table 9 and Table 13).

2.5 References

(1) Gross, R. A.; Ganesh, M.; Lu, W. Enzyme-Catalysis Breathes New Life into Polyester Condensation Polymerizations. *Trends Biotechnol.* **2010**, *28* (8), 435–443. https://doi.org/10.1016/j.tibtech.2010.05.004.

(2) Douka, A.; Vouyiouka, S.; Papaspyridi, L.-M.; Papaspyrides, C. D. A Review on Enzymatic Polymerization to Produce Polycondensation Polymers: The Case of Aliphatic Polyesters, Polyamides and Polyesteramides. *Prog. Polym. Sci.* **2018**, *79*, 1–25. https://doi.org/10.1016/j.progpolymsci.2017.10.001.

(3) Hilker, I.; Rabani, G.; Verzijl, G. K. M.; Palmans, A. R. A.; Heise, A. Chiral Polyesters by Dynamic Kinetic Resolution Polymerization. *Angew. Chem. Int. Ed.* **2006**, *45* (13), 2130–2132. https://doi.org/10.1002/anie.200503496.

(4) Chaudhary, A. K.; Lopez, J.; Beckman, E. J.; Russell, A. J. Biocatalytic Solvent-Free Polymerization To Produce High Molecular Weight Polyesters. *Biotechnol. Prog.* **1997**, *13* (3), 318–325. https://doi.org/10.1021/bp970024i.

(5) Kirk, O.; Christensen, M. W. Lipases from Candida Antarctica: Unique Biocatalysts from a Unique Origin. *Org. Process Res. Dev.* **2002**, *6* (4), 446–451. https://doi.org/10.1021/op0200165.

(6) Kobayashi, S. Recent Developments in Lipase-Catalyzed Synthesis of Polyesters. *Macromol. Rapid Commun.* **2009**, *30* (4–5), 237–266. https://doi.org/10.1002/marc.200800690.

(7) Lozano, P.; Diego, T. de; Carrié, D.; Vaultier, M.; Iborra, J. L. Lipase Catalysis in Ionic Liquids and Supercritical Carbon Dioxide at 150 °C. *Biotechnol. Prog.* **2003**, *19* (2), 380–382. https://doi.org/10.1021/bp025759o.

(8) Jiang, Y.; Woortman, A. J. J.; Ekenstein, G. O. R. A. van; Loos, K. A Biocatalytic Approach towards Sustainable Furanic–Aliphatic Polyesters. *Polym. Chem.* **2015**, *6* (29), 5198–5211. https://doi.org/10.1039/C5PY00629E.

(9) Ortiz, C.; Ferreira, M. L.; Barbosa, O.; Santos, J. C. S. dos; Rodrigues, R. C.; Berenguer-Murcia, Á.; Briand, L. E.; Fernandez-Lafuente, R. Novozym 435: The "Perfect" Lipase Immobilized Biocatalyst? *Catal. Sci. Technol.* **2019**, *9* (10), 2380–2420. https://doi.org/10.1039/C9CY00415G.

(10) Hillmyer, M. A.; Tolman, W. B. Aliphatic Polyester Block Polymers: Renewable, Degradable, and Sustainable. *Acc. Chem. Res.* **2014**, *47* (8), 2390–2396. https://doi.org/10.1021/ar500121d.

(11) Linko, Y.-Y.; Lämsä, M.; Wu, X.; Uosukainen, E.; Seppälä, J.; Linko, P. Biodegradable Products by Lipase Biocatalysis. *J. Biotechnol.* **1998**, *66* (1), 41–50. https://doi.org/10.1016/S0168-1656(98)00155-2.

(12) Linko, Y.-Y.; Wang, Z.-L.; Seppälä, J. Lipase-Catalyzed Synthesis of Poly(1,4-Butyl Sebacate) from Sebacic Acid or Its Derivatives with 1,4-Butanediol. *J. Biotechnol.* **1995**, *40* (2), 133–138. https://doi.org/10.1016/0168-1656(95)00039-S.

(13) Kosugi, Y.; Kunieda, T.; Azuma, N. Continual Conversion of Free Fatty Acid in Rice Bran Oil to Triacylglycerol by Immobilized Lipase. *J. Am. Oil Chem. Soc.* **1994**, *71* (4), 445–448. https://doi.org/10.1007/BF02540528.

(14) Poojari, Y.; Palsule, A. S.; Cai, M.; Clarson, S. J.; Gross, R. A. Synthesis of Organosiloxane Copolymers Using Enzymatic Polyesterification. *Eur. Polym. J.* **2008**, *44* (12), 4139–4145. https://doi.org/10.1016/j.eurpolymj.2008.07.043.

(15) Jiang, Z. Lipase-Catalyzed Synthesis of Aliphatic Polyesters *via* Copolymerization of Lactone, Dialkyl Diester, and Diol. *Biomacromolecules* **2008**, *9* (11), 3246–3251. https://doi.org/10.1021/bm800814m.

(16) Braiuca, P.; Ebert, C.; Basso, A.; Linda, P.; Gardossi, L. Computational Methods to Rationalize Experimental Strategies in Biocatalysis. *Trends Biotechnol.* **2006**, *24* (9), 419–425. https://doi.org/10.1016/j.tibtech.2006.07.001.

(17) Sarotti, A. M.; Spanevello, R. A.; Suárez, A. G. An Efficient Microwave-Assisted Green Transformation of Cellulose into Levoglucosenone. Advantages of the Use of an Experimental Design Approach. *Green Chem.* **2007**, *9* (10), 1137–1140. https://doi.org/10.1039/B703690F.

(18) Chang, S.-W.; Shaw, J.-F.; Yang, K.-H.; Shih, I.-L.; Hsieh, C.-H.; Shieh, C.-J. Optimal Lipase-Catalyzed Formation of Hexyl Laurate. *Green Chem.* **2005**, *7* (7), 547–551. https://doi.org/10.1039/B501724F.

(19) Itabaiana, I.; Sutili, F. K.; Leite, S. G. F.; Gonçalves, K. M.; Cordeiro, Y.; Leal, I. C. R.; Miranda, L. S. M.; Ojeda, M.; Luque, R.; Souza, R. O. M. A. de. Continuous Flow Valorization of Fatty Acid Waste Using Silica-Immobilized Lipases. *Green Chem.* **2013**, *15* (2), 518–524. https://doi.org/10.1039/C2GC36674F.

(20) Pellis, A.; Ferrario, V.; Cespugli, M.; Corici, L.; Guarneri, A.; Zartl, B.; Acero, E. H.; Ebert, C.; Guebitz, G. M.; Gardossi, L. Fully Renewable Polyesters *via* Polycondensation Catalyzed by Thermobifida Cellulosilytica Cutinase 1: An Integrated Approach. *Green Chem.* **2017**, *19* (2), 490–502. https://doi.org/10.1039/C6GC02142E.

(21) Azim, H.; Dekhterman, A.; Jiang, Z.; Gross, R. A. Candida Antarctica Lipase B-Catalyzed Synthesis of Poly(Butylene Succinate): Shorter Chain Building Blocks Also Work. *Biomacromolecules* **2006**, *7* (11), 3093–3097. https://doi.org/10.1021/bm060574h.

(22) Mahapatro, A.; Kalra, B.; Kumar, A.; Gross, R. A. Lipase-Catalyzed Polycondensations: Effect of Substrates and Solvent on Chain Formation, Dispersity, and End-Group Structure. *Biomacromolecules* **2003**, *4* (3), 544–551. https://doi.org/10.1021/bm0257208.

(23) Kulshrestha, A. S.; Gao, W.; Gross, R. A. Glycerol Copolyesters: Control of Branching and Molecular Weight Using a Lipase Catalyst. *Macromolecules* **2005**, *38* (8), 3193–3204. https://doi.org/10.1021/ma0480190.

(24) Carothers, W. H. Polymers and Polyfunctionality. *Trans. Faraday Soc.* **1936**, *32* (0), 39–49. https://doi.org/10.1039/TF9363200039.

(25) Jiang, Y.; Woortman, A. J. J.; Alberda van Ekenstein, G. O. R.; Loos, K. Enzyme-Catalyzed Synthesis of Unsaturated Aliphatic Polyesters Based on Green Monomers from Renewable Resources. *Biomolecules* **2013**, *3* (3), 461–480. https://doi.org/10.3390/biom3030461.

(26) Speight, J. G. *Reaction Mechanisms in Environmental Engineering: Analysis and Prediction*; Butterworth-Heinemann, 2018.

(27) Speight, J. G. *Environmental Organic Chemistry for Engineers*; Butterworth-Heinemann, 2016.

(28) Martin, K.; Spickermann, J.; Räder, H. J.; Müllen, K. Why Does Matrix-Assisted Laser Desorption/Ionization Time-of-Flight Mass Spectrometry Give Incorrect Results for Broad Polymer Distributions? *Rapid Commun. Mass Spectrom.* **1996**, *10* (12), 1471–1474. https://doi.org/10.1002/(SICI)1097-0231(199609)10:12<1471::AID-RCM693>3.0.CO;2-X.

(29) Spinella, S.; Ganesh, M.; Re, G. L.; Zhang, S.; Raquez, J.-M.; Dubois, P.; Gross, R. A. Enzymatic Reactive Extrusion: Moving towards Continuous Enzyme-Catalysed Polyester Polymerisation and Processing. *Green Chem.* **2015**, *17* (8), 4146–4150. https://doi.org/10.1039/C5GC00992H.

(30) Rueda, N.; Santos, J. C. S. dos; Torres, R.; Ortiz, C.; Barbosa, O.; Fernandez-Lafuente, R. Improved Performance of Lipases Immobilized on Heterofunctional Octyl-Glyoxyl Agarose Beads. *RSC Adv.* **2015**, *5* (15), 11212–11222. https://doi.org/10.1039/C4RA13338B.

(31) Santos, J. C. S. dos; Rueda, N.; Sanchez, A.; Villalonga, R.; Gonçalves, L. R. B.; Fernandez-Lafuente, R. Versatility of Divinylsulfone Supports Permits the Tuning of CALB Properties during Its Immobilization. *RSC Adv.* **2015**, *5* (45), 35801–35810. https://doi.org/10.1039/C5RA03798K.

3. The impact of diethyl furan-2,5-dicarboxylate as aromatic biobased monomers towards lipase-catalyzed synthesis of semi-aromatic copolyesters

3.1 Introduction

Furan-2,5-dicarboxylic acid (FDCA) has been given a lot of attention in recent years as (co)monomers, due to its ease of production from biomass and its aromaticity. FDCA is a biobased monomer synthesized by oxidation of 5-hydroxymethylfurfural, which is by turn the dehydration product of hexoses such as fructose and glucose.[1–3] There are many new research works, implementing FDCA as an alternative (co)monomer to petroleum-based terephthalic acid (TPA) that is vastly used in the synthesis of aromatic polyesters, notably polyethylene terephthalate (PET) and polybutylene terephthalate (PBT). This trend favoring FDCA stems from the structural similarities between both monomers as both are aromatic rings with two oppositely positioned carboxylic groups.[4,5] In addition, FDCA bioproduction route is easily accessible when compared to the challenging and inefficient TPA bioproduction.[6–9] When polymerized, aromatic polyesters produced from FDCA instead of TPA show very competitive properties that are in some cases being considered far superior to TPA-based polyesters.[10–12]

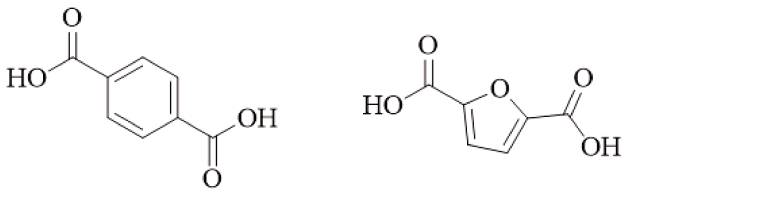

Terephthalic acid Furan-2,5-dicarboxylic acid

Scheme 17. Structures of terephthalic acid (TPA) and furan-2,5-dicarboxylic acid (FDCA).

In general, semi-aromatic polyesters are structurally designed on the basis of both aliphatic as well as aromatic (co)monomeric units. The incorporation of aromatic units into the polymer structure helps increasing the rigidity, hydrophobicity, and thermal properties of the polymeric backbone, whereas the aliphatic units in the form of aliphatic diacids or diols serve enhancing the flexibility of the polymeric structure and lowering its glass transition temperature (T_g).[13,14] Accordingly, the combination of aliphatic and aromatic groups in semi-aromatic polyesters such as PET, and PBT have shown a great enhancement of properties and expanded the scope of their applications, ranging from plastic bottles to synthetic fibers and food packaging.[15,16]

In recent years, many furan-based polyesters and polyamides have been synthesized,[17] and many research works focused on comparing them to their TPA-based counterparts.[18–20] For example, *via* a two-step polycondensation process in the presence of Titanium isopropoxide ($Ti(O\text{-}i\text{-}Pr)_4$) as catalyst, Knoop *et al.*[11] synthesized a series of polyethylene (PEF), polypropylene (PPF), and polybutylene (PBF) furanoates of medium molecular weights that are comparable to their TPA analogs, and showing less coloration. Moreover, furan-based polyesters have shown to present enhanced gas barrier properties when compared to their TPA counterparts.[21,22] Regarding their mechanical properties, PEF was found to be similar to PET in terms of its Young's modulus and maximum stress values. In contrast, PEF was shown to be significantly more brittle than PET.[23] In another interesting study, the PBF ductility was found to significantly increase as a function of the molecular weight, reaching Young's modulus and elongation values comparable to the reported values of commercial PBT when the number average molecular weight (M_n) was > 16,000 $g.mol^{-1}$. In contrast, lower values of Young's modulus and elongation at break were reported when the M_n was ~7,000 $g.mol^{-1}$. This difference was suggested to originate from the insufficient number of entanglements at lower molecular weight values.[12]

Although the literature is rich in examples of enzyme-catalyzed polyesterification to produce aliphatic polyesters, the synthesis of aromatic polyesters remains less studied mainly due to the need to use elevated reaction temperatures when dicarboxylic aromatic (co)monomers are used. Nevertheless, several promising attempts have been noted to synthesize aromatic and semi-aromatic polyesters *via* enzymatic catalysis, which can be manageable at lower temperatures by substituting diacid monomers with their methyl or ethyl diester analogous. However, such polyesters were ill-defined with their low molecular weights, mainly due to side reactions such as

ether formation as well as to the low temperature used, leading to phase separation of the end-product and limited the polymer growth.[24,25] In an attempt to overcome this limitation, Jian *et al.*[26] performed a two-step polycondensation reaction using Novozym 435 (N435) as a catalyst, which is a *Candida antarctica* lipase B (CALB) immobilized on an acrylic resin. The results obtained showed that for the polyesterification reaction between dimethyl furan-2,5-dicarboxylate (DMFDCA) and different aliphatic diols, being hexane-1,6-diol, octane-1,8-diol, and decane-1,10-diol at a temperature of 140 °C, the polyesters obtained possessed a high number average molecular weight (M_n) of 41,100, 41,000, and 51,600 g.mol^{-1}, respectively. Those values exceeded the values obtained at 80 °C by more than 10-folds. As enzymatic catalysis proved to be better suitable for oligomer production, several attempts to synthesize furan-based oligomers *via* enzymatic catalysis were approached in recent years, where different aromatic and semi-aromatic oligomers were produced.[27,28]Other attempts to synthesize semi-aromatic diesters *via* enzymatic catalysis were reported by Pellis *et al*.[29] Aliphatic diols varying in chain length between C_4-C_8 were reacted with several aromatic monomers such as diethyl furan-2,5-dicarboxylate, diethyl terephthalate, diethyl isophthalate, in addition to different isomers of pyridine dicarboxylic acid. The results showed that the reaction between 2,4-diethyl pyridine dicarboxylate and octane-1,8-diol in diphenyl ether led to the highest molecular weight (M_n = 14,300 g.mol^{-1}).

Although semi-aromatic polyesters such as PET and PBT or their furan counterparts possess good physical properties, they are however resistant to biodegradation.[30,31] To tackle this, semi-aromatic terpolyesters such as polybutylene adipate terephthalate (PBAT) were developed, consisting of aromatic and aliphatic units, showing adequate mechanical properties while being biodegradable at the same time.[32] In fact, the biodegradation of such copolyesters was due to the presence of aliphatic repeating units such as butylene adipate (BA) in PBAT, which were more susceptible to hydrolysis and microorganism attacks than the semi-aromatic butylene terephthalate (BT).[32,33] In a study conducted by Herrera *et al*.[34] PBAT with an adipate/terephthalate ratio of 60/40 was found to degrade at a faster rate than PBAT with a higher terephthalate content (40/60). Such findings could allow for an adequate control over the properties and degradation time of semi-aromatic copolyesters such as PBAT simply by tuning the adipate/terephthalate ratio. With the biodegradability advantage of such copolyesters, in addition to the advantages of furan based polyesters, research have been focusing in recent years on developing furan based copolyesters

such as polybutylene adipate furanoate (PBAF) aiming to produce biobased polymers which are also biodegradable and possess adequate properties allowing them to compete with TPA based polymers.[35–40]

Although enzymatically catalyzed synthesis of furan-based polyesters such as PBF, among other types were recently reported in the literature,[17,25,26] the enzymatic synthesis of furan-based terpolyesters, on the other hand, was less studied. Morales-Huerta *et al.*[41] synthesized poly(butylene furan-2,5-dicarboxylate-*co*-succinate) *via* the ring-opening polymerization of cyclic butylene furan-2,5-dicarboxylate and butylene succinate oligomers yielding copolyesters with a M_n ranging between 16,000 and 31,000 g.mol^{-1} where Novozym 435 was loaded at 40% w/w relative to the totality of the concentration of the monomers. On the other hand, the enzymatic polycondensation approach towards semi-aromatic copolyesters was reported by Maniar *et al*.[42] by reacting DMFDCA, 2,5-bis(hydroxymethyl)furan (BHMF), along with aliphatic linear diols and diacid ethyl esters. The highest M_n was achieved when using octane-1,8-diol reaching 16,000 g.mol^{-1} after 72 h under vacuum and a temperature varied between 80 and 95 °C.

Previously, we have introduced a statistical approach that allowed us to predict the M_n of poly(hexylene adipate) simply by tuning the values of certain parameters such as vacuum, enzyme loading and temperature.[43] In our current work, and based on the promising properties of furan-based terpolyesters, such as their excellent mechanical properties and biodegradability we investigate herein the enzyme-catalyzed synthesis of furan-based semi-aromatic terpolyesters by reacting diethyl furan-2,5-dicarboxylate (DEFDC), with variable aliphatic linear dicarboxylic esters, and diols. A special emphasis was made on the influence of furan loading, and the chain length of diols and diesters, and how such factors can influence the reactivity, molecular weight, and thermal properties of the end-product. In addition, amorphous fatty dimer diol such as Pripol 2033 ((9*Z*,12*Z*)-18-[(6*Z*,9*Z*)-18-hydroxyoctadeca-6,9-dienoxy]octadeca-9,12-dien-1-ol) was tested for its influence on improving the reactivity in the system where enzymatic catalysis was limited.

3.2 Results and discussion

Following the general procedure above, the polycondensation of different diols, with diethyl adipate and DEFDC in the presence of N435 (see Scheme 18) was conducted in diphenyl ether, as it was previously reported to be the more suitable solvent to achieve high conversion and molecular weights.[44–46] While maintaining the equimolarity between the diols and the diesters, the molar percent of DEFDC relative to the aliphatic diester was varied between 0 and 90%. Different aliphatic diols tested as (co)monomers were butane-1,4-diol, hexane-1,6-diol, octane-1,8-diol, decane-1,10-diol, and dodecane-1,12-diol.

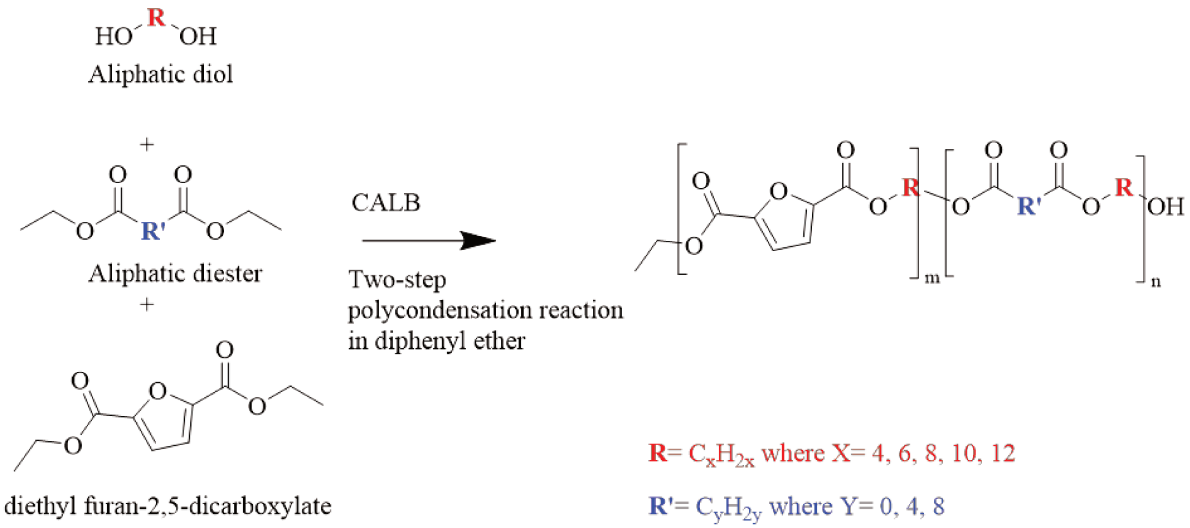

Scheme 18. Polycondensation reaction of variable diols, diethyl adipate, and DEFDC in the presence of N435 as catalyst.

The impact of the diol length and furan content on the final copolymer properties were both assessed in terms of copolymer composition (X-furan), conversion (%), yield by weight (%), number average molecular weight (M_n), dispersity ($Đ_M$) and degree of polymerization (D.P.) given in Table 15. Peak assignments are provided in Figure 25.

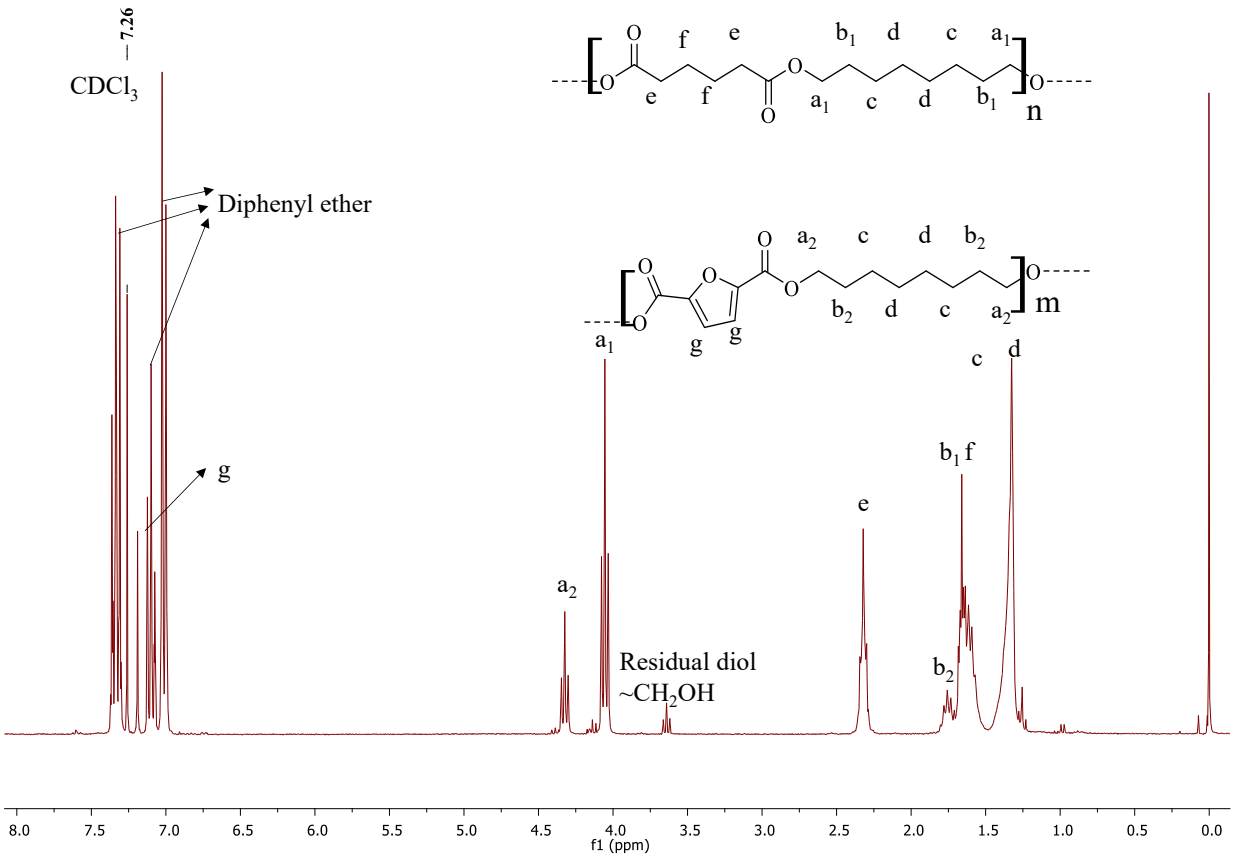

Figure 25. 1H NMR spectrum (CDCl3, 300 MHz) of the crude reaction of octane-1,8-diol, diethyl furan-2,5-dicarboxylate and diethyl adipate in diphenyl ether (1 mL), and the yielded copolyester after a two-step polycondensation reaction at 100 °C and 20% w/w enzyme.

Table 15. Molecular structure analysis (X-furan), % conversion, % yield, M_n, $Đ_M$ and D.P. of furan-based *co*-polyesters with variable furan content and aliphatic diols.

Entry	Diol[1]	DEFDC feed (%)[2]	X-furan (%)[3]	Conversion (%)[4]	Yield by weight (%)	M_n (g.mol^{-1})[5]	$Đ_M$[6]	D.P.[7]
1	**C_4**	**0**	0	98	85	16,000	1.80	80
2	**C_4**	10	12	86	68	4,900	1.93	24
3	**C_4**	25	27	95	62	1,300	6.9	6
4	**C_4**	50	-	-	-	-	-	-
5	**C_6**	0	0	97	91	9,200	1.80	40
6	**C_6**	10	12	95	77	9,400	1.61	41
7	**C_6**	25	27	98	82	11,100	2.13	48
8	**C_6**	50	51	98	87	9,600	2.09	41
9	**C_6**	75	75	96	90	3,800	1.91	16
10	**C_6**	90	78	48	0	-	-	-
11	**C_8**	0	0	94	88	9,000	1.94	35
12	**C_8**	10	12	95	87	10,900	1.82	42
13	**C_8**	25	27	95	86	8,900	1.75	34
14	**C_8**	50	49	91	74	9,900	1.91	38
15	**C_8**	75	75	96	84	7,500	2.14	28
16	**C_8**	90	87	96	87	4,700	1.85	18
17	**C_{10}**	0	0	95	98	9,100	2.05	32
18	**C_{10}**	10	12	95	93	8,300	1.91	29
19	**C_{10}**	25	27	95	92	8,600	1.78	30
20	**C_{10}**	50	50	94	83	10,300	1.84	35

21	**C_{10}**	75	74	95	92	7,300	2.04	35
22	**C_{10}**	90	89	97	99	8,500	2.27	29
23	**C_{12}**	0	0	95	98	7,700	2.07	25
24	**C_{12}**	10	11	95	97	9,900	2.01	31
25	**C_{12}**	25	26	96	93	9,700	2.21	31
26	**C_{12}**	50	50	95	95	8,700	1.97	27
27	**C_{12}**	75	74	95	89	6,300	1.98	20
28	**C_{12}**	90	88	97	100	7,300	2.19	23

[1] C4 = butane-1,4-diol, C6 = hexane-1,6-diol, C8 = octane-1,8-diol, C10 = decane-1,10-diol, C12 = dodecane-1,12-diol; [2] DEFDC feed (%) = represents the molar percentage of diethyl furan-2,5-dicarboxylate added, relative to the total diester amount; [3] X-furan (%) = defined as the molar fraction of alkylene furan-2,5-dicarboxylate repeating unit in the copolymer and determined *via* ^{1}H NMR as per equation 2: X-furan (%) = Ia2/(Ia1+ Ia2) x 100, where (Ix) represents the ^{1}H NMR integration of the relative peak; [4] Conversion (expressed in %) = represents the total amount of reacted diols in relative to the overall diols in the system and was calculated by ^{1}H NMR *via* equation 3: Conversion (%) = Ia1 + Ia2/(Ia1+ Ia2 + I(residual diol)) x 100, where (Ix) represents the ^{1}H NMR integration of the relative peak; [5] The number average molecular weight (M_n) was obtained from GPC analyses ($CHCl_3$, 23 °C, polystyrene standards); [6] Molar mass dispersity ĐM = M_w/M_n was obtained from GPC analyses ($CHCl_3$, 23 °C, polystyrene standards).

From Table 15, it was observed that the increase in DEFDC content had a negative impact on X-furan, conversion, yield, M_n, and D.P. of copolymers synthesized from shorter diols, mainly butane-1,4-diol and to a lesser extent hexane-1,6-diol, where the maximum quantities of furan successfully incorporated into these copolymer structures were 27 and 75%, achieving yields of 62 and 90% (as observed in entries 3 and 9), respectively. Increasing the feed molar percentage of DEFDC with these short diols limited the copolymer growth and led to a failure in precipitation, which was assumed to result from the low reactivity and the formation of short oligoesters that did not precipitate in methanol. No detectable conversion or yield was observed (see entry 4), when the DEFDC feed was increased to 50%, while only 48% conversion was calculated when the DEFDC feed was increased to 90% (as observed in entry 10); without any detectable yield. Similarly, the D.P. of the copolymers prepared with butane-1,4-diol was highly influenced by DEFDC feed, where increasing the DEFDC feed by only 10% led to a drop in D.P. from 80 (entry 1) to 24 (entry 2), and further decreased to 6 (entry 3) with 25% DEFDC. Inversely, the $Đ_M$ increased from 1.93 at 10% DEFDC in the feed up to 6.9 with 25% DEFDC, indicating a broad distribution in the molecular weight as a function of DEFDC addition. On the other hand, copolymers based on octane-1,8-diol, decane-1,10-diol, and dodecane-1,12-diol showed a stable conversion (>90%) and high yields without any noticeable variations as a function of DEFDC feed increase. The D.P. of copolymers based on octane-1,8-diol was partially affected at high DEFDC content, decreasing from 38 to 28 to 18 with the increase in DEFDC feed from 50 to 75 to 90%. Longer diols were not significantly affected by the increase in DEFDC feed %, where copolymers based on decane-1,10-diol and dodecane-1,12-diol maintained a relatively stable D.P. at high DEFDC feed. The formation of poly(alkylene alkanoate-*co*-alkylene furan-2,5-dicarboxylate) rather than poly(alkylene alkanoate) and poly (alkylene furan-2,5-dicarboxylate) homopolymers was confirmed by performing DOSY NMR scans. The spectrum provided in Figure 26 shows a single diffusion coefficient for the produced poly(dodecylene adipate-*co*-dodecylene furan-2,5-dicarboxylate) representing entry 26.

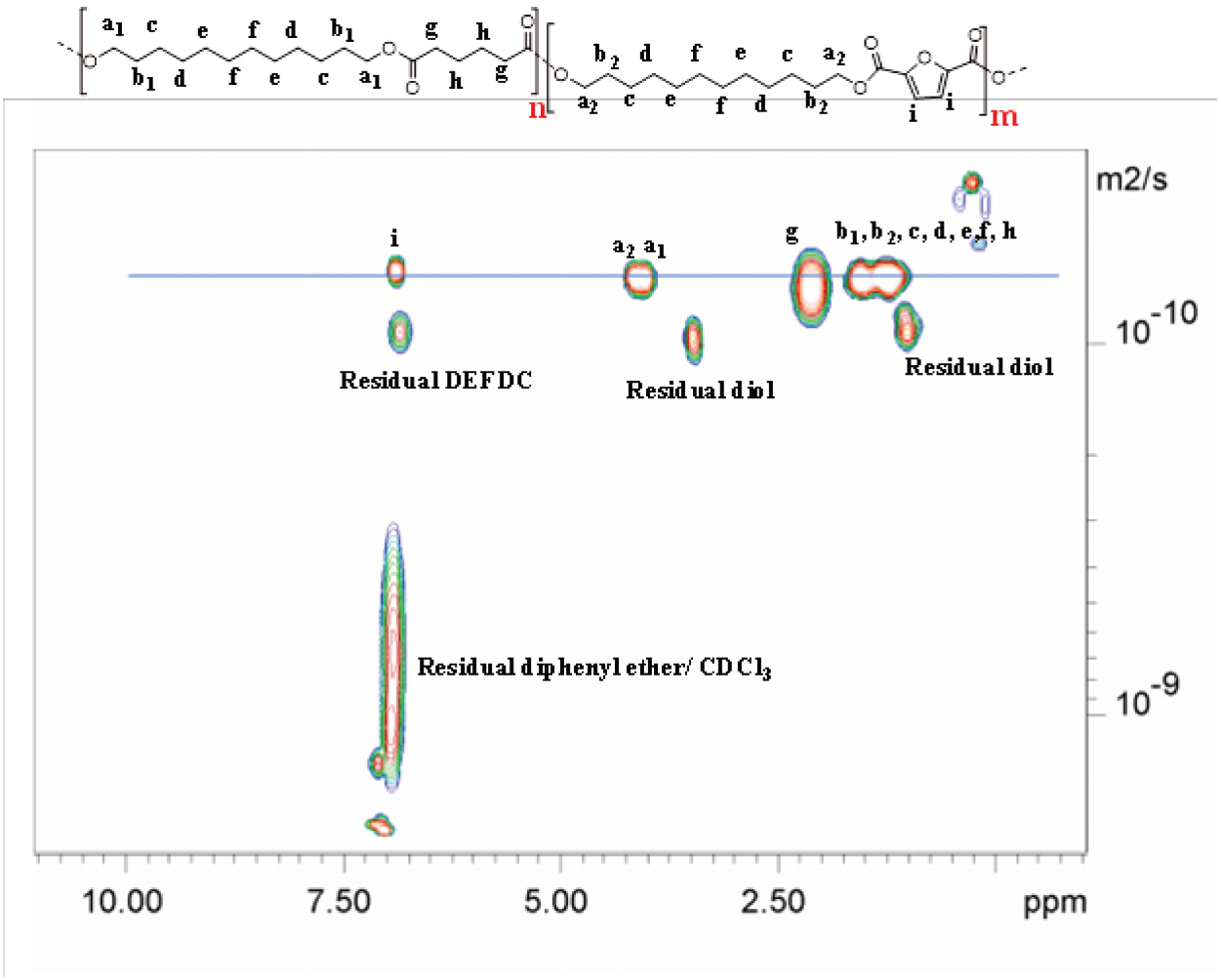

Figure 26. A DOSY NMR spectrum of poly(dodeyleneadipate-*co*-dodecylenefuranoate) (entry 26).

What was generally noticed from these results is that the limitation imposed by the increase in DEFDC feed became less significant as a function of increasing the diol length, where up to 90% DEFDC were successfully incorporated into the copolyesters based on octane-1,8-diol, decane-1,10-diol, and dodecane-1,12-diol. The superior catalytic efficiency of N435 or CALB catalysts towards longer diols in the presence of high furan content agreed well with the previously documented results by Jiang *et al.*[26] They suggested that besides the better selectivity of CALB towards longer diols, furan-based polyesters based on longer diols showed higher solubility in the reaction media (diphenyl ether), and lower melting points compared to those produced from

shorter diols which precipitated rapidly due to the reasons mentioned above and prevented polymer growth. Surprisingly though, and contrary to previous results in the literature,[45] increasing the diol length in the absence of DEFDC, did not seem to cause any increase in the D.P. of the corresponding aliphatic polyesters. On the contrary, the polymer based on butane-1,4-diol and diethyl adipate (entry 1) was found to possess the highest D.P. (80) amongst the aliphatic polyesters, while the D.P. was maintained within a range of (25-40) for polymers based on hexane-1,6-diol (entry 5), octane-1,8-diol (entry 11), decane-1,10-diol ((entry 17) and dodecane-1,12-diol (entry 23). However, it should be noted that the limitations in polymer growth could have stemmed from the diminishing in the mixing speed due to the increase in the viscosity of the samples, which might have posed a negative effect on the heat and mass transfer. In fact, it was observed that the mixing efficiency decreased rapidly in the reactions containing long diols, while it took more time to notice the same decrease when shorter diols were used. This observation could further justify the limited D.P. values with long diols.

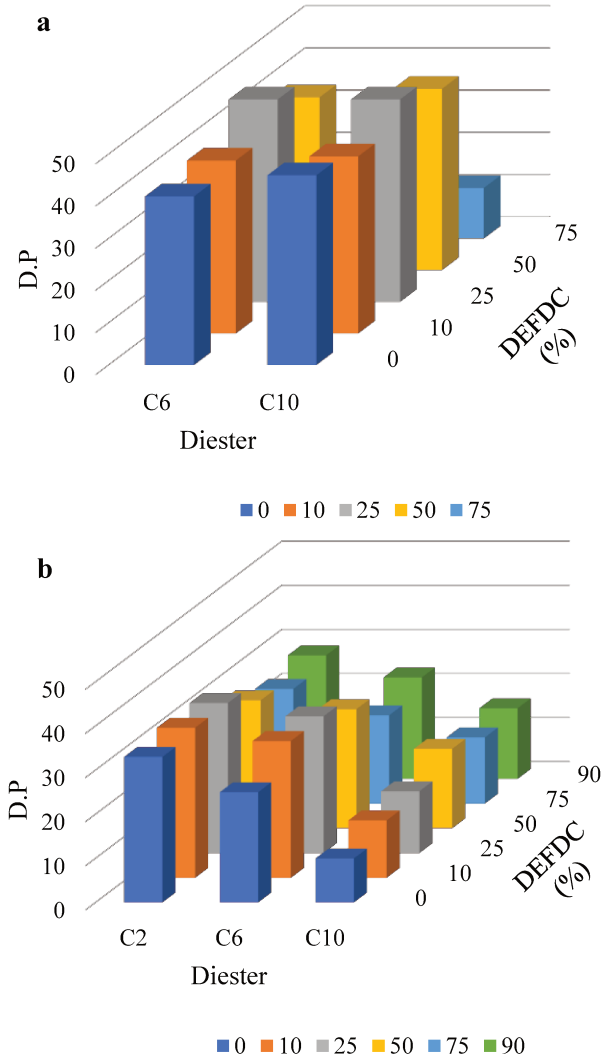

Figure 27.(a) the variation in D.P. of furan-based copolyesters with variable furan content based on hexane-1,6-diol and different aliphatic diesters. (b) the variation in D.P. of furan-based copolyesters with variable furan content based on dodecane-1,12-diol and different aliphatic diesters, where C2=1,2-diethyl oxalate, C6=1,6-diethyl adipate, and C10=1,10-diethyl sebacate.

The influence of the diester length was examined by comparing 1,2-diethyl oxalate (C_2), 1,6-diethyl adipate (C_6), and 1,10-diethyl sebacate (C_{10}). The results showing the evolution of D.P. as a function of diester length is given in Figure 27, and further results concerning the X-furan, conversion (%), yield (%), M_n (g.mol^{-1}), $Đ_M$, and D.P. are stated in Table 16.

Table 16. Molecular structure analysis (X-furan), % conversion, % yield, M_n, ÐM and D.P. of furan-based copolyesters with variable furan content and aliphatic diesters.

Entry	Diol/Diester[1]	DEFDC feed (%)[2]	X-furan (%)[3]	Conversion (%)[4]	Yield by weight (%)	M_n (g.mol^{-1})[5]	$Đ_M$[6]	D.P.[7]
29	C_6/C_2	0	-	-	0	-	-	-
30	C_6/C_2	10	-	-	0	-	-	-
31	C_6/C_2	25	-	-	0	-	-	-
32	C_6/C_{10}	0	0	98	91	12900	1.89	45
33	C_6/C_{10}	10	10	98	87	11800	1.91	42
34	C_6/C_{10}	25	26	97	74	12800	1.71	48
35	C_6/C_{10}	50	50	98	72	10800	1.84	43
36	C_6/C_{10}	75	74	96	63	2700	1.93	12
37	C_6/C_{10}	90	75	28	0	-	-	-
38	C_{12}/C_2	0	0	97	93	8600	2.28	33
39	C_{12}/C_2	10	14	97	95	8900	2.2	34
40	C_{12}/C_2	25	28	97	90	9400	2.14	34
41	C_{12}/C_2	50	50	98	94	8500	2.36	29
42	C_{12}/C_2	75	74	96	91	7900	2.19	26
43	C_{12}/C_2	90	87	97	96	8900	2.2	28
44	C_{12}/C_{10}	0	0	97	90	3600	2.14	10
45	C_{12}/C_{10}	10	14	97	84	4600	2.04	13
46	C_{12}/C_{10}	25	29	97	87	4900	1.93	14
47	C_{12}/C_{10}	50	54	98	85	6200	2.01	18
48	C_{12}/C_{10}	75	77	96	89	5100	2.09	15
49	C_{12}/C_{10}	90	n.d	n.d	95	5100	2.13	16

[1] C_6/C_2 = hexane-1,6-diol + diethyl oxalate, C_6/C_{10}= hexane-1,6-diol + diethyl sebacate, C_{12}/C_2 = dodecane-1,12-diol + diethyl oxalate, C_{12}/C_{10} = dodecane-1,12-diol + diethyl sebacate; **[2]** DEFDC feed (%) = represents the molar percentage of diethyl furan-2,5-dicarboxylate added, relative to the total diester amount; **[3]** X-furan (%) = defined as the molar fraction of alkylene furan-2,5-dicarboxylate repeating unit in the copolymer and determined *via* ^{1}H NMR as per equation 2: X-furan (%) = Ia2/(Ia1+ Ia2) x 100, where (I_x) represents the ^{1}H NMR integration of the relative peak; **[4]** Conversion (expressed in %) = represents the total amount of reacted diols in relative to the overall diols in the system and was calculated by ^{1}H NMR *via* equation 3: Conversion (%) = Ia1 + Ia2/(Ia1+ Ia2 + I(residual diol)) x 100, where (I_x) represents the ^{1}H NMR integration of the

relative peak; [5] The number average molecular weight (M_n) was obtained from GPC analyses ($CHCl_3$, 23 °C, polystyrene standards); [6] Molar mass dispersity $Đ_M = M_w/M_n$ was obtained from GPC analyses ($CHCl_3$, 23 °C, polystyrene standards); [7] D.P. = degree of polymerization = M_n/M_0 where M_o is the molecular weight of the repeating unit.

With the exception of 1,2-diethyl oxalate that did not yield any polymers when reacted against hexane-1,6-diol, the increase in the diester length from C6 to C10 did not have a significant impact on the molecular weight of the copolymers produced as observed in Figure 27 (a). On the other hand, in Figure 27 (b), reacting dodecane-1,12-diol with diethyl oxalate (C_2) in the presence or absence of DEFDC led to copolymers with a D.P. ranging between 26 and 34. The D.P. decreased on average with increasing the diester length down to a D.P. (20-31) with diethyl adipate (C_6) and a further decrease in D.P. down to (10-18) with diethyl sebacate (C_{10}). However, as mentioned before, the decrease in D.P. with longer diesters could have resulted from the high viscosity built up in the system that could have limited polymer growth. Moreover, unlike copolyesters based on hexane-1,6-diol, copolyesters based on dodecane-1,12-diol and regardless of the aliphatic diester used, did not show significant variations in term of conversion, yield, and D.P. as a function of increasing the DEFDC feed.

Taking advantage of the difference in reactivity between different chain length diols, a kinetic study was performed comparing hexane-1,6-diol and dodecane-1,12-diol in terms of conversion during the oligomerization step as a function of DEFDC content in the feed. The results showing the evolution of conversion in addition to X-furan representing the furan content (%) in the oligomers produced is given in Figure 28.

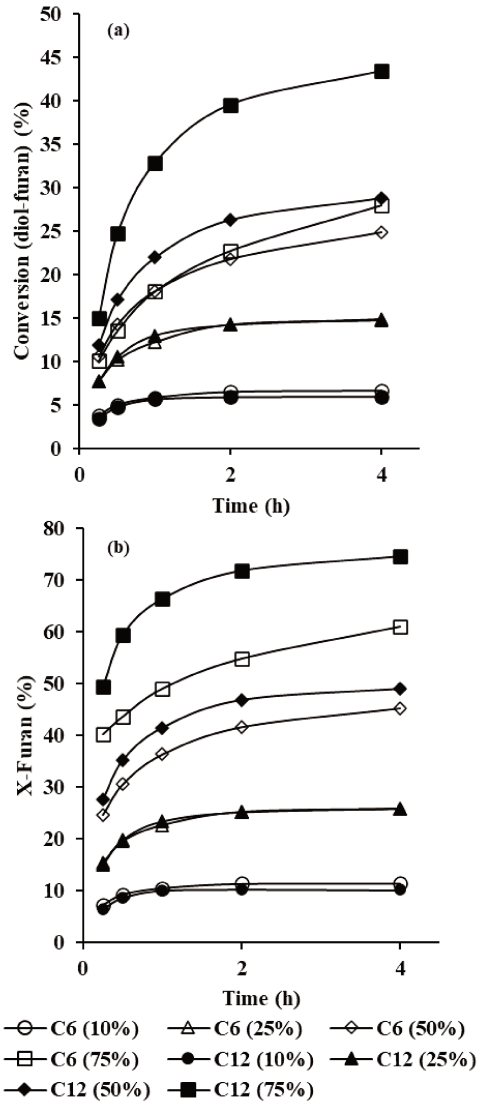

Figure 28. (a) Conversion of diols to furan-esters (expressed in %) during oligomerization, determined *via* ^{1}H NMR. Medium: diphenyl ether, N435: 20% w/w, temperature: 100 °C. (b) Microstructure of *co*-polyesters during oligomerization showing the evolution of furan content in oligomers produced, determined *via* ^{1}H NMR. Medium: diphenyl ether, N435: 20% w/w, temperature: 100 °C

From Figure 28, the reactions of two diols showed similar kinetic profiles at 10 and 25% DEFDC in the feed, where in both cases, the conversion representing the total amount of diols that reacted with DEFDC reached within a 2 h interval a constant value of 6% for C_6 (10%) and C_{12} (10%),

and 14% with C_6 (25%) and C_{12} (25%). Similarly, the amount of furan (X-furan) in the copolymer structure was similar with both diols reaching 10% with C_6 (10%) and C_{12} (10%), and 25% with C_6 (25%) and C_{12} (25%), respectively. Such values represented accurately the DEFDC in the feed. However, as the DEFDC feed content increased to 50% and 75%, variations in terms of conversion and X-furan were observed when comparing hexane-1,6-diol to dodecane-1,12-diol-based oligoesters, where at 50% DEFDC feed content, the conversion calculated for C_6 (50%) and C_{12} (50%) reached values of 25 and 29%, and the X-furan values were 45 and 49%, respectively. The superior reactivity of dodecane-1,12-diol with DEFDC was further confirmed at higher DEFDC content (75%), where for C_6 (75%), conversion did not increase beyond 29% after 4 h oligomerization time, compared to 43% with C_{12} (75%) within the same time limit. Similarly, the X-furan was limited to 61% with C_6 (75%) but was equivalent to the DEFDC feed percentage with C_{12} (75%) with a X-furan value of 75%. These results further confirmed the results obtained in Table 15, suggesting that in the presence of N435 as a catalyst, longer diols were more reactive towards DEFDC than their shorter counterparts. However, at low DEFDC content (<25%), and in the presence of diethyl adipate, the conversion of both seemed to proceed at a very similar rate regardless of the diol length.

As the reactivity differences between hexane-1,6-diol and dodecane-1,12-diol appeared to be more significant in the presence of high amounts of DEFDC, another kinetic study was performed comparing hexane-1,6-diol and dodecane-1,12-diol reactivity using the same system as detailed under the experimental section. The evolution of X-furan and X-adipate for both hexane-1,6-diol and dodecane-1,12-diol are given in Figure 29.

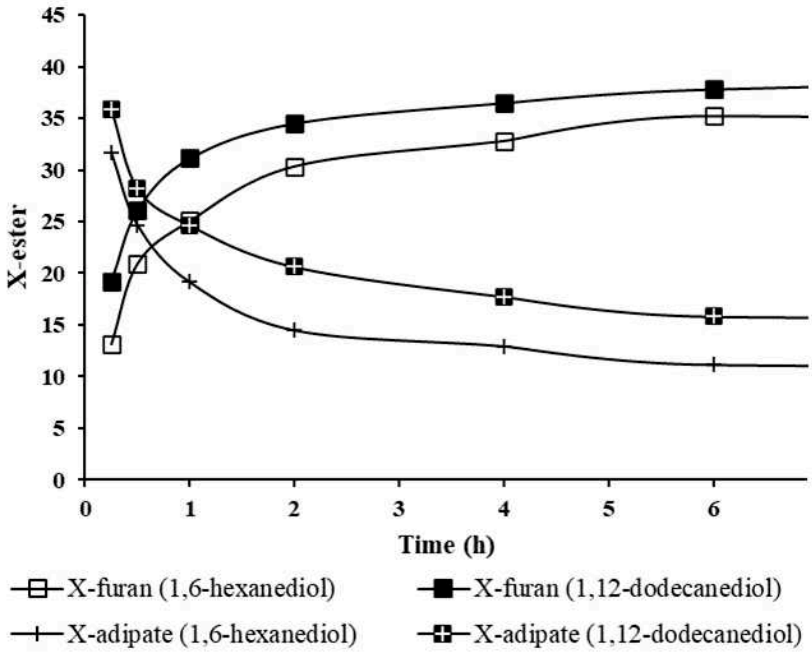

Figure 29. Microstructure of *co*-polyesters during oligomerization showing the evolution of furan (X-furan) and adipate content (X-adipate) in oligomers produced, determined *via* ^{1}H NMR. Reactants: hexane-1,6-diol (2 mmol), dodecane-1,12-diol (2 mmol), DEFDC (3 mmol), diethyl adipate (1 mmol). Medium: 1 mL diphenyl ether, N435: 20% w/w, temperature: 100 °C.

It was evident from Figure 29 that after only 15 mins from the start of the reaction, the oligoester structures were dominated by hexanediol-adipate and dodecanediol-adipate ester units recording 32 and 36% respectively, relative to the total esters formed in the system, while hexanediol-furan and dodecanediol-furan esters were limited to 13 and 19%, respectively. The domination of diol-adipate esters during the first minutes of the reaction resulted from the higher reactivity of diols towards aliphatic diesters under N435 mediated catalysis. As the reaction proceeds, the X-adipate for both diols started to decrease gradually while the X-furan increased simultaneously, where after 4 h, the X-adipate(hexane-1,6-diol) and X-adipate(dodecane-1,12-diol) decreased to reach values of 13 and 18%, whereas the X-furan(hexane-1,6-diol) and X-furan (dodecane-1,12-diol) increased to reach 33 and 37%, respectively. Unlike what was observed in Figure 28 in the case of hexane-1,6-diol; where the X-furan was limited to 61% after 4 h, the presence of the two diols in the same system allowed the oligoesters' microstructure to rearrange as the reaction proceeds to

reach after 4 to 6 h a microstructure that accurately represent the feed ratio of diols and esters based on the summation of X-furan of both hexane-1,6-diol and dodecane-1,12-diol.

These two kinetic studies showed how N435 showed minimal catalytic differences between hexane-1,6-diol and dodecane-1,12-diol at low DEFDC content, which is evident from the conversion profiles presented in Figure 28. On the other hand, it was also clear how in the presence of an aromatic group such as DEFDC, N435 tended to catalyze the transesterification reaction between dodecane-1,12-diol and DEFDC at a faster rate compared to similar reactions with hexane-1,6-diol. These observations suggest that in enzymatic catalysis based on N435, longer diols are better suitable to react against high furan content.

The impact of % N435 w/w loading was tested by comparing the polycondensation reaction of hexane-1,6-diol with diethyl adipate and DEFDC at 10 and 20% w/w N435 enzyme loading. The results in Table 17 showed modest variations in results at low DEFDC % (entries 50 and 54). However, as the DEFDC feed content increased, it became evident that a higher enzyme loading was necessary for conducting the reaction, where copolymers based on 10% N435 (see entries 52 and 53) had a minute amount of furan in their structures (3-4%), and a low conversion of 24 and 17%, respectively. While elevated conversions and yields were persistent in copolymers based on 20% N435 loading.

Table 17. Molecular structure analysis (X-furan), % conversion, % yield, M_n and $Đ_M$ of copolyesters with variable furan content and N435 % loading.

Entry	% N435 w/w	Diol[1]	DEFDC feed (%)[2]	X-furan[3]	Conversion (%)[4]	Yield by weight (%)	M_n (g.mol^{-1})[5]	$Đ_M$[6]
50	10	C_6	10	10	97	81	8,400	2.05
51	10	C_6	25	20	91	19	7,600	1.84
52	10	C_6	50	3	24	0	-	-
53	10	C_6	75	4	17	0	-	-
54	20	C_6	10	12	95	77	9,400	1.61
55	20	C_6	25	27	98	82	11,100	2.13
56	20	C_6	50	51	98	87	9,600	2.09
57	20	C_6	75	75	96	90	3,800	1.91

[1] C_6 = hexane-1,6-diol; [2] DEFDC feed (%) = represents the molar percentage of diethyl furan-2,5-dicarboxylate added, relative to the total diester amount; [3] X-furan (%) = Molar percent of alkylene furan-2,5-dicarboxylate unit in the copolymer; [4] Conversion (expressed in %) calculated *via* ^{1}H NMR; [5] The number average molecular weight (M_n) was obtained from GPC analyses ($CHCl_3$, 23 °C, polystyrene standards); [6] Molar mass dispersity $Đ_M = M_w/M_n$ was obtained from GPC analyses ($CHCl_3$, 23 °C, polystyrene standards).

As the reactivity of diols and the M_n of the copolyesters tend to decrease with high amounts of DEFDC, especially with shorter diols, small amounts of Pripol 2033 were incorporated in the reaction media as mentioned in the experimental section and observed in Scheme 19 in an attempt to overcome the limitations of producing copolyesters with high aromatic content *via* enzymatic catalysis. As observed in Table 18, the yield by weight and M_n increased significantly with the addition of Pripol 2033 from 68% and 2,700 g.mol^{-1} up to 90% and 5,300 g.mol^{-1} upon the addition of 10 and 20% of Pripol 2033 relative to DEFDC.

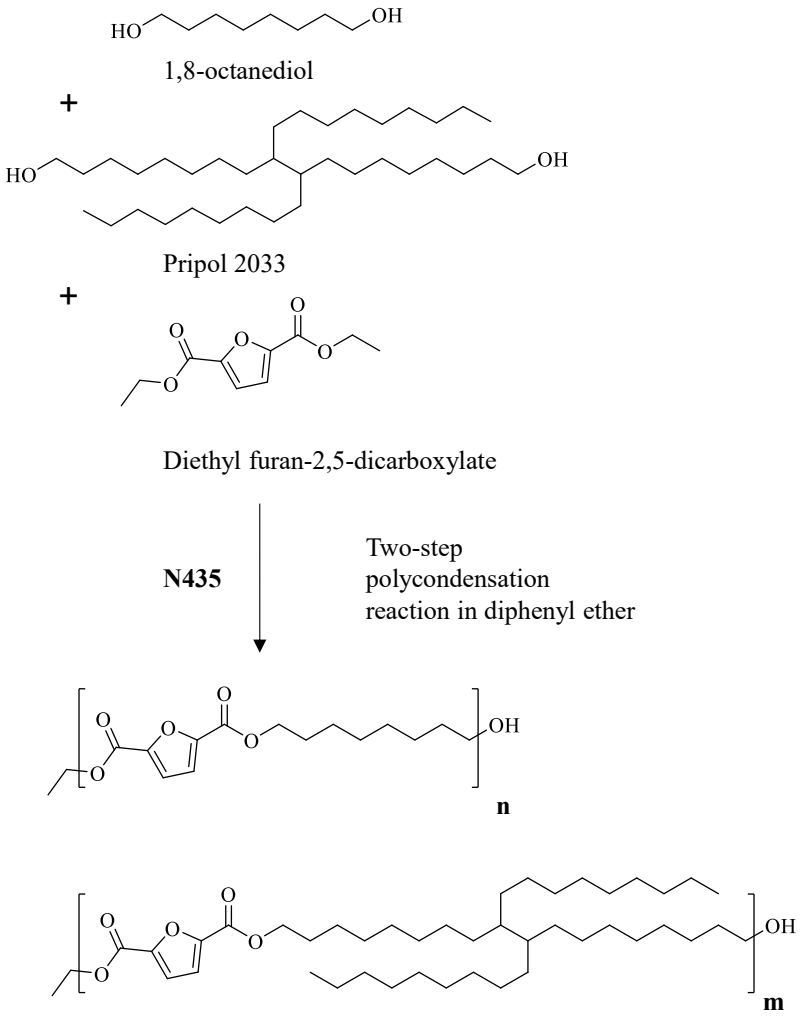

Scheme 19. Enzyme-catalyzed polycondensation reaction of octane-1,8-diol, Pripol 2033 and DEFDC.

Table 18. % conversion, % yield, M_n, $Đ_M$, T_m and ΔHm of *co*-polyesters based on octane-1,8-diol and DEFDC with or without Pripol 2033.

Entry	Pripol 2033 (%)	Conversion (%)	Yield by weight (%)	M_n (g.mol^{-1})	$Đ_M$	T_m	ΔH_m(J/g)
58	0	93	68	2,700	1.71	141	63
59	10	93	88	3,100	2.08	135	52
60	20	96	90	5,300	2.08	128	38

As semi-aromatic copolyesters based on small diols such as butane-1,4-diol were limited to small amounts of DEFDC (~25%) and to small molecular weights and yields, Pripol 2033 was used in a similar approach as before to enhance the polycondensation reaction in the presence of butane-1,4-diol. The reactions proceeded as observed in Scheme 20 in equimolar ratios between the diols and the diesters, where Pripol 2033 was added at 10, 25, and 50% relative to the diesters. Similar to what was observed before in the case of butane-1,4-diol at high DEFDC loading, and even after extending the reaction time for 72 h and increasing the volume of diphenyl ether up to 3 mL to avoid mixing issues, butane-1,4-diol did not react with DEFDC when the latter was added at 75% relative to the total diesters in the reaction, and no copolyesters were collected. In fact, the ^{1}H-NMR of the sample collected from the reaction media after 72 h did not show any peaks representing the formation of an ester bond between butane-1,4-diol and DEFDC. The same observation continued upon the addition of 10% Pripol 2033, with no detected changes in the reactivity towards DEFDC whether for butane-1,4-diol or for Pripol 2033. However, upon further increase in Pripol 2033 molar loading up to 25%, the X-furan detected in the ^{1}H-NMR sample was equivalent to the DEFDC molar feed percent (75%), with 56% resulting from the esterification of butane-1,4-diol and DEFDC and 19% of Pripol 2033 and DEFDC, and a high conversion ~99%. Likewise, when butane-1,4-diol and Pripol 2033 were in equimolar amounts, the reaction proceeded to reach a high conversion, and the X-furan reached 75% divided equally between butane-1,4-diol and Pripol 2033. The increase in Pripol 2033 feed ratio had a positive impact on reactivity and as a result, a higher M_n was achieved, reaching 7,700 and 12,000 g.mol^{-1} with 25 and 50% Pripol 2033.

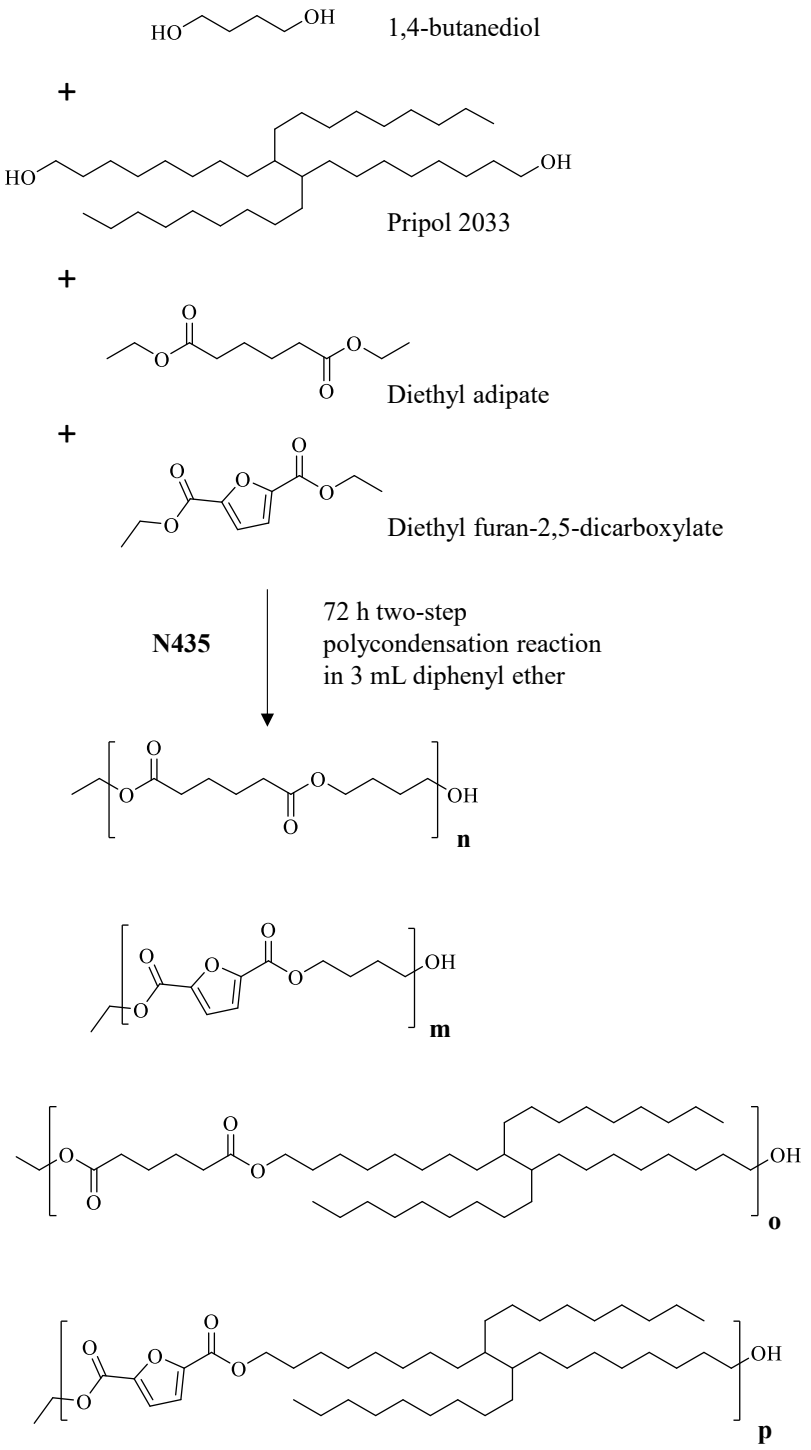

Scheme 20. Enzyme-catalyzed polycondensation reaction of butane-1,4-diol, Pripol 2033, diethyl adipate and DEFDC.

Table 19. X-furan, % conversion, % yield and M_n, of copolyesters based on octane-1,8-diol and DEFDC with or without Pripol 2033.

Entry	Pripol 2033 (%)	X-furan (1,4-BD)	X-furan (Pripol)	X-furan(total)	Conversion (%)	Yield by weight (%)	M_n (g.mol^{-1})
61	0	0	0	0	-	-	-
62	10	0	0	0	-	-	-
63	25	56	19	75	99	88	7,700
64	50	37	38	75	99	91	12,000

The DSC profiles of the prepared polymers were determined following the protocol stated in the experimental section. The results given in Figure 30 representing the entries in Table 15 showed the evolution of major melting endotherms (T_m) and crystallization enthalpies (ΔH_c) during the second heating cycle as a function of DEFDC molar ratio and diol length. Up to 25% DEFDC feed, the melting endotherms of the copolymers showed a gradual decrease as a function of the increase in DEFDC molar content, where longer diols showed higher melting endotherms. However, as the DEFDC content increased beyond 25%, the melting endotherms started increasing. Copolymers based on hexane-1,6-diol showed an increase in their melting endotherms from 34 °C at 25% DEFDC feed up to 81 and 119 °C at 50 and 75% DEFDC molar content. Similarly, copolymers based on octane-1,8-diol showed a similar increase in their melting endotherms exceeding that of hexane-1,6-diol based copolymers, where T_m increased from 49 °C at 25% DEFDC feed ratio up to 92, 124, and 134 °C for 50, 75, and 90% DEFDC feed ratio. Although the increase in DEFDC molar content also resulted in a positive shift in the melting endotherms of copolymers based on C_{10} and C_{12} diols, this increase was not as significant as those for shorter diols. It is to be noted that copolymers based on C_8, C_{10}, and C_{12} diols showed a second but minor melting endotherm at 50% DEFDC which appeared to fall within close proximity to the main endothermic peaks suggesting the coexistence of two crystalline structures. In fact, the thermal behavior of these copolyesters represented in Figure 30 and showing a decrease followed by an increase in the melting endotherms, and the coexistence of two crystalline phases at certain molar ratios, suggests a pseudo-eutectic behavior and isodimorphic cocrystallization.[47,48] The crystallization enthalpy, which was higher for aliphatic copolymers based on longer diols, showed a gradual decrease as a function

of DEFDC feed ratio until reaching a transitional point (~50% DEFDC), followed by an increase upon further DEFDC addition (>50% DEFDC). In fact, the pseudo-eutectic point in copolymers that is usually characterized by the coexistence of two crystalline phases and represents the minimal crystalline value, usually falls around equimolar monomer ratios, but it can vary according to the nature of the repeating unit.[47,49]The different crystal phases were later confirmed *via* WAXS analysis. Regarding the glass transition temperature (T_g), Table 20 depicts its evolution as a function of diol length and DEFDC molar content. Due to the high crystallinity in some samples, the T_g was not detected in all copolyesters. As observed in Table 20, the T_g appeared to increase as a function of increasing DEFDC % with all tested copolymers, but no specific pattern that relates the length of the tested diols to the value of T_g was observed. During the first heating cycle, and at 50% DEFDC molar feed, the polymer based on C_6 (entry 8) showed two glass transition temperatures at -47 and 43 °C belonging to adipate-rich and furan-rich blocks, respectively. However, during the second heating cycle, the T_g at 43 °C disappears and only a T_g at -40 °C is observed, suggesting that the furan-rich amorphous structures tend to dissolve in the melt and recrystallize thereafter with the cooling step. The same observation was noticed at 75% DEFDC (entry 9). Similarly, polymers based on C_8 diol showed similar behavior at 50 and 75% DEFDC feed (entries 14 and 15), but at 90% DEFDC (entry 16), only the T_g at 45 °C appeared during the first heating cycle, while no T_g was observed during the second heating cycle. The polymers based on C_{10} diol only showed two T_g at 75% DEFDC feed, while polymers based on C_{12} showed a direct transition towards an elevated T_g value (42 °C) with 75 and 90% DEFDC feed (entries 27 and 28). What was noticeable from these results was that although changes in the melting endotherms as a function of furan content were observed for all copolymers, their change was more pronounced with copolymers based on shorter diols achieving higher T_m values at high DEFDC content, which comes in agreement with previous reports in the literature associating the decrease in T_m to the increase in the number of methylene groups.[5,26] Regarding the influence of diester length on the DSC profiles of the copolymers produced, (Figure 31) shows the evolution of both the melting endotherms and crystallinity as a function of both DEFDC % and diester length. The increase in % DEFDC showed a similar effect on the DSC profiles as what was observed in . Variations in melting endotherms (°C) and crystallization enthalpies (J/g) as a function of diol length and furan content. However, no direct relation was found relating the evolution of the DSC profiles as a function of the diester length.

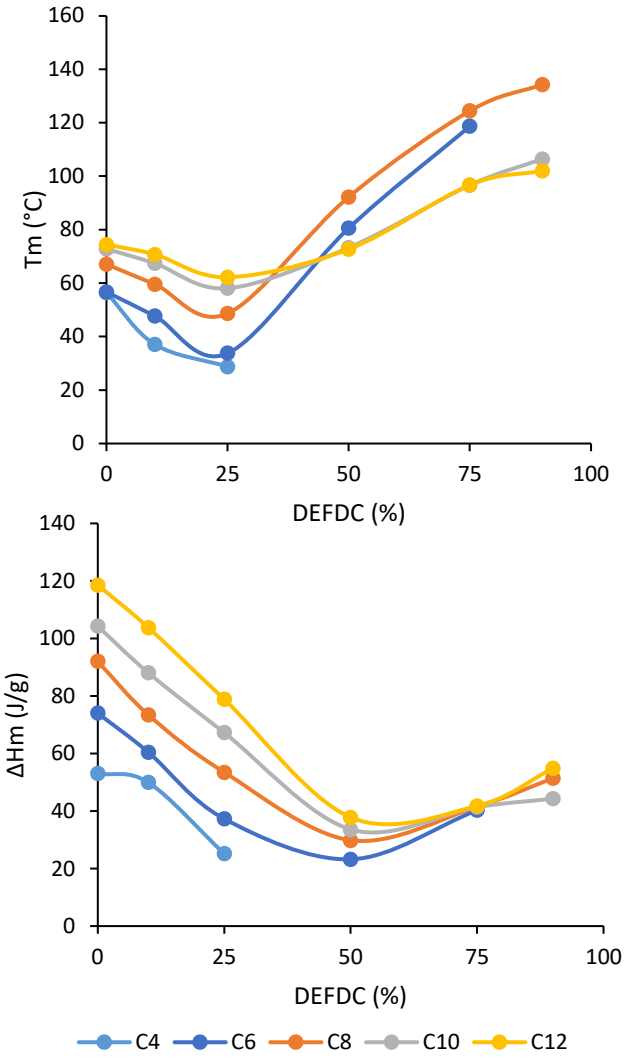

Figure 30. Variations in melting endotherms (°C) and crystallization enthalpies (J/g) as a function of diol length and furan content.

Table 20. The evolution of the glass transition temperature (T_g) as a function of diol length and DEFDC molar content.

			T_g (°C)	
Entry	**Diol**	**DEFDC feed (%)**	**1st heating cycle**	**2nd heating cycle**
1	**C4**	0	-57	-59
2	**C4**	10	-56	-56
3	**C4**	25	-52	-47
6	**C6**	10	-52	-53
7	**C6**	25	-50	-47
8	**C6**	50	(-47) (43)	-41
9	**C6**	75	(-30) (44)	-30
12	**C8**	10	-48	-51
13	**C8**	25	-50	-51
14	**C8**	50	(-48) (43)	-47
15	**C8**	75	(-31) (47)	-31
16	**C8**	90	45	-
19	**C10**	25	-47	-
20	**C10**	50	-45	-44
21	**C10**	75	(-37) (45)	-35
22	**C10**	90	46	-
25	**C12**	25	-38	-
26	**C12**	50	-38	-36
27	**C12**	75	41	-
28	**C12**	90	42	-

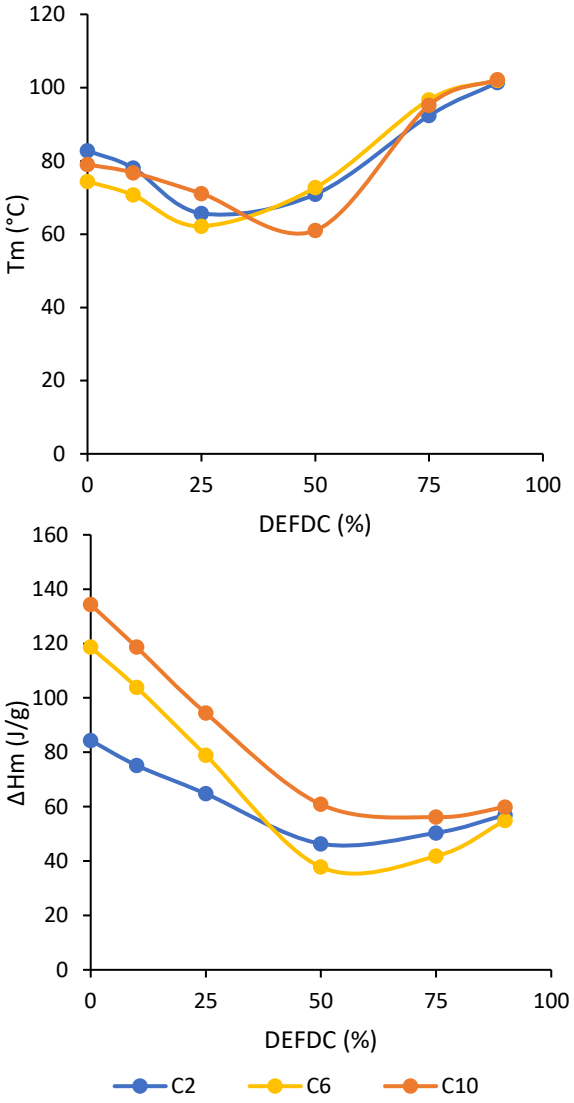

Figure 31. Variations in melting endotherms (°C) and crystallization enthalpies (J/g) as a function of diester length (C2= diethyl oxalate; C6= diethyl adipate; C10= diethyl sebacate) and furan content.

Regarding the thermal properties of the copolyesters based on Pripol 2033, octane-1,8-diol and DEFDC depicted in Scheme 19, and during the second heating cycle, all polymers showed an endothermic peak that gradually decreased as a function of increasing Pripol 2033 content, from 141 °C in entry 58 in the absence of Pripol 2033, down to 135 and 128 °C with 10 and 20% Pripol 2033, respectively (entries 59 and 60). Similarly, the crystallinity also decreased from 66 to 38 J/g (see Table 18).

The incorporation of Pripol 2033 at 25% along with butane-1,4-diol, diethyl adipate, and DEFDC as depicted in Table 19 resulted in a highly viscous yellow sticky liquid, which during the first heating cycle of the DSC, the copolymer given in entry 63, showed a T_g at -36 °C and

a broad melting endotherm peaking at 110 °C with an enthalpy of 16 J/g. The cooling cycle did not show any recrystallization peaks. During the second heating cycle, the first T_g increased by 6 °C up to -30 °C, followed by a cold crystallization peak at 39 °C. The T_m peaked at 109 °C with a slight decrease in enthalpy from 16 to12 J/g. The decrease in crystallinity might have risen from the incomplete crystallization during the second heating cycle and the close proximity between the crystallization and melting point. Regarding entry 64, the increase in Pripol 2033 feed to 50% led to the formation of a copolyester with a T_g appearing at -47 °C during the first heating cycle, and a T_m at 51 °C with an enthalpy not exceeding 5.5 J/g. During the second heating cycle, the T_g shifted slightly towards 43 °C, followed by a cold crystallization peak at 46 °C. Directly after crystallization, the T_m peaked at 77 °C, with minimal enthalpy that did not exceed 1 J/g. The big shift in the T_m peak from 51 °C during the first heating cycle to 77 °C on the second cycle, could have resulted from the presence of the cold crystallization and the melting peaks in very close quarters, masking any melting that might have occurred at similar intervals (see Figure 32). The copolymer in entry 64 appeared as a white flexible film. The decrease in T_g as a function of increasing Pripol 2033 content reflects an increase in the flexibility of the polymer structure and increases the distance between the rigid blocks which subsequently decreases the crystallinity and the crystallization rate.[50]

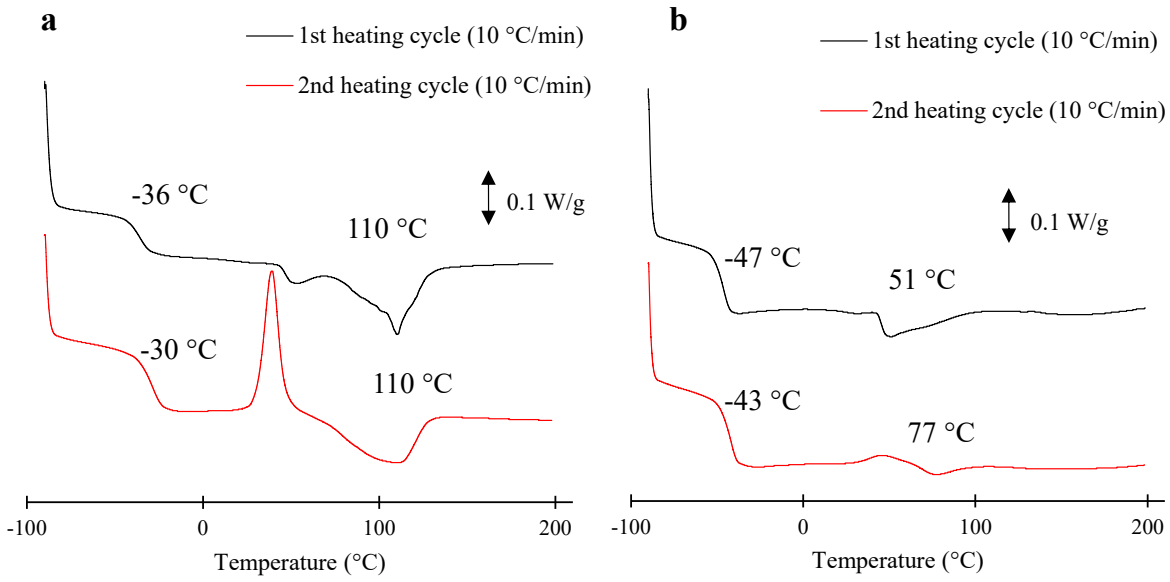

Figure 32. DSC profiles of entries 63 (a) and 64 (b) showing the 1st and 2nd heating cycle.

To further study the influence of the DEFDC molar content and diol length on the crystallinity of the copolymers, Wide-angle X-ray scattering (WAXS) was employed following the protocol stated under the experimental section. Regarding the influence of DEFDC feed %, copolymers based on octane-1,8-diol with DEFDC content varying between 0 and 90% were examined and compared (see Figure 33). For C_8 (0%), the WAXS profile was dominated by two major peaks at 22 ° and 25 ° which appeared to be very similar to the profiles of similar aliphatic polymers tested in the literature such as the case of poly(hexylene succinate).[51] Up to 25% DEFDC feed, the crystallinity continued to be dominated by poly(octylene adipate) crystals. However, upon the increase in DEFDC to 50%, a new peak started appearing at 17 ° with a significant decrease in the intensity of the peak at 22°, suggesting a mixture of poly(octylene adipate) and poly(octylene furanoate) crystal phases. Upon further increase in DEFDC % up to 75 and 90%, the peak at 20 ° completely disappears. These WAXS profiles of furan rich copolymers were very similar in pattern to what was previously reported in the literature with poly(octylene furanoate), suggesting that at high furan content; regardless of the presence of small amounts of diethyl adipate, the crystalline structures of the copolymers is dominated by the poly(octylene furanoate) crystal phase.[26]The pseudo-eutectic behavior of these copolyesters is thus confirmed by the WAXS results, and is a characterstic of isodimorphic copolymers showing adipate-rich crysalline phase at one side of the pseudo-eutectic region, furan-rich crystalline phase at the other, and the coexistance of both crystalline phases at the pseudo-eutectic point which is observed in the case of C_8(50%) in Figure 33. This does not mean that only one of the crystalline phases can exist at either sides of the the pseudo-eutectic region, but rather that the two crystalline phases coexist at any given ratio of the two repeating unit, but appear as a single crystalline phase resembling that of the the repeating unit present in abundance.[14,47,52]

The influence of diol length was studied by comparing the WAXS profiles of copolymers based on hexane-1,6-diol, octane-1,8-diol, decane-1,10-diol, and dodecane-1,12-diol at a constant 50% DEFDC molar ratio as observed in Figure 34. All tested copolymers appeared to be semi-crystalline in nature, where C_6 (50%) showed dominating peaks at 17 ° and 25 ° belonging to furan-rich blocks, in addition to a minor peak at 14 ° that appeared to move gradually to lower theta angles as a function of increasing the diol length, reaching 10 ° with C_{12} (50%), while maintaining a stable intensity. As the diol length increased, peaks at 17 ° started to diminish and new crystalline peaks at 21 ° belonging to the adipate-rich blocks started appearing, where C_8 (50%) showed a mixture of both poly(octylene adipate) and poly(octylene furanoate) crystal

blocks, C_{10} (50%) was dominated by poly(decylene adipate) crystals and small quantities of poly(decylene furanoate). However, with the longer dodecane-1,12-diol, the peak belonging to poly(dodecylene furanoate) disappeared, and the WAXS spectra was dominated with peaks at 21 ° and 25 ° suggesting the domination of poly(dodecylene adipate) blocks. From these results, it appeared that at equimolar DEFDC: diethyl adipate ratio, copolymers based on longer diols had a stronger tendency to form poly(alkylene adipate) rather than poly(alkylene furanoate) crystals, as opposed to copolymers based on shorter diols that had a quicker tendency to form the opposite. What was generally observed in our work, was that shorter diols reach the pseudo-eutectic transitional point at lower quantities of DEFDC, whereas evident in Figure 34, at 50% DEFDC, polymers based on smaller diols such as hexane-1,6-diol had already shifted towards furan-rich crystalline structures, octane-1,8-diol-based polymers appeared to be in very close proximity to the pseudo-eutectic point, while polymers based on decane-1,10-diol and dodecane-1,12-diol maintained an adipate-rich crystalline structures even at 50% DEFDC.

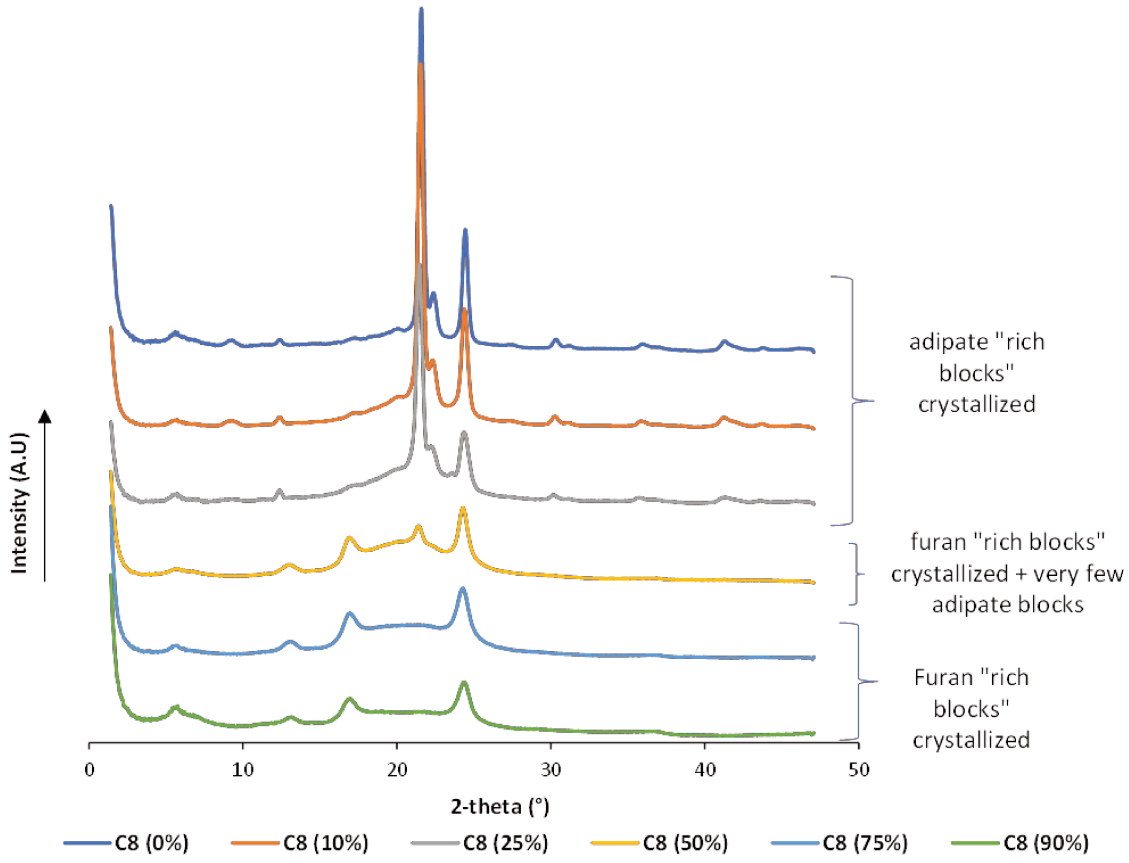

Figure 33. WAXS profiles of poly(octyleneadipate-*co*-octylenefuranoate) as a function of increasing the DEFDC content from 0 up to 90%.

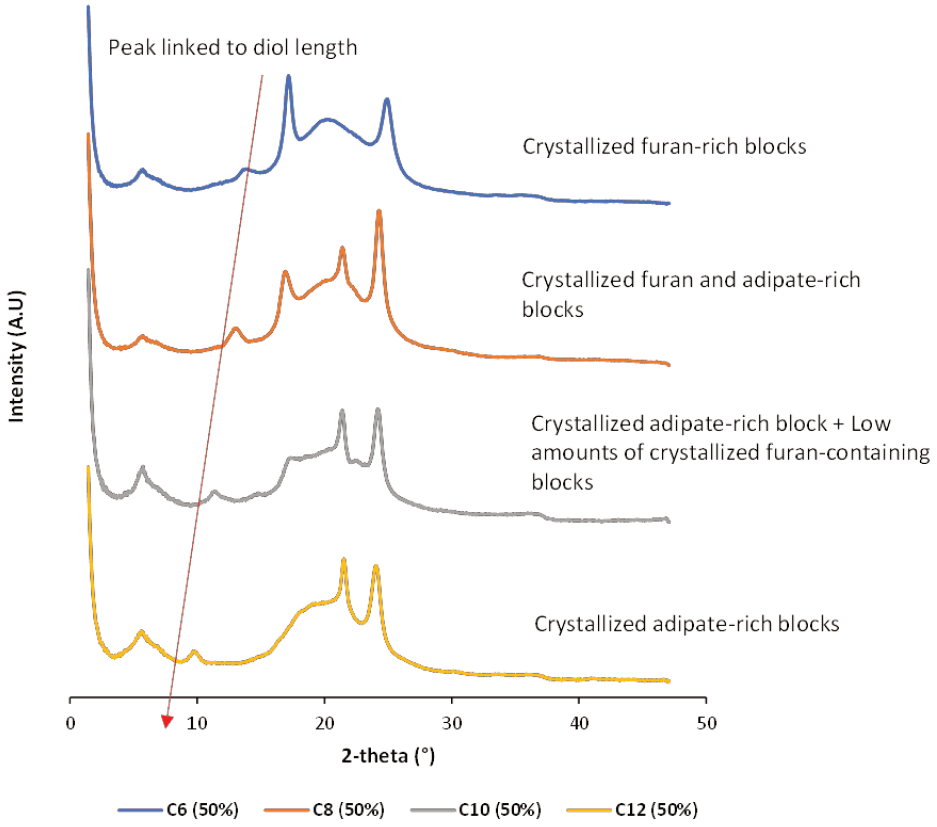

Figure 34. WAXS profiles of C_6 (50%), C_8 (50%), C_{10} (50%), C_{12} (50%) showing the evolution of the crystalline nature as a function of increasing the diol length while maintaining DEFDC loading at 50%.

3.3 Conclusion

The polycondensation reactions of different chain length aliphatic diols and diesters at a variable content of diethyl furan-2,5-dicarboxylate (DEFDC) were studied using Novozym 435 as biocatalyst. It was observed that increasing the diol length was essential to allow better reactivity towards DEFDC, where up to 90% DEFDC successfully reacted with long diols starting with octane-1,8-diol. On the other hand, reacting dodecane-1,12-diol with different

aliphatic diesters in presence of DEFDC showed no variations as a function of DEFDC feed but copolymers produced in the presence of long aliphatic diesters such as diethyl sebacate had low M_n when compared to reactions with diethyl oxalate and diethyl adipate that were relatively similar in results. The increase in N435 loading from 10 to 20% w/w did not seem to impose major changes when aliphatic monomers were in high excess, but it appeared to be essential in the success of the reactions when the amount of DEFDC was higher in the feed. The melting behavior and crystallinity of the prepared copolymers were principally affected by the DEFDC content, showing a decrease in the melting endotherm and crystallinity at low DEFDC content followed by an increase in both at elevated DEFDC content, where it was noticed that longer diols were somehow less affected by DEFDC content increase. All copolymers acquired a semi-crystalline structure, with both poly(alkylene alkanoate) and poly(alkylene furanoate) crystal blocks existing alone or together in the same polymeric structure depending on DEFDC content. The introduction of the amorphous Pripol 2033 improved the polymerization reaction in systems containing high furan content and butane-1,4-diol which otherwise did not yield any polymers without the long chain fatty dimer diol. Finally, this work introduced a green method to produce semi-aromatic furan based copolyesters that could be further optimized, studied, and compared with other semi-aromatic copolyesters already on the market such as polybutylene adipate terephthalate. Based on the findings of this work, and the feasibility of incorporating high amounts of DEFDC into the polyesters *via* enzymatic catalysis using strategies such as increasing the diol length, the next chapter will further explore the suitability of Novozym 435 in the synthesis of polyesters containing other cyclic compounds. Chapter 4 will therefore assess Novozym 435 in terms of its ability to catalyze the incorporation of cyclic compounds having more challenging properties (such as levoglucosan) and will shed light over the limitations and approaches that would allow for polymer growth enhancement, and how the regioselectivity of Novozym 435 can be advantageous in performing certain reactions that might not be accessible *via* other catalytic systems.

3.4 Materials and Methods

3.4.1 Materials

hexane-1,6-diol (97%), diethyl adipate (99%), sebacic acid (99%) and diphenyl ether (99%) were purchased from Sigma-Aldrich. butane-1,4-diol (99%), octane-1,8-diol (98%), dodecane-1,12-diol (98%) were purchased from Acros Organics. decane-1,10-diol (97%) and diethyl oxalate were purchased from Alfa Aesar. Furan-2,5-dicarboxylic acid (99.7%) was purchased from Satachem co. Pripol 2033 fatty dimer diol ((9*Z*,12*Z*)-18-[(6*Z*,9*Z*)-18-hydroxyoctadeca-6,9-dienoxy]octadeca-9,12-dien-1-ol) (≥96.5) was kindly provided by Croda Chemicals. Analytical grade methanol, absolute ethanol, and chloroform (99%) were purchased from VWR. All the reagents and solvents were used as received. Novozym 435 (N435), a *Candida antarctica* lipase B (CALB) immobilized on an acrylic resin was kindly provided by Novozymes. Chloroform D ($CDCl_3$) (99.8%) and deuterated dimethyl sulfoxide DMSO-d_6 were purchased from Euriso-Top.

3.4.2 Synthesis of diethyl furan-2,5-dicarboxylate (DEFDC)

5 g of furan-2,5-dicarboxylic acid (FDCA) were added to 60 mL of absolute ethanol and 2 mL of sulfuric acid and refluxed overnight under continuous stirring at 100 °C. The mixture was allowed to cool followed by evaporation to remove the excess amount of ethanol. The solution was added dropwise into distilled water under continuous stirring, resulting in FDCA precipitation. The product was washed multiple times with distilled water before suspending in 100 mL H_2O solution and neutralizing by adding 5% $NaCO_3$ and finally filtering using a Buchner funnel under vacuum application. The white crystalline powder obtained was dried overnight under high vacuum and the yield by weight achieved was >75% w/w. ^{1}H-NMR analysis confirmed the structure of diethyl furan-2,5-dicarboxylate (DEFDC) with no detectable impurities ^{1}H NMR ($CDCl_3$, 300 MHz): δ 1.39 (t, 6H), 4.4 (m, J = 7.1 Hz, 4H), 7.2 (s, 2H) ppm (see Figure 35).

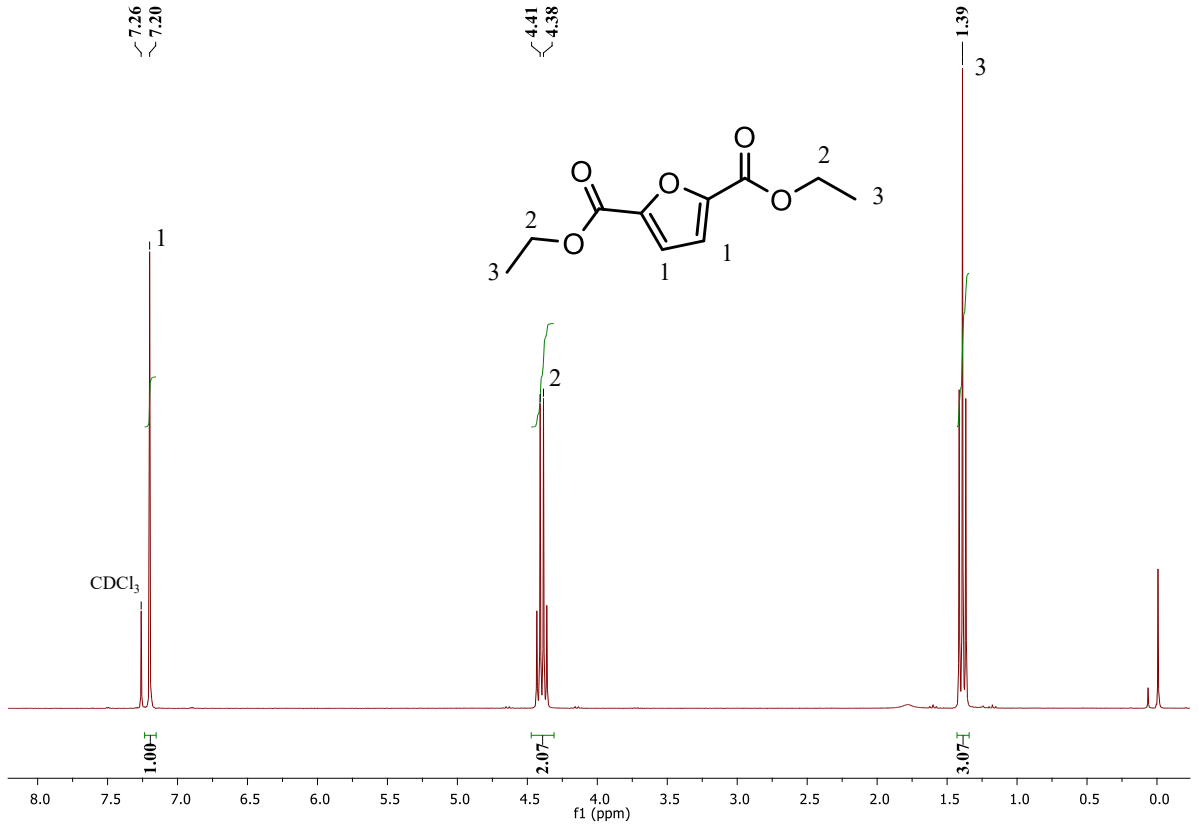

Figure 35. ^{1}H NMR spectrum ($CDCl_3$, 300 MHz) of diethyl furan-2,5-dicarboxylate: δ 7.20 (s, 2H), 4.40 (q, J = 7.1 Hz, 4H), 1.39 (t, J = 7.1 Hz, 6H).

3.4.3 General procedure for the enzymatic synthesis of poly(alkylene alkanoate-*co*-alkylene furan-2,5-dicarboxylate)

3.4.3.1 The effect of diol length (C_4 to C_{12}) and DEFDC molar ratio

Furan-based semi-aromatic copolyesters were prepared by reacting DEFDC and diethyl adipate with diols of different chain lengths varying from C_4 to C_{12}. As an example, the synthesis of poly(hexyleneadipate-*co*-hexylene furan-2,5-dicarboxylate) containing 25% furan was prepared as following: hexane-1,6-diol (4 mmol), diethyl adipate (2 mmol), and DEFDC (2 mmol) were weighed and added into a schlenk tube. A predetermined amount (20% w/w) of N435 relative to the total weight of hexane-1,6-diol (4 mmol) and diethyl adipate (4 mmol) was weighed and added to the mixture. 1 mL of diphenyl ether was added as a solvent of choice. The reaction proceeded under atmospheric pressure for 2 h at 100 °C (using an oil bath with continuous stirring kept constant at 350 rpm). Afterwards, the schlenk tube was attached to a

vacuum line, and the pressure was decreased gradually within 1 h to reach a predetermined value of 10 mbar to remove the byproduct (ethanol). The reaction was left to proceed for 24 h, then was stopped by adding an excess amount of chloroform under atmospheric pressure after a cooling step, followed by direct filtration to remove the N435 beads. The filtrate was then partially evaporated, and then added dropwise to excess amount of cold methanol under stirring to precipitate the obtained polymer. The mixture was then filtered, and the product obtained was left to dry at room temperature for 24 h before collecting and weighing.

3.4.3.2 The effect of diester length (C_2-C_6-C_{10}) and DEFDC molar ratio

Following the same procedure as before, the influence of diester length was examined by performing the copolymerization reaction between hexane-1,6-diol and different chain length diesters being diethyl oxalate (C_2), diethyl adipate (C_6), and diethyl sebacate (C_{10}), at variable DEFDC molar feed percent (0-90%). The same approach was used starting from dodecane-1,12-diol.

3.4.4 Effect of diol length on DEFDC conversion during oligomerization: "A comparison between hexane-1,6-diol and dodecane-1,12-diol based *co*-polyesters"

In the first part of this study and following the same procedure as before, different samples containing either hexane-1,6-diol or dodecane-1,12-diol, in addition to diethyl adipate and DEFDC were prepared keeping an equimolar ratio between the diol and diesters, while varying the DEFDC content from 10 to 75%. The conversion of DEFDC into alkylene furanoate was monitored by withdrawing samples at different time intervals and exploiting the ^{1}H NMR signals at δ= (4.32-4.34) of the methylene (-*O*-$\underline{CH_2}$-C_nH_{2n}-$\underline{CH_2}$-*O*-) of the alkylene furanoate, δ= (4.06-4.07) of the methylene (-*O*-$\underline{CH_2}$-C_nH_{2n}-$\underline{CH_2}$-*O*-) of the alkylene adipate, and δ= 3.65 of the methylene (*HO*-$\underline{CH_2}$-C_nH_{2n}-$\underline{CH_2}$-*OH)* of the residual diol. Conversion of DEFDC during oligomerization was calculated *via* the ratio of the signal representing alkylene furanoate at δ= (4.32-4.34) relative to the summation of signals representing alkylene furanoate, alkylene adipate and residual diols at δ= (4.32-4.34), δ= (4.06-4.07), and δ= 3.65, respectively.

In the second part of this study, hexane-1,6-diol and dodecane-1,12-diol were added into the same reaction in equimolar amounts and reacted against 75% DEFDC and 25% of diethyl adipate while maintaining an equimolar ratio between the diols and diesters. The conversion of DEFDC into either hexylene furanoate or dodecylene furanoate was monitored *via* ^{1}H NMR in the same fashion as previously mentioned and by taking advantage of the Global spectral deconvolution technique to distinguish between overlapping signals of hexylene furanoate and dodecylene furanoate. The aim was to monitor how two different chain length diols could compete in the same reaction media.

3.4.5 Effect of N435 % loading

hexane-1,6-diol was chosen as a model monomer to see the effect of enzyme loading on the polymerization reaction. Similar to the general procedure mentioned above, hexane-1,6-diol was reacted with diethyl adipate and DEFDC at different molar percentages (10, 25, 50, and 75%), the N435 % loading was varied between 10 and 20%, while maintaining similar reaction conditions.

3.4.6 Effect of fatty dimer diol (Pripol 2033)

The effect of Pripol 2033 was tested in two experimental parts. In the first experimental approach, octane-1,8-diol and Pripol 2033 were reacted with DEFDC in equimolar (diol-diester) ratios (4 mmol). Pripol 2033 was added at 10 and 20% relative to DEFDC, the reactions proceeded for 2 h at 100 °C in 1 mL diphenyl ether and 20% w/w N435 loading, followed by 24 h under vacuum (10 mbar). The polyesters synthesized were compared in terms of conversion, X-furan, M_n and their thermal properties.

In the second experimental procedure, butane-1,4-diol and Pripol 2033 were reacted against diethyl adipate (25%) and DEFDC (75%). Pripol 2033 was added at 10, 25, and 50% relative to the diesters while maintaining an equimolar (diol-diester) ratio (4 mmol). The reactions proceeded for 2 h at 100 °C in 3 mL diphenyl ether and 20% w/w N435 loading, followed by

72 h under vacuum (10 mbar). The polyesters synthesized were compared in terms of conversion, X-furan, M_n and their thermal properties.

3.4.7 Analytical methods

3.4.7.1 Nuclear Magnetic Resonance (NMR) analysis

The ^{1}H NMR spectra of the monomers, and the recovered polymer were recorded at room temperature on a Bruker Avance 300 instrument (delay time = 3 s, number of scans = 32) at 300.13 MHz using either $CDCl_3$ or DMSO-d_6 as solvents. Chemical shifts (ppm) are given in δ-units and were calibrated using the residual signal of $CDCl_3$ and DMSO-d_6 at 7.26 ppm and 2.5 ppm, respectively. Additionally, ^{1}H NMR was used to confirm conversion and determine its rate (as mentioned in the previous section). DOSY spectra were recorded on Avance II 400 Bruker spectrometer (9.4 T) regulated at 298 K respectively in $CDCl_3$ and toluene d8. Data acquisition and analysis were performed using the Bruker TopSpin 3.2 and MestReLab 6.0.

3.4.7.2 Gel Permeation Chromatography (GPC) analysis

Gel permeation chromatography (GPC) analysis was performed in chloroform as eluent (flow rate of 1 mL/min) at 23 °C using Alliance e2695 (Waters) apparatus and with a sample concentration around 10-15 mg.mL^{-1}. A refractive index detector Optilab T-rEX (Wyatt Technology) was used as a detector, and a set of columns: HR1, HR2 and HR4 (Water Styragel) were utilized. The molecular weight calibration curve was obtained using monodisperse polystyrene standards.

3.4.7.3 Differential scanning calorimetry (DSC)

The thermal transition was recorded with a Differential Scanning Calorimetry (DSC) on a TA Discovery DSC 25 using a cooling-heating-cooling-heating method. First, samples of ~10 mg

were sealed in aluminum pans, the temperature was equilibrated at - 90 °C, followed by a heating ramp of 10 °C/min to 200 °C, then a cooling ramp of 10 °C/min to - 90 °C, and a second heating ramp of 10 °C/min to 200 °C. The thermograms were analyzed using TA instruments TRIOS software.

3.4.7.4 Wide-angle X-ray scattering (WAXS)

Wide-angle X-ray scattering (WAXS) analysis were performed on a Xeuss 2.0 apparatus (Xenocs) equipped with a micro source using a Cu Kα radiation (λ= 1.54 Å) and point collimation (beam size: 500×500µm²). The sample to detector distance, around 15 cm, was calibrated using silver behenate as standard. Through view 2D diffraction patterns are recorded on a Pilatus 200k detector (Dectris). Integrated intensity profiles were computed from the 2D patterns using the Foxtrot® software. Exposure time: 15 min.

3.5 References

(1) van Putten, R.-J.; van der Waal, J. C.; de Jong, E.; Rasrendra, C. B.; Heeres, H. J.; de Vries, J. G. Hydroxymethylfurfural, A Versatile Platform Chemical Made from Renewable Resources. *Chem. Rev.* **2013**, *113* (3), 1499–1597. https://doi.org/10.1021/cr300182k.

(2) Kröger, M.; Prüße, U.; Vorlop, K.-D. A New Approach for the Production of 2,5-Furandicarboxylic Acid by in Situ Oxidation of 5-Hydroxymethylfurfural Starting from Fructose. *Top. Catal.* **2000**, *13* (3), 237–242. https://doi.org/10.1023/A:1009017929727.

(3) Koopman, F.; Wierckx, N.; de Winde, J. H.; Ruijssenaars, H. J. Efficient Whole-Cell Biotransformation of 5-(Hydroxymethyl)Furfural into FDCA, 2,5-Furandicarboxylic Acid. *Bioresour. Technol.* **2010**, *101* (16), 6291–6296. https://doi.org/10.1016/j.biortech.2010.03.050.

(4) Huang, Y.-T.; Wong, J.-J.; Huang, C.-J.; Li, C.-L.; Jang, G.-W. B. 2,5-Furandicarboxylic Acid Synthesis and Use. In *Chemicals and Fuels from Bio-Based Building Blocks*; John Wiley & Sons, Ltd, 2016; pp 191–216. https://doi.org/10.1002/9783527698202.ch8.

(5) Sousa, A. F.; Vilela, C.; Fonseca, A. C.; Matos, M.; Freire, C. S. R.; Gruter, G.-J. M.; Coelho, J. F. J.; Silvestre, A. J. D. Biobased Polyesters and Other Polymers from 2,5-Furandicarboxylic Acid: A Tribute to Furan Excellency. *Polym. Chem.* **2015**, *6* (33), 5961–5983. https://doi.org/10.1039/C5PY00686D.

(6) Dutta, S.; De, S.; Saha, B. A Brief Summary of the Synthesis of Polyester Building-Block Chemicals and Biofuels from 5-Hydroxymethylfurfural. *ChemPlusChem* **2012**, *77* (4), 259–272. https://doi.org/10.1002/cplu.201100035.

(7) Qian, X. Mechanisms and Energetics for Brønsted Acid-Catalyzed Glucose Condensation, Dehydration and Isomerization Reactions. *Top. Catal.* **2012**, *55* (3), 218–226. https://doi.org/10.1007/s11244-012-9790-6.

(8) Román-Leshkov, Y.; Chheda, J. N.; Dumesic, J. A. Phase Modifiers Promote Efficient Production of Hydroxymethylfurfural from Fructose. *Science* **2006**, *312* (5782), 1933–1937. https://doi.org/10.1126/science.1126337.

(9) Collias, D. I.; Harris, A. M.; Nagpal, V.; Cottrell, I. W.; Schultheis, M. W. Biobased Terephthalic Acid Technologies: A Literature Review. *Ind. Biotechnol.* **2014**, *10* (2), 91–105. https://doi.org/10.1089/ind.2014.0002.

(10) Burgess, S. K.; Karvan, O.; Johnson, J. R.; Kriegel, R. M.; Koros, W. J. Oxygen Sorption and Transport in Amorphous Poly(Ethylene Furanoate). *Polymer* **2014**, *55* (18), 4748–4756. https://doi.org/10.1016/j.polymer.2014.07.041.

(11) Knoop, R. J. I.; Vogelzang, W.; Haveren, J. van; Es, D. S. van. High Molecular Weight Poly(Ethylene-2,5-Furanoate); Critical Aspects in Synthesis and Mechanical Property Determination. *J. Polym. Sci. Part Polym. Chem.* **2013**, *51* (19), 4191–4199. https://doi.org/10.1002/pola.26833.

(12) Zhu, J.; Cai, J.; Xie, W.; Chen, P.-H.; Gazzano, M.; Scandola, M.; Gross, R. A. Poly(Butylene 2,5-Furan Dicarboxylate), a Biobased Alternative to PBT: Synthesis, Physical Properties, and Crystal Structure. *Macromolecules* **2013**, *46* (3), 796–804. https://doi.org/10.1021/ma3023298.

(13) Burgess, S. K.; Leisen, J. E.; Kraftschik, B. E.; Mubarak, C. R.; Kriegel, R. M.; Koros, W. J. Chain Mobility, Thermal, and Mechanical Properties of Poly(Ethylene Furanoate) Compared to Poly(Ethylene Terephthalate). *Macromolecules* **2014**, *47* (4), 1383–1391. https://doi.org/10.1021/ma5000199.

(14) Terzopoulou, Z.; Papadopoulos, L.; Zamboulis, A.; Papageorgiou, D. G.; Papageorgiou, G. Z.; Bikiaris, D. N. Tuning the Properties of Furandicarboxylic Acid-Based Polyesters with Copolymerization: A Review. *Polymers* **2020**, *12* (6), 1209. https://doi.org/10.3390/polym12061209.

(15) Llevot, A.; Grau, E.; Carlotti, S.; Grelier, S.; Cramail, H. Renewable (Semi)Aromatic Polyesters from Symmetrical Vanillin-Based Dimers. *Polym. Chem.* **2015**, *6* (33), 6058–6066. https://doi.org/10.1039/C5PY00824G.

(16) Larrañaga, A.; Lizundia, E. A Review on the Thermomechanical Properties and Biodegradation Behaviour of Polyesters. *Eur. Polym. J.* **2019**, *121*, 109296. https://doi.org/10.1016/j.eurpolymj.2019.109296.

(17) Silvianti, F.; Maniar, D.; Boetje, L.; Loos, K. Green Pathways for the Enzymatic Synthesis of Furan-Based Polyesters and Polyamides. In *Sustainability & Green Polymer*

Chemistry Volume 2: Biocatalysis and Biobased Polymers; ACS Symposium Series; American Chemical Society, 2020; Vol. 1373, pp 3–29. https://doi.org/10.1021/bk-2020-1373.ch001.

(18) Gandini, A.; Silvestre, A. J. D.; Neto, C. P.; Sousa, A. F.; Gomes, M. The Furan Counterpart of Poly(Ethylene Terephthalate): An Alternative Material Based on Renewable Resources. *J. Polym. Sci. Part Polym. Chem.* **2009**, *47* (1), 295–298. https://doi.org/10.1002/pola.23130.

(19) Gomes, M.; Gandini, A.; Silvestre, A. J. D.; Reis, B. Synthesis and Characterization of Poly(2,5-Furan Dicarboxylate)s Based on a Variety of Diols. *J. Polym. Sci. Part Polym. Chem.* **2011**, *49* (17), 3759–3768. https://doi.org/10.1002/pola.24812.

(20) Jiang, M.; Liu, Q.; Zhang, Q.; Ye, C.; Zhou, G. A Series of Furan-Aromatic Polyesters Synthesized *via* Direct Esterification Method Based on Renewable Resources. *J. Polym. Sci. Part Polym. Chem.* **2012**, *50* (5), 1026–1036. https://doi.org/10.1002/pola.25859.

(21) Vannini, M.; Marchese, P.; Celli, A.; Lorenzetti, C. Fully Biobased Poly(Propylene 2,5-Furandicarboxylate) for Packaging Applications: Excellent Barrier Properties as a Function of Crystallinity. *Green Chem.* **2015**, *17* (8), 4162–4166. https://doi.org/10.1039/C5GC00991J.

(22) Wang, J.; Liu, X.; Zhang, Y.; Liu, F.; Zhu, J. Modification of Poly(Ethylene 2,5-Furandicarboxylate) with 1,4-Cyclohexanedimethylene: Influence of Composition on Mechanical and Barrier Properties. *Polymer* **2016**, *103*, 1–8. https://doi.org/10.1016/j.polymer.2016.09.030.

(23) Lepoittevin, B.; Roger, P. Poly(Ethylene Terephthalate). In *Handbook of Engineering and Speciality Thermoplastics*; John Wiley & Sons, Ltd, 2011; pp 97–126. https://doi.org/10.1002/9781118104729.ch4.

(24) Cruz-Izquierdo, Á.; Broek, L. A. M. van den; Serra, J. L.; Llama, M. J.; Boeriu, C. G. Lipase-Catalyzed Synthesis of Oligoesters of 2,5-Furandicarboxylic Acid with Aliphatic Diols. *Pure Appl. Chem.* **2015**, *87* (1), 59–69. https://doi.org/10.1515/pac-2014-1003.

(25) Jiang, Y.; Woortman, A. J. J.; Alberda van Ekenstein, G. O. R.; Petrović, D. M.; Loos, K. Enzymatic Synthesis of Biobased Polyesters Using 2,5-Bis(Hydroxymethyl)Furan as the Building Block. *Biomacromolecules* **2014**, *15* (7), 2482–2493. https://doi.org/10.1021/bm500340w.

(26) Jiang, Y.; Woortman, A. J. J.; Ekenstein, G. O. R. A. van; Loos, K. A Biocatalytic Approach towards Sustainable Furanic–Aliphatic Polyesters. *Polym. Chem.* **2015**, *6* (29), 5198–5211. https://doi.org/10.1039/C5PY00629E.

(27) Skoczinski, P.; Espinoza Cangahuala, M. K.; Maniar, D.; Albach, R. W.; Bittner, N.; Loos, K. Biocatalytic Synthesis of Furan-Based Oligomer Diols with Enhanced End-Group Fidelity. *ACS Sustain. Chem. Eng.* **2020**, *8* (2), 1068–1086. https://doi.org/10.1021/acssuschemeng.9b05874.

(28) Baraldi, S.; Fantin, G.; Carmine, G. D.; Ragno, D.; Brandolese, A.; Massi, A.; Bortolini, O.; Marchetti, N.; Giovannini, P. P. Enzymatic Synthesis of Biobased Aliphatic–Aromatic Oligoesters Using 5,5′-Bis(Hydroxymethyl)Furoin as a Building Block. *RSC Adv.* **2019**, *9* (50), 29044–29050. https://doi.org/10.1039/C9RA06621G.

(29) Pellis, A.; Comerford, J. W.; Weinberger, S.; Guebitz, G. M.; Clark, J. H.; Farmer, T. J. Enzymatic Synthesis of Lignin Derivable Pyridine Based Polyesters for the Substitution of Petroleum Derived Plastics. *Nat. Commun.* **2019**, *10* (1), 1762. https://doi.org/10.1038/s41467-019-09817-3.

(30) Mueller, R.-J. Biological Degradation of Synthetic Polyesters—Enzymes as Potential Catalysts for Polyester Recycling. *Process Biochem.* **2006**, *41* (10), 2124–2128. https://doi.org/10.1016/j.procbio.2006.05.018.

(31) Müller, R.-J.; Kleeberg, I.; Deckwer, W.-D. Biodegradation of Polyesters Containing Aromatic Constituents. *J. Biotechnol.* **2001**, *86* (2), 87–95. https://doi.org/10.1016/S0168-1656(00)00407-7.

(32) Jian, J.; Xiangbin, Z.; Xianbo, H. An Overview on Synthesis, Properties and Applications of Poly(Butylene-Adipate-*Co*-Terephthalate)–PBAT. *Adv. Ind. Eng. Polym. Res.* **2020**, *3* (1), 19–26. https://doi.org/10.1016/j.aiepr.2020.01.001.

(33) Kijchavengkul, T.; Auras, R.; Rubino, M.; Selke, S.; Ngouajio, M.; Fernandez, R. T. Biodegradation and Hydrolysis Rate of Aliphatic Aromatic Polyester. *Polym. Degrad. Stab.* **2010**, *95* (12), 2641–2647. https://doi.org/10.1016/j.polymdegradstab.2010.07.018.

(34) Herrera, R.; Franco, L.; Rodríguez-Galán, A.; Puiggalí, J. Characterization and Degradation Behavior of Poly(Butylene Adipate-*Co*-Terephthalate)s. *J. Polym. Sci. Part Polym. Chem.* **2002**, *40* (23), 4141–4157. https://doi.org/10.1002/pola.10501.

(35) Wu, B.; Xu, Y.; Bu, Z.; Wu, L.; Li, B.-G.; Dubois, P. Biobased Poly(Butylene 2,5-Furandicarboxylate) and Poly(Butylene Adipate-*Co*-Butylene 2,5-Furandicarboxylate)s: From Synthesis Using Highly Purified 2,5-Furandicarboxylic Acid to Thermo-Mechanical Properties. *Polymer* **2014**, *55* (16), 3648–3655. https://doi.org/10.1016/j.polymer.2014.06.052.

(36) Matos, M.; Sousa, A. F.; Fonseca, A. C.; Freire, C. S. R.; Coelho, J. F. J.; Silvestre, A. J. D. A New Generation of Furanic Copolyesters with Enhanced Degradability: Poly(Ethylene 2,5-Furandicarboxylate)-*Co*-Poly(Lactic Acid) Copolyesters. *Macromol. Chem. Phys.* **2014**, *215* (22), 2175–2184. https://doi.org/10.1002/macp.201400175.

(37) Sousa, A. F.; Guigo, N.; Pożycka, M.; Delgado, M.; Soares, J.; Mendonça, P. V.; Coelho, J. F. J.; Sbirrazzuoli, N.; Silvestre, A. J. D. Tailored Design of Renewable Copolymers Based on Poly(1,4-Butylene 2,5-Furandicarboxylate) and Poly(Ethylene Glycol) with Refined Thermal Properties. *Polym. Chem.* **2018**, *9* (6), 722–731. https://doi.org/10.1039/C7PY01627A.

(38) Wu, L.; Mincheva, R.; Xu, Y.; Raquez, J.-M.; Dubois, P. High Molecular Weight Poly(Butylene Succinate-*Co*-Butylene Furandicarboxylate) Copolyesters: From Catalyzed Polycondensation Reaction to Thermomechanical Properties. *Biomacromolecules* **2012**, *13* (9), 2973–2981. https://doi.org/10.1021/bm301044f.

(39) Yu, Z.; Zhou, J.; Cao, F.; Wen, B.; Zhu, X.; Wei, P. Chemosynthesis and Characterization of Fully Biomass-Based Copolymers of Ethylene Glycol, 2,5-Furandicarboxylic Acid, and Succinic Acid. *J. Appl. Polym. Sci.* **2013**, *130* (2), 1415–1420. https://doi.org/10.1002/app.39344.

(40) Zhou, W.; Wang, X.; Yang, B.; Xu, Y.; Zhang, W.; Zhang, Y.; Ji, J. Synthesis, Physical Properties and Enzymatic Degradation of Bio-Based Poly(Butylene Adipate-*Co*-Butylene Furandicarboxylate) Copolyesters. *Polym. Degrad. Stab.* **2013**, *98* (11), 2177–2183. https://doi.org/10.1016/j.polymdegradstab.2013.08.025.

(41) Morales-Huerta, J. C.; Ciulik, C. B.; Ilarduya, A. M. de; Muñoz-Guerra, S. Fully Bio-Based Aromatic–Aliphatic Copolyesters: Poly(Butylene Furandicarboxylate-*Co*-Succinate)s Obtained by Ring Opening Polymerization. *Polym. Chem.* **2017**, *8* (4), 748–760. https://doi.org/10.1039/C6PY01879C.

(42) Maniar, D.; Jiang, Y.; Woortman, A. J. J.; van Dijken, J.; Loos, K. Furan-Based Copolyesters from Renewable Resources: Enzymatic Synthesis and Properties. *ChemSusChem* **2019**, *12* (5), 990–999. https://doi.org/10.1002/cssc.201802867.

(43) Nasr, K.; Meimoun, J.; Favrelle-Huret, A.; Winter, J. D.; Raquez, J.-M.; Zinck, P. Enzymatic Polycondensation of hexane-1,6-diol and Diethyl Adipate: A Statistical Approach Predicting the Key-Parameters in Solution and in Bulk. *Polymers* **2020**, *12* (9), 1907. https://doi.org/10.3390/polym12091907.

(44) Azim, H.; Dekhterman, A.; Jiang, Z.; Gross, R. A. Candida Antarctica Lipase B-Catalyzed Synthesis of Poly(Butylene Succinate): Shorter Chain Building Blocks Also Work. *Biomacromolecules* **2006**, *7* (11), 3093–3097. https://doi.org/10.1021/bm060574h.

(45) Mahapatro, A.; Kalra, B.; Kumar, A.; Gross, R. A. Lipase-Catalyzed Polycondensations: Effect of Substrates and Solvent on Chain Formation, Dispersity, and End-Group Structure. *Biomacromolecules* **2003**, *4* (3), 544–551. https://doi.org/10.1021/bm0257208.

(46) Debuissy, T.; Pollet, E.; Avérous, L. Enzymatic Synthesis of a Bio-Based Copolyester from Poly(butylene succinate) and Poly((R)-3-hydroxybutyrate): Study of Reaction Parameters on the Transesterification Rate https://pubs.acs.org/doi/pdf/10.1021/acs.biomac.6b01494 (accessed Apr 22, 2021). https://doi.org/10.1021/acs.biomac.6b01494.

(47) Pérez-Camargo, R. A.; Arandia, I.; Safari, M.; Cavallo, D.; Lotti, N.; Soccio, M.; Müller, A. J. Crystallization of Isodimorphic Aliphatic Random Copolyesters: Pseudo-Eutectic Behavior and Double-Crystalline Materials. *Eur. Polym. J.* **2018**, *101*, 233–247. https://doi.org/10.1016/j.eurpolymj.2018.02.037.

(48) Mincheva, R.; Delangre, A.; Raquez, J.-M.; Narayan, R.; Dubois, P. Biobased Polyesters with Composition-Dependent Thermomechanical Properties: Synthesis and Characterization of Poly(Butylene Succinate-*Co*-Butylene Azelate). *Biomacromolecules* **2013**, *14* (3), 890–899. https://doi.org/10.1021/bm301965h.

(49) Liang, Z.; Pan, P.; Zhu, B.; Inoue, Y. Isomorphic Crystallization of Aliphatic Copolyesters Derived from hexane-1,6-diol: Effect of the Chemical Structure of Comonomer Units on the Extent of Cocrystallization. *Polymer* **2011**, *52* (12), 2667–2676. https://doi.org/10.1016/j.polymer.2011.04.032.

(50) Kwiatkowska, M.; Kowalczyk, I.; Kwiatkowski, K.; Szymczyk, A.; Jędrzejewski, R. Synthesis and Structure – Property Relationship of Biobased Poly(Butylene 2,5-Furanoate) – Block – (Dimerized Fatty Acid) Copolymers. *Polymer* **2017**, *130*, 26–38. https://doi.org/10.1016/j.polymer.2017.10.009.

(51) Bai, Z.; Liu, Y.; Su, T.; Wang, Z. Effect of Hydroxyl Monomers on the Enzymatic Degradation of Poly(Ethylene Succinate), Poly(Butylene Succinate), and Poly(Hexylene Succinate). *Polymers* **2018**, *10* (1), 90. https://doi.org/10.3390/polym10010090.

(52) Ceccorulli, G.; Scandola, M.; Kumar, A.; Kalra, B.; Gross, R. A. Cocrystallization of Random Copolymers of ω-Pentadecalactone and ε-Caprolactone Synthesized by Lipase Catalysis. *Biomacromolecules* **2005**, *6* (2), 902–907. https://doi.org/10.1021/bm0493279.

4. Enzymatic synthesis of levoglucosan based polyesters and *co*-polyesters.

4.1 Introduction

Amongst the different products issued from biomass, cellulose is the most abundant one, constituting more than 50% of the overall biomass weight.[1,2] While other constituents of the biomass such as hemicellulose and lignin are also present, certain processes can be utilized to separate them apart from, allowing a more selective valorization of each component such as the Kraft and Organosolv procedures.[3–5]

The importance of cellulose stems from the wide array of products that it can convert to, including their use in different fields and applications. This polysaccharide consisting of thousands of linearly arranged β-1,4 linked D-glucose units can be chemically converted to glucose and furan-based derivatives. The use of cellulose as a precursor to produce such molecules is an important aspect of the environmental sustainability, especially that cellulose unlike starch, is not in competition with food sourcing.[1,6,7]

Levoglucosan (Scheme 21) is an anhydrous derivative of glucose that is produced mainly *via* starch and cellulose pyrolysis.[8,9] The increasing focus on levoglucosan production and other related anhydro carbohydrates from cellulose is due to the likelihood of these molecules to be valorized in multiple fields such as the polymer industry and pharmaceuticals.[10] In addition to its promising applications, the pyrolysis process of cellulose can be efficiently upscaled for commercial use with minimal impact on the environment due to the solvent-free nature of this process.[5]

As aforementioned, different approaches have been studied and optimized for converting cellulose into ethanol, lipids, glucose, and other important molecules. However, the use of pure levoglucosan has not been completely neglected. In fact, some studies have focused on pure levoglucosan to produce certain molecules with attractive applications. One of the main issues limiting the use of levoglucosan is its highly hydrophilic nature. Indeed, the hydrophilicity of levoglucosan prevents the use of certain organometallic catalysts, and limits reactions with

certain hydrophobic moieties. In addition to the aforementioned limitations, the localization of the hydroxyl groups on levoglucosan in the axial position provides a certain degree of structural stability due to certain intermolecular interactions (hydrogen bonding). This occurs mainly between the C2 and C4 hydroxyl groups, in addition to the hydrogen bonding between the oxygen positioned on C6 and the hydroxyl group at the C3 carbon as observed in Scheme 21. The high structural stability however decreases the reactivity of levoglucosan towards other moieties.[11,12]

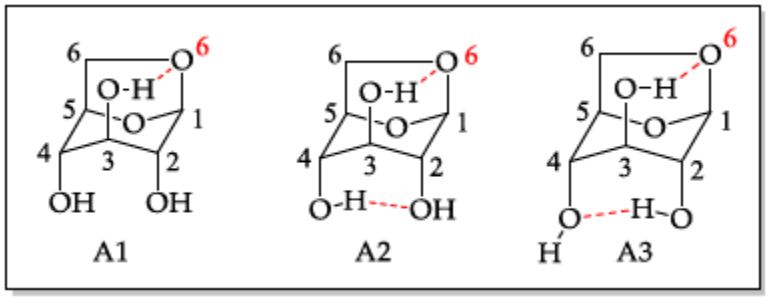

Scheme 21. Conformational structures for levoglucosan in the axial position (in red: hydrogen bonding).[13]

Nevertheless, the esterification of levoglucosan has been reported in the literature.[14–16] Galletti *et al.*[17] reported the enzyme-catalyzed esterification and transesterification of levoglucosan with different acids and vinyl esters. The study also compared between different enzymes and solvents and compared yields after performing 5 days reactions. The use of acetonitrile and 1-(2-hydroxyethyl)-3-methylimidazolium dicyanamide [MOEMIm][dca] ionic liquid was favored and resulted in better yields. An example is provided in Scheme 22, showing the reaction between levoglucosan and vinyl acetate catalyzed *via* Novozym 435 in [MOEMIm][dca], and the structures of the obtained esters. The main product was 4-O-acetyl levoglucosan represented as structure (a) in scheme, with 61% yield. The other structures did not exceed 9% yield each.

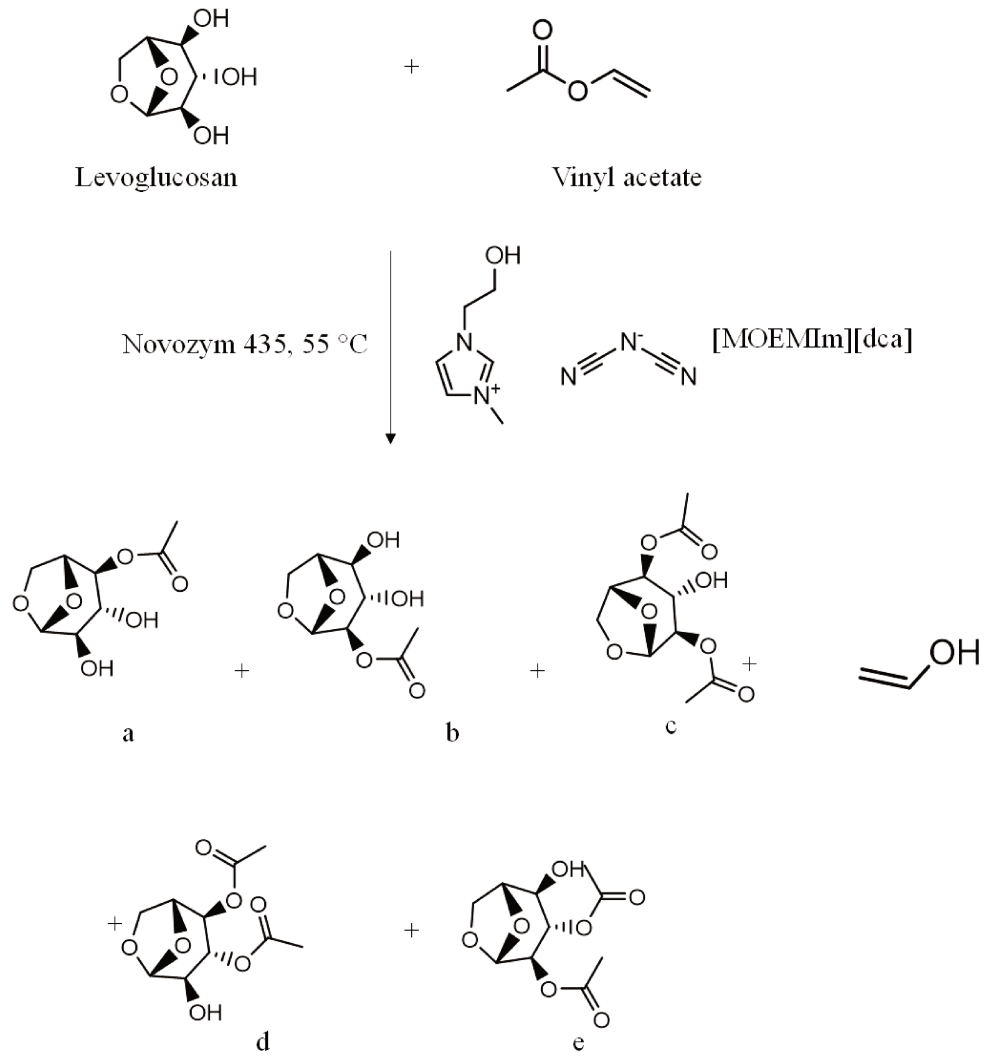

Scheme 22. Enzyme-catalyzed reaction between levoglucosan and vinyl acetate in ionic liquid.[17]

While using vinyl esters led to good yields in both ionic liquid and acetonitrile, acids on the other hand, resulted in good yields only in the presence of Lewis acid-type ionic liquids. Regarding the enzyme type, Novozym 435 and PS (lipase from *Pseudomonas cepacea* immobilized on ceramic particles) were found to be better suited than *Candida cylindracea*. In another recent work, Avelar do Nascimento *et al.*[13] examined the lipase-catalyzed transesterification of levoglucosan with several ethyl esters in acetonitrile. Comparing between different enzymes, it was found that N435 exhibited similar selectivity towards C2 and C4 hydroxyl groups for most esters, while both PSIM (*Burkholderia cepacia*) and CALB_epoxy (CALB immobilized on Epoxy resin Purolite) showed preference towards the hydroxyl group located on C4.

Based on these findings, the successful esterification of levoglucosan with multiple esters, in addition to the equireactivity towards the C2 and C4 hydroxyl groups, we perform for the first time, in collaboration with Prof. Ivaldo Itabaiana Jr and his team, the enzyme-catalyzed polycondensation of levoglucosan with different chain length diesters and diols aiming to produce levoglucosan-based copolymers and terpolymers. The use of different chain length monomers was based on our previous work and previous reports in the literature that showed lipases have a preference and a better catalytic performance towards longer aliphatic moieties.[18,19]

4.2 Results and discussion

The reaction of levoglucosan with excess amounts of diethyl adipate is depicted in Scheme 23 and detailed in section 4.4.2. The conversion was determined *via* ^{1}H NMR analysis on the crude sample recovered at the end of the reaction before any purification.

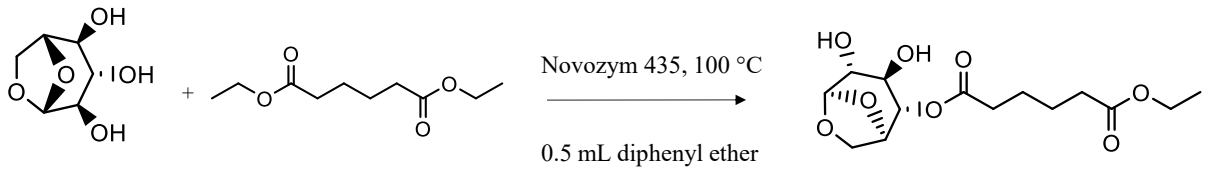

Scheme 23. Enzyme-catalyzed reaction of levoglucosan and diethyl adipate in 0.5 mL diphenyl ether. *Note that the reaction might have occurred at positions C2, C3 and C4 hydroxyl groups, but was simplified in the scheme.*

From the ^{1}H NMR spectrum given in Figure 36, it was clear that the reactivity between levoglucosan and diethyl adipate was minimum, where after 24 h of the reaction, the ^{1}H NMR showed high amounts of unreacted diethyl adipate. Conversion did not exceed 18% and was calculated by subtracting the amount of unreacted diethyl adipate represented by the end group (4') at 4.03 ppm from the total amount of diethyl adipate (reacted + unreacted) represented by (2') and (2") at 2.28 and 2.35 ppm, respectively. In fact, it was even visually evident that high amounts of levoglucosan remained undissolved in the reaction media even after a 24 h reaction, suggesting that the poor solubility of levoglucosan in the reaction media is a major limiting factor in the polycondensation reaction.

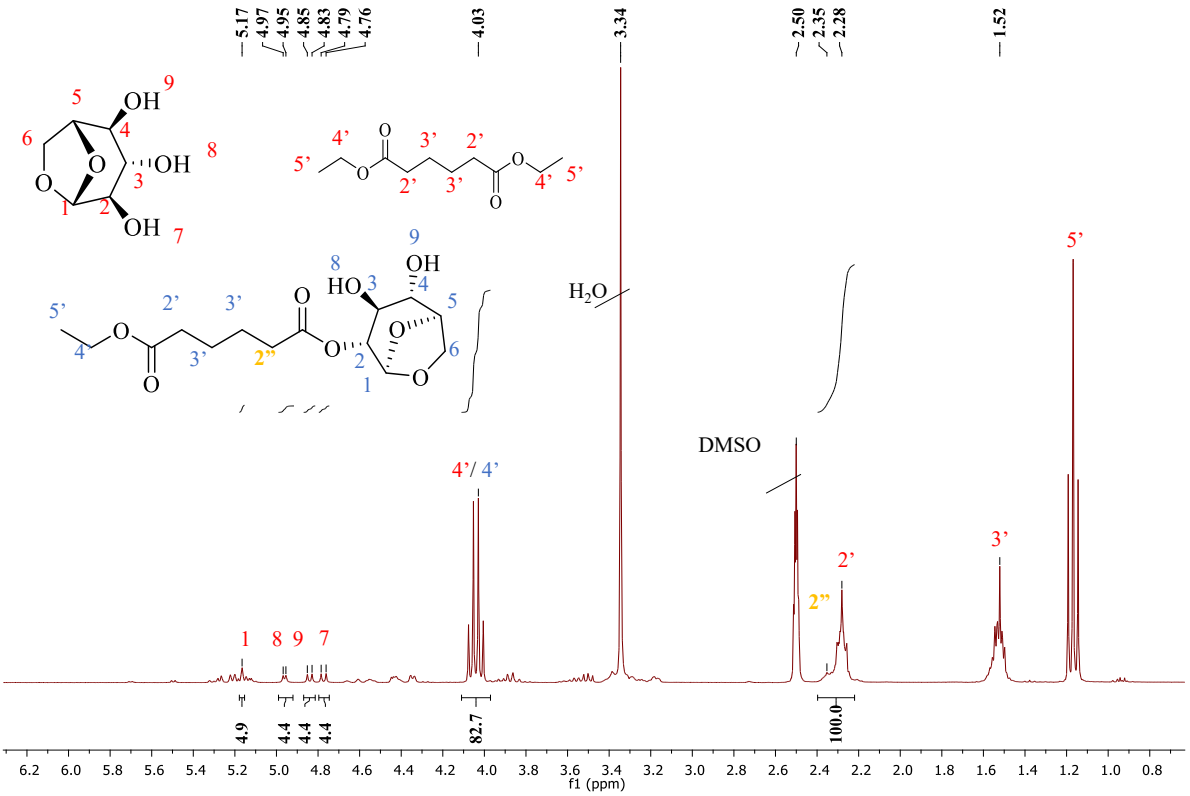

Figure 36. ^{1}H NMR spectrum (DMSO-d_6, 300 MHz) of the product obtained from the reaction between levoglucosan and diethyl adipate.

In the second approach detailed in 4.4.3.2, levoglucosan in combination with an aliphatic diol got reacted against diethyl adipate in both bulk and solvent conditions (i.e., in diphenyl ether) as observed in Scheme 24.

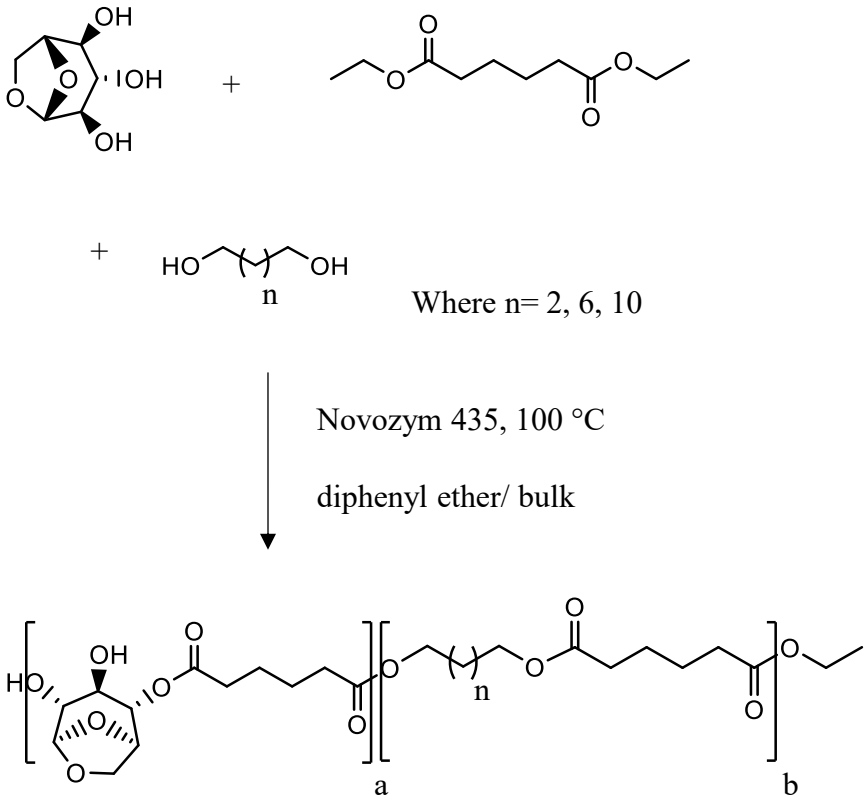

Scheme 24. Enzyme-catalyzed reaction between levoglucosan, diethyl adipate and different chain length diols (butane-1,4-diol, octane-1,8-diol, and dodecane-1,12-diol) in bulk and solvent conditions.

In an attempt to overcome the poor reactivity and polymer growth observed before; levoglucosan was added at lower amounts, being 25 and 50% relative to diethyl adipate, overall while maintaining an equimolar diol: diester ratio by incorporating butane-1,4-diol, octane-1,8-diol, or dodecane-1,12-diol as comonomers. As presented in Table 21, the influence of medium nature, levoglucosan molar loading and diol length were all assessed in terms of molecular microstructure (X-levo), yield by weight and number average molecular weight (M_n), where X-levo is defined as the percentage of levoglucosan incorporated into the polymeric structure and is calculated following Equation 4.

Equation 4. X-levo (%) showing the percentage amount of levoglucosan incorporated into the polymeric structure.

$$\boldsymbol{X-levo}(\%) = \boldsymbol{I_{levo-ester}}/(\boldsymbol{I_{levo-ester}} + \boldsymbol{I_{diol-ester}}),$$

where ($I_{levo\text{-}ester}$) represents the ^{1}H NMR integration value of the peak representing levoglucosan ester at ~ 2.38 ppm, while $I_{diol\text{-}ester}$ represents the ^{1}H NMR integration value of the peak representing diol-ester at ~ 2.28 ppm. (An example of ^{1}H NMR peak assignments is given later in the chapter in Figure 37 and confirmed with 2D COSY (Figure 38)

From Table 21, it is observed that when butane-1,4-diol was used as a comonomer with levoglucosan and diethyl adipate, the ^{1}H NMR spectrum did not show any detectable evidence about the reaction between levoglucosan and diethyl adipate in diphenyl ether, and no precipitate was collected (entry 1). On the other hand, minimal traces were detected when the reaction was conducted in bulk conditions (entry 2). However, the yield by weight did not exceed 17%. Increasing the diol length up to C_8 with octane-1,8-diol showed a positive impact on reactivity when the reaction was performed in diphenyl ether (entry 3), where the introduction of levoglucosan at 25 mol % in the feed, led to a polymer with a M_n of 5,300 g.mol^{-1}, 62% yield by weight, and 14% of levoglucosan were detected in the polymer microstructure after precipitation. On the other hand, performing the same reaction in bulk conditions (entry 4) led to a lower M_n of 3,300 g.mol^{-1}, a similar 58% yield by weight, but the levoglucosan detected in the microstructure of the precipitated polymer did not exceed 3%. It must be noted that the conversion was not calculated in this case as any residual levoglucosan present at the end of the reaction did not get dissolved in $CDCl_3$. Similarly, peaks related to unreacted diethyl adipate observed as a quartet peak at ~ 4.08 ppm representing the CH_2 in the end group, interlapped with other peaks such as the *endo* hydrogen on the C6 of levoglucosan.

Increasing levoglucosan feed loading to 50% in the presence of octane-1,8-diol, led to a significant drop in yield to 11 and 9% w/w in diphenyl ether and bulk conditions, respectively (entries 5 and 6). The amount of levoglucosan detected in the microstructure did not exceed 14%, suggesting a large remaining portion of unreacted levoglucosan.

Although the increase in diol length from C_8 to C_{12} in dodecane-1,12-diol (entries 7 and 8) did not show any positive or negative influence on the amount of X-levo compared to the reactions with octane-1,8-diol, the yield by weight significantly increased to 47 and 48%, and the M_n recorded 2,200 and 2,500 g.mol^{-1} in diphenyl ether and bulk, respectively. The yield increase

might have resulted from the fact that lipases catalyze the transesterification reactions of longer diols in a more efficient manner.[18,19]

In all tested samples, the M_n was limited <5,300 g.mol^{-1} and the dispersity did not exceed 1.6. It was also evident from the results in Table 21, that the detected amount of levoglucosan (X-levo) before precipitation (measured at the end of the reaction) was significantly higher than X-levo detected in the precipitated polymer, suggesting that although higher amounts of levoglucosan did react, the chain growth was rather limited, together with the fact that a certain amount of low molecular weight oligomers did not precipitate. These observations could have resulted from a number of factors, such as the weak selectivity of N435 towards secondary diols leading to poor reactivity towards the hydroxyl groups of levoglucosan, in addition to the intermolecular interactions occurring within the levoglucosan structure as seen in Scheme 21. This might have further limited reactivity.[13,20]Another major limiting factor, is the high polarity of levoglucosan which limits its solubility and interaction with diesters.[5,17,21]

Table 21. Molecular structure analysis (X-levo), % yield, M_n, and $Đ_M$ of levoglucosan-based *co*-polyesters with variable levoglucosan content and aliphatic diols in bulk and diphenyl ether conditions.

Entry	Aliphatic diol[1]	Levoglucosan feed (%)[2]	Medium	X-levo (Before precipitation)[3]	X-levo (After precipitation)[4]	Yield by weight (%)	M_n(g.mol^{-1})[5]	Dispersity ($Đ_M$) [6]
1	C_4	25	Diphenyl ether	0	0	0	ND	ND
2	C_4	25	Bulk	Traces	Traces	17	4700	1.32
3	C_8	25	Diphenyl ether	15	13	62	5300	1.53
4	C_8	25	Bulk	12	3	58	3300	1.51
5	C_8	50	Diphenyl ether	25	8	11	3000	1.24
6	C_8	50	Bulk	30	14	9	4100	1.1
7	C_{12}	50	Diphenyl ether	22	12	47	2200	1.44
8	C_{12}	50	Bulk	23	12	48	2500	1.4

[1] C_4 = butane-1,4-diol, C_8 = octane-1,8-diol, C_{12} = dodecane-1,12-diol. [2] Levoglucosan feed (%) = represents the molar percentage of levoglucosan added, relative to the total diol amount. [3] X-levo (before precipitation) = defined as the molar fraction of levoglucosan ester repeating unit in the copolymer at the end of the reaction and determined *via* ^{1}H NMR as per equation 4. [4] X-levo (after precipitation) = defined as the molar fraction of levoglucosan ester repeating unit in the copolymer in the polymer structure collected after precipitation and determined *via* ^{1}H NMR as per equation 4.[5] The number average molecular weight (M_n) was obtained from GPC analyses ($CHCl_3$, 23 °C, polystyrene standards). [6] Molar mass dispersity $Đ_M = M_w/M_n$ was obtained from GPC analyses ($CHCl_3$, 23 °C, polystyrene standards).

The amount of levoglucosan successfully incorporated into the polymeric structure was limited to a maximum of 14% in all tested reactions of Table 21 . We have therefore substituted diethyl adipate (C_6) with the longer diethyl sebacate (C_{10}) and proceeded with the reaction as observed in and detailed in Scheme 25 and detailed in section 4.4.3.2.

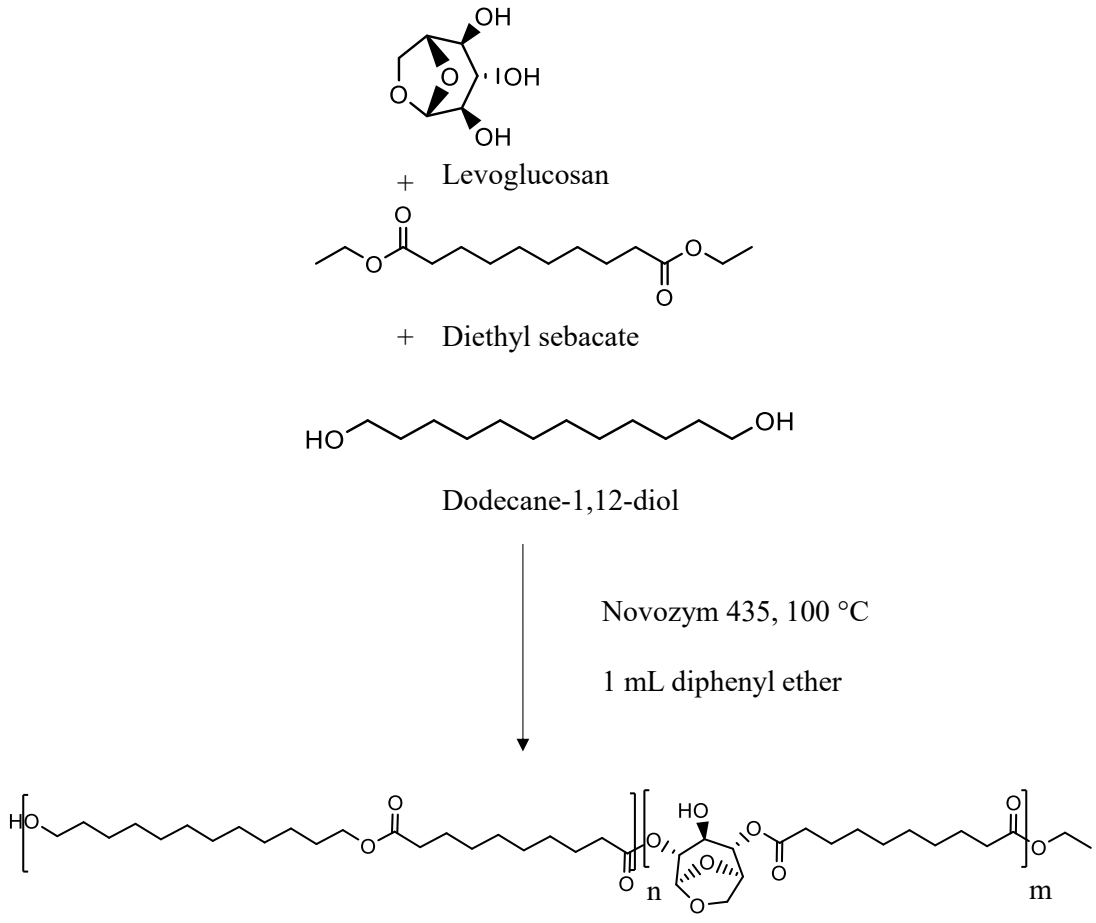

Scheme 25. Enzyme-catalyzed reaction between levoglucosan, diethyl sebacate and dodecane-1,12-diol in diphenyl ether.

As depicted in Table 22, increasing the length of the diester had a positive influence on reactivity in general. Apart from entry 12, the yield by weight exceeded 80% in all reactions, with a slight superiority to reactions performed in diphenyl ether. Additionally, the detected X-levo in the precipitated polymers increased significantly and was better related to the feed ratio of levoglucosan with up to 35% detected in entry 11. In addition, the M_n almost doubled in value compared to the reactions performed with diethyl adipate. These results suggest that increasing the length of the diester had a positive effect on the enzyme-catalyzed

polycondensation of levoglucosan, which comes in agreement with previous reports in the literature stating a similar increase in reactivity as a function of increasing the chain length of the diacids.[19,22,23]

Table 22. Molecular structure analysis (X-levo), % yield, M_n, and $Đ_M$ of levoglucosan-based *co*-polyesters with variable levoglucosan content in bulk and diphenyl ether conditions.

Entry	Aliphatic diol[1]	Levoglucosan feed (%)[2]	Medium	X-levo (before precipitation)[3]	X-levo (after precipitation)[4]	Yield by weight (%)	M_n (g.mol^{-1})[5]	Dispersity ($Đ_M$)[6]
9	**C_{12}**	25	Diphenyl ether	18	14	94	5400	1.82
10	**C_{12}**	25	Bulk	11	6	88	3900	1.83
11	**C_{12}**	50	Diphenyl ether	40	35	81	4300	1.73
12	**C_{12}**	50	Bulk	34	30	58	4000	1.68

[1] C_4 = butane-1,4-diol, C_8 = octane-1,8-diol, C_{12} = dodecane-1,12-diol. [2] Levoglucosan feed (%) = represents the molar percentage of levoglucosan added, relative to the total diol amount. [3] X-levo (before precipitation) = defined as the molar fraction of levoglucosan ester repeating unit in the copolymer at the end of the reaction and determined *via* ^{1}H NMR as per equation 4. [4] X-levo (after precipitation) = defined as the molar fraction of levoglucosan ester repeating unit in the copolymer in the polymer structure collected after precipitation and determined *via* ^{1}H NMR as per equation 4.[5] The number average molecular weight (M_n) was obtained from GPC analyses ($CHCl_3$, 23 °C, polystyrene standards). [6] Molar mass dispersity $Đ_M = M_w/M_n$ was obtained from GPC analyses ($CHCl_3$, 23 °C, polystyrene standards).

^{1}H NMR and 2D COSY NMR were used to confirm the microstructure of the terpolymers produced. As a case study in this chapter, entry 11 in Table 22 was selected based on its high levoglucosan incorporation (35%), high yield of 81%, and good M_n of 4,300 g.mol^{-1}. The structure of the polyester was confirmed *via* ^{1}H NMR (Figure 37) and COSY analysis, where starting from C2 of levoglucosan, we were able to assign the rest of the peaks following the homonuclear correlations patterns as shown in Figure 38. The X-levo calculated *via* Equation is visually depicted in Figure 37 and is based on the integration ratio of levoglucosan ester represented by 2'(red) relative to the total diesters in the reaction represented by 2' (blue) and 2' (red) at 2.28 and 2.38, respectively. In addition, the formation of a terpolymer between the respective monomers rather than two separate copolymers was confirmed by performing DOSY NMR scans. The spectrum provided in Figure 39 shows a single diffusion coefficient representing entry 12.

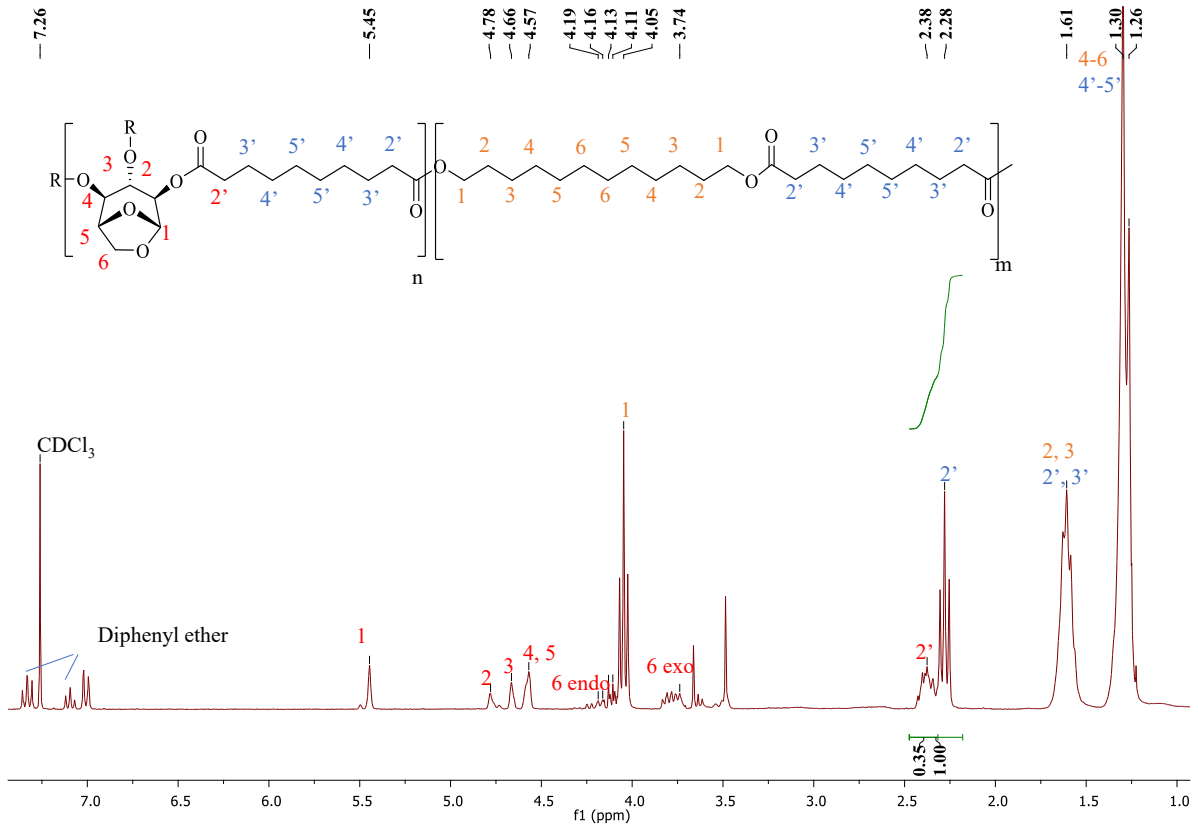

Figure 37. ^{1}H NMR spectrum and peak assignment for entry 11, where R can represent an ester or a hydrogen atom. ^{1}H NMR (300 MHz, $CDCl_3$) δ 5.45 (s, 1H), 4.78 (s, 1H), 4.66 (s, 1H), 4.57 (s, 1H), 4.15 (dd, J = 16.9, 7.3 Hz, 1H), 4.05 (t, 4H), 3.78 (dd, J = 5.9 Hz, 1H), 2.38 (s, 4H), 2.28 (t, 4H), 1.74 – 1.49 (m, 16H), 1.28 (d, J = 9.7 Hz, 26H). *Note: the regioselectivity towards C2 in levoglucosan is chosen arbitrarily and might occur at C3 and C4.*

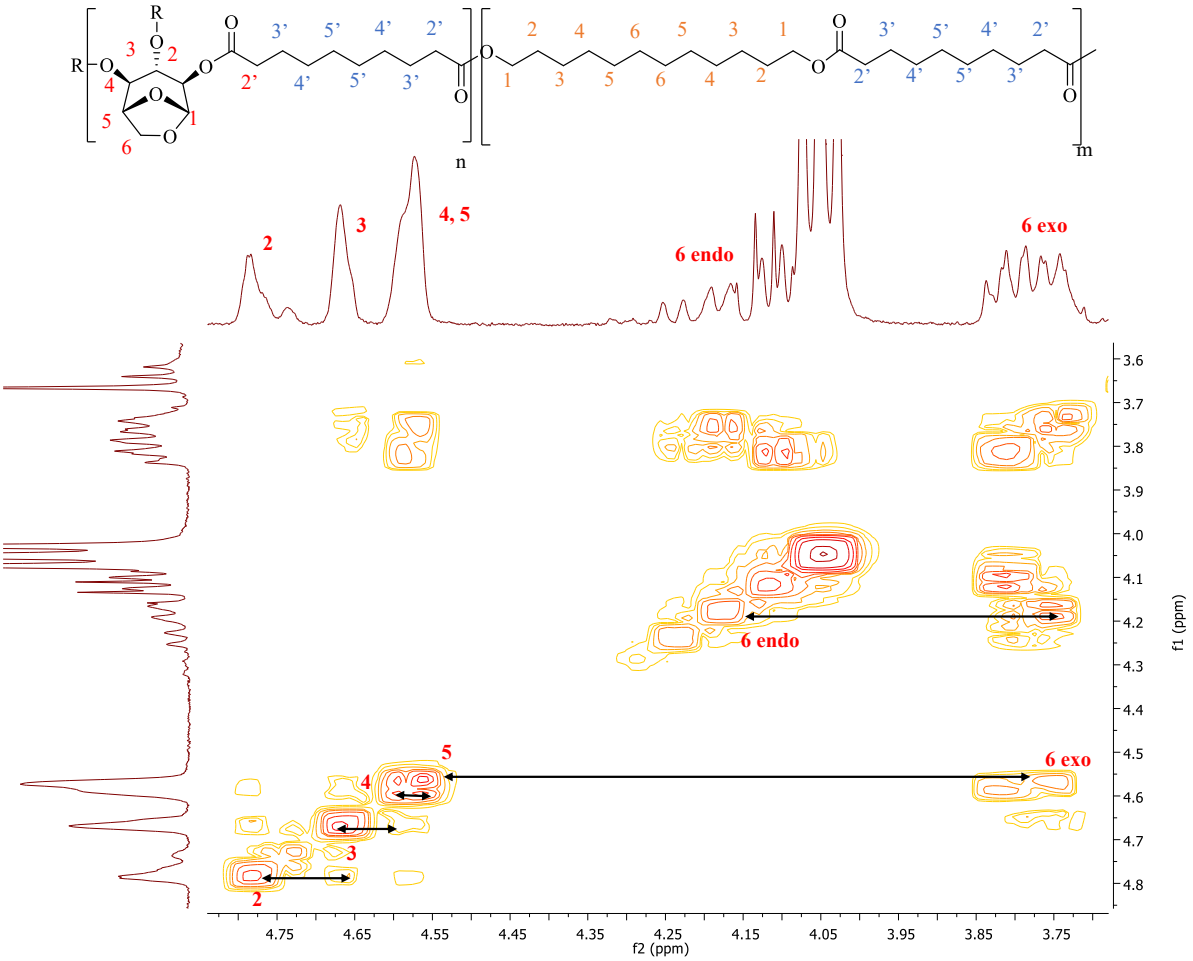

Figure 38. An enlarged 2D-COSY NMR (300 MHz, $CDCl_3$) spectra of entry 11 showing the correlation between adjacent protons of levoglucosan and was used to confirm the microstructure of the polymer produced.

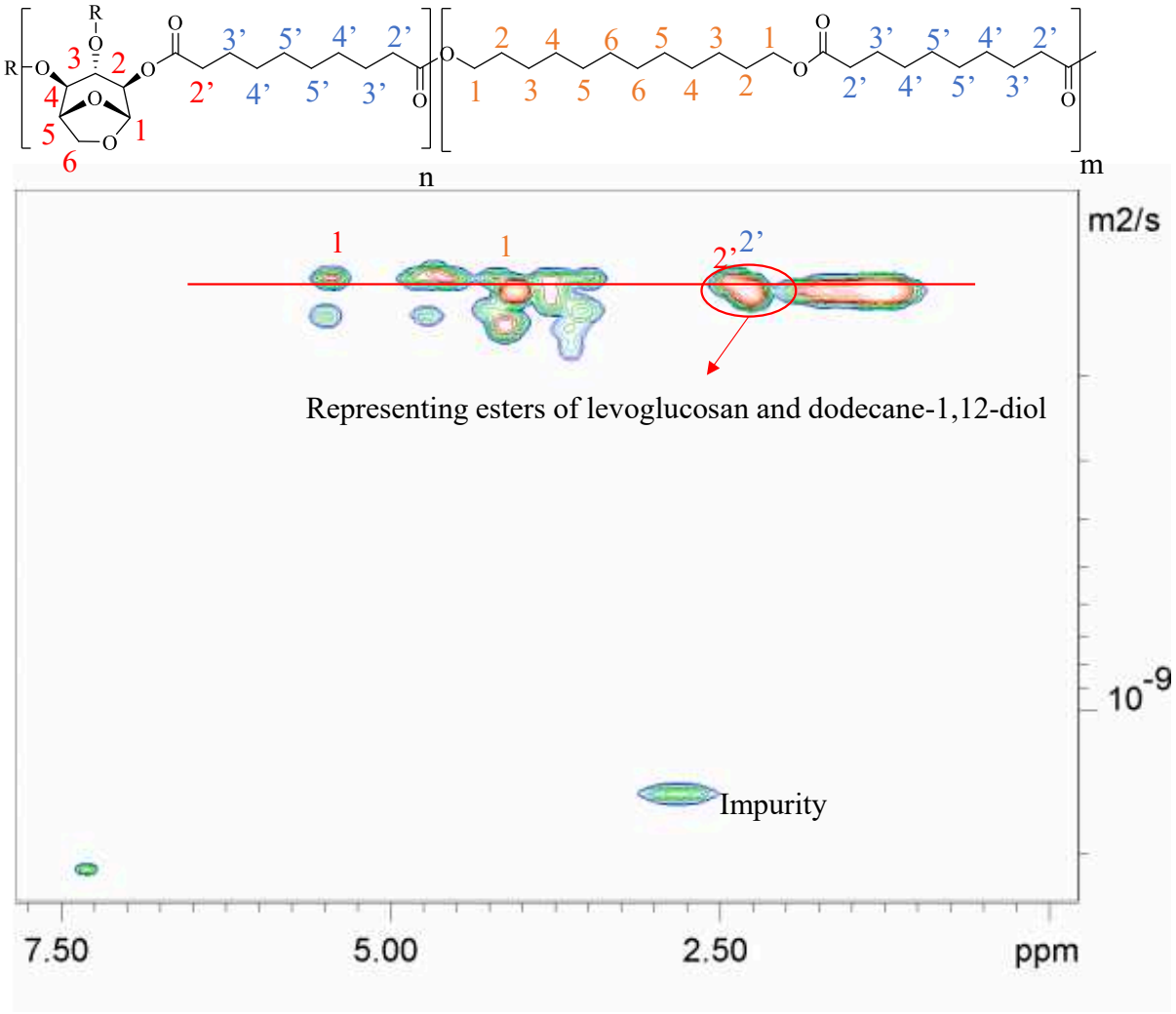

Figure 39. A DOSY NMR (400 MHz, $CDCl_3$) spectrum of a levoglucosan based polymer (entry 12).

In another approach to incorporate levoglucosan into a polymeric structure, diethyl adipate was substituted with divinyl adipate, as presented in Scheme 26 and detailed in section 4.4.3.3.

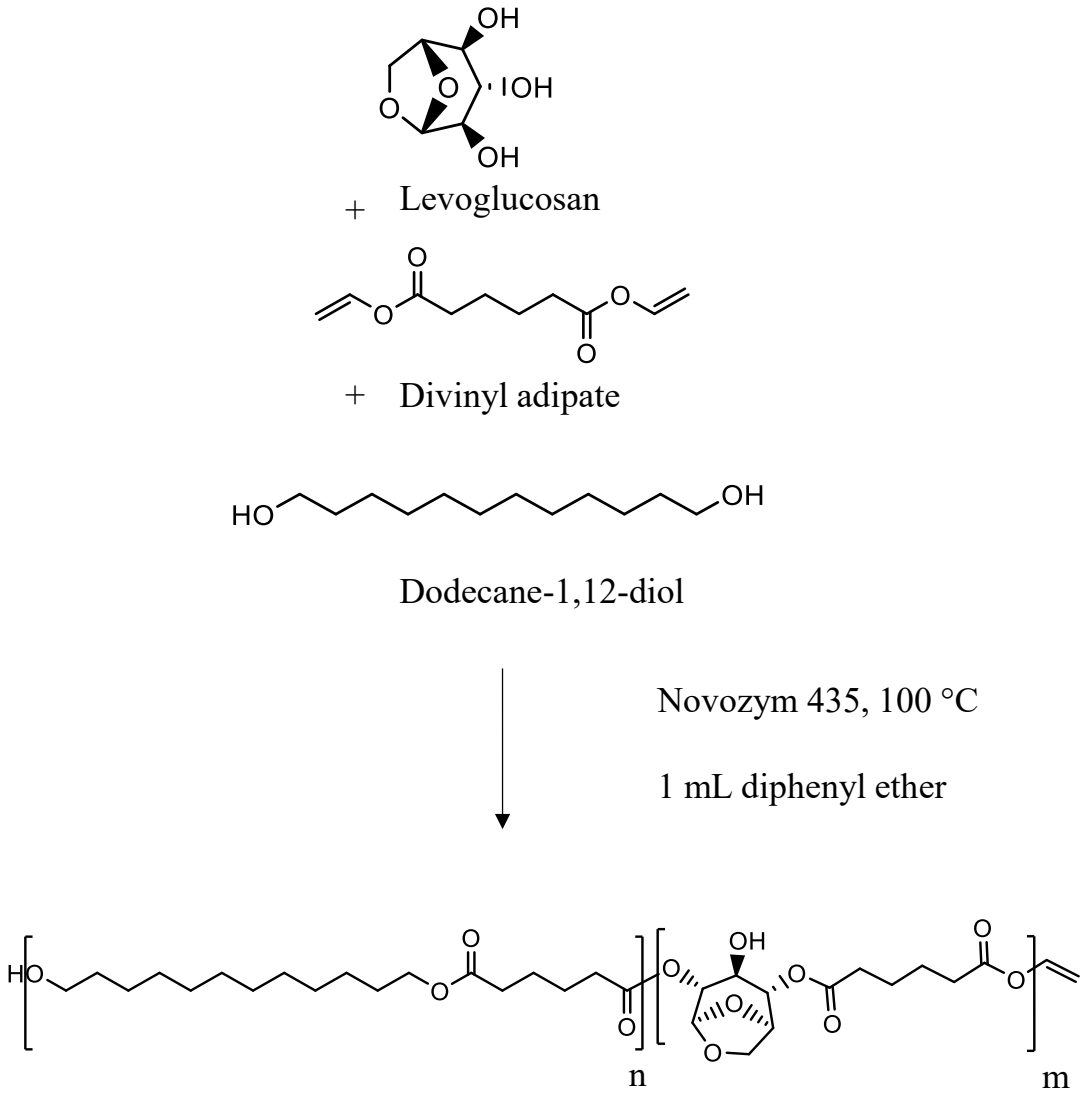

Scheme 26. Enzyme-catalyzed reaction between levoglucosan, divinyl adipate and dodecane-1,12-diol in diphenyl ether.

The advantage of using divinyl esters is due to the production of ethenol as a byproduct, which tautomerizes under normal conditions to the more stable acetaldehyde. Besides being a highly volatile substance it can easily evacuate the system, preventing the backward reaction which is a limiting factor in polycondensation reactions.[24] From Figure 40, it was evident that levoglucosan fully reacted with divinyl adipate, where the ^{1}H NMR spectra of a sample taken after 24 h of the reaction showed the formation of two esters, an ester of levoglucosan and divinyl adipate (X-levo = 46%) and an ester of dodecane-1,12-diol and divinyl adipate at 54%, which is in good agreement with the feed molar ratio of the reacting monomers. This

observation confirms that the reactivity of levoglucosan towards divinyl esters is superior to that towards diethyl adipate that only led to X-levo value of 22% (entry 7). Surprisingly, the polymer growth appeared to be limited since the precipitation did not yield any polymers. In one research work, the limitations in polymer growth were related to the hydrolysis of the vinyl esters during the reaction due to the use of high amounts of enzymes containing bound water.[25] Therefore, further experimentation and structural analysis could shed light on the underlying causes.

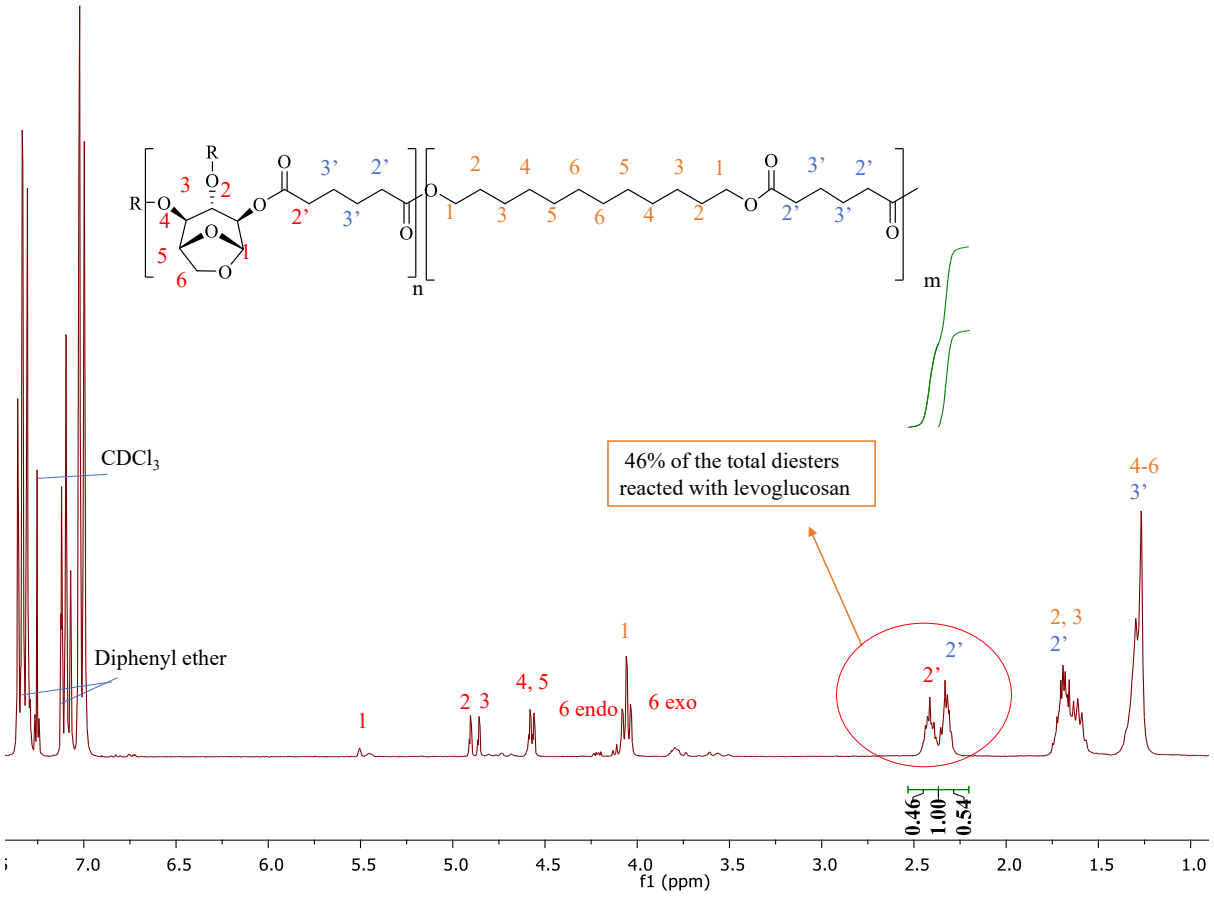

Figure 40. ^{1}H NMR (300MHz, $CDCl_3$) spectrum of the reaction between levoglucosan, divinyl adipate, and dodecane-1,12-diol. (Sample withdrawn after 24 h from the start of the reaction).

Like the effect of levoglucosan incorporation on the thermal behavior of the final polymer, Figure 41 depicts the effect of increasing the amount in levoglucosan on the polymer synthesized *via* reacting levoglucosan, dodecane-1,12-diol and diethyl adipate (entries 9 and 11 in Table 22, in addition to a reference reaction without levoglucosan). The glass transition temperature (T_g) was only detected for entry 11 (T_g = 31 °C) due to the high content of levoglucosan that led to a decrease in crystallinity and an increase in the amorphous phase. The melting endotherm and crystallinity showed significant variations as a function of the levoglucosan content. As observed, the incorporation of only 14% levoglucosan into the polymeric structure led to a decrease in the melting point by around 8 °C and a drop in crystallinity from 134 J/g down to 97 J/g. Similarly, a further increase in levoglucosan to 35% led to a further decrease in the melting endotherm and crystallinity to 57 °C and 56 J/g, respectively. This trend is similar to what was observed in our work on diethyl furan-2,5-dicarboxylate (DEFDC) in Chapter 3 that showed a similar decrease in both crystallinity and melting point as the DEFDC content increases up to a certain percentage and was linked to the isodimorphic behavior that is usually observed with certain random copolymers.[26,27]

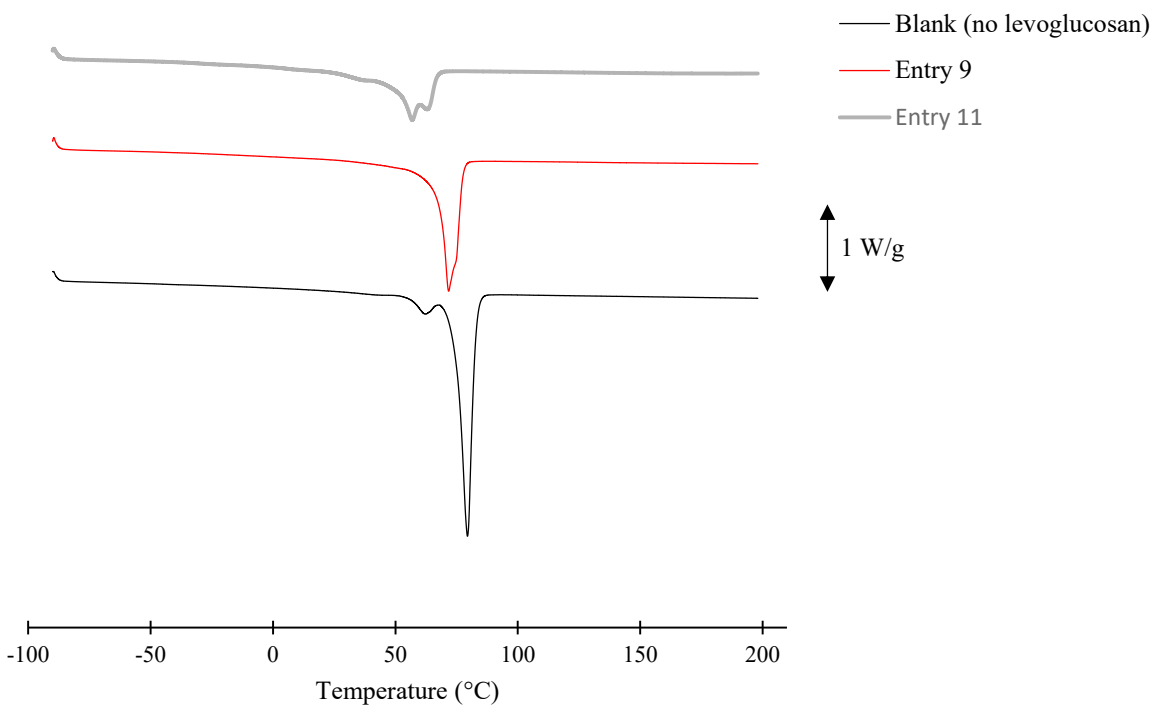

Figure 41. Variations in melting endotherms (°C) and crystallization enthalpies (J/g) as a function of increasing levoglucosan incorporation into the polymer structure. (Blank: no levoglucosan, and entries 9 and 11).

4.3 Conclusion

It was evident from the results that although the reaction between levoglucosan and diethyl adipate was not feasible, the incorporation of aliphatic diols alongside levoglucosan in the reactions with diethyl alkanoates improved reactivity and polymer growth. The N435-catalyzed polycondensation of levoglucosan was enhanced by increasing the aliphatic diol and diester chain length, showing the highest X-levo value of 35% with dodecane-1,12-diol and diethyl sebacate, and a M_n of 4,300 g.mol^{-1}. It was also observed that while substituting diethyl adipate with divinyl adipate resulted in higher X-levo at the end of the reaction, the polymer growth was rather limited as no precipitates were collected. Regarding the thermal properties of the produced copolyesters, both the melting endotherm and crystallinity decreased as a function of the increased amount of levoglucosan incorporated in the polymeric structure. Finally, this work introduces for the first time the successful enzyme-catalyzed

polycondensation of levoglucosan to produce a series of levoglucosan-containing terpolymers. Further work should build on these findings to optimize reactivity and analyze the properties of such polymers and their possible applications.

4.4 Materials and Methods

4.4.1 Materials

Levoglucosan (99%) was acquired from Chem-Impex Int'l Inc. Diethyl adipate (99%), and diphenyl ether (99%) were purchased from Sigma-Aldrich. Butane-1,4-diol (99%), octane-1,8-diol (98%), dodecane-1,12-diol (98%) were purchased from Acros Organics. furan-2,5-dicarboxylic acid (99.7%) was purchased from Satachem co. Divinyl adipate was purchased from Tokyo Chemical Industry. Analytical grade methanol, absolute ethanol, and chloroform (99%) were purchased from VWR. All the reagents and solvents were used as received. Novozym 435 (N435), a *Candida antarctica* lipase B (CALB) immobilized on a porous acrylic resin was kindly provided by Novozymes. Chloroform D ($CDCl_3$) (99.8%) and deuterated dimethyl sulfoxide DMSO-d_6 were purchased from Euriso-Top.

4.4.2 Enzymatic polycondensation of levoglucosan and diethyl adipate

Levoglucosan (2 mmol) and diethyl adipate (3 mmol) were weighed and added into a schlenk tube. 20% w/w of N435 (relative to the total weight of the monomers) was weighed and added to the mixture. 0.5 mL of diphenyl ether was added as a solvent of choice and the reaction was commenced with no additional steps. The reaction proceeded under atmospheric pressure for 2 h at 100 °C (using an oil bath with continuous stirring kept constant at 350 rpm). Afterwards, the schlenk tube was attached to a vacuum line, and the pressure was decreased gradually in 1 h to reach 10 mbar to remove byproduct (ethanol). After applying the vacuum, the reaction was left to proceed for 24 h and got stopped by adding an excess amount of chloroform under atmospheric pressure after a cooling step, followed by direct filtration to remove the N435 beads. The filtrate was then partially evaporated using a rotavap, followed by the addition of

excess amount of cold methanol to precipitate the obtained polymer. The mixture was then filtered, and the product obtained was left to dry at room temperature for 24 h before collecting and weighing. The polyesters synthesized were compared in terms of conversion, X-levo and M_n.

4.4.3 Enzymatic polycondensation approach towards biobased levoglucosan-containing *co*-polyesters.

4.4.3.1 Influence of aliphatic diol length.

Levoglucosan in addition to an aliphatic diol and diethyl adipate were reacted *via* a two-step reaction following a similar approach to the one stated in the previous section. Keeping an equimolar diol: diester ratio, levoglucosan was added at 25-50 mol% relative to the total diols in the reaction, and the effect of its molar loading was assessed. In addition, the effect of diol length was assessed by performing the polycondensation reaction with butane-1,4-diol (C_4), octane-1,8-diol (C_8) and dodecane-1,12-diol (C_{12}). The reactions were performed in bulk and diphenyl ether for comparison.

4.4.3.2 Influence of increasing the length of the diester.

In a similar approach to the previous section, diethyl adipate (C_6) was substituted with diethyl sebacate (C_{10}) to assess the influence of increasing the diester length. The reaction was performed against dodecane-1,12-diol and levoglucosan at 25 and 50 mol% relative to the total diols present.

4.4.3.3 Influence of substituting diethyl adipate with divinyl adipate.

Levoglucosan (2 mmol), dodecane-1,12-diol (2 mmol) were reacted against divinyl adipate (4 mmol) catalyzed *via* a 20% w/w N435 in diphenyl ether. The reaction proceeded in a two-step reaction similar to the previous sections.

4.4.4 Analytical methods

4.4.4.1 Nuclear Magnetic Resonance (NMR) analysis

The ^{1}H NMR, 2D-COSY spectra were recorded at room temperature on a Bruker Avance 300 instrument (delay time = 3 s, number of scans = 32) at 300.13 MHz using either $CDCl_3$ or DMSO-d_6 as solvents. Chemical shifts (ppm) are given in δ-units and were calibrated using the residual signal of $CDCl_3$ and DMSO-d_6 at 7.26 ppm and 2.5 ppm, respectively. DOSY spectra was recorded on Avance II 400 Bruker spectrometer (9.4 T) regulated at 298 K respectively in $CDCl_3$. Additionally, ^{1}H NMR was used to confirm conversion and determine its rate. Data acquisition and analysis were performed using the Bruker TopSpin 3.2 and MestReLab 6.0.

4.4.4.2 Gel Permeation Chromatography (GPC) analysis

Gel permeation chromatography (GPC) analysis was performed in chloroform as eluent (flow rate of 1 mL/min) at 23 °C using Alliance e2695 (Waters) apparatus and with a sample concentration around 10-15 $mg.mL^{-1}$. A refractive index detector Optilab T-rEX (Wyatt Technology) was used as a detector, and a set of columns: HR1, HR2 and HR4 (Water Styragel) were utilized. The molecular weight calibration curve was obtained using monodisperse polystyrene standards.

4.4.4.3 Differential scanning calorimetry (DSC)

The thermal transition was recorded with a Differential Scanning Calorimetry (DSC) on a TA Discovery DSC 25 using a cooling-heating-cooling-heating method. First, samples of ~10 mg were sealed in aluminum pans, the temperature was equilibrated at - 90 °C, followed by a heating ramp of 10 °C/min to 200 °C, then a cooling ramp of 10 °C/min to - 90 °C, and a second heating ramp of 10 °C/min to 200 °C. The thermograms were analyzed using TA instruments TRIOS software.

4.5 References

(1) Yu, J.; Paterson, N.; Millan, M. The Primary Products of Cellulose Pyrolysis in the Absence of Extraparticle Reactions. *Fuel* **2019**, *237*, 911–915. https://doi.org/10.1016/j.fuel.2018.10.059.

(2) Fisher, T.; Hajaligol, M.; Waymack, B.; Kellogg, D. Pyrolysis Behavior and Kinetics of Biomass Derived Materials. *J. Anal. Appl. Pyrolysis* **2002**, *62* (2), 331–349. https://doi.org/10.1016/S0165-2370(01)00129-2.

(3) Ragauskas, A. J.; Williams, C. K.; Davison, B. H.; Britovsek, G.; Cairney, J.; Eckert, C. A.; Frederick, W. J.; Hallett, J. P.; Leak, D. J.; Liotta, C. L.; Mielenz, J. R.; Murphy, R.; Templer, R.; Tschaplinski, T. The Path Forward for Biofuels and Biomaterials. *Science* **2006**, *311* (5760), 484–489. https://doi.org/10.1126/science.1114736.

(4) Bozell, J. J.; Black, S. K.; Myers, M.; Cahill, D.; Miller, W. P.; Park, S. K. Solvent Fractionation of Renewable Woody Feedstocks: Organosolv Generation of Biorefinery Process Streams for the Production of Biobased Chemicals. *Biomass Bioenergy* **2011**, *35* (10), 4197–4208. https://doi.org/10.1016/j.biombioe.2011.07.006.

(5) Junior, I. I.; Nascimento, M. A. do; Souza, R. O. M. A. de; Dufour, A.; Wojcieszak, R. Levoglucosan: A Promising Platform Molecule? *Green Chem.* **2020**, *22* (18), 5859–5880. https://doi.org/10.1039/D0GC01490G.

(6) Lin, Y.-C.; Cho, J.; Tompsett, G. A.; Westmoreland, P. R.; Huber, G. W. Kinetics and Mechanism of Cellulose Pyrolysis. *J. Phys. Chem. C* **2009**, *113* (46), 20097–20107. https://doi.org/10.1021/jp906702p.

(7) Maduskar, S.; Maliekkal, V.; Neurock, M.; Dauenhauer, P. J. On the Yield of Levoglucosan from Cellulose Pyrolysis. *ACS Sustain. Chem. Eng.* **2018**, *6* (5), 7017–7025. https://doi.org/10.1021/acssuschemeng.8b00853.

(8) Pecha, M. B.; Arbelaez, J. I. M.; Garcia-Perez, M.; Chejne, F.; Ciesielski, P. N. Progress in Understanding the Four Dominant Intra-Particle Phenomena of Lignocellulose Pyrolysis: Chemical Reactions, Heat Transfer, Mass Transfer, and Phase Change. *Green Chem.* **2019**, *21* (11), 2868–2898. https://doi.org/10.1039/C9GC00585D.

(9) Şerbănescu, C. Kinetic Analysis of Cellulose Pyrolysis: A Short Review. *Chem. Pap.* **2014**, *68* (7), 847–860. https://doi.org/10.2478/s11696-013-0529-z.

(10) Rover, M. R.; Aui, A.; Wright, M. M.; Smith, R. G.; Brown, R. C. Production and Purification of Crystallized Levoglucosan from Pyrolysis of Lignocellulosic Biomass. *Green Chem.* **2019**, *21* (21), 5980–5989. https://doi.org/10.1039/C9GC02461A.

(11) Smrčok, Ľ.; Sládkovičová, M.; Langer, V.; Wilson, C. C.; Koóš, M. On Hydrogen Bonding in 1,6-Anhydro-β-d-Glucopyranose (Levoglucosan): X-Ray and Neutron Diffraction and DFT Study. *Acta Crystallogr. B* **2006**, *62* (5), 912–918. https://doi.org/10.1107/S010876810602489X.

(12) Quiquempoix, L.; Bogdan, E.; Wells, N. J.; Le Questel, J.-Y.; Graton, J.; Linclau, B. A Study of Intramolecular Hydrogen Bonding in Levoglucosan Derivatives. *Mol. J. Synth. Chem. Nat. Prod. Chem.* **2017**, *22* (4). https://doi.org/10.3390/molecules22040518.

(13) Avelar do Nascimento, M.; Ester Gotardo, L.; Miguez Bastos, E.; C. L. Almeida, F.; A. C. Leão, R.; O. M. A. de Souza, R.; Wojcieszak, R.; Itabaiana, I. Regioselective Acylation of Levoglucosan Catalyzed by Candida Antarctica (CaLB) Lipase Immobilized on Epoxy Resin. *Sustainability* **2019**, *11* (21), 6044. https://doi.org/10.3390/su11216044.

(14) Carmen Cruzado, M.; Martin-Lomas, M. The Regioselectivity of Tributyltin Ether-Mediated Benzylation of 1,6-Anhydro-β-d-Hexoipyranoses. *Carbohydr. Res.* **1988**, *175* (2), 193–199. https://doi.org/10.1016/0008-6215(88)84142-9.

(15) Ward, D. D.; Shafizadeh, F. Some Esters of Levoglucosan. *Carbohydr. Res.* **1982**, *108* (1), 71–79. https://doi.org/10.1016/S0008-6215(00)81891-1.

(16) Regioselective Acylation of 1,6-Anhydro-β-D-Glucopyranose Catalysed by Lipases. *Tetrahedron Asymmetry* **1993**, *4* (12), 2441–2444. https://doi.org/10.1016/S0957-4166(00)82220-X.

(17) Galletti, P.; Moretti, F.; Samorì, C.; Tagliavini, E. Enzymatic Acylation of Levoglucosan in Acetonitrile and Ionic Liquids. *Green Chem.* **2007**, *9* (9), 987–991. https://doi.org/10.1039/B702031G.

(18) Jiang, Y.; Woortman, A. J. J.; Ekenstein, G. O. R. A. van; Loos, K. A Biocatalytic Approach towards Sustainable Furanic–Aliphatic Polyesters. *Polym. Chem.* **2015**, *6* (29), 5198–5211. https://doi.org/10.1039/C5PY00629E.

(19) Mahapatro, A.; Kalra, B.; Kumar, A.; Gross, R. A. Lipase-Catalyzed Polycondensations: Effect of Substrates and Solvent on Chain Formation, Dispersity, and End-Group Structure. *Biomacromolecules* **2003**, *4* (3), 544–551. https://doi.org/10.1021/bm0257208.

(20) Pyo, S.-H.; Hatti-Kaul, R. Selective, Green Synthesis of Six-Membered Cyclic Carbonates by Lipase-Catalyzed Chemospecific Transesterification of Diols with Dimethyl Carbonate. *Adv. Synth. Catal.* **2012**, *354* (5), 797–802. https://doi.org/10.1002/adsc.201100822.

(21) Hu, X.; Wu, L.; Wang, Y.; Mourant, D.; Lievens, C.; Gunawan, R.; Li, C.-Z. Mediating Acid-Catalyzed Conversion of Levoglucosan into Platform Chemicals with Various Solvents. *Green Chem.* **2012**, *14* (11), 3087–3098. https://doi.org/10.1039/C2GC35961H.

(22) Mahapatro, A.; Kumar, A.; Gross, R. A. Mild, Solvent-Free ω-Hydroxy Acid Polycondensations Catalyzed by Candida Antarctica Lipase B. *Biomacromolecules* **2004**, *5* (1), 62–68. https://doi.org/10.1021/bm0342382.

(23) Nasr, K.; Meimoun, J.; Favrelle-Huret, A.; Winter, J. D.; Raquez, J.-M.; Zinck, P. Enzymatic Polycondensation of 1,6-Hexanediol and Diethyl Adipate: A Statistical Approach Predicting the Key-Parameters in Solution and in Bulk. *Polymers* **2020**, *12* (9), 1907. https://doi.org/10.3390/polym12091907.

(24) Dai, S.; Xue, L.; Zinn, M.; Li, Z. Enzyme-Catalyzed Polycondensation of Polyester Macrodiols with Divinyl Adipate: A Green Method for the Preparation of Thermoplastic Block Copolyesters. *Biomacromolecules* **2009**, *10* (12), 3176–3181. https://doi.org/10.1021/bm9011634.

(25) Uyama, H.; Inada, K.; Kobayashi, S. Lipase-Catalyzed Synthesis of Aliphatic Polyesters by Polycondensation of Dicarboxylic Acids and Glycols in Solvent-Free System. *Polym. J.* **2000**, *32* (5), 440–443. https://doi.org/10.1295/polymj.32.440.

(26) Arandia, I.; Meabe, L.; Aranburu, N.; Sardon, H.; Mecerreyes, D.; Müller, A. J. Influence of Chemical Structures on Isodimorphic Behavior of Three Different Copolycarbonate Random Copolymer Series. *Macromolecules* **2020**, *53* (2), 669–681. https://doi.org/10.1021/acs.macromol.9b02078.

(27) Pérez-Camargo, R. A.; Arandia, I.; Safari, M.; Cavallo, D.; Lotti, N.; Soccio, M.; Müller, A. J. Crystallization of Isodimorphic Aliphatic Random Copolyesters: Pseudo-Eutectic Behavior and Double-Crystalline Materials. *Eur. Polym. J.* **2018**, *101*, 233–247. https://doi.org/10.1016/j.eurpolymj.2018.02.037.

5. General conclusion and perspective

The general objective of this research work was to develop an efficient, ecofriendly synthetic approach towards the synthesis of biobased polyester *via* enzymatic catalysis based on Novozym 435, a lipase B from *Candida antarctica* immobilized on a porous acrylic resin. In **Chapter 1**, we generally discussed biobased polymers in terms of their different production methods, sourcing and challenges encountered. In this chapter, we showed the importance of moving towards greener synthetic methods that do not compete with food supply, mainly food waste, lignocellulosic biomass and microalgae. Different enzymes used in polymerization were assessed in terms of their different classifications and how they are used in polymerization reactions. Among the different enzymes mentioned, lipases were found to be the most common for the synthesis of polyesters, particularly we have focused on the applications of Novozym 435. This enzyme was successfully used in the literature to catalyze the synthesis of different polyesters, polyamides and other polymers through polycondensation or ring-opening polymerization. In addition, this chapter also discussed the different parameters that can influence enzyme-catalyzed reactions, such as the solvent, temperature, and the nature of the reactants. It was evident that lipases were generally better active in non-polar solvents, and low temperatures not exceeding a 100 °C. The nature and structure of the monomers were a major factor affecting the end-product of lipase-catalyzed reactions, with an evident preference towards aliphatic diols and diesters. In **Chapter 2**, we developed a statistical model that allows a proper prediction of the number average molecular weight (M_n) of polyesters based on hexane-1,6-diol and diethyl adipate by tuning certain parameters during the reaction such as the temperature, enzyme loading amount, and vacuum level. From these results, it was determined that enhancing the vacuum power and temperature led to a significant increase in M_n. In addition, the recyclability of Novozym 435 was assessed, and it was successfully reused for three consecutive cycles in both bulk and solution conditions, confirming the efficiency and eco-friendly nature of this enzyme. Based on the findings of our work, we continued to explore the capabilities of Novozym 435 in **Chapter 3** towards the synthesis of semi-aromatic copolymers and terpolymers based on diethyl furan-2,5-dicarboxylate. The biobased furan-based monomer was successfully reacted with several aliphatic diols with a superior reactivity towards long chain diols ($\geq C_8$). This was further confirmed by performing a kinetic study comparing between hexane-1,6-diol and dodecane-1,12-diol reactivity towards diethyl furan-

2,5-dicarboxylate. Based on these findings, the incorporation of long diols such as Pripol 2033 alongside short diols such as butane-1,4-diol was found to aid the polymerization reaction to yield polymers with high furan content and an acceptable molecular weight. It was also noticed that higher amounts of Novozym 435 were necessary for a successful polymerization reaction when higher amounts of diethyl furan-2,5-dicarboxylate were reacted. In contrast, increasing the enzyme amount from 10 to 20% w/w showed no effect on the properties of aliphatic polymers. The thermal and crystallography analysis of furan-based polymers showed the formation of semi-crystalline structures, with both poly(alkylene alkanoate) and poly(alkylene furanoate) crystal blocks. The successful synthesis of furan-based polyesters *via* enzymatic catalysis was encouraging to pursue the polymerization of other non-aliphatic monomers, such as levoglucosan, an anhydrous derivative of glucose produced from the pyrolysis of carbohydrates like cellulose or starch. Therefore, in **Chapter 4**, we were able to produce polymers with variable amounts of levoglucosan. Although the high polarity of levoglucosan, strong intermolecular interactions within its structure, and the absence of primary hydroxyl groups were all limiting polymer growth and reactivity, the use of long chain diols and diesters was found to be a suitable approach to enhance polymerization and levoglucosan incorporation into the polymeric structure, reaching up to 35% levoglucosan when reacted alongside dodecane-1,12-diol and diethyl sebacate.

Throughout our work, we have successfully used Novozym 435 to synthesize several biobased polymers with interesting properties. The different approaches used through this study did not only confirm the suitability of Novozym 435 in polymer synthesis, but also improved our understanding of enzymatic catalysis in polymer synthesis, especially in terms of advantages and limitations. Although the efficiency of enzymatic catalysis at the moment, still do not compete with more vigorous approaches based on some metal-based catalysts, it does offer a set of advantages that can allow enzymes to compete and even surpass other catalytic systems in specific applications and fields. Taking advantage of the regioselectivity of enzymes can allow a certain degree of control over certain polymeric structures, that might not be accessible *via* other approaches. In addition, the use of enzymes can prove to be better suited for polymers intended to be used in drug delivery and medical applications, when safety is of high concern. Therefore, future work could enlarge our findings to enhance enzyme-based catalysis, and further study the properties and applications of polymers produced *via* enzymatic catalysis. Other approaches can aim at improving the synthetic process by substituting traditional methods such as in-solution and in-bulk batch techniques with more efficient ones. For

example, the use of reactive extrusion (REx) can be a promising approach to improve the efficiency of enzymatic catalysis in terms of time, energy, and solvent use. Such approach would also allow the transition from a batch-based towards a continuous manufacturing process, especially that the recyclable nature of Novozym 435 could allow for its reuse in multiple cycles. Other approaches such as the combination of multiple enzymes with different properties and selectivity could allow the manufacturing of novel polymers that might be otherwise not possible through alternative catalytic systems. Moreover, current and future advances in enzyme immobilization techniques and protein engineering, can lead to enzymes towards a more competing position in polymer synthesis, and possibly towards a superior position for certain applications. It is also very important to mention that certain enzymes such as lipases can catalyze the depolymerization of polyesters and polyamides under certain conditions, such as in aqueous media. From the different approaches to improve polymeric breakdown, embedding enzymatic particles within the polymer matrix can speed-up polymer degradation. Therefore, future work can focus on developing efficient systems where the enzymes that are used for polymerization can be efficiently redirected *via* minimal modifications to act as catalysts for polymer breakdown. Finally, the application of enzymatic catalysis for polymerization and depolymerization is still considered as novel, and not extensively discovered, and therefore its future is abundant in possibilities that awaits unfolding.